# The relationship between *ADAMTS13* genotype and phenotype in congenital thrombotic thrombocytopenic purpura and characterisation of ADAMTS13 mutants

Mary Imy Underwood

Thesis submitted to University College London for the degree of Doctor of Philosophy

University College London 2015

I, Mary Imy Underwood confirm that the work presented in this thesis is my own. Where information has been derived from other sources, I confirm that this has been indicated in the thesis.

…….

## Abstract

Congenital thrombotic thrombocytopenic purpura (TTP) is a thrombotic microangiopathy, usually involving *ADAMTS13* gene defects. ADAMTS13 processes the multimeric plasma glycoprotein Von Willebrand factor making it less reactive to platelets. Patients differ in terms of disease severity and evidence suggests a relationship between *ADAMTS13* genotype and disease phenotype. Over 140 mutations have been identified in patients but only ~30% of these has been expressed *in vitro*. The aim of this thesis was to study certain *ADAMTS13* mutations identified in a homozygous form in congenital TTP patients to assess *in vitro* their effect on the secretion and activity of ADAMTS13 and to assess their contribution to disease phenotype. ADAMTS13 mutants (p.R102H, p.I143T and p.Y570C) and wild type (WT) were expressed in HEK293T cells. The p.R102H mutation partially affected the secretion of ADAMTS13 and reduced the catalytic efficiency of the mutant but not to the extent predicted based upon levels measured in patient plasma. Expressing this mutant with three *ADAMTS13* polymorphisms (p.Q448E, p.P618A and p.A900V) which were also identified in the patient with this mutation further reduced the secretion and activity of ADAMTS13. When these three polymorphisms were expressed separately in WT ADAMTS13, the p.P618A polymorphism reduced the secretion and subsequently the activity of ADAMTS13 suggesting that this polymorphism in particular was responsible for the reduction observed. These results highlight the importance of *ADAMTS13* polymorphisms. The p.I143T and p.Y570C mutations severely affected ADAMTS13 secretion. Immunofluorescence studies showed localisation of these mutants within the ER but less extensive localisation within the *cis* Golgi compared to WT ADAMTS13. The p.I143T mutant was characterised further and was shown to be degraded by the cell proteasome. Addition of a chemical chaperone (betaine) appeared to rescue the secretion defect caused by the p.I143T mutation. This may have future therapeutic implications for the treatment of some congenital TTP patients.

## Acknowledgements

I would like to thank my supervisors Dr. Ian Mackie, Professor Samuel Machin and Professor Flora Peyvandi for their help and support throughout the last four years. I also would like to thank all staff at the Haemostasis Research Unit in UCL and the Angelo Bianchi Bonomi Hemophilia and Thrombosis Centre, Milan, in particular Dr. Isabella Garagiola. I would also like to thank Dr. Raimondo De Cristofaro, Dr. Stefano Lancelloti, Mr George Chennel and Mr Tomas Adejumo for their technical support. Finally I would like to thank my family for their support throughout.

## Contents

## Figures

Tables

## Abbreviations used in this thesis

| | |
|---|---|
| 4PBA | 4-phenylbutyric acid |
| ADAM | A disintegrin and metalloprotease |
| ADAMTS | A disintegrin-like and metalloprotease with thrombospondin type 1 motif |
| ALLN | N-acetyl-L-leucinyl-L-leucinyl-norleucinal |
| BiP | Binding immunoglobulin protein |
| BSA | Bovine serum albumin |
| $C_A$ | N-terminal cysteine-rich domain residues 440-531 |
| $C_B$ | C-terminal cysteine-rich domain residues 532-555 |
| CFTR | Cystic fibrosis transmembrane receptor |
| CI | Confidence interval |
| CUB | Complement C1r/C1s, sea urchin epidermal growth factor and bone morphogenetic protein 1 |
| Cy3 | Cyanine 3 |
| CV | Coefficient of variation |
| DAPI | 4',6-diamidino-2-phenylindole |
| DEPC | Diethylpyrocarbonate |
| DMEM | Dulbecco's modified eagle's medium |
| DMSO | Dimethyl sulfoxide |
| DTCS | Disintegrin-like, TSP-1, cysteine-rich and spacer domains |
| ECL | Enhanced chemiluminescence |
| ECM | Extracellular matrix |
| EDTA | Ethylenediaminetetraacetic acid |
| EGF | Epidermal growth factor |
| ER | Endoplasmic reticulum |
| ERAD | ER associated degradation |
| *Escherichia Coli* | *E. coli* |
| FBS | Fetal bovine serum |
| FFP | Fresh frozen plasma |
| FITC | Fluorescein isothiocyanate |
| FPLC | Fast performance liquid chromatography |

| | |
|---|---|
| FRET | Fluorescence resonance energy transfer |
| FVIII | Factor VIII |
| G3PDH | Glyceraldehyde 3-phosphate dehydrogenase |
| GPCC | Global Pearson correlation coefficient |
| HEPES | N-2-hydroxyethylpiperazine-N-2-ethane sulfonic acid |
| HRP | Horse radish peroxidase |
| HUS | Haemolytic uraemic syndrome |
| IS | Ischaemic stroke |
| KO | Knock-out |
| LB | Luria-Bertani |
| LDH | Lactate dehydrogenase |
| $M_1$ | Manders correlation coefficient 1 |
| $M_2$ | Manders correlation coefficient 2 |
| MAF | Minor allele frequency |
| MAHA | Microangiopathic haemolytic anemia |
| MG132 | Carbobenzoxy-Leu-Leu-leucinal |
| MI | Myocardial infarction |
| mRNA | Messenger RNA |
| NAC | N-acetylcysteine |
| NP40 | Nonidet P-40 |
| PAGE | Polyacrylamide gel electrophoresis |
| PBS | Phosphate buffered saline |
| PBST | Phosphate buffered saline containing 0.05% Tween 20 |
| PCC | Pearson correlation coefficient |
| PDI | Protein disulphide isomerase |
| PEI | Polyethylenimine |
| PMSF | Phenylmethylsulfonyl fluoride |
| PNP | Pooled normal plasma |
| QC | Quality control |
| RIPA | Radioimmunoprecipitation assay |
| RT | Reverse transcription |
| SD | Standard deviation |
| SDS | Sodium dodecyl sulphate |

| | |
|---|---|
| SELDI-TOF | Surface-enhanced laser desorption/ionization time-of-flight |
| SRC | Spearman's rank correlation coefficient |
| TBE | Tris-borate-EDTA |
| TBS | Tris buffered saline |
| TBST | Tris buffered saline containing 0.05% Tween 20 |
| TMA | Thrombotic microangiopathy |
| TMAO | Trimethylamine N-oxide |
| TPCC | Thresholded Pearson correlation coefficient |
| TSP | Thrombospondin |
| TTP | Thrombotic thrombocytopenic purpura |
| ULVWF | Ultra large Von Willebrand factor |
| UPR | Unfolded protein response |
| UPS | Ubiquitin-proteasome system |
| VWD | Von Willebrand disease |
| VWF | Von Willebrand factor |
| VWF73 | Peptide of VWF consisting of residues 1596-1668 |
| WT | Wild type |

# Chapter 1 Introduction

## 1.1 Von Willebrand Factor

### 1.1.1 VWF gene, synthesis, secretion

The gene encoding Von Willebrand factor (VWF) is situated on chromosome 12 (Ginsburg *et al*, 1985) and spans ~178 kilobases, containing 52 exons (Mancuso *et al*, 1989). The 9kb *VWF* messenger RNA (mRNA) encodes a 2813 amino acid precursor that contains a 22 amino acid long signal peptide, a 741 amino acid long propeptide and a 2050 amino acid long mature subunit (Sadler, 1998) (Figure 1-1). VWF is synthesised within vascular endothelial cells (Jaffe *et al*, 1973) and megakaryocytes (Sporn *et al*, 1985;Nachman *et al*, 1977) and is stored within endothelial cells in Weibel-Palade bodies (Wagner *et al*, 1982) and within α-granules in megakaryocytes (Cramer *et al*, 1985).

During synthesis VWF undergoes glycosylation with the addition of twelve N-linked and ten O-linked glycan side chains on each mature monomer unit (Titani *et al*, 1986). A small proportion of the N-linked and O-linked glycans contain the ABO (H) group antigen (Matsui *et al*, 1992;Canis *et al*, 2010). ABO blood group is an important determinant of plasma VWF levels. Blood group O is associated with lower mean WVF antigen levels compared to groups A, B and AB. These levels however are still within the normal range (Gill *et al*, 1987).

Covalent dimerisation of VWF monomers occurs in the endoplasmic reticulum (ER) (Wagner & Marder, 1984), with the formation of disulphide bonds between cysteine residues in the cysteine knot (CK) domain of VWF (Katsumi *et al*, 2000) (Figure 1-1). Multimerisation of these dimers occurs in the Golgi (Wagner & Marder, 1984) with the formation of disulphide bonds between the D3 domains of VWF dimers (Marti *et al*, 1987) (Figure 1-1). The propeptide D1-D2 domains are required for VWF multimerisation, acting as a disulphide isomerase (Mayadas & Wagner, 1992).

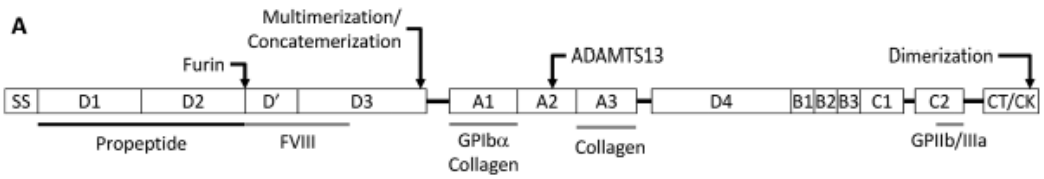


**Figure 1-1 VWF domain structure**

The domain structure of VWF is shown. Regions important for interaction with other proteins are also shown. Image from: (Yee & Kretz, 2014).

After glycosylation, furin removes the VWF propeptide, which then assists in the trafficking of both mature multimeric VWF and the cleaved propeptide to Weibel-Palade bodies (endothelial cells) or α-granules (platelets) (Wagner *et al*, 1991). Each VWF monomer is ~250kDa, stored ultra large forms of VWF (ULVWF) are typically >20,000 kDa in size (Sadler, 1998).

ULVWF multimers are secreted into the bloodstream from endothelial cells in a constitutive-like manner (Giblin *et al*, 2008) and in response to agonists. The majority of VWF within endothelial cells is secreted constitutively. In contrast to endothelial cells, megakaryocytes do not constitutively secrete VWF, but release it in response to agonists. In cultured endothelial cells, VWF secretion is stimulated by a variety of agents including histamine (Hamilton & Sims, 1987), thrombin (Levine *et al*, 1982), fibrin (Ribes *et al*, 1987), calcium ionophore A23187 (Loesberg *et al*, 1983), the vasopressin analogue 1-desamino-8-D-arginine vasopressin (DDAVP) (Mannucci *et al*, 1975) and phorbol myristate acetate (Loesberg *et al*, 1983).

### 1.1.2 VWF function

VWF exists both in the circulation and in the extracellular matrix (ECM) (Rand *et al*, 1980;Rand *et al*, 1982) and plays an important role in primary haemostasis by recruiting platelets to sites of vessel injury. A deficiency of VWF can lead to Von Willebrand disease (VWD), one of the most common inherited human bleeding disorders.

Shear stress is an important determinant of VWF function as it has the ability to significantly change the confirmation of VWF. This structural change modulates the

exposure of ligand binding sites within the VWF protein. Within the circulation VWF can exist in a globular and an extended form (Siedlecki *et al*, 1996) (Figure 1-2).


**Figure 1-2 VWF changes its shape in response to shear stress**

VWF can adopt a globular shape under low shear stress and with increasing shear stress can unfold. Image from: (Siedlecki *et al*, 1996).

As blood flows through a vessel, velocity is maximal in the centre and falls to zero at the vessel wall. Conversely the gradient of velocity, or shear rate is maximal at the vessel wall and falls to zero at the centre. Typical shear rates in small arteries where the procoagulant activity of VWF is predominant, is typically within the range of $1{,}000s^{-1}$ (Schneider *et al*, 2007). VWF was shown to display a reversible globule-stretch transition at a critical shear rate ($\gamma$crit) of $5{,}000s^{-1}$ in the absence of any adsorbing surface (Schneider *et al*, 2007). At $\gamma$crit VWF changed from its globular (estimated diameter 2μM) to stretched form (15μM) (Schneider *et al*, 2007). In the presence of platelets $\gamma$crit decreased to $3{,}500s^{-1}$ (Schneider *et al*, 2007). The $\gamma$crit *in vivo* is expected to be lower than this due to the increased viscosity of blood and the binding or adsorption of platelets to the surface of VWF. Larger VWF multimers unravel more readily in response to shear stress (Zhang *et al*, 2009).

Vessel wall damage leads to the exposure of collagen rich matrix which normally lies beneath the cell monolayer. Globular VWF can recognise newly exposed collagen (via its A3 domain) which leads to its recruitment to the damaged vessel wall. The major binding site for type I and type III collagen lies within the A3 domain of VWF (Cruz *et al*, 1995;Lankhof *et al*, 1996;Romijn *et al*, 2001). Binding sites within the A1 domain for type I and type III collagen have also been identified (Morales *et al*, 2006;Bonnefoy *et al*, 2006b). VWF can additionally bind to collagen VI via its A1 domain (Mazzucato *et al*, 1999). These different types of collagen are situated predominantly in different regions of the ECM, enabling VWF to participate in the initiation of coagulation when the vessel wall is damaged to different degrees (Vanhoorelbeke & Deckmyn, 2003). The A1 domain of VWF can also bind to heparin-like molecules (Fujimura *et al*, 1987) and to sulfatides (Christophe *et al*, 1991), playing a potentially important role in the immobilisation of soluble VWF onto complex ECMs (Ruggeri, 1997).

Once VWF is immobilised it can subsequently unfold by local shear stress exerted on the tethered VWF molecule by flowing blood (Siedlecki *et al*, 1996) revealing previously hidden ligand binding sites such as platelet binding sites. VWF is important for initial platelet tethering and subsequent platelet adhesion (Sadler, 1998). Initial contact occurs between the glycoprotein (GP) Ib-IX-V complex on platelets (Sakariassen *et al*, 1986) and the A1 domain of VWF (Fujimura *et al*, 1986) (Figure 1-1). Blocking GPIb prevents the binding of platelets to VWF strings (Dong *et al*, 2002). This platelet receptor is exposed on the surface of unactivated platelets and has significant affinity for VWF, whereas the VWF A1 domain binding site is not exposed when VWF is in its globular state. This receptor binds to endothelial anchored VWF in the presence of venous and arterial fluid shear stress (Dong *et al*, 2002).

The GPIIb-IIIa complex on platelets is important for platelet aggregation but is not sufficient for platelet adhesion as this interaction is relatively slow (Savage *et al*, 1996). VWF does not promote thrombus growth when platelet GPIIb-IIIa is absent (Chauhan *et al*, 2006). The GPIIb-IIIa complex on resting platelets does not bind to VWF. This receptor is exposed after platelet activation by thrombin or other agonists

(Fujimoto *et al*, 1982). The binding site for GPIIb-IIIa lies within the VWF C2 domain (Girma *et al*, 1986).

Savage *et al* showed that platelet binding to fibrinogen was fully efficient only at wall shear rates below 600-900$s^{-1}$, with maximal platelet deposition at 50$s^{-1}$ (Savage *et al*, 1996). Conversely adhesion to VWF was minimal at 50$s^{-1}$ and maximal at 1500s-1. VWF is therefore important for platelet adhesion (via GPIb) and platelet aggregation (via GPIIb-IIIa) under high shear stress. Larger VWF multimers have an increased ability to support platelet adhesion and aggregation (Federici *et al*, 1989;Moake *et al*, 1986).

VWF acts as a carrier for Factor VIII (FVIII) stabilising the protein (Weiss *et al*, 1977). In the absence of VWF, Factor VIII is rapidly removed from the circulation (Tuddenham *et al*, 1982). This is evident in patients with severe VWD, who not only have undetectable levels of VWF but have Factor VIII levels <10% of normal (Sadler, 1998). A minimal proteolytic fragment compromising the D' and D3 domains of VWF has been reported to bind to FVIII (Foster *et al*, 1987).

VWF has been shown to self-associate at the interface of soluble and surface bound VWF (Savage *et al*, 2002;Barg *et al*, 2007). VWF formed a web like structure (Barg *et al*, 2007) and this association was rapidly reversible (Savage *et al*, 2002). The ability of VWF multimers to self-associate may further contribute to its ability to prevent bleeding.

### 1.1.3 ADAMTS13 regulates the size of VWF

VWF is stored and released from platelets and endothelial cells as ULVWF. ULVWF however is not normally detected in blood, but instead a series of lower molecular weight multimeric forms, ranging in size typically from 500 to 20,000 kDa are present (Zhou *et al*, 2010). These lower molecular weight forms exist because ULVWF is cleaved by the enzyme ADAMTS13 (A disintegrin-like and metalloprotease with thrombospondin type 1 motif) (Furlan *et al*, 1998b;Furlan *et al*, 1997;Furlan *et al*, 1998a;Tsai & Lian, 1998). By cleaving VWF, ADAMTS13 down-regulates platelet aggregation and prevents excessive thrombus growth.

ADAMTS13 cleaves VWF at the Tyr1605-Met1606 peptide bond within the A2 domain of VWF (Furlan *et al*, 1996;Tsai, 1996). The scissile bond is unavailable for cleavage when VWF is in its native, globular state. Unfolding of the VWF A2 domain exposes the scissile bond and cryptic exosites (Figure 1-3).

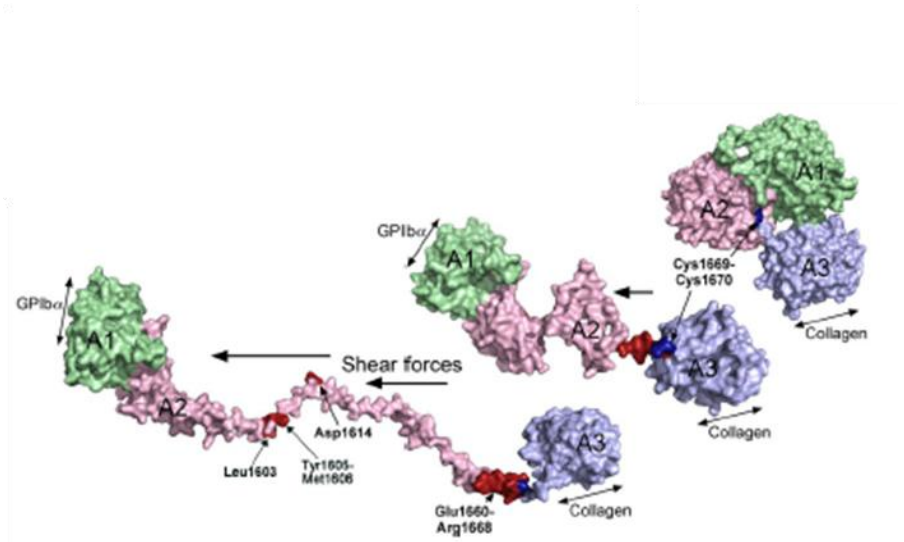


**Figure 1-3 Shear flow leads to the unfolding of VWF**

The molecular structure of the A1-A2-A3 domain is shown. In its globular form (far right), the A3 domain collagen binding site is exposed. Shear stress leads to unravelling of the A2 domain exposing the site for ADAMTS13 cleavage and platelet binding sites. Image adapted from (Crawley *et al*, 2011).

ADAMTS13 cleaves ULVWF during secretion from endothelial cells and further cleaves VWF in the circulation. Endothelial cell derived ULVWF strings bind to platelets and are cleaved within seconds to minutes in the presence of normal plasma or partially purified ADAMTS13. In contrast the strings persist in the absence of ADAMTS13 (Dong *et al*, 2002), suggesting that cleavage of VWF occurs on the surface of endothelial cells. ADAMTS13 has been shown to bind to endothelial cells which may facilitate the ability of ADAMTS13 to cleave ULVWF (Vomund & Majerus, 2009). This interaction may potentially involve CD36 on the surface of endothelial cells, as *in vitro* ADAMTS13 has been shown to bind to CD36 (Davies *et al*, 2006).

VWF can be cleaved by ADAMTS13 in the circulation. Under shear flow the tensile force on a VWF multimer increases with the square of multimer length and is highest

in the middle, providing a mechanism for haemostatic regulation of VWF size in the circulation (Zhang *et al*, 2009). A VWF A2 domain typically unfolds at 11pN, this tensile force may correspond to the force encountered by a 200mer VWF multimer in arterioles and capillaries (Zhang *et al*, 2009). ADAMTS13 can limit thrombus growth directly at the site of ongoing thrombus generation (Shida *et al*, 2008) and so may further regulate the size of VWF under these circumstances.

## 1.2 The *ADAMTS13* gene, synthesis and secretion

### 1.2.1 Gene

The human *ADAMTS13* gene is located on chromosome 9 at position 9q34, spanning 37 kb and contains 29 exons (Levy *et al*, 2001). Seven isoforms produced by alternative splicing have been described (Zheng *et al*, 2001). The *ADAMTS13* mRNA of the primary isoform is approximately 5 kb and encodes a protein of 1,427 amino acids (Zheng *et al*, 2001).

The *ADAMTS13* gene consists of a signal peptide, propeptide, metalloprotease, disintegrin- like, thrombospondin-1 repeat (TSP-1), cysteine-rich, ADAMTS spacer, seven additional TSP-1 repeats and two complement C1r/C1s, sea urchin epidermal growth factor and bone morphogenetic protein 1 (CUB) domains (Zheng *et al*, 2001) (Figure 1-4).

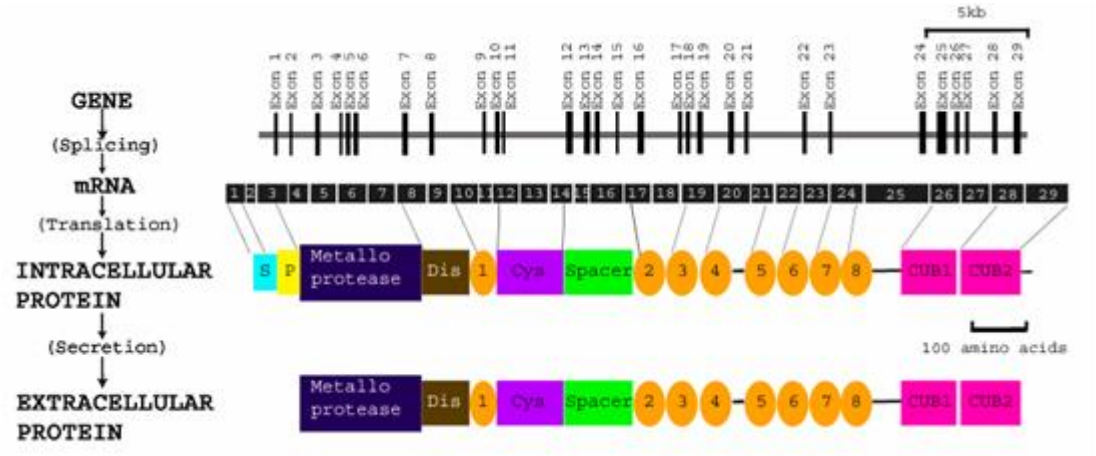


**Figure 1-4 ADAMTS13 from gene to protein**

*ADAMTS13* gene organisation is shown along with the protein domain structure. Image adapted from (Zheng *et al*, 2001).

### 1.2.2 Synthesis

ADAMTS13 is mainly synthesised in hepatic stellate cells (Zheng *et al*, 2001;Uemura *et al*, 2005;Zhou *et al*, 2005) but *ADAMTS13* mRNA or protein has been detected in several other cells and tissues including megakaryocytes/platelets (Suzuki *et al*, 2004;Liu *et al*, 2005), endothelial cells (Turner *et al*, 2006) and renal podocytes (Manea *et al*, 2007a). Plasma ADAMTS13 is highly glycosylated, with ten potential N-linked glycosylation sites (Zheng *et al*, 2001), two in the metalloprotease domain, one in the cysteine-rich, three in the spacer, one in the TSP-1:2, one in the TSP-1:4, one in the CUB-1 and one in the CUB-2 domain. Nine of these sites have been identified as glycosylation sites within plasma and recombinant ADAMTS13 (Sorvillo *et al*, 2014) (TSP-1:4 was not identified). ADAMTS13 has seven predicted O-fucosylation sites, one in each TSP-1 domain with the exception of TSP-1:4 (Zheng *et al*, 2001). Six of these sites (TSP-1:2, TSP-1:3, TSP-1:5, TSP-1:6, TSP1-7, TSP1-8) have been identified as glycosylation sites in human and recombinant ADAMTS13 (Ricketts *et al*, 2007;Sorvillo *et al*, 2014). Several potential C-mannosylation sites have been identified within ADAMTS13. There is evidence to suggest the existence of two putative C-mannosylation sites within plasma and recombinant ADAMTS13 (Sorvillo *et al*, 2014).

### 1.2.3 Secretion

ADAMTS13 circulates in plasma at a concentration of 0.5-1 μg/ml (Soejima *et al*, 2006), with an estimated half-life of two to three days (Furlan *et al*, 1999). Glycosylation is important for the secretion of ADAMTS13. Disruption of O-fucosylation has been reported to reduce ADAMTS13 secretion from transfected HEK293 cells (Ricketts *et al*, 2007) and N-glycosylation in the ER is also critical for the efficient secretion of ADAMTS13 from HEK293T cells (Zhou & Tsai, 2009). Amino acid substitution at a potential C-mannosylation site in the TSP-1 domain (p.W387A) led to reduced secretion of ADAMTS13, suggesting that C-mannosylation at this site is also important for secretion (Ling *et al*, 2013).

In endothelial cells, ADAMTS13 secretion is targeted to the vascular lumen which is mediated by an interaction between the CUB domains of ADAMTS13 and the

detergent-resistant and cholesterol-enriched lipid rafts in the apical surface of these cells (Shang *et al*, 2006;Zhou *et al*, 2009b).

## 1.3 The ADAMTS13 protein

### 1.3.1 The ADAMTS family

ADAMTS13 is a metalloprotease belonging to the ADAMTS family (Levy *et al*, 2001). The ADAMTS family includes nineteen soluble multi-domain zinc-proteases, which share a conserved multi-domain structure with sequence similarity to the ADAM (A disintegrin and metalloprotease) proteases (Andreini *et al*, 2005). Both protein families have a conserved catalytic metalloprotease domain, a signal peptide, a propeptide, a disintegrin-like domain and a cysteine-rich region (Figure 1-5). ADAMTS proteins lack the epidermal growth factor (EGF) like and transmembrane domains present in ADAM proteins and instead contain a TSP-1 sequence repeat motif and an ADAMTS spacer domain (Figure 1-5). The C-terminal region contains a variable number of additional TSP-1 repeats (from fourteen in ADAMTS9 and 20, to none in ADAMTS4) (Apte, 2004).

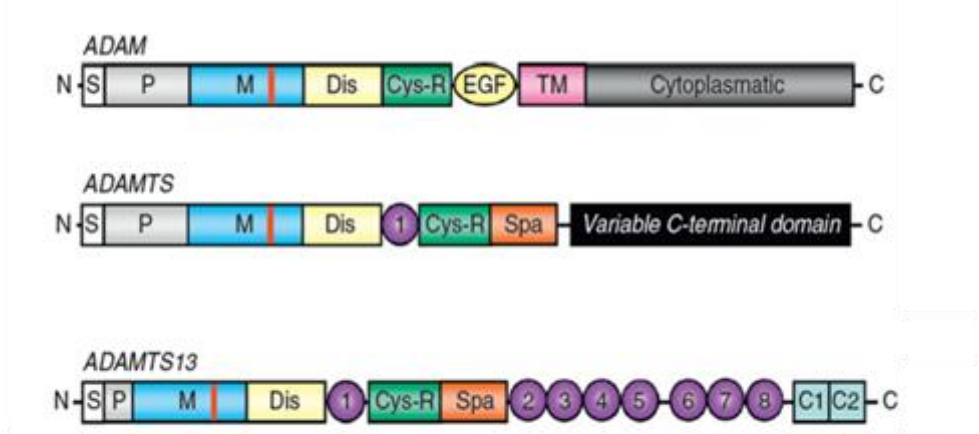


**Figure 1-5 Domain structure of the ADAM and ADAMTS protease family and ADAMTS13**

Signal peptide (S), propeptide (P), metalloprotease domain (M) (location of the zinc-binding motif is shown in red), disintegrin-like domain (Dis), cysteine-rich domain (Cys-R), EGF domain (EGF), transmembrane domain (TM), first TSP-1 repeat (1), spacer domain (Spa), TSP-1 repeats 2 to 8 (2-8), two CUB domains (C1, C2). Image adapted from (Lancellotti & De Cristofaro, 2011).

ADAMTS13 developed before the divergence of fish and tetrapod lineages at least 360 million years ago (Majerus *et al*, 2003). ADAMTS13 is most closely related to ADAMTS2, 3 and 14, which process collagen (Huxley-Jones *et al*, 2005). The function of the other ADAMTS proteases includes cleavage of the matrix metalloproteoglycans aggrecan, versican and brevican (ADAMTS1, 4, 5, 8, 9 and 15) and inhibition of angiogenesis (ADAMTS1 and 8) (Jones & Riley, 2005).

### 1.3.2 ADAMTS13

The crystal structure of the region encompassing the disintegrin-like, TSP-1, cysteine-rich and spacer domain (DTCS) of ADAMTS13 has been solved (Akiyama *et al*, 2009) and the metalloprotease domain modelled based upon the crystal structure of ADAMTS1, 4 and 5. The 3D molecular structure of ADAMTS13 (metalloprotease→spacer domain) is shown in Figure 1-6 along with the VWF A2 domain ribbon structure which interacts with these domains.

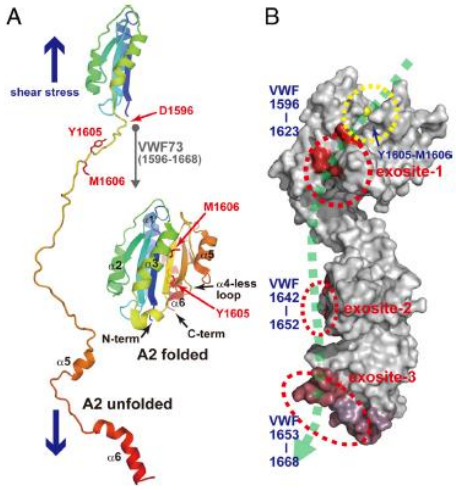


**Figure 1-6 ADAMTS13 DTCS**

Figure A shows the folded and unfolded structure of the VWF A2 domain. The molecular structure of the modelled metalloprotease domain along with the DTCS model is shown in B. The dotted green line represents a VWF molecule. Exosites important for VWF binding are shown in red and yellow. Image from: (Akiyama *et al*, 2009).

### 1.3.3 Propeptide

The ADAMTS13 propeptide domain is shorter compared to other ADAMTS family proteins. Deletion of this region does not appear to affect the secretion, folding or enzymatic activity of ADAMTS13 *in vitro* (Majerus *et al*, 2003) and so this domain appears to be dispensable for these purposes.

### 1.3.4 Metalloprotease domain

The metalloprotease domain of the ADAMTS family members are characterised by a reprolysin-type zinc ($Zn^{2+}$) binding signature (HEXXHXXGXXHD) which consists of three conserved histidine (H) residues and a catalytic glutamic acid. The glutamic acid polarises a water molecule which is stabilised by the $Zn^{2+}$ ion. The $Zn^{2+}$ binding motif is followed by a tight methionine turn (Zheng *et al*, 2001).

The metalloprotease domain has two potential calcium ($Ca^{2+}$) binding sites. One of these sites (low affinity site) does not appear to be important for ADAMTS13 function (Gardner *et al*, 2009) but may be structurally important. The second $Ca^{2+}$ binding site (high affinity site) appears to be important for ADAMTS13 function. The amino acids important for $Ca^{2+}$ binding at the second site are present in a loop close to the ADAMTS13 active site suggesting that $Ca^{2+}$ binding provides structural integrity to this loop (Gardner *et al*, 2009).

ADAMTS13 cleaves VWF at the position Tyr1605-Met1606. Substitution of these residues with alanine was shown to greatly reduce the proteolytic efficiency of ADAMTS13 (Pruss *et al*, 2008). Substitution of methionine with leucine showed no significant change in activity using a VWF115 peptide but a 26% decrease when using full length VWF. This data highlights the requirement for a large and hydrophobic amino acid at this position (P1' residue) (Pruss *et al*, 2008). The proteolysis of Tyr1605Phe and Tyr1605Trp variants was comparatively normal to wild type (WT) demonstrating the importance of the aromatic side chain at position 1605 (P1 residue) (Pruss *et al*, 2008).

There are a number of VWF binding subsites within the metalloprotease domain. The ADAMTS13 S1 pocket which accommodates P1 may involve the hydrophobic

residues Leu151 and Val195 (Xiang *et al*, 2011) and the functional $Ca^{2+}$ ion. Amino acids Asp252-Pro256 of ADAMTS13 are important in shaping the docking site of P1' contributing to the S1' pocket (de Groot *et al*, 2010). The VWF P3 residue (Leu1603) appears to have an essential role in the proteolysis of the scissile bond whereas the adjacent P2 residue (Val1604) plays a minor role (Xiang et al 2010). Mutagenesis studies identified the amino acid residues Leu198, Leu232 and Leu 274 as important elements of the S3 subsite (Xiang *et al*, 2011).

Studies using C-terminal truncated recombinant ADAMTS13 constructs showed that the metalloprotease domain alone is unable to cleave plasma VWF (Soejima *et al*, 2003;Zheng *et al*, 2003) or a short A2 domain peptide, GST-VWF73-His at the correct site (Ai *et al*, 2005), suggesting that the domains downstream of the metalloprotease domain are responsible for determining substrate specificity. Indeed a chimeric variant of ADAMTS5 (which normally cleaves aggrecan), engineered to contain the ADAMTS13 TSP-1, cysteine-rich and spacer domains, was shown to cleave VWF (although at a different peptide bond within the A2 domain) (Gao *et al*, 2012). This demonstrates the importance of these domains for substrate specificity.

### 1.3.5 Disintegrin-like domain

The disintegrin-like domain of ADAMTS proteins share sequence similarity to snake venom disintegrins but lack the canonical disintegrin cysteine arrangement (Apte, 2004). The disintegrin-like domain of ADAMTS13 does not appear to function like a disintegrin-like domain but bears greater structural similarity to the cysteine-rich domain, with folding similarities existing between the disintegrin-like domain and the N-terminal portion of the cysteine-rich domain (residues 440-531, designated the $C_A$ domain) of ADAMTS13 (Akiyama *et al*, 2009).

Additionally unlike the ADAM family metalloproteases the ADAMTS disintegrin-like domain contains a linker region that extends around the back of the metalloprotease domain and positions the disintegrin-like domain at one end of the active-site cleft (Gerhardt *et al*, 2007;Mosyak *et al*, 2008). The crystal structure of the ADAMTS13 disintegrin-like domain shows that the disintegrin domain abuts the metalloprotease domain catalytic site, suggesting that the surface of the disintegrin-

like domain leading to the catalytic site functions as a VWF binding site (Akiyama *et al*, 2009).

The disintegrin-like domain appears to be important for VWF binding. Addition of the disintegrin-like domain to the ADAMTS13 metalloprotease domain restored the specific cleavage of GST-VWF73-His at the Tyr-Met bond (Ai *et al*, 2005). This domain also bound dose dependently to GST-VWF73-His and also dose dependently inhibited cleavage of FRETS-VWF73 by full length ADAMTS13.

Indeed a VWF binding exosite exists within the disintegrin-like domain of ADAMTS13 (exosite 1), consisting of the amino acids: Arg326, Glu327, His328, Asp330, Arg349, Leu350 and Val352 (Akiyama *et al*, 2009). The cluster of charged residues may collaboratively interact with Asp1614, Glu1615 and Lys1617 within VWF. These ADAMTS13 amino acids and the corresponding interacting amino acids within VWF have been previously shown *in vitro* to be important for the interaction between ADAMTS13 and VWF (Zanardelli *et al*, 2006;de Groot *et al*, 2009).

### 1.3.6 TSP-1 domain

The TSP-1 domain is homologous to the type 1 repeat of thrombospondin-1 and -2 and contains six cysteine amino acids. The TSP-1 domain of ADAMTS13 is stiff and rod-like (Akiyama *et al*, 2009). The core of TSP-1 is stabilised by stacked layers of tryptophan, arginine and hydrophobic residues and is capped by disulphide bonds at bond ends. This stacked structure is referred to as the CWR layered core (Akiyama *et al*, 2009).

The addition of the TSP-1 domain to the metalloprotease domain of ADAMTS13 restored the specific cleavage of GST-VWF73-His at the Tyr-Met bond. Additionally the TSP-1 domain alone bound dose dependently to GST-VWF73-His and dose dependently inhibited cleavage of FRETS-VWF73 by full length ADAMTS13 and an ADAMTS13 variant truncated after the spacer domain (Ai *et al*, 2005). The TSP-1 domain may interact with VWF residues Gln1624-Val1630 (Gao *et al*, 2008). However this interaction appears to be non-essential and the primary role of the TSP-

1 domain may be to spatially position the VWF binding exosites within the other ADAMTS13 domains (Akiyama *et al*, 2009).

### 1.3.7 Cysteine-rich domain

The cysteine-rich domain contains ten conserved cysteine residues; the N-terminal portion of the cysteine-rich domain $C_A$, has a fold structurally homologous to that of the cysteine-rich domains of ADAMs, despite the lack of sequence similarity. The disintegrin-like and $C_A$ domains have only 17% identity in their amino acid sequences however their tertiary structures are similar. They share an N-terminal α-helix, two pairs of double-stranded antiparallel β-sheets and three disulphide bonds, constituting the core structure of these domains (Akiyama *et al*, 2009).

The remaining C-terminal portion of the cysteine-rich domain (resides 532-555, $C_B$) is highly conserved in amino acid sequence among ADAMTS family proteins. Although the $C_B$ domain has no apparent secondary structure it has a series of turns stabilised by a pair of disulphide bonds and forms a rod shape with its C and N termini ~25A apart (Akiyama *et al*, 2009).

This domain appears to be important for VWF binding. The cysteine-rich domain alone was shown to bind dose dependently to GST-VWF73-His and to dose dependently inhibit cleavage of FRETS-VWF73 by full length ADAMTS13 (Ai *et al*, 2005). A VWF binding exosite (exosite 2) may exist in the cysteine-rich region, consisting of amino acids: His476, Ser477, Gln478, Arg448, Phe494-Met496 (Akiyama *et al*, 2009). This may interact with the VWF region encompassing amino acids: Ile1642-Gln1652 (Gao *et al*, 2008).

### 1.3.8 Spacer domain

The spacer domain contains no cysteine amino acids, has a variable length in ADAMTS family members and is the least homologous domain. It folds into a single globular domain with ten β-strands in a jelly roll topology, forming two antiparallel β-sheets that lie almost parallel to each other. The hydrophobic aromatic residues forming the core of the β-sandwich are highly conserved. In contrast loops located on the distal side of the molecule are highly variable in length and amino acid sequence

among ADAMTS proteins. The N and C-termini of the spacer domain are in close proximity and thus the TSP-1:2 domain following the spacer domain should be in close proximity to the $C_A$/spacer domain junction, not at the distal side of the spacer domain (Akiyama *et al*, 2009). The B6-B7 loop in the spacer domain plays a pivotal role in the interactions between the $C_A$ and spacer domain (Akiyama *et al*, 2009).

Addition of the spacer domain to the metalloprotease domain restored the specific cleavage of GST-VWF73-His at the Tyr-Met bond (Ai *et al*, 2005). The spacer domain additionally bound dose dependently to GST-VWF73-His and dose dependently inhibited the cleavage of FRETS-VWF73 by full length ADAMTS13 and ADAMTS13 truncated after the spacer domain (Ai *et al*, 2005).

A VWF binding site, exosite 3, consisting of the residues Arg568, Pro590, Leu591, Phe592, Leu637, Pro638, Leu591, Phe592, Arg660, Tyr661, Tyr665, and Leu688 exists within the spacer domain. Some of these amino acids lie on two distal loops on the spacer domain (Akiyama *et al*, 2009). The importance of some of these residues for this interaction has been demonstrated *in vitro* (Pos *et al*, 2010). The amino acid Arg659 may also contribute to the ADAMTS13 spacer-VWF A2 domain interaction (Jin *et al*, 2010). This region binds to Asp1653-Arg1668 in the VWF A2 domain (Akiyama *et al*, 2009).

Exposure of cryptic binding sites within the VWF A2 domain requires the extraction of the adjacent molecular plug formed by the vicinal disulphide bond (Cys1669-Cys1670) and uncoupling of the C-terminal α-helix in which residues Glu1660-Arg1668 reside. As this region is predicted to unfold first, even partial unfolding of the VWF A2 domain could be sufficient for the spacer domain to bind (Chen *et al*, 2009).

### 1.3.9 TSP-1:2→TSP-1:8, CUB-1 and CUB-2 domains

The TSP-1 repeats are homologues to the type 1 repeat of thrombospondin-1 and -2. The TSP-1:2→TSP-1:8 repeats are variable in sequence. The TSP-1:4 domain of ADAMTS13 contains just four cysteine residues, two of which are predicted to be unpaired. All of the TSP-1 repeats except for TSP-1:4 are predicted to be O-glycosylated. There are six potential CD36 binding sites within the TSP-1 repeats,

with CSVSCG recognition sites in four TSP-1 repeats and two CSASCG recognition sites in two of the TSP-1 repeats (Davis *et al*, 2009). ADAMTS13 is the only member of the ADAMTS family to contain CUB domains. These domains are present within proteins known to be important for developmental regulation, such as bone morphogenetic protein-1 (Bork & Beckmann, 1993).

The TSP-1:2→8 and CUB domains have been shown to mediate binding of recombinant ADAMTS13 to a constitutively exposed surface on globular VWF. Interaction occurs between the TSP-1:5→TSP-1:8 and/or the CUB domains (Zanardelli *et al*, 2009). This interaction does not result in ADAMTS13 cleavage (Zanardelli *et al*, 2009;Feys *et al*, 2009a) and is reversible and non-covalent (Feys *et al*, 2009a). This interaction also occurs in normal human plasma, with ADAMTS13-VWF complexes representing approximately 3% of total ADAMTS13 (Feys *et al*, 2009a). This domain may be important for the initial docking of ADAMTS13 to VWF and its localisation at the site of the growing thrombus *in vivo*, but dispensable when ADAMTS13 activity is measured under static conditions.

The importance of the C-terminal domains has been demonstrated in mice. Mice encode two forms of the *ADAMTS13* gene, some mouse strains encode full length ADAMTS13 (129/Sv) and some strains of mice such as C57BL/6 encode a short form of ADAMTS13 lacking the distal C-terminal domains due to the insertion of a retrotransposon in intron 23 of the *ADAMTS13* gene (Banno *et al*, 2004;Zhou *et al*, 2007). Banno *et al* analysed and generated 129/Sv-genetic background congenic mice that carried the short form of ADAMTS13 (*ADAMTS13*$^{S/S}$) and compared this to the WT mice with the long form (*ADAMTS13*$^{L/L}$). *In vitro* thrombogenesis using blood from both mice was measured under flow by perfusing whole blood over a collagen-coated surface in a parallel flow chamber. At a shear rate of 5000s-1, thrombogenesis was accelerated in *ADAMTS13*$^{S/S}$ compared to *ADAMTS13*$^{L/L}$, but there was no significant difference at 1000s$^{-1}$. Both *in vivo* thrombus formation in ferric-chloride injured arterioles and thrombocytopenia induced by collagen plus epinephrine challenge was more dramatic in *ADAMTS13*$^{S/S}$ than in *ADAMTS13*$^{L/L}$ but less than in *ADAMTS13*$^{-/-}$ (Banno *et al*, 2009).

It has been proposed that the TSP-1:2→8 domains may negatively regulate ADAMTS13 activity. In mice the proteolysis of endothelial platelet decorated strings by ADAMTS13 truncated after the spacer domain was similar to full length ADAMTS13. In contrast removal of the CUB domains was found to abolish proteolysis of endothelial platelet-decorated VWF strings. Activity of an ADAMTS13 variant truncated after the TSP-1:6 domain resulted in reduced activity when compared to ADAMTS13 truncated after the spacer domain (De Maeyer *et al*, 2010). The authors hypothesise that the catalytic site and/or spacer domain of ADAMTS13 are shielded by the TSP2-8 tail, an interaction that could be disrupted after the initial docking of the CUB domains, enabling interaction of the catalytic site and spacer domain with the A2 domain of VWF. Alternatively conformational changes that may occur in ADAMTS13 after the deletion of these regions could explain the differences observed. It is unclear therefore whether the TSP-1:2→8 domains negatively regulate ADAMTS13 activity (De Maeyer *et al*, 2010).

## 1.4 ADAMTS13 cleavage of VWF

As described VWF binding exosites exist in the metalloprotease domain and within the disintegrin-like domain, cysteine-rich region and spacer domain of ADAMTS13. These exosites interact with discontinuous regions of VWF (Akiyama *et al*, 2009). The overall structure of the ADAMTS13 DTCS resembles a distorted W-shape in which three protruding regions: disintegrin-like, $C_A$ and spacer domain are connected by 2 elongated structural modules: TSP-1 and $C_B$. The homologous disintegrin-like and $C_A$ domains are separated and related by a pseudo-90° screw rotation with a ~45A translation along TSP-1. The VWF-binding exosites are on the linearly aligned discontinuous surface of the disintegrin-like, $C_A$ and spacer domains transversing the W-shaped molecule (Akiyama *et al*, 2009).

The multiple interactions that exist between VWF and ADAMTS13 are illustrated in Figure 1-7. According to this model (Crawley *et al*, 2011) ADAMTS13 and VWF make contact through their C-terminal domains. As a consequence of changes in local shear stress conditions, confirmational changes in VWF lead to the exposure and binding of exosites present in the N-terminal region of the VWF A2 domain and ADAMTS13, which positions the scissile bond in the catalytic cleft of ADAMTS13.

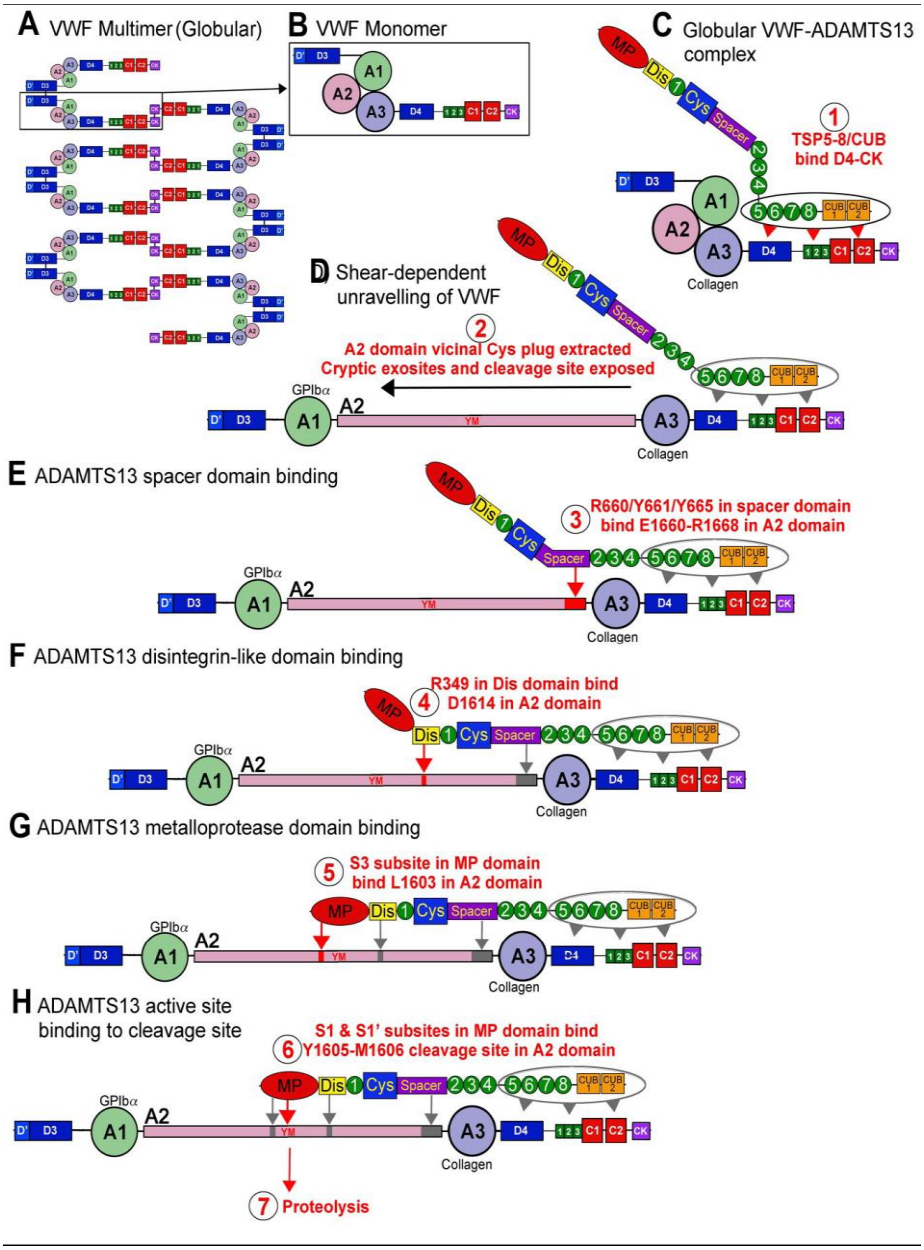


**Figure 1-7 ADAMTS13 cleavage of VWF**

Crawley *et al* proposed that the cleavage of ADAMTS13 occurs in 7 distinct steps, as follows: ADAMTS13 can reversibly bind to globular VWF (step 1). When shear stress induces the unfolding of VWF, additional exosite binding sites on VWF are revealed (step 2). The ADAMTS13 spacer domain recognises residues Glu1660-Arg1668 (step 3) revealed when the vicinal Cys disulphide bind plug is extracted from the hydrophobic core of the A2 domain. This increases the affinity of ADAMTS13 for VWF. An ADAMTS13 disintegrin-like exosite involving Arg349 recognises a complementary site of VWF compromising VWF1614 in a critical but low affinity interaction (step 4). Thereafter an essential contact is made between VWF Leu1603 and a complementary S3 subsite in ADAMTS13 involving Leu198, Leu232 and Leu274 (step 5). Together these interactions bring the Tyr1605-Met1606 scissile bond over the ADAMTS13 active site. This allows the P1 (1605) and P1' (1606) residues to engage their respective S1 and S1' subsite pockets involving Leu151/Val195 (S1) and Asp252-Pro256 (S1') respectively (step 6). Once cleavage has taken place (step 7) there is a reduction in the affinity between ADAMTS13 and VWF, enabling ADAMTS13 to recycle. Image from: (Crawley *et al*, 2011).

Deletion of residues Gln1624-Arg1641 within a VWF peptide substrate (GST-VWF73-His) did not change the rate of cleavage of VWF by various ADAMTS13 variants (Gao *et al*, 2008). These residues therefore do not appear to be essential for enzyme recognition, at least in the context of VWF73. As deletion of these amino acids reduced the distance between the scissile bond and auxiliary binding sires in the ADAMTS13 cysteine-rich and spacer domains, it suggests that ADAMTS13 does not require a fixed spatial relationship between the scissile bond and auxiliary exosite binding sites on the substrate. This ability to accommodate a large change in substrate structure suggests that ADAMTS13 is relatively flexible and can alter the relationships between the distal domains that bind VWF, which may be important for substrate recognition. Fluid shear stress *in vivo* may induce a spectrum of conformational changes in VWF. The flexibility of ADAMTS13 would enable it to bind to VWF in a variety of contexts and combinations (Gao *et al*, 2008).

The ADAMTS13 DTCS crystal structure supports this hypothesis. VWF73 is more than 200Å long at its maximum extension which is almost twice the distance between the catalytic site and the distal exosite-3 in the current ADAMTS13 model (Akiyama *et al*, 2009). ADAMTS13 appears to be able to accommodate by an induced fit mechanism, a partially unfolded VWF73 segment.

### 1.4.1 Factors affecting cleavage of VWF by ADAMTS13

ADAMTS13 is constitutively secreted as an active enzyme (Majerus *et al*, 2003) and no specific physiological inhibitor is known. Several factors have been shown to affect the interaction between ADAMTS13 and VWF (both positively and negatively). Some of these factors may only play a role under certain pathological circumstances.

The substrate VWF is an important determinant of ADAMTS13 cleavage. VWF glycans have been shown to both positively and negatively affect VWF cleavage by ADAMTS13. O-linked glycans, N-linked glycans and more specifically ABO blood group antigens and terminal sialic acid on VWF influence binding and ADAMTS13 proteolysis (Bowen & Collins, 2004;O'Donnell *et al*, 2005;McKinnon *et al*, 2008;McGrath *et al*, 2010;McGrath *et al*, 2013;Nowak *et al*, 2014) . In fact platelet

derived VWF has a different glycosylation profile rendering it more resistant to proteolysis by ADAMTS13 (McGrath *et al*, 2013).

Mutations within the VWF A2 domain (such as those present in patients with type 2A VWD) can increase the susceptibility of VWF to ADAMTS13 cleavage (Hassenpflug *et al*, 2006). Similarly, mutations within the VWF A1 domain (such as those present in patients with type 2B VWD), increase the affinity by which VWF can bind to GpIb, which in turn enhances ADAMTS13 cleavage (De Cristofaro *et al*, 2006;Rayes *et al*, 2007;Rayes *et al*, 2010). *In vitro* oxidation of Met1606 impairs ADAMTS13 mediated VWF proteolysis by reducing substrate binding affinity (Chen *et al*, 2010;Lancellotti *et al*, 2010;Pozzi *et al*, 2012)

Inorganic ions have been shown to affect both ADAMTS13 and VWF. $Ca^{2+}$ and $Zn^{2+}$ ions, bind to the metalloprotease domain of ADAMTS13, exerting both a functional and structural effect (Furlan *et al*, 1996;Anderson *et al*, 2006;Gardner *et al*, 2009;Pozzi *et al*, 2012). However concentrations of $Zn^{2+}$>3mM can inhibit ADAMTS13 activity (Anderson *et al*, 2006). A $Ca^{2+}$ binding site exists within the A2 domain of VWF stabilising it and impeding its unfolding, consequently protecting it from cleavage (Zhou *et al*, 2011). Chloride ions can bind to the VWF A1 domain, stabilising the folded conformation of VWF A1-A2-A3 domains (De Cristofaro *et al*, 2005;De Cristofaro *et al*, 2006). At concentrations exceeding physiological levels, $Mg^{2+}$ ions can enhance cleavage of ULVWF under flow (Dong *et al*, 2008).

Other proteins present within the circulation may also affect the interaction between ADAMTS13 and VWF. Factor H, a regulator of complement activation, was shown in one study to bind to VWF and enhance its proteolysis (Feng *et al*, 2013b). In contrast in another study it inhibited VWF proteolysis by ADAMTS13 (Rayes *et al*, 2014) and therefore its role needs to be further clarified.

Heparin has been shown to bind to the VWF A1 domain and enhance VWF proteolysis (Nishio *et al*, 2004). However heparin could indirectly inhibit proteolysis by binding to endothelial cells (Vomund & Majerus, 2009), as the binding of ADAMTS13 to endothelial cells, enhances VWF proteolysis.

Platelet GpIb binding to the VWF A1 domain promotes A2 domain unfolding by inducing conformational changes in the A1-A2 domains increasing the tensile force experienced by VWF multimers under shear stress (Nishio *et al*, 2004;Shim *et al*, 2008). P-selectin has been shown to interact with ULVWF strings on the surface of activated endothelium, potentially facilitating ADAMTS13 cleavage *in vitro* (Padilla *et al*, 2004). However it appears to have no effect in *vivo* in *P-selectin* knock-out (KO) mice (Chauhan *et al*, 2007).

The light chain of FVIII has been shown to accelerate VWF proteolysis by ADAMTS13 *in vitro* (Cao *et al*, 2008a;Cao *et al*, 2012;Skipwith *et al*, 2010). However patients with severe haemophilia A display normal cleavage of VWF by ADAMTS13 *in vivo* (Chen *et al*, 2013).

Thrombospondin-1 has been shown to protect VWF from proteolysis, competing with ADAMTS13 for binding to VWF A2 and A3 domains (Bonnefoy *et al*, 2006a;Wang *et al*, 2010). The binding of haemoglobin to the VWF A2 domain prevents the cleavage of VWF (Studt *et al*, 2005;Zhou *et al*, 2009a) and shigatoxin 1 and 2 have been shown to bind to VWF A1 and A2 domains and inhibit cleavage of ULVWF strings (Nolasco *et al*, 2005;Lo *et al*, 2013).

### 1.4.2 Disulphide bond reduction of VWF by ADAMTS13

In addition to cleaving VWF, ADAMTS13 has been shown to reduce disulphide bonds that may form between VWF multimers under high shear conditions. This is hypothesised to inhibit self-association of plasma VWF multimers into fibrillar structures which have an increased ability to bind to platelets (Yeh *et al*, 2010). Free thiols within ADAMTS13 which appear to be responsible for this disulphide bond reducing activity are mainly situated within the C-terminal TSP-1 and CUB domains (Yeh *et al*, 2010;Bao *et al*, 2014). The free thiols present in these distal domains inhibit thrombus formation under high shear stress *in vitro* and *in vivo*, independent of ADAMTS13 proteolytic activity (Bao *et al*, 2014). The concentrations of ADAMTS13 used in these experiments were higher than the physiological quantities normally present in the circulation and so its role under physiological and pathological conditions still remains to be determined.

### 1.4.3 VWF and ADAMTS13 cleavage

Coagulation (thrombin, plasmin, FXa) (Crawley *et al*, 2005) and leukocyte proteases (Ono *et al*, 2006;Hiura *et al*, 2010) have been shown to cleave ADAMTS13, but this may only occur under specific pathological conditions.

Proteases other than ADAMTS13 have been shown to cleave VWF such as leukocyte proteases (Buzza *et al*, 2008;Raife *et al*, 2009;Hollestelle *et al*, 2011) and plasmin (Tersteeg *et al*, 2014). Plasmin, generated by plasminogen activation via the urokinase plasminogen activator or the thrombolytic drug streptokinase, cleaves VWF and degrades platelet VWF complexes in the absence of ADAMTS13, both *in vitro* and *in vivo* (Tersteeg *et al*, 2014). Plasmin has been suggested as a potential alternative mechanism to cleave VWF when there is severe ADAMTS13 deficiency.

## 1.5 Thrombotic thrombocytopenic purpura

### 1.5.1 Signs and symptoms

The original description of TTP described a pentad of thrombocytopenia, microangiopathic haemolytic anemia (MAHA), neurological symptoms, renal impairment and fever (Moschcowitz, 1924). However TTP patients can present without the full pentad, up to 35% of patients do not have neurological signs at presentation and renal abnormalities and fever are not prominent features (Scully *et al*, 2012). TTP is characterised today by thrombocytopenia, MAHA, widespread microvascular thrombi and consequent clinical sequelae due to ischaemic end organ damage. The presence of thrombocytopenia and MAHA is not specific to TTP, but is characteristic of a number of other diseases known as thrombotic microangiopathies (TMAs). TMAs include haemolytic uraemia syndrome (HUS), disseminated intravascular coagulation, haemolysis, elevated liver enzymes and low platelet count (HELLP) and antiphospholipid syndrome. The pathophysiology of these diseases however differs from that of TTP, which is characterised generally by a deficiency of ADAMTS13. The diagnosis of TTP remains clinical but the measurement of ADAMTS13 activity within patient plasma can help to confirm the diagnosis and monitor the course of the disease.

Patients may present with TTP with thrombocytopenia; central neurological problems (confusion, headache, paresis, aphasia, dysarthria, visual problems, encephalopathy, and coma); jaundice; renal impairment (proteinuria, microhaematuria); cardiac involvement (chest pain, heart failure, and hypotension); gastrointestinal tract (abdominal pain) or fever (Scully *et al*, 2012). Neurological involvement was the most prevalent symptom (78% of cases) in one cohort of TTP patients with 10% of patients presenting with coma. Cardiac involvement accounted for 42% of presenting features (Scully *et al*, 2008).

Median platelet count in patients is normally 10-30x$10^9$/l; median haemoglobin levels on admission are typically 80-100g/l with schistocytes on the blood film. Patients have low haptoglobulin levels, raised reticulocyte counts due to haemolysis, along with a negative direct Coombs test and elevated levels of lactate dehydrogenase (LDH) (Scully *et al*, 2012).

### 1.5.2 Incidence

The annual incidence of TTP has been estimated as 2-6 per million of the population (Terrell *et al*, 2005;Scully *et al*, 2008;Miller *et al*, 2004). These estimates are based on studies from the USA and the UK. The incidence of TTP in the USA in one study was 3.8 (95% confidence interval [CI]:2.4-5.1) (Miller *et al*, 2004) and in another study the incidence of TTP-HUS patients with severe ADAMTS13 deficiency was 1.74 (95% CI: 2.4-5.1) (Terrell *et al*, 2005). The incidence of TTP has been estimated as 6 cases per million population per year in the UK (Scully *et al*, 2008).

The median age of acute TTP presentation is during the third to fourth decade, in one cohort of TTP patients 7% presented during childhood (<18 years) whereas 93% presented as adults (>18 years) (Moatti-Cohen *et al*, 2012). The disease typically affects women, with a ratio of approximately 2:1 (Moatti-Cohen *et al*, 2012). At least half of all acute episodes of TTP are in women of childbearing age (Scully *et al*, 2014).

### 1.5.3 Pathophysiology

Patients with thrombotic thrombocytopenia purpura (TTP) generally have a deficiency in the enzyme ADAMTS13. This deficiency leads to the accumulation of ULVWF multimers within the circulation. Larger molecular weight multimers of VWF have an increased affinity for platelet receptors such as glycoproteins Ib/V/IX and IIb/IIIa (Federici *et al*, 1989) and unfold more readily in response to shear stress (Zhang *et al*, 2009). ULVWF is therefore more effective than the largest normal forms of plasma VWF in supporting shear-induced platelet aggregation (Moake *et al*, 1986). The consequence of this is uncontrolled formation of platelet-rich thrombi in the microcirculation, which can lead to occlusion. These thrombi contain little fibrin but are abundant in VWF (Asada *et al*, 1985).

TTP occurs in two forms: congenital TTP, due to homozygous or compound heterozygous mutations in the *ADAMTS13* gene (Levy *et al*, 2001), or acquired TTP, often characterised by the development of anti-ADAMTS13 autoantibodies. Congenital TTP accounts for approximately 5% of TTP cases (Scully *et al*, 2008).

### 1.5.4 Triggers:infection

Patients with TTP can have single or recurrent TTP episodes. Infection is recognised to be a triggering causal factor for acute TTP as it can precipitate an episode in patients with other predisposing causal factors (such as low ADAMTS13 activity). In one cohort 41% of acute TTP episodes were associated with infection (Morgand *et al*, 2014). Some *in vitro* studies suggest that inflammatory cytokines may affect ADAMTS13 and VWF levels and also their interaction. The release of VWF from HUVECS was shown to be dose dependently increased in the presence of the inflammatory cytokines TNF-α and IL-8 (Bernardo *et al*, 2004). However another study did not find the same effect of TNFα (Cao *et al*, 2008b).

The cytokines IFN-γ, IL-4 and TNF-α reduced *ADAMTS13* mRNA and proteolytic activity in hepatic stellate cells and HUVECs, in a dose dependent manner. Incubation of IFN-γ, IL-4 and TNF-α with purified recombinant ADAMTS13 however did not inhibit its proteolytic activity (Cao *et al*, 2008b). In contrast the effect of TNF-α was not confirmed in another study (Claus *et al*, 2005). Additionally

cleavage of endothelial VWF by ADAMTS13 in the presence of IL-6 under conditions of flow (but not under static conditions) has been shown to be inhibited (Bernardo *et al*, 2004), suggesting that some cytokines can affect ADAMTS13 mediated cleavage. Together these *in vitro* studies suggest that inflammation associated with infection may affect normal levels of VWF and/or ADAMTS13 and their interaction, precipitating a TTP episode.

### 1.5.5 Triggers: Pregancy

Pregnancy also appears to be a triggering causal factor for the onset of TTP in a number of patients. Pregnancy associated TTP is reported to represent 5-10% of all adult TTP cases (George *et al*, 2008;Scully *et al*, 2008;Fujimura & Matsumoto, 2010;Moatti-Cohen *et al*, 2012) and is estimated to occur in 1 in 198,000 pregnancies (Moatti-Cohen *et al*, 2012).

Patients present with TTP primarily from the second trimester to the postpartum period (Moatti-Cohen *et al*, 2012;Scully *et al*, 2014) but fetal loss/morbidity appears to be highest in the first (Moatti-Cohen *et al*, 2012) and second trimester (Scully *et al*, 2014) of pregnancy. If pregnant TTP patients are untreated it can lead to significant morbidity and mortality for the child (Fujimura *et al*, 2009;Moatti-Cohen *et al*, 2012;Scully *et al*, 2014).

In normal pregnancies plasma VWF increases steadily during gestation with the appearance of ULVWF (Stirling *et al*, 1984). Treatment of endothelial cells with oestrogens (Harrison & McKee, 1984) has been shown to increase VWF synthesis. Healthy, pregnant women have lower ADAMTS13 activity compared to women who are not pregnant (Sanchez-Luceros *et al*, 2004;Mannucci *et al*, 2001). ADAMTS13 may be consumed under these conditions due to the high levels of VWF released during pregnancy, precipitating a TTP episode.

### 1.5.6 Treatment

Patients with TTP are treated with plasma exchange or infusion which acts as a source of ADAMTS13 for the patients. In patients with acquired TTP plasma exchange also removes antibodies which may bind and inhibit ADAMTS13. Patients

with acquired TTP may also be treated with immunosuppressive drugs (George, 2010). ADAMTS13 has a half-life of two to three days (Furlan *et al*, 1999), however the regular infusion of plasma approximately every two to three weeks appears to be sufficient in most congenital patients to prevent episodes (Kinoshita *et al*, 2001).

## 1.6 Congenital TTP

Congenital TTP is suspected in patients with TTP and an ADAMTS13 activity level below 5% of normal, in the absence of anti-ADAMTS13 antibodies. These patients can therefore also be described as having a congenital ADAMTS13 deficiency. There are over 100 congenital TTP patients worldwide (Scully *et al*, 2012). Although congenital TTP patients have persistently low levels of ADAMTS13 in the circulation some patients may be asymptomatic until childhood or adulthood. Based on information gathered from reported congenital TTP patients in the literature, 48% developed TTP in the neonatal period, 31% during childhood (2 months to 18 years) and 21% during adulthood (Lotta *et al*, 2010).

Neonates typically have severe neonatal jaundice and blood examinations show schistocytes together with red cell anisocytosis (Scully *et al*, 2006). Patients presenting during the neonatal period or childhood typically have thrombocytopenia, MAHA, jaundice and elevated LDH, although some children may have isolated thrombocytopenia (Scully *et al*, 2012).

Patients may also present during adulthood. Pregnancy is commonly associated with disease onset (Fujimura *et al*, 2009;Moatti-Cohen *et al*, 2012;Scully *et al*, 2014). Rarely patients may not develop symptoms until their 50s or 60s (Fujimura *et al*, 2011). Asymptomatic male cases have been reported usually because they have affected relatives (Bestetti *et al*, 2003;Garagiola *et al*, 2008;Palla *et al*, 2009).

The p.R1060W mutation is commonly found in Caucasian patients who first present with TTP during pregnancy. This mutation was present in 73% of patients in one cohort (Scully *et al*, 2014) and 80% of patients in another cohort (Moatti-Cohen *et al*, 2012). However this mutation has not been identified in Japanese pregnancy onset patients (Fujimura *et al*, 2009). Congenital TTP presents more frequently than

acquired TTP during pregnancy. In one cohort 66% of women presenting with TTP for the first time had late onset TTP (Scully *et al*, 2014).

The clinical severity of disease episodes varies between patients. Some have asymptomatic episodes of thrombocytopenia and anemia, whereas others have multi-organ failure (Schneppenheim *et al*, 2003).

### 1.6.1 *ADAMTS13* mutations

Genetic defects within *ADAMTS13* were first identified in 2001 (Levy *et al*, 2001) in patients with familial, congenital TTP. These genetic defects were inherited in an autosomal recessive manner. Since then over 140 mutations have been identified within the *ADAMTS13* gene in patients with congenital TTP (Hing *et al*, 2013;Feys *et al*, 2009b;Klukowska *et al*, 2010;He *et al*, 2010;Deal *et al*, 2012;Rossio *et al*, 2013;Lotta *et al*, 2012;Ma *et al*, 2006;Scully *et al*, 2014) (Table S 6). Patients have homozygous or compound heterozygous mutations in the *ADAMTS13* gene. These mutations are distributed throughout the gene. The majority of mutations are missense mutations, causing either secretion and/or catalytic activity defects of the ADAMTS13 protein (Lotta *et al*, 2010).

### 1.6.2 *ADAMTS13* polymorphisms

A number of non-synonymous coding polymorphisms have been identified within the *ADAMTS13* gene. The effect of these polymorphisms on the secretion and activity of ADAMTS13 has been studied for some of these polymorphisms (p.R7W, p.Q448E, p.P475S, p.P618A, p.A732V, p.A900V, p.A1033T) (Kokame *et al*, 2002;Plaimauer *et al*, 2006;Tao *et al*, 2006;Rurali *et al*, 2013;Edwards *et al*, 2012). Notably two of the polymorphisms, p.P475S and p.P618A lead to significantly reduced ADAMTS13 activity *in vitro* compared to WT (Kokame *et al*, 2002;Plaimauer *et al*, 2006). Certain polymorphisms are more common in certain ethnic groups for example the p.P475S polymorphism is common in the Japanese population but not Caucasians (Kokame *et al*, 2002;Levy *et al*, 2001).

### 1.6.3 Mouse models of congenital TTP

*ADAMTS13* KO mice have been produced to replicate the severe deficiency of ADAMTS13 found in patients with congenital TTP. These models have contributed to our understanding of the disease, demonstrating ADAMTS13 cleavage of VWF *in vivo*. In mice ADAMTS13 deficiency is necessary but not sufficient for the development of TTP.

*ADAMTS13* KO mice do not spontaneously develop TTP (Motto *et al*, 2005;Banno *et al*, 2006). Pregnancy, a TTP trigger in humans, does not induce the disease in *ADAMTS13* KO mice (Motto *et al*, 2005;Banno *et al*, 2006). In *ADAMTS13* KO mice no schistocytes were found in WT or KO mice (Motto *et al*, 2005;Banno *et al*, 2006), there was no thrombocytopenia and histopathological analysis showed that WT and KO mouse tissue was indistinguishable (Motto *et al*, 2005). There were no significant differences in blood cell counts, plasma haptoglobin levels and platelet aggregation in response to collagen and botrocetin (Banno *et al*, 2006). There was a difference in multimeric pattern with the presence of ULVWF in the KO but not the WT mice in Banno's model, but ULVWF was present in both WT and KO mice in Motto's model. In Motto's model mice expressed the truncated version of ADAMTS13 (*ADAMTS13*$^{S/S}$) whereas in Banno's model they expressed full length ADAMTS13 (*ADAMTS13*$^{L/L}$).

Although *ADAMTS13* KO mice do not spontaneously develop TTP they are in a prothrombotic state (Motto *et al*, 2005;Banno *et al*, 2006). After perfusion of the calcium ionophore A23187 (to stimulate ULVWF release), *ADAMTS13* KO mice showed significantly prolonged adhesion of platelets compared to WT mice (Motto *et al*, 2005). After 3.5 minutes of perfusion of blood from WT and KO mice over a collagen coated surface in a parallel flow chamber, the thrombus grew rapidly in *ADAMTS13* KO mice, which was significantly different to WT mice (Banno *et al*, 2006). When mice were challenged with collagen, mortality was not different between WT and KO mice but platelet counts were significantly lower in KO mice compared to WT mice (Banno *et al*, 2006). Furthermore when tested *in vivo* thrombosis models, *ADAMTS13* KO mice showed accelerated arterial thrombosis

formation leading to faster occlusion of injured blood vessels (Chauhan *et al*, 2006;Banno *et al*, 2009;Laje *et al*, 2009;Niiya *et al*, 2009).

In one of the *ADAMTS13* KO models, mice (on a C57BL/6J background) were backcrossed with CASA/Rk mice (Motto *et al*, 2005), a strain which has approximately 5 to 10 fold higher VWF levels compared to the C57BL/6J mouse strain used (Mohlke *et al*, 1999). Mean plasma levels increased 40 to 50% after this backcross and multimeric VWF was different between WT and KO mice. There was a significant decrease in platelet count in KO mice compared to WT mice with 21% of the KO mice severely thrombocytopenic at baseline. The KO mice exhibited significantly decreased survival compared to WT mice. In some of the *ADAMTS13* KO mice there was spontaneous development of severe microangiopathic changes in the peripheral blood along with widespread VWF rich and fibrin-poor hyaline thrombi in the small vessels of multiple organs. However the mice still did not develop TTP.

A TTP like disease however developed in some mice, on a specific genetic background after challenge with shigatoxin (Motto *et al*, 2005). Challenge of C57BL/6J WT and KO mice with shigatoxin led to no consistent change in red blood cell or platelet count in both mice, with similar mortality in both groups. However differences were observed between *ADAMTS13* WT and KO mice on the CASA/Rk background, with significant difference in survival and platelet cont. Also some of the *ADAMTS13* KO mice developed TTP like symptoms (Motto *et al*, 2005). However there was no correlation between elevated plasma VWF levels and mortality, baseline platelet count or thrombocytopenia. The requirement for VWF in this model was experimentally confirmed by showing that CASA/Rk mice deficient in both VWF and ADAMTS13 were not susceptible to shigatoxin induced TTP (Chauhan *et al*, 2008).

In another *ADAMTS13* KO model, TTP could be induced in mice after they were challenged with recombinant VWF containing ULVWF (Schiviz *et al*, 2012). Recombinant human ADAMTS13 protected the mice from developing TTP. Recently a new mouse model of TTP has been developed, with the development of TTP in mice expressing a VWF mutant resistant to ADAMTS13 cleavage (Morioka

*et al*, 2014). The authors found lower molecular weight forms of VWF present in the circulation of these mice, suggesting that other proteases may have cleaved VWF in these mice.

*ADAMTS13* KO mice therefore do not spontaneously develop TTP but are in a prothrombotic state. They require an additional trigger for disease development, suggesting that other environmental and genetic factors are important in the development of TTP. This resembles somewhat the situation in humans as some patients only develop TTP after a trigger such as infection of pregnancy but does not explain apparent spontaneous TTP development.

Furthermore *ADAMTS13* KO mice do not develop TTP during pregnancy which is a well-known trigger for TTP development in humans. The hameodynamics formed by anatomical differences in the vasculature network of mice and humans significantly differ and so there are limitations in using mice as a model. Although mouse models have aided our understanding they do not fully reflect the disease as seen in humans.

### 1.6.4 Residual ADAMTS13 activity

Despite having severe ADAMTS13 deficiency the clinical presentation of patients with congenital TTP is highly variable. Patients vary with respect to the age of disease onset, number of relapses and need for plasma exchange/infusion. Some may initially present with TTP during the neonatal period or during infancy (Assink *et al*, 2003) whilst others may present as adults (Camilleri *et al*, 2008;Tao *et al*, 2006). Some patients require regular prophylactic plasma infusions whereas others rarely require plasma infusion (Fujimura *et al*, 2011). The onset of TTP in some patients may be spontaneous with no identifiable trigger, whilst in other cases it may be the result of an environmental trigger such as infection or pregnancy (Donadelli *et al*, 2006;Fujimura *et al*, 2011;Palla *et al*, 2009).

Evidence suggests that there may be a relationship between *ADAMTS13* genotype and phenotype, with the particular *ADAMTS13* mutations present in congenital TTP patients accounting for some of the heterogeneity observed in patients with congenital TTP. It has been observed that the age of disease onset is similar between both siblings and unrelated patients with the same *ADAMTS13* genotype (Figure

1-8). The p.R1060W mutation has been observed in a relatively large number of patients and has been mainly identified in patients with pregnancy onset TTP (Moatti-Cohen *et al*, 2012;Scully *et al*, 2014). The p.E1382RfsX6 (Schneppenheim *et al*, 2006) and p.R692C (Levy *et al*, 2001;Snider *et al*, 2004;Kim *et al*, 2014) mutation have been predominantly found in patients that present with TTP during childhood.

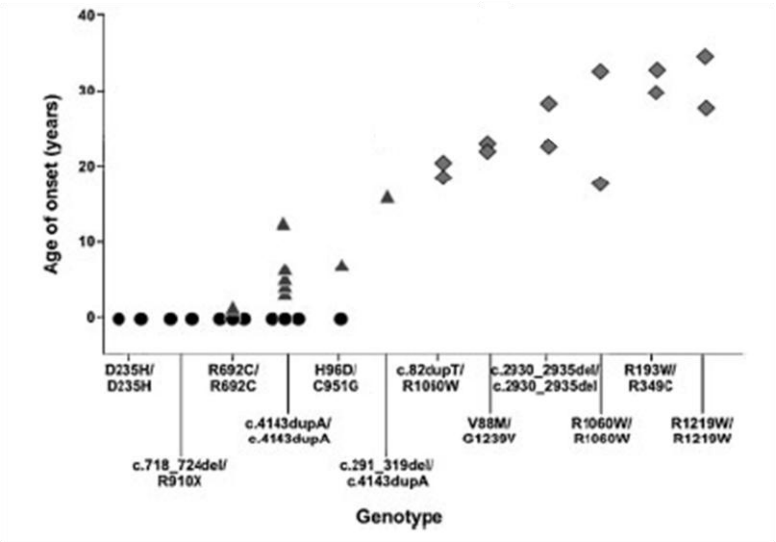


**Figure 1-8 Relationship between *ADAMTS13* genotype and age of disease phenotype**

Circles represent patients with neonatal disease onset, triangles childhood onset (>2 months to 18 years), diamond patients with adult onset. Image adapted from (Lotta *et al*, 2010).

Residual ADAMTS13 activity currently undetectable by routine ADAMTS13 assays has been measured using SELDI-TOF (surface-enhanced laser desorption/ionization time-of-flight) to investigate the relationship between residual ADAMTS13 activity and disease phenotype (Lotta *et al*, 2012). ADAMTS13 activity >0.5% of PNP was measured in 90% of patients studied (26/29). Median plasma activity was 3.08% range <0.5%-6.77%.

Lower levels of ADAMTS13 activity were associated with an earlier age at first TTP episode requiring plasma infusion. Lower levels were associated with a higher annual incidence of TTP episodes and with the prescription of fresh frozen plasma (FFP) prophylaxis (Lotta *et al*, 2012). ADAMTS13 activity <2.74% appeared to discriminate between patients who had a first episode requiring FFP under 18 and

prescription of FFP. The relationship between *ADAMTS13* genotypes (that occurred more than once in the literature) and residual ADAMTS13 activity and age at first TTP episode requiring FFP is shown in Figure 1-9. Siblings with the same genotype and unrelated individuals (with the p.R1060W mutation) had a similar age of disease onset.

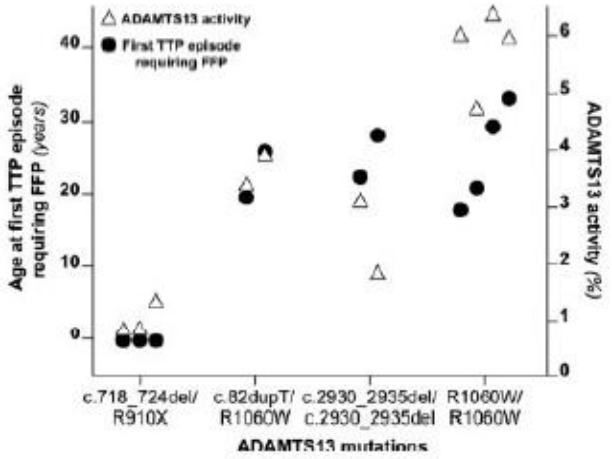


**Figure 1-9 Relationship between *ADAMTS13* genotype and residual ADAMTS13 activity and age at first episode requiring FFP**

Image from: (Lotta *et al*, 2012).

Patients with homozygous mutations in the N-terminal region (n=4) displayed lower residual activity compared to those with homozygous mutations in the C-terminal region (n=8) (Figure 1-10).

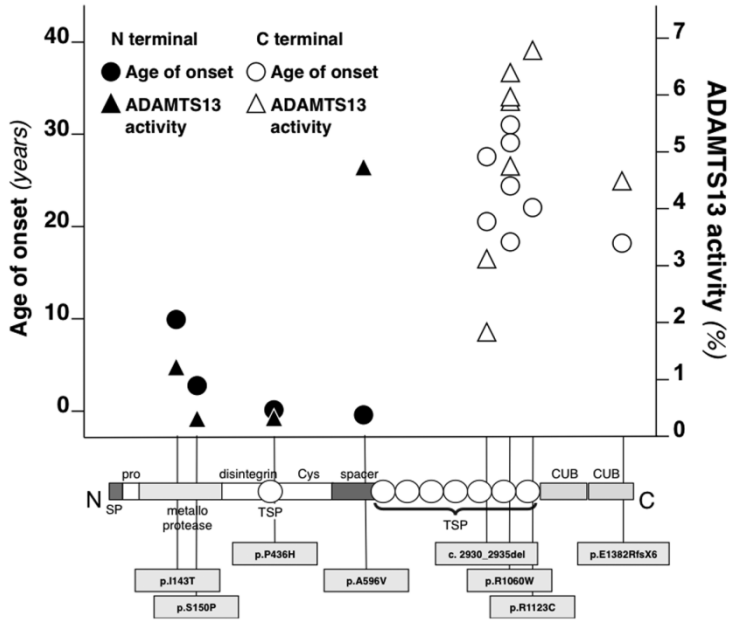


**Figure 1-10 Residual ADAMTS13 activity in patients homozygous for *ADAMTS13* mutations**

Image from: (Lotta *et al*, 2012).

There were some exceptions with some patients having relatively high residual activity with an early age of disease at first episode requiring FFP or frequent recurrences demonstrating the importance of other factors (genetic and environmental) (Lotta *et al*, 2012). These studies were performed in a small number, often related individuals, so although they suggest a relationship may exist it would need to be confirmed in a larger number of unrelated patients, however this is difficult because of the rarity of the disease.

Environmental triggers (e.g. infections) and associated physiological or pathological conditions (e.g. pregnancy and autoimmune disorders) are hypothesised to induce an increase in VWF antigen levels which exceed the levels which residual active ADAMTS13 enzyme can normally degrade, leading to the precipitation of an acute TTP episode.

## 1.7 Acquired TTP

Acquired TTP patients may have TTP secondary to other diseases such as HIV, infection, drugs or transplantation. However the majority of patients have acquired acute idiopathic TTP. It is not associated with a specific underlying precipitating factor and antibodies to ADAMTS13 can be detected. In up to 90% of cases these are IgG (Rieger *et al*, 2005) although IgM (Scheiflinger *et al*, 2003) and IgA (Ferrari *et al*, 2007) antibodies have also been described. Antibodies which inhibit the activity of ADAMTS13 (Tsai & Lian, 1998;Peyvandi *et al*, 2004;Ferrari *et al*, 2007) or possibly increase its clearance (Scheiflinger *et al*, 2003) have been identified in patients with idiopathic acquired TTP.

Not all acquired TTP patients have an acquired ADAMTS13 deficiency, with some patients having normal or moderately reduced ADAMTS13 activity (Bettoni *et al*, 2012;Mori *et al*, 2002;Bohm *et al*, 2005). The incidence of acquired TTP-HUS in the US has been estimated as 4.46 cases per million of the population per year (95% CI:3.43-5.50) (Terrell *et al*, 2005).

The ADAMTS13 cysteine-rich and spacer domains have been shown to be the primary autoimmune target in patients with TTP (Soejima *et al*, 2003;Klaus *et al*, 2004;Luken *et al*, 2005). Residues Pro660, Tyr661 and Tyr665 in the spacer domain represent a core binding site for antibodies (Pos *et al*, 2010). Antibodies directed towards other regions of ADAMTS13 such as the propeptide, TSP-1, TSP-1:2→8 and CUB have also been detected less frequently (Klaus *et al*, 2004;Zheng *et al*, 2010).

Early studies performed before the identification of ADAMTS13 demonstrated the presence of anti-CD36 antibodies in patients with acquired TTP (Tandon *et al*, 1994;Schultz *et al*, 1998). This has not been investigated further since the identification of ADAMTS13, but is an interesting finding given that CD36 may be the binding site for ADAMTS13 on endothelial cells (Davis *et al*, 2009).

There have been no studies to analyse whether *ADAMTS13* genetic defects could contribute to anti-ADAMTS13 antibody formation in patients with acquired TTP. By

definition patients with congenital TTP do not have anti-ADAMTS13 antibodies so the *ADAMTS13* gene is normally only analysed in patients with no anti-ADAMTS13 autoantibodies. Three patients heterozygous for the p.R1060W mutation were also reported to have detectable antibodies to ADAMTS13 (Camilleri *et al*, 2008). However this may have been coincidental as the p.R1060W mutation has been detected in a number of congenital TTP patients with no anti-ADAMTS13 antibodies, both in a heterozygous and homozygous form (Camilleri *et al*, 2012;Moatti-Cohen *et al*, 2012;Scully *et al*, 2014). The antibodies detected may have been transient non-specific or low titre antibodies.

### 1.7.1 Baboon models of acquired TTP

In baboons, four days of ADAMTS13 functional inhibition using a mouse monoclonal antibody directed towards the metalloprotease domain was sufficient to induce a TTP-like disease, in the absence of inciting triggers (Feys *et al*, 2010). The baboons had severe thrombocytopenia, MAHA, a rise in serum LDH levels and the presence of platelet and VWF-rich thrombi in the kidneys, heart, brain and spleen, thus providing a model for acquired TTP.

The situation in baboons appears to be different to *ADAMTS13* KO mice which do not spontaneously develop TTP. The authors proposed that the discrepancies between this model and mouse models may be due to differences in the physiology of mice and primates. This model mimicked the early stages of the disease and demonstrated the importance of ADAMTS13 in disease development.

## 1.8 New therapeutic options for TTP

New therapeutic options are currently being explored for the treatment of TTP. Plasma exchange has significantly improved the outcome of patients with TTP. Death in TTP patients has been dramatically reduced from 90% to approximately 10-20% (Scully *et al*, 2012). Plasma exchange/infusion however does have its disadvantages. It is time consuming and expensive, citrate reactions and allergic reactions can occur and there is also the risk of venous thromboembolism, which occurred in 6.5% of patients in one cohort (McGuckin *et al*, 2014).

Recombinant ADAMTS13 is currently in development for use as an alternative to plasma exchange/infusion in patients (Plaimauer & Scheiflinger, 2004). It could be used to treat congenital TTP patients who have little or no functional ADAMTS13. In an *ADAMTS13* KO model of TTP administration of ADAMTS13 prevented the onset of TTP symptoms (Schiviz *et al*, 2012). In acquired TTP inhibitory antibodies may inhibit the infused recombinant ADAMTS13. An *in vitro* study showed that reasonable doses of recombinant ADAMTS13 could overcome neutralising inhibitors and restore ADAMTS13 activity, and so its use in patients with acquired TTP may also be beneficial (Plaimauer *et al*, 2011).

The efficacy and safety of the nanobody ALX-0081 as adjunctive therapy to plasma exchange in patients with acquired TTP is now being assessed in the TITAN trial, which is a Phase II, single-blind, randomised, placebo-controlled trial (Holz, 2012). This nanobody is directed towards the A1 domain of VWF and specifically inhibits its interaction with the GPIb-IX-V platelet receptor glycoprotein, thereby preventing VWF-mediated platelet aggregation. A humanised nanobody (ALX-0681) targeting the A1 domain of VWF has been tested in the baboon TTP model (Callewaert *et al*, 2012). This nanobody targets the same region as ALX-0081, but its mode of administration is slightly different. Prophylactic administration of ALX-0681 not only prevented the rapid onset of thrombocytopenia after ADAMTS13 inhibition but prevented the appearance of schistocytes, intravascular haemolysis and an increase in LDH levels. Administration of this drug soon after the onset of TTP was not able to dissolve already formed thrombi within the vessels of various organs but prevented the progressive formation of aggregates. This drug when administered to humans is anticipated to reduce the time to normalisation of platelet count and the number of plasma exchange sessions to achieve remission. Importantly there was no indication of relevant bleeding or signs of intracranial bleeding or internal organ bleeding (Callewaert *et al*, 2012).

A similar drug to ALX-0081 (ARC1779) has been tested previously in a clinical trial which was unfortunately prematurely terminated. ARC1779 is a nucleic acid macromolecule (aptamer) targeting the A1 domain of VWF preventing the interaction between VWF and the GPIb-IX-V receptor. Prior to the premature termination of the clinical trial, nine patients were treated with either ARC1779 or

placebo as an adjunct to plasma exchange (two placebo, seven ARC1779). Clinical response was achieved in four of seven subjects in the ARC1779 treated subjects and in none of the placebo treated patients during the two week infusion protocol. The number of patients included in this trial was too small to enable conclusions to be drawn regarding the efficacy of this drug. However the drug did not appear to lead to bleeding and sustained suppression of VWF activity was achieved during the two week treatment period (Cataland *et al*, 2012).

Rituximab is a chimeric monoclonal antibody that targets CD20 on the surface of B-lymphocytes. It has been successfully used in the treatment of some TTP patient's refractory to immunosuppressive drugs (Sallah *et al*, 2004;Ahmad *et al*, 2004;Fakhouri *et al*, 2005;Scully *et al*, 2007). It may ameliorate the symptoms of TTP by eradicating specific B-cell clones responsible for the production of ADAMTS13 autoantibodies (Stasi, 2010). It has not been tested in a randomised Phase III trial but has been tested in a phase II trial (Scully *et al*, 2011). In Caucasian patients treatment with rituximab led to a reduction in the number of plasma exchanges required to achieve remission and an overall reduction in inpatient days (excluding those patients in intensive care). There were no serious side effects reported with this drug.

N-acetylcysteine (NAC) is an FDA approved drug which is also approved for use in pregnancy (George *et al*, 2014). It is commonly used to reduce the viscosity of mucous secretion in respiratory disorders. NAC's free sulfhydryl group allows it to decrease the molecular size of mucin and therefore viscosity by reducing the disulphide bonds that produce mucin polymers (Von Langenbeck, 1966). NAC has been shown to cleave VWF *in vitro* and *in vivo* in mice (Chen *et al*, 2011). NAC reduced multimers under static conditions and endothelial VWF strings under conditions of flow. It reduced disulphide bonds within the A1 domain of VWF, inhibited platelet agglutination in a concentration dependent manner in the presence of ristocetin and it inhibited collagen binding in a concentration dependent manner. NAC also reduced circulating VWF multimers *in vivo* in mice and reduced thrombi formation in WT and *ADAMTS13* KO mice treated with NAC. There was no difference in bleeding time between the mice treated with NAC compared to

controls. NAC also prevented *in vitro* platelet aggregation in response to ADP and collagen.

A recent case report has suggested it may potentially be a useful therapeutic option (Li *et al*, 2014). A patient with acquired TTP who did not respond to corticosteroids or rituximab, was treated with success with NAC in conjunction with plasma exchange, corticosteroids and rituximab (Li *et al*, 2014). The patient's platelet count began to improve two to three days after NAC treatment (within six days or rituximab treatment). The Puget Sound blood centre has begun a pilot study of NAC in patients with suspected TTP (NCT01808521, URL: https://clinicaltrials.gov/, accessed 17th June 2014), to determine if changes in VWF function can be detected in humans receiving NAC and if NAC is tolerated when administered between plasma exchange procedures.

Substitution of four to five residues in exosite 3 of ADAMTS13 has been shown to generate ADAMTS13 variants (M4:R660K/F592Y/R568K/Y661F and M5: R660K/F592Y/R568K/Y661F/Y665F) with increased specific activity to FRETS-VWF73 and multimeric VWF. Levels were increased 4- to 5- fold and 10- to 12- fold respectively (Jian *et al*, 2012). These variants were more resistant than WT ADAMTS13 to inhibition by anti-ADAMTS13 antibodies from a number of patients with acquired TTP. This variant has not been tested in animal models but may be a promising therapeutic option in the future to treat patients with acquired TTP.

Gene therapy has been investigated in *ADAMTS13* KO mice as a potential therapy for patients with congenital TTP. Systemic administration of adenovirus encoding *ADAMTS13* (Trionfini *et al*, 2009;Jin *et al*, 2013) and *in utero* lentiviral transfer of *ADAMTS13* (Niiya *et al*, 2009) have been successfully performed in *ADAMTS13* KO mice. Additionally autologous transplantation of haematopoietic progenitor cells, transduced *ex vivo* with a lentiviral vector encoding *ADAMTS13* (Laje *et al*, 2009) has led to ADAMTS13 expression in *ADAMTS13* KO mice. In these models functional ADAMTS13 was effectively expressed in the mice. Furthermore gene transfer of *ADAMTS13* was shown to prevent the development of shigatoxin induced TTP in mice (Jin *et al*, 2013). However the use of gene therapy to treat TTP does not appear to be a possible therapeutic option in the near future.

## 1.9 ADAMTS13 deficiency in the setting of other diseases

Some case control studies have found an association between low ADAMTS13 antigen and risk of myocardial infarction (MI) (Bongers *et al*, 2009;Crawley *et al*, 2008;Andersson *et al*, 2012) and ischaemic stroke (IS) (Lambers *et al*, 2013;Andersson *et al*, 2012). However it remains to be determined whether the reduced levels of ADAMTS13 measured in these studies was a cause or consequence of the pathogenesis of these diseases. With this is mind, some groups have investigated the effect of ADAMTS13 deficiency *in vivo* in mouse models of these diseases to assess the contribution of ADAMTS13 to disease pathogenesis.

In ischaemia/reperfusion models of MI and IS the absence of ADAMTS13 led to an increase in the size of the infarct (De Meyer *et al*, 2012;Doi *et al*, 2012;Gandhi *et al*, 2012b;Khan *et al*, 2012;Fujioka *et al*, 2010;Fujioka *et al*, 2012;Zhao *et al*, 2009) and an increased number of inflammatory cells entering the site (Fujioka *et al*, 2010;Khan *et al*, 2012;Gandhi *et al*, 2012b). Addition of recombinant ADAMTS13 to WT or KO mice reduced the infarct and number of inflammatory cells at the site (De Meyer *et al*, 2012;Doi *et al*, 2012;Zhao *et al*, 2009). The anti-thrombotic and anti-inflammatory effects appeared to be mediated through VWF as *VWF* KO and *VWF/ADAMTS13* double KO mice had smaller infarcts and a decreased number of inflammatory cells (Zhao *et al*, 2009;Kleinschnitz *et al*, 2009;Gandhi *et al*, 2012b;Khan *et al*, 2012).

ADAMTS13 deficiency in *ApoE* KO, atherosclerosis prone mice led to the formation of larger atherosclerotic plaques containing more inflammatory cells (Gandhi *et al*, 2012a;Jin *et al*, 2012). These effects appeared to be mediated through VWF (Gandhi *et al*, 2014) as *VWF* KO and *VWF/ADAMTS13* KO mice appeared to have smaller lesion sizes and a reduced number of inflammatory cells.

Together these mouse models suggest that a severe deficiency in ADAMTS13 may contribute to the pathogenesis of diseases such as MI and IS by potentially preventing the thrombotic occlusion of the microvasculature during the post-ischaemic reperfusion stage (Doi *et al*, 2012). Ischaemia is a rapid inducer of Weibel-Palade body release thus making the infarct area highly thrombogenic

(Pinsky *et al*, 1996). ADAMTS13 has been shown to have anti-inflammatory properties (Chauhan *et al*, 2008) and its deficiency leads to a worse disease phenotype in a mouse model of atherosclerosis. These results have implications for patients with congenital TTP, who may have a worse prognosis after development of these diseases.

## 1.10 *ADAMTS13* genetic variation in diseases other than TTP

Mutations or polymorphisms within *ADAMTS13* have been described for some diseases such as HUS (Feng *et al*, 2013a), venous thrombosis (Lotta *et al*, 2013), coronary heart disease (Schettert *et al*, 2010), IS (Hanson *et al*, 2009), response to ACE inhibitors (Rurali *et al*, 2013) and malaria (Kraisin *et al*, 2014). However many of the studies were performed in a small number of patients and the effect of some of these polymorphisms or mutations *in vivo* still remains to be determined.

## 1.11 Aims of thesis

I hypothesise that the clinical and laboratory phenotype of patients with congenital TTP will relate to their *ADAMTS13* mutations and the effect that these mutations have on ADAMTS13 expression and activity *in vitro*. The aim of this study was to express *ADAMTS13* mutations identified in a homozygous form in congenital TTP patients to assess their effect on the secretion and activity of ADAMTS13. For the mutations that severely affected the secretion of ADAMTS13 I aimed to investigate the localisation of these mutations within the cell. For those mutants that were secreted I aimed to analyse the catalytic activity of the secreted protein. Finally for those mutations which were predicted to affect splicing of the *ADAMTS13* gene, I aimed to create a mini gene to analyse this *in vitro*.

# Chapter 2 Materials and methods

## 2.1 *In silico* analysis of *ADAMTS13* missense mutations

Human ADAMTS13 was aligned with ADAMTS13 orthologs using clustalW2 multiple sequence alignment tool (URL: http://www.ebi.ac.uk/Tools/msa/clustalw2/; accessed 17th June 2014). The amino acid sequence of *Homo Sapiens* ADAMTS13 was aligned with the amino acid sequence of ADAMTS13 from the following species: *Taeriopygia guttata* (zebra finch), *Gallus gallus* (chicken), *Bos taurus* (cattle), *Ovis aries* (sheep), *Gorilla gorilla gorilla* (western lowland gorilla), *Pan troglodytes* (chimpanzee), *Nomascus leucogenys* (northern white cheeked gibbon), *Pango abelli* (Sumatran orangutan), *Papio anubis* (olive baboon), *Calithrix jacchus* (white tufted ear marmoset), *Saimiri boliviensis boliviensis* (Bolivian squirrel monkey), *Otolemur garretti* (small-eared galago), *Mus musculus* (house mouse), *Cricetulus griseus* (Chinese hamster), *Cavia porcellus* (domestic guinea pig), *Canis lupus familiaris* (domestic dog), *Felis catus* (domestic cat), *Ailuropoda melanoleuca* (giant panda), *Equus caballus* (domestic horse), *Sarophilus harrisii* (Tasmanian devil) and *Danio Rerio* (zebra fish). Sequences within the region affected by mutations or non-synonymous polymorphisms in the patients studied are only shown. The affected amino acids are highlighted in yellow.

Similarly the ADAMTS13 amino acid sequence of *Homo sapiens* was aligned with the ADAMTS13 sequence of paralogs using the clustalW2 multiple sequence alignment tool. ADAMTS13 was aligned with the sequences of ADAMTS1, 2, 3, 4, 5, 6, 7, 8, 9, 10, 12, 13, 14, 15, 16, 17, 18, 19, 20 (all from *Homo Sapiens*). The GI numbers of all sequences are shown in the appendix (Table S 1).

SNPs3D (URL: http://www.snps3d.org/; accessed 17th June 2014), SIFT human SNPs tool (URL: http://sift.jcvi.org/www/SIFT_chr_coords_submit.html; accessed 17th June 2014) and Polyphen-2 (URL: http://genetics.bwh.harvard.edu/pph2/; accessed 17th June 2014) were used to predict the functional effect of mutations and non-synonymous polymorphisms on *ADAMTS13*.

## 2.2 Creation of *ADAMTS13* missense mutations

### 2.2.1 Sequencing *ADAMTS13* cDNA

*ADAMTS13* missense mutations and polymorphisms were introduced into a pcDNA 3.1/V5-His TOPO ® vector (Life technologies) containing the complete *ADAMTS13* cDNA sequence (kindly provided by Dr. F. Scheiflinger, Baxter Bioscience). ADAMTS13 was therefore expressed with a C-terminal V5 epitope and polyhistidine tag (6xHis tag). The entire *ADAMTS13* cDNA within the vector was first sequenced to ensure there were no unexpected deletions or mutations within its sequence. The primers used are shown in the appendix (Table S 2).

Sequencing was carried out using the principle of dye-terminator DNA sequencing, originally described by Sanger (Sanger *et al*, 1977). This was set up with the big dye terminator v3.1 cycle sequencing kit (Life technologies) using 3.2μM of primer and 1μg of plasmid DNA. The cycle sequencing reaction was set up as follows:

| | | | |
|---|---|---|---|
| 96°C | 10 seconds | } | x 25 cycles |
| 50°C | 5 seconds | | |
| 60°C | 4 minutes | | |

Polymerase chain reaction (PCR) products were purified using sephadex and loaded onto an automated ABI Prism 310 genetic analyser (Life technologies).

### 2.2.2 Site directed mutagenesis

Missense mutations and polymorphisms were introduced by site directed mutagenesis. The primers used for site directed mutagenesis are shown in the appendix (Table S 3 and Table S 4). The mutagenesis reaction was set up using the QuickChange II XL site directed mutagenesis kit (Agilent technologies) using 10-50ng of DNA in the absence or presence of 5% dimethyl sulfoxide (DMSO).

The PCR conditions used were as follows:

| | | | |
|---|---|---|---|
| 95°C | 1 minute | | x1 cycle |
| 95°C | 50 seconds | } | x18 cycles |
| 60°C | 50 seconds | | |
| 68°C | 5 minutes | | |
| 68°C | 7 minutes | | x1 cycle |

### 2.2.3 DpnI digestion and agarose gel electrophoresis

The restriction enzyme DpnI (1µl) was added to the reaction mix for 1 hour at 37°C to digest unmutated vector. The DpnI digested DNA was run on a 1.5% agarose gel prepared in TBE (Tris-Borate-EDTA (Ethylenediaminetetraacetic acid), 89mM Tris, 89mM boric acid, 2mM EDTA, pH 8.3). To 100ml of prepared agarose 1µl of ethidium bromide was added and for loading 5µl of loading buffer (0.25% bromophenol blue, 10% glycerol in TBE) was added to 5µl of water and 1µl of DpnI digested DNA. This was run at 120V for ~30 minutes.

### 2.2.4 Transformation

Transformation was performed after detection of a band on a 1.5% agarose gel, after DpnI digestion. Transformation was carried out either using TOP10 one shot chemically competent *Escherichia Coli* (*E. coli*) (Life technologies), XL10-Gold ultracompetent *E. coli* (Agilent technologies) or Sure 2 supercompetent *E. coli* (Agilent technologies). Briefly cells were incubated with 1-2µl of DpnI digested DNA (after addition of beta mercaptoethanol to the XL10-Gold and Sure 2 supercompetent cells) for 30 minutes on ice. The cells were then heated at 42°C for 30 seconds followed by incubation on ice for 2 minutes. S.O.C medium (Life technologies) was added to Top10 cells and $NZY^+$ broth (prepared according to the manufacturer's instructions) was added to the XL10-Gold ultracompetent cells and Sure 2 supercompetent cells (as recommended by the manufacturers). *E. coli* were then incubated at 37°C for 1 hour with shaking (250rpm). After this *E. coli* were plated onto LB (Luria-Bertani) agar (Anachem Ltd) containing 50µg/ml ampicillin and left overnight at 37°C (~16 hours). Plates were stored at 4°C until further analysis.

### 2.2.5 Mini preparation

For mini preparation a single *E. coli* colony was picked using a 1µl sterile inoculation loop (Greiner Bio-One Ltd) and added to 5ml of LB media (Anachem Ltd) containing 50µg/ml ampicillin. The cultures were left to grow overnight at 37°C with shaking at 250rpm for approximately 16 hours.

The next day cultures underwent mini preparation using a commercial kit, according to the manufacturer's instructions (Qiagen). Before mini preparation glycerol stocks of the *E. coli* were prepared by adding 190µl of 80% glycerol (MP Biomedicals) to 810µl of culture.

In brief the cultures were centrifuged at 15,700g for 3 minutes and the supernatant removed. The pelleted *E. coli* were resuspended in 250µl of resuspension buffer containing RNase. After, 250µl of alkaline lysis buffer was added, followed by neutralisation buffer (350µl) 5 minutes later. Samples were spun at 15,700g for 10 minutes to precipitate and remove proteins, cell debris and chromosomal DNA from the cell lysate samples.

The cell supernatant was then passed through a silica membrane column, to which the plasmid DNA bound. The column was washed with PE buffer containing ethanol, to wash away impurities, followed by elution with 30µl of water.

The extracted plasmid DNA was quantified using a nano-drop spectrophotometer (ThermoFischer Scientific) and the purity assessed by running on a 1% agarose gel (Chapter 2.2.3).

### 2.2.6 Sequencing of construct to confirm presence of mutation

After site directed mutagenesis *ADAMTS13* was sequenced to confirm the presence of the nucleotide change introduced. Sequencing was either carried out using the ABI Prism 310 genetic analyser (Life technologies) as described (Chapter 2.2.1) or using a Ceq™ 8000 genetic analysis system (Beckman Coulter). Reactions were set up using GenomeLab DTCS Quick start kit (Beckman Coulter).

The cycle sequencing PCR was set up as follows:

| | | | |
|---|---|---|---|
| 96°C | 30 seconds | } | x 30 cycles |
| 50°C | 30 seconds | | |
| 60°C | 4 minutes | | |

PCR products were purified as recommended by the manufacturer. The primers used to sequence *ADAMTS13* cDNA to confirm the presence of these nucleotide variations are shown in the appendix (Table S 2).

### 2.2.7 Large scale plasmid preparation

Once it was confirmed that the desired nucleotide change had been introduced into the plasmid without disrupting the surrounding *ADAMTS13* sequence, maxi-preparation was carried out in order to produce large quantities of plasmid DNA for subsequent experiments. As with mini preparation (Chapter 2.2.5) this was performed using a commercial kit (Qiagen).

Briefly *E. coli* were resuspended in buffer P1, followed by addition of buffer P2 to enable cell lysis. This was neutralised by the addition of buffer P3. The lysates were cleared by centrifugation and then loaded onto an anion-exchange tip where plasmid DNA selectively bound. RNA, proteins and other impurities were removed by a medium salt wash and pure plasmid DNA was eluted using a high salt solution. The DNA was concentrated and desalted by isopropanol precipitation and collected by centrifugation.

The quantity of plasmid DNA extracted was measured using a nano-drop (ThermoFischer Scientific) and the quality was assessed on a 1% agarose gel (Chapter 2.2.3).

## 2.3 Transient transfection of ADAMTS13 variants

### 2.3.1 HEK 293T cells

HEK293T cells (LGC standards) were seeded in T75 flasks (VWR) and maintained in DMEM media containing L-glutamine (Dulbecco's Modified Eagle's Medium, Life technologies) with the addition of 10% fetal bovine serum (FBS, Life technologies) and 100 units/ml of penicillin and 0.1mg/ml streptomycin.

### 2.3.2 Transient transfection

Confluent HEK293T cells (~80% confluent) seeded in 90mm petri dishes (VWR) were used for transient transfection. Approximately one hour before transfection media was exchanged for OptiMEM reduced serum media containing glutamax (Life technologies) and 1% L-glutamine (Life technologies). For transfection 33µg of *ADAMTS13* vector DNA was diluted in 625µl of 150mM sodium chloride (NaCl). In addition 1µg of the pRL-TK plasmid (Promega) was added, in order to enable normalisation of the transfection efficiency for subsequent experiments. Similarly 75µl of 10mM PEI (polyethylenimine, prepared in water, Polysciences Europe) was diluted in 625µl of 150mM NaCl. After this 700µl of diluted PEI was added dropwise to the diluted DNA and left for 15-20 minutes to form the transfection complex. This transfection complex was then added slowly dropwise to the cells.

After four days supernatant and cell lysate samples from the transiently transfected cells were harvested. A protease inhibitor PMSF (phenylmethylsulfonyl fluoride) was added to the supernatant samples (final concentration 1mM). Supernatant samples were spun at 3000g for 10 minutes to remove cell debris and then stored at -80°C.

Cell lysate samples were harvested using a cell lysis buffer from a commercial kit (*Renilla* luciferase assay system, Promega) according to the manufacturer's instructions. In brief cells were washed with PBS (phosphate buffered saline, Life technologies) followed by incubation on ice for 15 minutes with 1ml of 1x lysis buffer containing 1mM PMSF. Cells were scraped off the surface of the petri dish and frozen at -80°C. Cells were later freeze thawed three times followed by spinning

at 15,700g for 15 minutes at 4°C. The supernatant obtained after spinning was used for subsequent analysis and stored at -80°C.

### 2.3.3 Normalisation after transient transfection

In order to normalise the transfection efficiency luminescence was measured in cell lysate samples. This luminescence was produced by the *Renilla* luciferase reporter enzyme that the pRL-TK co-transfected vector expressed when it was incubated with its substrate. This luminescence was subsequently measured using the *Renilla* luciferase assay system (Promega).

Luminescence was measured using a BMG Fluostar Optima microplate reader (BMG Labtech) set to luminescence mode. A protocol was created on the machine to automate the measurement of luminescence. The temperature of the machine was set to 25°C.

The production and measurement of luminescence was measured according to the recommendations in the *Renilla* luciferase assay system (Promega). In brief *Renilla* luciferase solution was prepared by adding 1x *Renilla* luciferase substrate to 1x *Renilla* luciferase buffer. A sufficient quantity was prepared so that 100µl could be added to each sample and also so that there was a final dead volume of 600µl. The pump of the microplate reader was primed with this solution. Following this 20µl of each cell lysate sample was added to a well of a white 96 well plate (ThermoFischer Scientific). Background luminescence was measured using negative control cell lysate samples (samples which had not been transfected with either pRL-TK or *ADAMTS13*). This background luminescence was measured every time luminescence was measured for a given experiment at least five times. The average value was then subtracted from the value of the other test samples.

The pump injected 100µl of *Renilla* luciferase solution into each well and luminescence readings were taken over a period of 24 seconds every 0.5 seconds. The change in luminescence was calculated over the period 4 to 14 seconds. This meant that luminescence was calculated approximately 2 seconds after the *Renilla*

luciferase solution had been added to the cell lysate sample, over a period of 10 seconds as recommended by the manufacturer (Promega).

The values calculated for the change in luminescence were used to normalise results. Values were normalised according to the lowest luminescence value measured, taken as 1. The remaining samples were expressed as a proportion of this based on their luminescence.

### 2.3.4 Concentrating media

Supernatant samples were concentrated 20 -100 fold using centrifugal filter devices with a ~100kDa cut-off (Millipore). Samples were spun at 3000g for 10-15 minutes at 4°C.

## 2.4 Creation of stable lines

HEK 293 cells (LGC standards) were cultured as described for HEK 293T cells (Chapter 2.3.1). Confluent cells (~70%) were seeded in 90mm petri dishes, two plates of cells were used for each transfection. Media was removed from the cells, followed by washing with PBS. Trypsin (Life technologies) was then added to both plates to remove the cells from the surface. The cells from both plates were then resuspended in 800µl of DMEM (not containing FBS or penicillin/streptomycin). After this 30µg of DNA was added to the cells and left for 1 minute.

The cell suspension was transferred to a 4mm electroporation cuvette (ThermoFischer Scientific) and immediately pulsed at 280V with a resistance of 1500µF using an Equibio/Easyject plus electroporator (ThermoFischer Scientific). Cells were then immediately resuspended in 10ml of DMEM media (with 10% FBS and penicillin/streptomycin) and were then seeded in petri dishes.

One week after transfection the antibiotic geneticin (Life technologies) was added to the media of cells in order to select for clones stably expressing ADAMTS13. A number of clones were picked and the quantity of ADAMTS13 produced was measured using an ADAMTS13 antigen ELISA. A clone was selected which expressed the greatest quantity of ADAMTS13 and used for subsequent experiments.

For the secretion defect mutant, a clone was picked based on the quantity of ADAMTS13 that could be detected within the cell using western blotting.

## 2.5 Western blotting

Cell lysate or supernatant samples were loaded onto Criterion XT 4-12% Bis-Tris precast polyacrylamide gels (Bio-Rad laboratories). Cell lysate samples (unless otherwise stated) were loaded under reducing conditions, 3x cell lysate was loaded with 1x reducing buffer (150mM Tris-HCl pH 6.8, 40% glycerol, 8% SDS (sodium dodecyl sulphate), 10% beta mercaptoethanol, 0.25% bromophenol blue). Unless otherwise stated, 3x supernatant was loaded with 1x non-reducing buffer (150mM Tris-HCl pH 6.8, 20% glycerol, 8% SDS, 0.25% bromophenol blue). The volume of supernatant or cell lysate obtained after transient transfection was loaded according to the transfection efficiency (up to 15µl of cell lysate and 40µl of supernatant). Samples were heated at 100°C for 5 minutes, and then briefly vortexed before they were loaded onto the gel. Precision plus dual colour standard ladder (Bio-Rad laboratories) was run with samples to ensure that the ADAMTS13 detected was of the correct size.

SDS gels were run using XT MOPS buffer (Bio-Rad laboratories). Gels were run at 100V for 15 minutes in order to concentrate the samples in the stacking part of the gel. Following this the voltage was increased to 200V for a further 45 minutes.

Protein was transferred onto Amersham Hybond ECL (enhanced chemiluminescence) 0.45µm nitrocellulose membranes (GE Healthcare) using the Criterion trans blot system (Bio-Rad laboratories). Samples were transferred for 30 minutes at 100V with Towbin blotting buffer (25mM Tris, 192mM glycine, 20% methanol). An ice pack was added also to reduce the temperature and a magnetic stirrer was placed inside the buffer to ensure a homogenous solution during transfer.

After transfer, membranes were blocked with TBS (Tris Buffered saline, 20mM Tris, 100mM NaCl, pH 7.4) containing 5% milk for 1 hour with agitation (45rpm). After blocking the membrane was incubated overnight at 4°C with a monoclonal mouse anti-V5 (Life technologies) antibody (directed against the C-terminal V5 tag the

recombinant protein expressed), diluted 1/2000 in TBST (TBS with 0.05% Tween 20) (Sigma) containing 5% milk. Membranes were then washed three times with TBST followed by incubation for 90 minutes with an ECL anti-mouse IgG polyclonal HRP (horseradish peroxidase) antibody (GE Healthcare) diluted 1/500 in TBST containing 5% milk. Membranes were washed again three times followed by incubation with supersignal west pico chemiluminescent substrate (ThermoFischer Scientific). The signal was captured using Amersham Hyperfilm ECL (GE Healthcare) and developed manually using Carestream ® Kodak ® autoradiography GBX fixer/replenisher and developer/replenisher (Sigma).

## 2.6 ADAMTS13 antigen ELISA

Supernatant samples were analysed using either an in-house ADAMTS13 antigen ELISA (Feys *et al*, 2007) or a commercial kit: Imubind ADAMTS13 ELISA (Sekisui Diagnostics).

### 2.6.1 In-house ADAMTS13 antigen ELISA

For the in-house ADAMTS13 antigen ELISA microplates were coated with 4μg/ml of the monoclonal antibody 20A5 (Katholieke Universiteit Leuven, directed again ADAMTS13 TSP-1:2→TSP-1:5 domains) diluted in PBS, 120μl per well. This was left overnight at 4°C. The next day the primary antibody was removed and the wells were washed three times in PBST (PBS containing 0.1% Tween 20), followed by blocking with PBS containing 3% milk for 90 minutes.

Wells were then washed five times in PBST followed by incubation with 100μl of sample. The default dilution for all samples, including the standard was 1 in 2. Samples were diluted in PBS containing 0.3% milk. After an hour samples were removed and the plate was washed five times with PBST. The biotinylated secondary antibody, 5C11 (Katholieke Universiteit Leuven, directed against TSP-1:2→TSP-1:5 domains of ADAMTS13) was next added (100μl per well), diluted in PBS to a final concentration of 2μg/ml.

Following this the plate was washed five times, followed by incubation with streptavidin peroxidase conjugate (Merck Chemicals), diluted 1/10,000 in PBS

containing 0.3% milk for 1 hour. After the plate was washed 4 times in PBST and the substrate was added to the plate: one 15mg OPD tablet (O-phenylenediamine dihydrochloride) dissolved in citrate phosphate buffer (0.1M, pH 5), with hydrogen peroxide. The colour was left to develop for ~30 minutes. The reaction was stopped using 2M sulphuric acid and the absorbance was measured at 490nm.

The standard curve was created using pooled normal plasma (PNP). PNP was diluted one in two in PBS (containing 0.3% milk) to give the 100% standard. This was diluted by doubling dilutions (100%, 50%, 25%, 12.5%, 6.25%, and 3.125%). ADAMTS13 antigen levels in samples were expressed as a percentage of PNP. Two controls (with normal and low ADAMTS13 antigen levels) were run on each ELISA.

The 5C11 antibody was biotinylated using EZ-Link Sulfo-NHS-SS-biotin (ThermoFischer Scientific) kit according to the manufacturer's recommendations. The antibody was dialysed in PBS before biotinylation (dialysis tubing with a >12,000 molecular weight cut off, Sigma). The detection limit of the ELISA was 3% of PNP and the normal range 44-148%.

The intra and inter assay coefficient of variation (CV) was 2% and 6% respectively at normal ADAMTS13 antigen levels (90% of PNP). The intra and inter assay CV was 8% and 12% respectively, when measured at low ADAMTS13 antigen levels (3% of PNP).

### 2.6.2 Commercial ADAMTS13 antigen ELISA

The laboratory normal range for the commercial kit: Imubind ADAMTS13 ELISA (Sekisui Diagnostics) is 485-1242ng/ml. The coating antibody is a polyclonal antibody and the capture antibody a biotinylated antibody both directed against the TSP-1:5→TSP-1:7 domains of ADAMTS13. Low ADAMTS13 antigen samples were diluted 1 in 5. By modifying the default dilution (1 in 20) to a 1 in 5 dilution ADAMTS13 antigen as low as 10ng/ml could be detected.

The intra and inter assay CV was 4% and 7% respectively as stated by the manufacturers. In house the intra and inter assay CV calculated at low antigen levels

(120ng/ml) was 6% and 10% respectively and at very low antigen levels (calculated at 10ng/ml) was 18% and 19% respectively.

## 2.7 ADAMTS13 activity assay: FRETS-VWF73

ADAMTS13 activity was measured using FRET (fluorescence resonance energy transfer) (Kokame *et al*, 2005) with minor modifications (Mackie *et al*, 2013). In brief, a modified VWF peptide (FRETS-VWF73) was used as a substrate for ADAMTS13 in this assay. When cleaved by ADAMTS13 this peptide produced fluorescence which was measured. Fluorescence was measured every 5 minutes for 75 minutes.

ADAMTS13 activity values were expressed as a percentage of PNP. The detection limit and normal range of the assay was 2.5% and 60-123% respectively. For low activity samples the incubation time of samples with substrate was increased and calculated using the linear portion of the rate curve (5-145 minutes).

The intra and inter assay CV was 2% and 6% respectively at 98% ADAMTS13 activity (5-75 minutes). The intra and inter assay CV at 5% ADAMTS13 activity was 22% and 21% respectively and at 10% ADAMTS13 activity was 13% and 7% respectively (5-145 minutes).

## 2.8 Immunofluorescence

Localisation of WT and mutant ADAMTS13 within the cell ER and Golgi was investigated using immunofluorescent labelled antibodies and confocal microscopy. Antibodies directed against ADAMTS13 and either the ER or Golgi were used.

### 2.8.1 Culturing and transfecting cells

Each cover glass (22x22mm, thickness: 0.13-0.16mm, VWR) was placed into separate wells of a six well culture plate (VWR) and sterilised by submersion in 100% ethanol. After 30 minutes the cover glasses were transferred to a new sterile six well plate using sterile tweezers and left to air dry in a sterile cabinet. HEK293T cells were then seeded onto the cover glasses.

Confluent HEK 293T cells (~80%) seeded onto cover glasses underwent transient transfection as described previously with minor modifications (Chapter 2.3.2). OptiMEM media was not added to cells before transfection took place. The volumes of DNA and PEI were scaled down (0.66µg DNA, 12.5µl of 150mM NaCl, 1.5µl PEI).

### 2.8.2 Immunofluorescent staining of cells

Media was removed from the cells 24 hours after transfection and the cells were washed with PBS. Following this cells were fixed with 4% paraformaldehyde (dissolved in PBS by heating, Sigma), 400µl was added slowly, dropwise to each cover glass. Paraformaldehyde cross-links proteins via methylene bridges preserving cellular structure (Jamur & Oliver, 2010). After 30 minutes the paraformaldehyde was removed and the cells were washed three times in PBS for 10 minutes.

Cells were then permeabilised to enable antibody entry into the cell, by incubating the fixed cells with 0.2% Triton X-100 (Sigma) for 10 minutes. Following this cells were blocked overnight at 4°C by incubation with 3% bovine serum albumin (BSA) (Sigma) containing 0.3M glycine (VWR) (dissolved in PBS). The next day, cells were incubated for 10 minutes at room temperature with PBS containing 10% heat inactivated serum from rabbit and from goat, (heat inactivated by heating at 56°C for 20 minutes, then spun at 15,700g for 15 minutes) (Sigma). The cells were washed again in PBS, then incubated simultaneously with two primary antibodies: i) a chicken polyclonal anti-V5 antibody (diluted 1/500) (Bethyl Laboratories Inc) in order to detect ADAMTS13; along with either ii) a mouse monoclonal anti-GM130 antibody (diluted 1/250) (BD Biosciences) (*cis* Golgi marker), or iii) a mouse monoclonal anti-protein disulphide isomerase (PDI) antibody (diluted 1/200) (RL90, Abcam) as a marker of the ER. Antibodies were diluted in 3% BSA; 100µl of diluted antibody was added to each cover glass. Cells were incubated with antibodies for three hours at 4°C.

Cells were then washed three times for 10 minutes, followed by permeabilisation again for 10 minutes with 0.2% Triton X-100. Following this cells were incubated in the dark, for 30 minutes at 4°C with 100µl of diluted fluorescently labelled

secondary antibody. A rabbit FITC (Fluorescein isothiocyanate) conjugated polyclonal anti-chicken antibody (Life technologies, diluted 1/50) was used to detect the primary anti-V5 antibody. A goat polyclonal Cy3 (Cyanine 3) conjugated anti-mouse antibody (Millipore, diluted 1/200) was used to detect the ER or Golgi primary antibody. The stock Cy3 was diluted 1 in 2 in glycerol and stored at -20° C (as recommended by the manufacturer) to give the Cy3 working solution and so the antibody was diluted 1/100 from the working Cy3 solution. When preparing the dilutions for the fluorescently conjugated antibodies, light was excluded as much as possible. Antibodies were diluted in PBS containing 3% BSA.

The cells were washed in the dark, four times with PBS, for 10 minutes (all remaining steps were carried out in the dark). One drop of Vectashield ® mounting media containing 4', 6-diamidino-2-phenylindole (DAPI) (Vector Laboratories) to stain for nuclei was added to each cover glass. A clean microscope slide (76x26mm, 0.8-1, Appelton Woods) was then placed on top of the cover glass, centering the cover glass onto the microscope slide. The microscope slide was carefully inverted so that the cover glass was on top. The cover glass was sealed onto the microscope slide using nail polish. The slides were then stored in the fridge in the dark before viewing.

### 2.8.3 Confocal microscopy

Cells were viewed using a spinning disk confocal microscope (Perkin Elmer) with a Volocity acquisition system, built on a Zeiss inverted microscope. Cells were imaged as soon as possible, normally one or two days after staining, a maximum of two weeks after staining. Cover glasses were cleaned with ethanol before they were viewed.

Images were captured using either a x63 or x100 immersion oil objective. Representative images of the cells were taken from two to three slides for each experiment to minimise the amount of bleaching taking place. Images were taken from a number of different fields in each slide, well separated from each other again to minimise bleaching. The confocal microscope takes images at different levels within a specimen producing 'optical' sections. This sequence of 'optical sections' is

known as a z series. The z series is collected by coordinating the movement of the fine focus of the microscope with image collection. When images of a desired cell (or group of cells) within a field of view were to be taken the microscope was set to image from the region just above the cells down to the region just below the cells. This ensured that only the images required were taken (i.e. so that images of areas devoid of cells were not taken). This was to prevent bleaching, exposing the cells to as little light as possible.

The spacing between each image in a z series (the z-space) was set to 0.359μm for each x63 and x100 objective. This spacing fulfilled the Nyquist criteria. According to the Nyquist sampling theorem (Oppenheim *et al*, 1983) in order to resolve two points and to avoid under or over-sampling, the z-spacing should be equal to the axial resolution between the two points divided by at least two. Voxels (the three dimensional equivalent of pixels), larger than those specified by the Nyquist criteria would under sample an image, create artefacts and result in false colocalisation. Collecting images with voxels smaller than the Nyquist value would result in the re-imaging of sections and longer exposure times which could lead to photobleaching.

Untransfected, unlabelled cells were imaged to assess whether autofluorescence was produced by the cells. There was no apparent autofluorescence. Single labelled controls (i.e. FITC or Cy3 staining alone) were used to assess bleed-through. Bleed-through is the passage of fluorescence emission in an inappropriate detection channel caused by an overlap of emission spectra (Bolte & Cordelieres, 2006). There was no apparent bleed-through.

Cross-talk occurs when several fluorochromes are excited with the same wavelength at a time because their excitation spectra partially overlap (Bolte & Cordelieres, 2006). Cross talk was minimised by sequentially scanning the sample: one laser was activated and the corresponding emission collected, followed by excitation of the next laser and detection of emission.

For each experiment the exposure times were first set for each channel to be imaged using a randomly chosen cell expressing WT ADAMTS13. The same exposure times were then used to image negative control samples. Test samples (WT and mutant

protein) were then imaged using the same exposure times. At each position images were taken in the order FITC, Cy3 and then DAPI. The objective then moved to the next position to take the next image. This method of imaging the cells as opposed to imaging all the FITC staining of each z stack followed by imaging all the Cy3 staining is more suitable for colocalisation analysis as it prevents the shifting of voxels between images.

To view DAPI staining, excitation was at 405nm and emission at 455/460nm. To view FITC staining, excitation was at 488nm and emission at 527/555nm. Finally for Cy3 staining excitation was at 568nm and emission at 615/670nm.

## 2.9 Immunofluorescence quantitation

The degree of colocolisation between ADAMTS13 and the Golgi was quantified using Volocity 3D image analysis software (Perkin Elmer). The 'co-localization' option was selected under the quantitation tab.

The images obtained after confocal microscopy were represented as a series of voxels, akin to pixels but representing space in addition to length and width. These voxels were given a value for each channel (wavelength) in which images were taken. A 14 bit channel was used to image the cells so each voxel was given a value between 0 and 16384 depending upon the intensity of the signal captured by the microscope, in this case having three different values for the three different wavelengths at which the images were viewed. For colocalisation analysis channel 1 was set to show the values obtained at a wavelength of 568nm. At this wavelength the fluorescently labelled Golgi was measured. Channel 2 was set to show the values obtained at a wavelength of 488nm. At this wavelength the fluorescently labelled ADAMTS13 could be measured.

Thresholds were first set to exclude voxels from the analysis which constituted background 'noise.' These were set by selecting a region of the image in which there were no cells. The software then calculated the threshold value for each channel separately by calculating the mean value of the voxel intensities (in a particular

channel) in the region of interest plus three standard deviations (SD). The same threshold for each channel was used throughout the analysis.

Clearly defined cells within an image were selected for analysis. The region of interest was selected using the freehand tool. Only cells with no saturated voxels were used to carry out the quantitation analysis. If there were other cells or parts of cells within the same region of the Z-stack, in the region of interest, these cells were excluded from the analysis.

## 2.10 Proteasome/lysosome inhibition

Confluent HEK 293 cells plated in 90mm petri dishes (VWR), stably expressing ADAMTS13 were incubated with either 10μM MG132 (carbobenzoxy-Leu-Leu-leucinal) (Merck Chemicals), 6μM ALLN (N-acetyl-L-leucinyl-L-leucinyl-norleucinal) (Merck chemicals, prepared in DMSO according to the manufacturer's instructions), 0.1μM Bafilomycin A1 (Sigma, prepared in DMSO according to the manufacturer's instructions), 50mM ammonium chloride (prepared in sterile water) or with 0.1% DMSO (Sigma). After 5 hours cell lysate and supernatant samples were harvested as described (Chapter 2.3.2). Supernatant was concentrated as described above ~100 fold (Chapter 2.3.4). For SDS gel electrophoresis, 15μl of cell lysate and 30μl of supernatant was loaded.

## 2.11 Betaine experiments

Betaine is a chemical chaperone and has been recently shown to aid the secretion of a Factor VIII mutant (Roth *et al*, 2012). In order to investigate whether betaine could aid the secretion of an ADAMTS13 secretion defect mutant, confluent HEK 293 cells plated in 90mm petri dishes (VWR) stably expressing ADAMTS13 were incubated in the presence or absence of 100mM betaine (prepared in sterile water). After 96 hours cell lysate and supernatant samples were harvested as described previously (Chapter 2.3.2). Supernatant was concentrated as described previously ~100 fold (Chapter 2.3.4).

### 2.11.1 SDS-PAGE

For SDS-PAGE (polyacrylamide gel electrophoresis), 15µl of cell lysate and 30µl of supernatant was loaded. To ensure better separation of cell lysate samples, samples were also run on Criterion XT tris-acetate 3-8% precast polyacrylamide gel, with XT tricine running buffer (Bio-Rad Laboratories). These samples were run with laemmli buffer (Bio-Rad laboratories) with 5% beta mercaptoethanol, 10µl cell lysate, 20µl of supernatant.

### 2.11.2 Deglycosylation experiments

Cell lysate samples (10µl) were digested with PNGase F (New England BioLabs) according to the manufacturer's instructions. The digested and undigested products then underwent gel electrophoresis on 3-8% Tris-acetate gels. Similarly cell lysate and supernatant samples (10µl) were digested with the restriction enzyme Endoglycosidase H (New England Biolabs) according to the manufacturer's instructions.

## 2.12 Purification of ADAMTS13

ADAMTS13 expressed by stable line cells was purified using a Fast Performance Liquid Chromatography (FPLC) system (GE Healthcare) using a 5ml HisTrap HP affinity column (GE Healthcare). The column was first stripped of its $Ni^{2+}$ ions using stripping solution (20mM sodium phosphate, 0.5M NaCl, 50mM EDTA, pH 7.4) followed by washing (20mM sodium phosphate, 20mM imidazole, 0.5M NaCl, pH 7.4). The column was then recharged with zinc using 100mM ZnCl solution. The column was stripped and recharged with $Zn^{2+}$ as during the purification procedure in previous experiments it was found that the $Ni^{2+}$ within the column displaced the ADAMTS13 $Zn^{2+}$ ions.

The column was washed with binding buffer (20mM HEPES, 20mM imidazole, 500mM NaCl, pH 7.4). After this 20mM imidazole was added to the stable line supernatant to prevent non-specific binding and this was then passed through the column. Following this, elution buffer was passed through the column (20mM HEPES, 500mM imidazole, 0.5M NaCl, pH 7.4). The eluted protein was collected in

2.5ml fractions and the fractions containing ADAMTS13 were identified by an increased absorbance of UV light.

Fractions containing the eluted protein were pooled together and the buffer exchanged (20mM HEPES, 150mM NaCl, pH 7.4) using an Ecno-Pac 10G column (Bio-Rad).

After purification the purity was confirmed using SDS electrophoresis and the quantity of ADAMTS13 purified was measured using an Imubind ADAMTS13 antigen ELISA (Sekisui Diagnostics).

### 2.12.1 Coomassie blue staining

SDS-PAGE was carried out using equal volumes of the following: i. unpurified supernatant (collected from WT or p.R102H mutant ADAMTS13 stable lines), ii. flow through supernatant obtained after purification (of both WT and p.R102H mutant) and iii. purified WT and p.R102H mutant ADAMTS13. SDS-PAGE was carried out as described in Chapter 2.5 under reducing conditions. After SDS-PAGE the gel was removed from its casing and placed briefly in distilled water followed by incubation with Coomassie dye (Bio-Rad) for 45 minutes with gentle agitation (45rpm). The Coomassie dye was removed and the gel was then washed with distilled water twice for one hour to remove the Coomassie stain (agitated at 45rpm). The gel was then washed overnight with distilled water.

### 2.12.2 Western blotting

Western blotting was carried out as described in Chapter 2.5, with minor modifications. A rabbit anti-human polyclonal anti-ADAMTS13 antibody diluted 1/200 (Santa Cruz Biotechnology, Inc) was used for the primary antibody. For the secondary antibody an anti-rabbit HRP conjugated secondary antibody, diluted 1/20,000 was used (Dako UK Ltd).

## 2.13 ADAMTS13 catalytic activity in purified ADAMTS13

VWF multimer analysis and time course experiments were performed with the assistance of Dr. Stefano Lancellotti

### 2.13.1 VWF multimer analysis

ADAMTS13 (2nM) was incubated with full length pooled VWF (10µg/ml) and ristocetin (1.5mg/ml) with 20mM HEPES, 5mM $CaCl_2$, pH 7.5. This was incubated at 37°C. At 30 minute intervals, 10µl sub samples were removed and added to 290µl of sample buffer (10mM Tris, 1mM $Na_2EDTA$, 2% SDS, 0.006% bromophenol blue, pH 8.0).

Samples underwent agarose gel electrophoresis. Samples were heated at 56°C for 30 minutes before loading. Agarose gels were prepared fresh. For stacking an agarose concentration of 0.8% was prepared (0.125M Tris, 0.1% SDS, pH 6.8) and for running a concentration of 2% was prepared (0.375M Tris, 0.1% SDS, pH 8.8).

Electrophoresis was carried out at 10°C (electrophoresis buffer: 0.05M Tris, 0.384M Glycine, 0.1% SDS, pH 8.3/8.6). The gel was run at 32mA for ~30 minutes. The current was then decreased to 10mA and the gel was run overnight.

Transfer was carried out at 2A at 10°C for 4 hours (transfer buffer: 0.05M $Na_2HPO_4$, 0.05M $NaH_2PO_4$, 0.04% SDS, pH 7.4). After transfer the membrane was blocked with 5% milk for 1 hour. The membrane was incubated with a polyclonal rabbit anti VWF antibody (Dako), diluted 1/7500 in 3% milk. This was left overnight with shaking at 4°C.

The next day the membrane was washed three times in TBST, followed by incubation with a goat polyclonal anti rabbit HRP conjugated antibody diluted 1/20,000 in 1% milk (Dako) for one hour. The membranes were then washed three times in TBST followed by incubation with ECL western blotting detection reagents (GE Healthcare). Chemiluminescence was measured using a ChemiDoc XRS+ system (Bio-Rad).

### 2.13.2 Time course experiment

Time course experiments under pseudo first order conditions were set up using FRETS-VWF73 as a substrate to analyse $K_{cat}/K_m$ values. ADAMTS13 (2nm) was incubated with FRETS-VWF73 (2μM) for 480 minutes. Fluorescence was measured every 5 minutes.

## 2.14 *In silico* analysis of splice site mutation

The effect of the mutation predicted to affect splicing was analysed using two different online tools: Berkeley Drosophila Genome Project splice site prediction (URL: http://www.fruitfly.org/seq_tools/splice.html; accessed 17th June 2014) and CRYP-SKIP (URL: cryp-skip.img.cas.cz/; accessed 17th June 2014). Both tools indicate regions within the DNA sequence under analysis which are likely to be donor or acceptor sites and assign a score to these sites. The higher the score assigned to a given site the more likely this site is to be used for splicing.

## 2.15 Whole blood RNA extraction

### 2.15.1 Blood collection

Blood was collected separately from two healthy volunteers in PAXgene Blood RNA tubes according to the manufacturer's instructions (PreAnalytix). The PAXgene Blood RNA tubes were incubated for two hours to ensure lysis of the blood cells.

### 2.15.2 RNA extraction

The RNA from blood collected in the PAX gene RNA tubes was extracted using PAXgene blood RNA kit (PreAnalytix) according to the manufacturer's guidelines. Blood was centrifuged at 3000g for 10 minutes and the supernatant removed. To the pellet 4ml of RNase-free water was added, followed by mixing with a vortex. This was centrifuged for 10 minutes at 3000g, the supernatant was removed and the pellet was resuspended in 350μl of resuspension buffer by vortex mixing. This was followed by the addition of 300μl of binding buffer and 40μl proteinase K and mixed using a vortex for 5 seconds. The samples were then incubated for 10 minutes at $55^0$C at 400rpm.

The lysate was then added to a PAXgene shredder spin column and centrifuged at 16,000g for 3 minutes. Flow through was transferred to a new tube followed by the addition of 350µl of absolute ethanol and mixing with a vortex. The samples were then transferred to the PAXgene RNA spin column and centrifuged at 16,000g. The flow through was discarded and the column was washed with 350µl of wash buffer 1, followed by centrifugation at 16,000g. Following this 80µl of DNase I incubation mix was added to the spin column and left for 15 minutes. After, 350µl of wash buffer I was added to the column and the column was spun at 16,000g for 1 minute. The flow through was discarded and the column was washed twice with 500µl of wash buffer 2, followed by centrifugation at 16,000g for 1 minute.

After, 40µl of elution buffer was added to the membrane of the spin column and centrifuged at 16,000g for 1 minute to elute the RNA. This was repeated and the eluted samples were incubated at $65^0$C for 5 minutes, followed by immediate transfer to ice. The quantity of RNA extracted was measured using a nano-drop spectrophotometer (ThermoFischer Scientific).

### 2.15.3 Reverse transcription

Reverse transcription (RT) of the RNA was carried out using an Advantage RT-for-PCR kit according to the manufacturer's instructions (Takara Bio Europe/Clontech). To 12.5µl of the purified RNA, 1µl of the random hexamer primer was added. Control RNA (human placental total RNA) was also reverse transcribed. To 1µl of this, 11.5µl of diethylpyrocarbonate (DEPC) treated water (provided in the kit) was added and 1µl of random hexamer primer. Hexamer primers are oligonucleotides of six base pairs synthesised randomly to cover a range of sequences that have the potential to bind and anneal to random points within an mRNA sequence.

The RNA was heated to enable primer binding at $70^0$C for 2 minutes and then immediately placed on ice. Reaction buffer, dNTPs, recombinant RNase inhibitor and MMLV reverse transcriptase was added to the RNA, which was then incubated at $42^0$C for 1 hour to enable RT to take place.

Following this samples were heated at $94^0$C for 5 minutes to stop RT and to destroy any DNase activity. The samples were diluted in DEPC-treated water to a final volume of 100µl.

### 2.15.4 PCR amplification of cDNA

The cDNA obtained after RT (5 or 10µl) was added to 1x reaction buffer (Life technologies), 1.5mm $MgCl_2$ (Life technologies), 400µM dNTPs (Life technologies), 200nM of primer, 1U of amplitaq DNA polymerase (Life technologies) and made up to a final volume of 50µl with sterile water. For each PCR reaction, two normal controls, a positive and negative control were set up also. The primer pairs used were F6/RevJP and F6/R6 (primer sequences are shown in the appendix Table S 5) along with glyceraldehyde 3-phosphate dehydrogenase (G3PDH) forward (F') and reverse (R') primers (provided by the kit) which bind to the housekeeping G3PDH gene. G3PDH is an enzyme important in glycolysis. Housekeeping genes are genes expressed in all cells of an organism. Primer F6 bound within exon 2, primer R6 bound within exon 3 and primer RevJP bound within exon 6. The PCR was set up as follows:

| | | | |
|---|---|---|---|
| 94°C | 3 minutes | | x1 cycle |
| 94°C | 30 seconds | } | x30 cycles |
| 62°C | 30 seconds | | |
| 72°C | 30 seconds | | |
| 72°C | 4 minutes | | x1 cycle |

The products were run on a 2% agarose gel prepared in TBE (Chapter 2.2.3). Samples were run with one of the following DNA ladders: pUC mix marker 8 (ThermoFischer Scientific), DNA ladder marker X (Roche) or gene ruler 100bp plus DNA ladder (ThermoFischer Scientific).

## 2.16 PCR amplification of genomic DNA for cloning

### 2.16.1 PCR using primers SpliceA/B and SpliceA/C

Genomic DNA from a control with normal (WT) *ADAMTS13* or from the patient with the splice site mutation was used for PCR. To 2µl of genomic DNA, 1x reaction

buffer (ThermoFischer Scientific), 100µM dNTPs (Life technologies), 200nM of primer and 1U of Pfu DNA polymerase (ThermoFischer Scientific) was added and made up to a final volume of 50µl with sterile water. PCR was carried out in the absence of DMSO and a negative control was set up with each PCR reaction. The conditions which were used for the PCR set up using primer SpliceA/B and Splice A/C were as follows:

| | | | |
|---|---|---|---|
| 95°C | 3 minutes | | x1 cycle |
| 95°C | 30 seconds | } | x25 cycles |
| 58°C | 30 seconds | | |
| 72°C | 4 minutes | | |
| 72°C | 7 minutes | | x1 cycle |

The PCR products were run on a 2% agarose gel as described in Chapter 2.15.4. Primer sequences are shown in the appendix (Table S 5).

### 2.16.2 PCR using primers SpliceD/E and SpliceA/F

Genomic DNA from a control with normal (WT) *ADAMTS13* or from the patient with the splice site mutation was used for PCR. To 1.5µl of genomic DNA 1x reaction buffer (ThermoFischer Scientific), 125µM dNTPs (Life technologies), 400nM of primer, 5% DMSO and 1U of Pfu DNA polymerase (ThermoFischer Scientific) was added and made up to a final volume of 50µl with water. A negative control was set up with each PCR reaction.

The conditions which were used for the PCR set up using primers SpliceD/E were as follows:

| | | | |
|---|---|---|---|
| 95°C | 2 minutes | | x1 cycle |
| 95°C | 30 seconds | } | x30 cycles |
| 58°C | 30 seconds | | |
| 72°C | 2 minutes | | |
| 72°C | 10 minutes | | x1 cycle |

The conditions used for nested PCR using primers SpliceA/F were as follows:

| | | | |
|---|---|---|---|
| 95°C | 2 minutes | | x1 cycle |
| 95°C | 30 seconds | } | x30 cycles |
| 61°C | 30 seconds | | |
| 72°C | 2 minutes | | |
| 72°C | 10 minutes | | x1 cycle |

Primer sequences are shown in the appendix (Table S 5).

### 2.16.3 Purification of PCR products

PCR products were purified using a QIAquick purification kit (Qiagen) according to the manufacturer's instructions. In brief PBI buffer was added to the PCR mix, which was then added to the QIAqick column and spun at 17,900g for 1 minute to bind the DNA. The DNA was washed using buffer PE and spun at 17,900g for 1 minute. The DNA was eluted in 30µl water by spinning the column for 1 minute at 17,900g. The purified product was visualised on a 2% agarose gel, as described in Chapter 2.15.4.

### 2.16.4 Gel purification

DNA was extracted from agarose gels using a QIAquick gel extraction kit (Qiagen). In brief buffer BG was added to the gel containing the DNA to be extracted, followed by incubation at 50$^0$C for 10 minutes with mixing using a vortex in between to dissolve the gel. Once this had dissolved isopropanol was added to the sample and mixed. This was applied to a QIAquick column and centrifuged for 1 minute at 10,000g to bind the DNA. The flow through was discarded and the DNA was washed with buffer QG by spinning for 1 minute at 10,000g to remove any traces of agarose. The DNA was washed again with buffer PE by centrifuging at 10,000g for 1 minute. The DNA was eluted with 40µl water. The purified product was visualised on a 2% agarose gel, as described in Chapter 2.15.4.

## 2.17 Topoisomerase (TOPO) cloning

PCR fragments were cloned using a pcDNA$^{TM}$ 3.1 Directional TOPO ® Expression kit (Life technologies). This kit enables directional blunt-end PCR product cloning

into the pcDNA3.1D/V5-His-TOPO® vector. This vector is supplied linearised with both ends adapted with topoisomerase. The vector is shown in Figure 2-1.

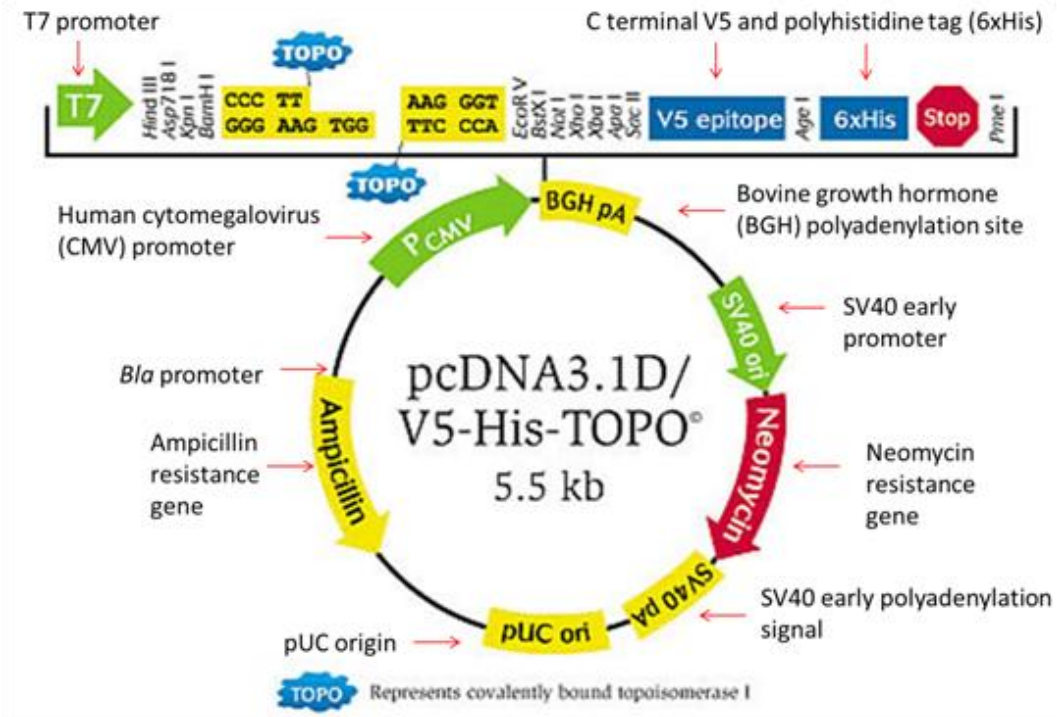


**Figure 2-1 pcDNA3.1D/V5-His-TOPO® vector**

The CMV promoter/enhancer allows high level expression of the inserted protein within mammalian cells. The V5-epitope enables the recombinant protein to express a C-terminal V5 epitope tag for protein detection, the 6xhistidine tag enables the protein to express a C-terminal polyhistidine tag for protein purification. The T7 promoter allows for *in vitro* transcription of the protein in the sense direction and the BGH polyadenylation signal enables efficient transcription termination and polyadenylation of the mRNA. The SV40 early promoter and SV40 early polyadenylation signal enable expression of the neomycin resistance gene and episomal replication in cells expressing the SV40 large T antigen. The neomycin gene enables selection of cells containing the vector using the antibiotic geneticin. The pUC origin enables high copy number replication and growth of the vector in *E. coli*. The *bla* promoter enables expression of the ampicillin resistance gene. The ampicillin resistance gene enables selection of *E. coli* expressing the vector. Note that this vector is the same vector that contains *ADAMTS13* full length cDNA. Image is adapted from (URL: https://www.lifetechnologies.com/order/catalog/product/K490001?ICID=search-product, accessed 17th June 2014).

Topoisomerase I functions as both a restriction enzyme and a ligase. Biologically it cleaves and rejoins DNA during replication. Topoisomerase I from *Vaccina* virus recognises the sequence 5'-(C/T)CCTT-3', cleaving it and forming a covalent bond with the phosphate group of the 3' thymidine (Shuman, 1991). This enzyme cleaves one DNA strand enabling the DNA to unwind, religates the ends of the cleaved strands and then releases itself from the DNA. The ability of this enzyme to religate together DNA is harnessed in this vector.

This kit requires the PCR product to be cloned to start with the DNA sequence CACC. The vector contains a single strand GTGG overhang at the 5' end of the linearised vector and a blunt end (no GTGG) at the 3' end. This 4 nucleotide overhang invades the double stranded DNA of the PCR product and anneals to the CACC sequence introduced into the PCR product by the primer. The Topoisomerase I can subsequently ligate the PCR product into the correct direction. This is illustrated in Figure 2-2.

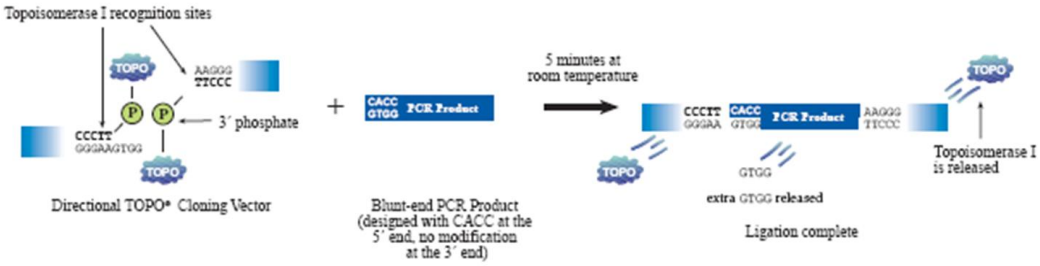


**Figure 2-2 Overview of TOPO cloning process**

Image is adapted from (URL: http://www.lifetechnologies.com/uk/en/home/life-science/cloning/topo/topo-resources/the-technology-behind-topo-cloning.html, accessed 17th June 2014).

The TOPO cloning reaction was set up by adding 1-4µl of the PCR product, 1µl of salt solution and 1µl of TOPO vector (final volume 6µl). The reaction was incubated for 5 minutes at room temperature, and then placed on ice. Following this 2µl of the cloning reaction was transformed into TOP10 one shot chemically competent *E. coli* (Life technologies) as described Chapter 2.2.4.

### 2.17.1 Restriction digest

Some of the cloned PCR products formed using primers SpliceA/C were digested with the following restriction enzymes: StuI (New England Biolabs), BstXI (New England Biolabs) and XbaI (Takara Bio Europe/Clontech). A total volume of 20µl was used, along with 1µl of the restriction enzyme, 1x restriction enzyme buffer and 2-17µl of the DNA obtained from mini preparation.

For StuI digestion of the cloned PCR product formed using primers SpliceA/F, 1µl of enzyme (New England Biolabs) was added to 1x NE buffer 4, with 10µl of the DNA

to be digested (with concentrations varying from 20-100ng/µl) and made up to a final volume of 50µl with sterile water.

# Chapter 3 Transient transfection of *ADAMTS13* missense mutants

## 3.1 Introduction

### 3.1.1 Congenital TTP and *ADAMTS13* mutations

To date over 140 different mutations within the *ADAMTS13* gene have been identified in patients with congenital TTP (Table S 6). These genetic defects are inherited in an autosomal recessive manner (Levy *et al*, 2001). Of those identified, 62% are missense mutations, 19% are deletions, 3% are insertions, 6% are splice site and 10% are nonsense mutations. These mutations are distributed throughout the whole of the *ADAMTS13* gene.

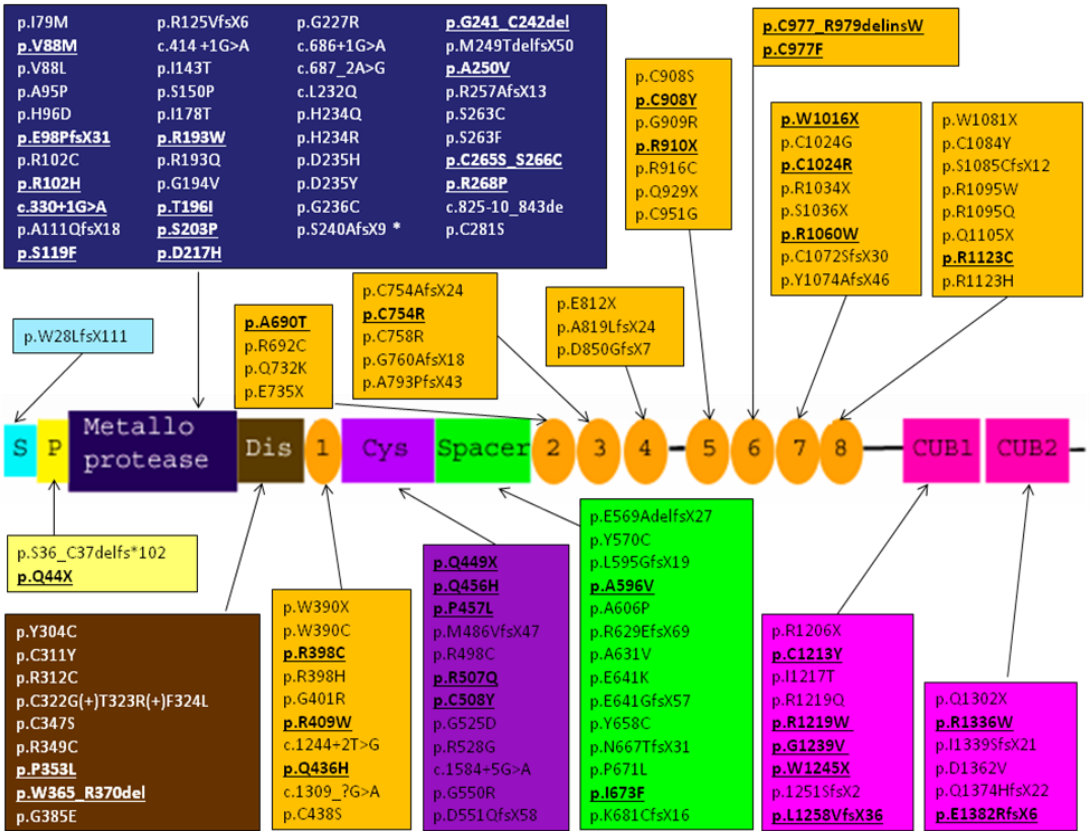


**Figure 3-1 Location of *ADAMTS13* gene mutations identified in patients with congenital TTP**

Mutations that have been expressed *in vitro* are underlined and in bold. Schematic *ADAMTS13* diagram modified from (Zheng *et al*, 2001).

Evidence suggests that there is an association between residual ADAMTS13 activity and *ADAMTS13* genotype. Residual ADAMTS13 activity in turn has been associated with clinical severity of disease in terms of the first episode requiring fresh frozen plasma (FFP) and the annual rate of TTP episodes (Lotta *et al*, 2012). Therefore, it is important to understand the mechanisms and to what extent different mutations within *ADAMTS13* affect its function. Of the mutations identified, approximately 30% have been expressed *in vitro* (Figure 3-1 and Table S 7). *ADAMTS13* mutations affect the secretion and/or the activity of ADAMTS13 (Figure 3-2). The majority of mutants expressed *in vitro* (86%) lead to reduced secretion (<50%) of WT ADAMTS13.

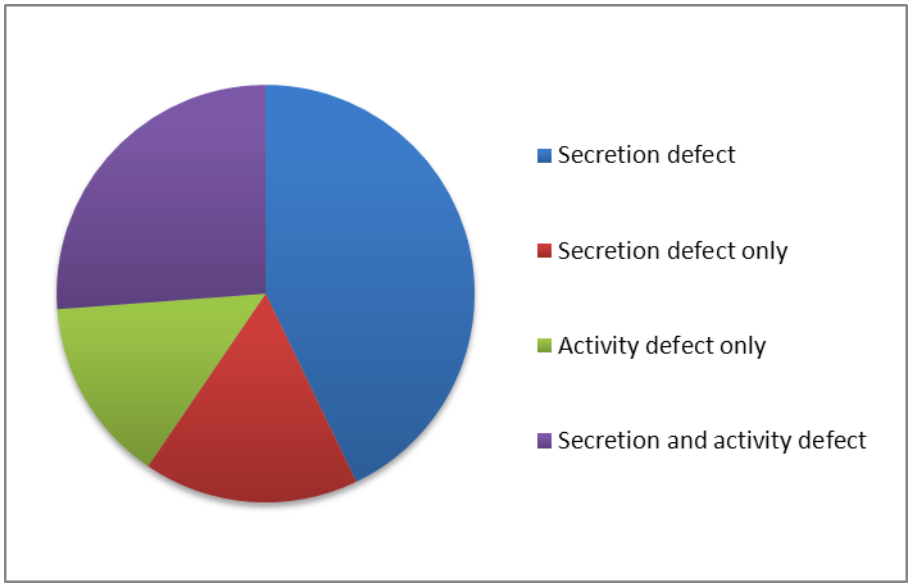


**Figure 3-2 *In vitro* expression of *ADAMTS13* mutants**

Activity defect is defined as a specific activity <50% of WT and a secretion defect as ADAMTS13 antigen <50% of WT. The 50% cut-off was arbitrarily chosen. 'Secretion defect only' are mutants with <50% ADAMTS13 antigen but >50% specific activity. 'Activity defect only' are those mutants with >50% ADAMTS13 antigen but <50% ADAMTS13 activity. 'Secretion and activity defect' are those mutants with <50% ADAMTS13 antigen and <50% specific activity. In some cases no ADAMTS13 was secreted or levels were very low (<10%) and so it is unknown whether the specific activity was reduced in addition to the secretion. These mutations are shown in blue and are described as 'secretion defect' mutants. The c.330+1G>A splicing mutation was not included in this analysis. For mutations analysed in more than one study average values were used.

### 3.1.2 Congenital ADAMTS13 deficient patients homozygous for *ADAMTS13* mutations

It is particularly desirable to study patients homozygous for *ADAMTS13* mutations in order to study genotype/phenotype relationships that may exist. Although useful information can also be obtained by studying compound heterozygotes, there is the possibility that the *ADAMTS13* gene on a particular chromosome may be expressed more often than the corresponding *ADAMTS13* gene on the other homologous chromosome. For example, ADAMTS13 mutant a on chromosome 9a may be expressed 70% of the time whereas ADAMTS13 mutant b on chromosome 9b may be expressed 30% of the time. Therefore, assuming that the ADAMTS13 antigen and activity measured in the plasma of a compound heterozygote patient is the result of 50/50 expression of each mutant, may not be strictly correct.

The majority of mutations that have been expressed *in vitro* were identified in a compound heterozygous state. Of the 43 mutations which have been analysed *in vitro*, only 16 have been found in a homozygous state in at least one patient in the literature, highlighting the need to characterise more mutations which have been identified in a homozygous state in patients (Table 3-1).

| No | Protein/cDNA change | Domain | Age | Antigen* | Reference | *In vitro* |
|---|---|---|---|---|---|---|
| 1 | p.S36_C37delfs*102 | MP | 8 months | <1% # | (Lotta *et al*, 2012), this study | This study |
| 2 | p. R102H | MP | 18 years | 42% # | (Camilleri *et al*, 2012), this study | This study (Camilleri et al, 2012) |
| 3 | | MP | Adult, preg | NA | (Scully *et al*, 2014) | |
| 4 | p.S119F | MP | 14 years | 5% # | (Feys *et al*, 2009b), personal communication | Antigen <10% of WT, specific activity 50% of WT (Feys *et al*, 2009b) |
| 5 | | MP | 17 years | NA | (Meyer *et al*, 2008) | |
| 6 | c.414+1G>A | MP | 4 years | <3% | (Matsumoto *et al*, 2004) | Splice site analysed *in vivo* (Matsumoto et al, 2004) |
| 7 | p.I143T | MP | 7 years | <1% | (Lotta *et al*, 2012) | This study |
| 8 | p.R193W | MP | NA, preg | 11% | (Fujimura *et al*, 2009) | Antigen ~25% of WT, no activity detected (Matsumoto et al, 2004) |
| 9 | p.T196I | MP | 3 years | <10ng/ml | (Camilleri *et al*, 2012) | Antigen 4% of WT, no activity detected (Camilleri et al, 2012) |
| 10 | c.687-2 A>G | MP | Neonatal | NA | (Studt *et al*, 2005) | - |
| 11 | p.L232Q | MP | Neonatal | NA | (Schneppenheim *et al*, 2003) | - |
| 12 | p.D235H | MP | 21 months | NA | (Assink *et al*, 2003) | - |
| 13 | | MP | 12 months | NA | (Assink *et al*, 2003) | - |
| 14 | p.G236C | MP | Adult, preg | <60ng/ml | (Moatti-Cohen *et al*, 2012) | - |
| 15 | p.C311Y | Dis | 23 months | NA | (Assink *et al*, 2003) | - |
| 16 | p.R349C | Dis | 22 years, preg | NA | (He *et al*, 2010) | - |
| 17 | p.R409W | TSP-1 | Neonatal | <10ng/ml | (Camilleri *et al*, 2012) | Antigen <3% of WT, no activity detected (Camilleri et al, 2012) |
| 18 | p.Q436HfsX23 | TSP-1 | Neonatal | <1% # | (Lotta *et al*, 2012) | - |
| 19 | p.Q449X | Cys | Neonatal | <3% | (Ishizashi *et al*, 2007;Kokame *et al*, 2002) | Antigen similar to WT but minimal activity (Kokame et al, 2002) |
| 20 | | Cys | Childhood | NA | (Fujimura *et al*, 2011;Kokame *et al*, 2002) | |
| 21 | c.1584+5G>A | Cys | 4 years | NA | (Levy *et al*, 2001) | - |
| 22 | p.D551QfsX58 | Cys | 13 months | 22ng/ml | (Alsultan *et al*, 2013) | - |
| 23 | | Cys | Neonatal | NA | (Alsultan *et al*, 2013) | |
| 24 | p.L595GfsX19 | Spa | Neonatal | NA | (Savasan *et al*, 2003) | - |
| 25 | p.Y570C | Spa | 10 years | <1% | (Metin *et al*, 2013) | This study |
| 26 | p.A596V | Spa | Neonatal | NA | (Veyradier *et al*, 2004) | Antigen <3% of WT, no detectable activity (Camilleri et al, 2012) |
| 27 | | Spa | 18 months | 11ng/ml | (Camilleri *et al*, 2012) | |
| 28 | p.E641GfsX57 | Spa | 4 years | Undetectable | (Alsultan *et al*, 2013) | - |
| 29 | p.Y658C | Spa | 34 years, preg | NA | (Lee *et al*, 2011) | - |

| | | | | | | |
|---|---|---|---|---|---|---|
| 30 | p.R692C | TSP-1:2 | Neonatal | NA | (Levy *et al*, 2001) | - |
| 31 | | | Neonatal | NA | (Levy *et al*, 2001) | |
| 32 | | | Neonatal | NA | (Levy *et al*, 2001) | |
| 33 | | | 2 months | NA | (Snider *et al*, 2004) | |
| 34 | | | 2 days | Undetectable | (Kim *et al*, 2014) | |
| 35 | | | 17 months | Undetectable | (Kim *et al*, 2014) | |
| 36 | p.E735X | TSP-1:2 | 2 years | Undetectable | (Borgi *et al*, 2013) | - |
| 37 | p.C754AfsX24 | TSP-1:3 | 4 months | NA | (Fujimura *et al*, 2011) | - |
| 38 | | | Neonatal | NA | (Fujimura *et al*, 2011) | |
| 39 | p.C754R | TSP-1:3 | 5 years | <10ng/ml | (Camilleri *et al*, 2012) | Antigen 4% of WT, undetectable activity (Camilleri et al, 2012) |
| 40 | | | 3 years | <10ng/ml | (Camilleri *et al*, 2012) | |
| 41 | p.G760AfsX18 | TSP-1:3 | 7 months | NA | (Assink *et al*, 2003) | - |
| 42 | p.C977_R979delinsW | TSP-1:6 | 23 years | <1% # | (Palla *et al*, 2009) | 1% antigen, specific activity 6% of WT (Palla *et al*, 2009) |
| 43 | | | 29 years | <1% # | (Palla *et al*, 2009) | |
| 44 | p.C977F | TSP-1:6 | 24 years, preg | 38ng/ml | (Camilleri *et al*, 2012) | Antigen <3% WT, undetectable activity (Camilleri et al, 2012) |
| 45 | p.C1024R | TSP-1:7 | 63 years | 0.7% # | (Fujimura *et al*, 2011;Taguchi *et al*, 2012) | Antigen 10% of WT, activity 30% WT. (Taguchi et al, 2012) |
| 46 | p.R1060W | TSP-1:7 | 33 years | 11ng/ml | (Camilleri *et al*, 2008) | Antigen <5% of WT, activity similar to WT (Camilleri et al, 2012) |
| 47 | | | 18 years | 5% # | (Lotta *et al*, 2010) | - |
| 48 | | | Adult, preg | NA | (Scully *et al*, 2014) | |
| 49 | | | Adult, preg | NA | (Scully *et al*, 2014) | |
| 50 | | | Adult, preg | NA | (Scully *et al*, 2014) | |
| 51 | | | Adult, preg | NA | (Scully *et al*, 2014) | |
| 52 | | | Adult, preg | NA | (Scully *et al*, 2014) | |
| 53 | p.W1081X | TSP-1:8 | 11 years | NA | (Fujimura *et al*, 2011) | |
| 54 | p.R1123C | TSP-1:8 | Neonatal | <62.5ng/ml # | (Donadelli *et al*, 2006) | Ag similar to WT no detectable activity (Donadelli et al, 2006) |
| 55 | p.R1219W | CUB-2 | 35 years | <62.5ng/ml # | (Donadelli *et al*, 2006) | Undetectable antigen, activity 62% of WT (Donadelli et al, 2006) |
| 56 | | | 21 years | <62.5ng/ml # | (Donadelli *et al*, 2006) | |
| 57 | p.D1362V | CUB-2 | 31 years, preg | 2% # | (Calderazzo *et al*, 2012) | - |
| 58 | p.E1382RfsX6 | CUB-2 | Neonatal | NA | (Manea *et al*, 2007a) | Antigen 3-14%, activity 10% of WT (Garagiola et al, 2008;Pimanda et al, 2004) |
| 59 | | | 3 years | Undetectable # | (Manea *et al*, 2007b) | |
| 60 | | | 18 months | Undetectable # | (Manea *et al*, 2007b) | |

| | | | | | | |
|---|---|---|---|---|---|---|
| 61 | | | 2 years | Undetectable [#] | (Manea *et al*, 2007b) | |
| 62 | | | 14 years | NA | (Schneppenheim *et al*, 2006) | |
| 63 | | | NA | NA | (Schneppenheim *et al*, 2006) | |
| 64 | | | 4 years | NA | (Schneppenheim *et al*, 2006) | |
| 65 | | | 4.5 years | NA | (Schneppenheim *et al*, 2006) | |
| 66 | | | Neonatal | NA | (Schneppenheim *et al*, 2006) | |
| 67 | | | Neonatal | NA | (Klukowska *et al*, 2010) | |
| 68 | | | Neonatal | NA | (Klukowska *et al*, 2010) | |
| 69 | | | 18 years | NA | (Lotta *et al*, 2012) | |

**Table 3-1 Patients in the literature with homozygous genotype**

Patients in the literature with homozygous genotype published after this thesis was commenced are highlighted in pink. NA- not available either not measured or could not obtain information. Preg indicates pregnancy onset. MP: metalloprotease, Dis: Disintegrin-like, Cys: cysteine-rich, Spa: spacer.*Antigen is expressed as a % of PNP or in ng/ml depending on the ADAMTS13 antigen ELISA used to measured antigen *in vivo*. 100% PNP is approximately 740 +/-110ng/ml (Imubind assay).[#] indicates where it is known that antigen was measured in the patient during remission.

I aimed to study *in vitro, ADAMTS13* mutations which had been identified in a homozygous state in patients with congenital TTP. I set out to study a range of different mutations falling into three categories: i.) mutations causing a severe secretion defect by reduced antigen and activity levels without altering splicing (which I have defined here as a type 1a defect), ii.) mutations with a modestly reduced or normal secretion level but dysfunctional protein (which I have defined here as a type 2 defect) and iii.) mutations affecting splicing and causing a severe secretion defect by reduced antigen and activity (which I have defined here as a type 1b defect). A severe secretion defect was characterised by a severe reduction in both antigen and activity levels. Antigen level values <10% of normal WT ADAMTS13 was arbitrarily chosen to describe a severe reduction in antigen levels. A severe activity defect was defined here as an activity level <5% of WT. This value was chosen as congenital TTP patients have an ADAMTS13 activity <5% of normal (Scully *et al*, 2012).

A number of mutations have been identified in a homozygous state in patients with congenital TTP in the UCL Haemostasis Research Unit and the Angelo Bianchi Bonomi Hemophilia and Thrombosis Centre, Milan. The majority of these mutations were predicted to lead to a type 1 deficiency based on antigen levels measured in patient plasma. Therefore, there were a number of potential type 1 mutations available to work with. Of all the mutations present in both centres there was one (p.R102H), which appeared to a type 2 defect. In order to identify other type 2 defects that could be studied, I carried out a literature search, examining the ADAMTS13 antigen levels measured in the plasma of patients with homozygous *ADAMTS13* gene mutations. Where this information was unavailable the authors were contacted for further information. Results of this search are shown in Table 3-1. This literature search was performed in July 2010. New patients with homozygous mutations which have been identified since then are also shown in the table, highlighted in pink.

At the time I found that the only known type 2 defects that had been described were the p.R102H and p.R193W mutations. The p.R193W mutation had been expressed previously by other groups. This exercise suggested that type 2 defects are rare and most *ADAMTS13* gene mutations lead to a secretion defect and a type 1 deficiency.

### 3.1.3 Congenital TTP patients with missense mutations

I attempted to characterise *in vitro* four mutations using both transient and stable line transfections. Three of these were missense mutations and will be described within this Chapter and in Chapters 4-7. The fourth mutation, a splice site mutant will be discussed separately in Chapter 8.

The clinical history of patients 1 and 2 (Metin *et al*, 2013) and patient 3 (Camilleri *et al*, 2012) have been previously described and are summarised in Table 3-2. All three patients had undetectable ADAMTS13 activity in their plasma in the absence of detectable anti-ADAMTS13 antibodies. The ADAMTS13 activity of patient 1 was also measured using a more sensitive SELDI-TOF mass spectrometry assay (detection limit <0.5% PNP). The patient had undetectable plasma ADAMTS13 activity when measured with this assay also (Lotta *et al*, 2012).

Patients 1 and 2 had undetectable ADAMTS13 antigen levels in their plasma, whereas ADAMTS13 antigen could be detected in patient 3. The ADAMTS13 antigen level was measured in patient plasma before treatment or more than three weeks after plasma exchange/infusion in patients 1 and 3. Plasma was not available in patient 2 during this time and so was measured during the acute phase of disease.

Patients 1 and 2 presented with TTP during adolescence. Patient 3 developed TTP during her third trimester of pregnancy. The mutations present in these patients localise within different regions of the *ADAMTS13* gene (Figure 3-3). Patients 1 and 3 have mutations which localise within the metalloprotease domain of ADAMTS13, while patient 2 has a mutation within the spacer domain.

The parents of patients 1 and 2 were consanguineous and both were Turkish. In Turkey 20-29% of marriages are consanguineous (Hamamy, 2012). Two further Turkish patients, with a homozygous *ADAMTS13* genotype have been identified and published in the literature (Table 3-1) (Metin *et al*, 2013;Studt *et al*, 2005;Lotta *et al*, 2012). Therefore, approximately 6% of patients (4/69) with homozygous *ADAMTS13* mutations are Turkish. This number may be an underestimate as the *ADAMTS13* gene in patients with suspected ADAMTS13 deficiency, is normally sequenced in specialised centres in other countries.

The parents of patient 3 are not consanguineous but the patient came from a small community. Interestingly another patient with the same mutations and non-synonymous polymorphisms as patient 3 has been identified (Table 3-1). This patient also comes from a similar small community as patient 3.

Offspring of consanguineous unions may be at increased risk of expression of autosomal recessive disorders. Therefore, patients from consanguineous unions with a congenital ADAMTS13 deficiency may have homozygous mutations in other genes which could potentially contribute to the disease severity and possibly ADAMTS13 levels.

| **Patient** | **1** | **2** | **3** |
|---|---|---|---|
| Sex/ Ethnicity/Consanguinity | Male/Turkish/Yes | Female/Turkish/Yes | Female/Caucasian/No |
| Consanguineous | Yes | Yes | No, but both parents from the same small community |
| Current age | 25 | 20 | 27 |
| Age at presentation/ diagnosis | 7/13 | 10/13 | 18 |
| Episodes: age and triggers | i.7, ii.8 (infection), iii.11, iv.13*,v.16 (unknown) | i.10 (unknown), ii.13* (menarche) | i.18* (Pregnancy), ii.unrelated to pregnancy |
| Other | No persistent renal or neurological involvement | Neurological involvement at diagnosis but no sequelea | Patient has had three live births |
| Treatment | Plasma infusion every 6 weeks | Plasma infusion every 3 weeks | Plasma exchange every two weeks during pregnancy, plasma exchange after episode |
| ADAMTS13 activity (% PNP) | <6% [a] | <6% [a] | <5% [b] |
| ADAMTS13 antigen (% PNP) | <1% [c] | <1% [c] | 42%±5.4 (mean±SD) [d, $] |
| ADAMTS13 antibodies | Negative | Negative | Negative |
| *ADAMTS13* mutations | p.I143T (Isoleucine→ Threonine) | p.Y570C (Tyrosine → Cysteine) | p.R102H (Arginine → Histidine) |
| *ADAMTS13* polymorphisms | p.Q448E (Glutamine → Glutamic acid) | p.R7W (Arginine → Tryptophan)<br>p.P618A (Proline → Alanine) | p.Q448E (Glutamine → Glutamic acid)<br>p.P618A (Proline → Alanine)<br>p.A900V (Alanine → Valine) |

**Table 3-2 Clinical characteristics of patients**

*Episode TTP diagnosed; [a]detection limit 6%, normal range: 46-160%; [b]detection limit 5%, normal range: 50-160%; [c]detection limit 1%, normal :>45%; [d]detection limit 3%, normal range:44-148%; [$]antigen measured on four separate occasions. ADAMTS13 activity measured using collagen binding assay, all mutations and polymorphisms present are homozygous in patients.

Patient 1

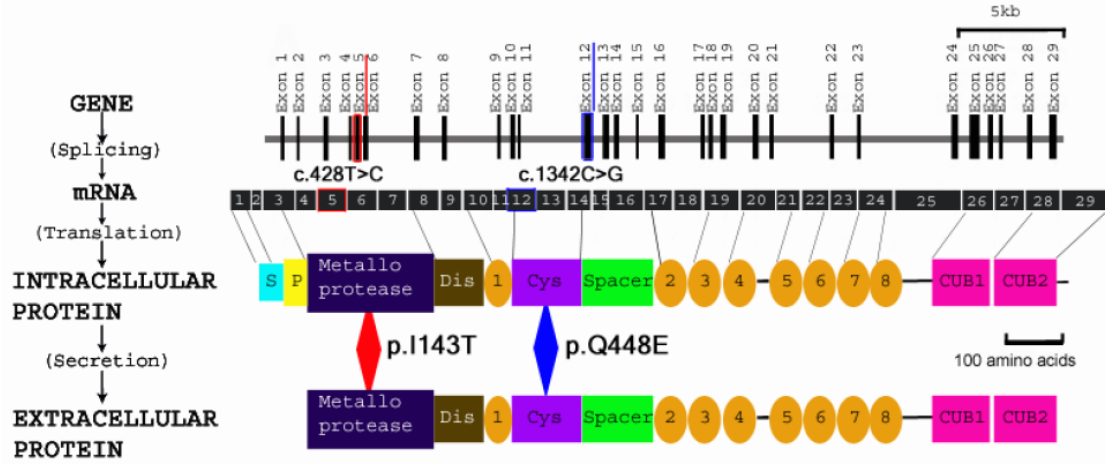


Patient 2

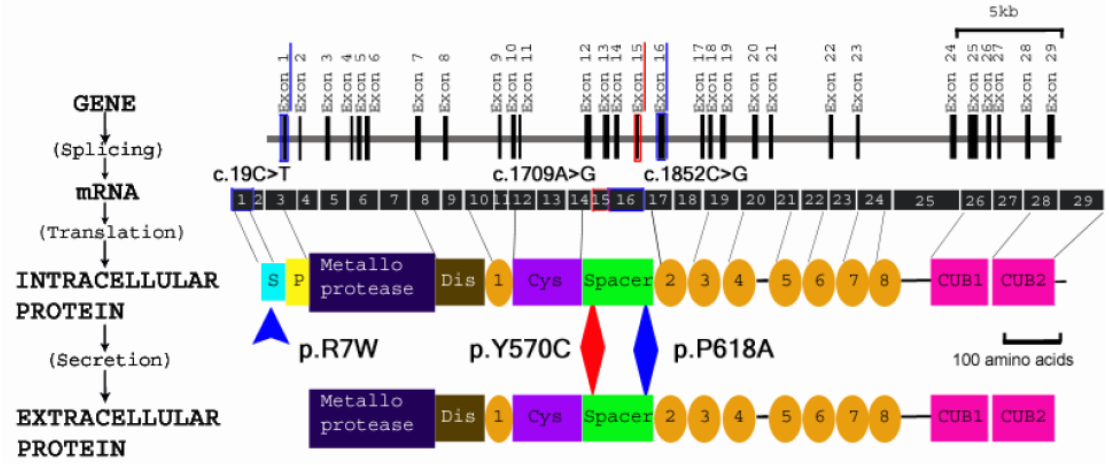


Patient 3

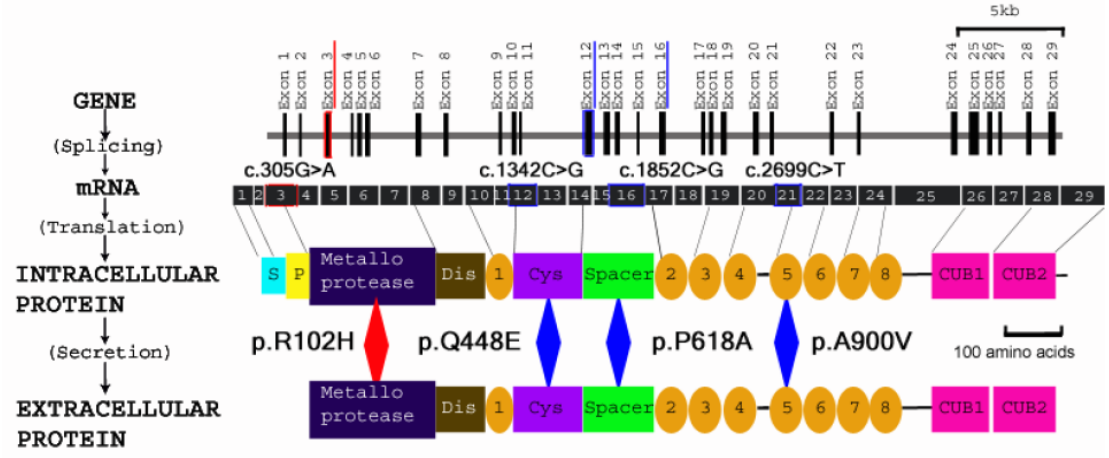


**Figure 3-3 Location of *ADAMTS13* mutations and polymorphisms in the *ADAMTS13* gene, mRNA and protein in patients 1, 2 and 3**

Image adapted from: (Zheng *et al*, 2001).

## 3.2 *In silico* analysis of mutations and polymorphisms

Conservation of the amino acids affected by mutations in the three patients was investigated by aligning the protein sequence of human ADAMTS13 with either the protein sequence of ADAMTS13 in other animals (ADAMTS13 orthologs) or with the protein sequence of other human ADAMTS proteins (ADAMTS13 paralogs). Results are shown in Figure 3-4 and Figure 3-5, in the regions affected by these amino acids. The amino acids affected by mutations in the patients are highlighted in yellow.

All three mutations are highly conserved in ADAMTS13 orthologs (Figure 3-4). The Y (tyrosine) residue at position 570 (patient 2) is also conserved in ADAMTS paralogs. The I (isoleucine) residue at position 143 (patient 1) is present in most ADAMTS13 proteins but is replaced with a valine (V) residue in ADAMTS 1, 4, 5, 8 and 15 (Figure 3-5). Both isoleucine and valine are neutral amino acids whereas threonine (T) is polar.

The conservation of the R (arginine) in ADAMTS paralogs is more variable. An R is present in ADAMTS 4, 13, 17, 19; a histidine (H) residue in ADAMTS1, 5, 6, 9, 15; an asparagine (N) in ADAMTS 3, 8, 14, 20; a serine in ADAMTS 7, 12; a threonine in ADAMTS 16, 18; a leucine in ADAMTS2 and a glutamine in ADAMTS 10. All of these amino acids are polar.

**p.I143**

```
Taeniopygia 166 VAGPDVYLYHREDTERYILANLNIGAELLRDASLGAHFRVHLMQMLVLREPEAEVNITTN 225
Gallus      30  VAGPDVYMYHQEDTERYILTNLNIGAELLRDASLGAHFRVHLMQMLVLREPEVNVNITTN 89
Bos         73  AVGPDVHRTHGEETERYVLTNLNMGSELLRDPSLGAQFRVHLVKMVILTQPEDAPEITAN 132
Ovis        179 AVGPDVQRTHGEETERYVLTNLNMGSELLRDPSLGAQFRVHLVKMVILTQPEDAPKITAN 238
Gorilla     91  AVGPDVFQAHQEDTERYVLTNLNIGAELLRDPSLGAQFRVHLVKMVILTEPEGAPNITAN 150
Pan         91  AVGPDVFQAHQEDTERYVLTNLNIGAELLRDPSLGAQFRVHLVKMVILTEPEGAPNITAN 150
ADAMTS13    87  AVGPDVFQAHQEDTERYVLTNLNIGAELLRDPSLGAQFRVHLVKMVILTEPEGAPNITAN 146
Nomascus    89  AVGLMSFQAHQEDTERYVLTNLNIGAELLRDPSLGAQFRVHLVKMVILTEPEGAPNITAN 148
Pango       87  AVGPDVFQAHQEDTERYVLTNLNIGAELLRDPSLGAQFRVHLVKMVILTEPEGAPNITAN 146
Papio       89  AVGPDVFQAHQEDTERYVLTNLNIGAELLRDPSLGAQFRVHLVKMVILTEPEGAPNITAN 148
Callithrix  85  AVGPDVFQAHQEDTERYVLTNLNIGAELLRDPSLGVQFRVHLVKMVILTEPE-------- 136
Saimin      87  AVGPDVFQAHQEDTERYVLTNLNIGAELLRDPSLGAQFRVHLVKMVILTEPESAPNITAN 146
Otolemur    71  AVGPDVYQAHQEDTERYVLTNLNIGSELLRDPSLGTQFQMHLVKMVILREPQDAPNITAN 130
Mus         89  AVGPDVSRAHQEDTERYVLTNLNIGSELLRNPSLGVQFQVHLVKLITLSDSESTPNITAN 148
Cricetulus  89  AVGPDVYQVHQEDTERYVLTNLNIGSKLLRDPSLGAQFQVHLVKLIILSDSESIPNITTN 148
Cava        87  AVGPDVHQAHQEDTERYVLTNLHIGSDLLRDPSLGVQVQVYLVKLLILTEPEDAPNITAN 146
Canus       237 AVGPDVYQAHQEDTERYVLTNLNMGSELLRDPSLGAQFQVHLVKMVILTQPEDAPNITAN 296
Felis       228 AVGPDVYQAHQEDTERYVLTNLNMGSELLRDPSLGTQFQVHLVKMVTLTQPEDAPNITAN 287
Ailuropoda  182 AVGPDVYQAHQEDTERYVLTNLNTGSELLRDPSLGAQFRVHLVKLVILTQPEDAPNITAN 241
Equus       78  AVGPDVYQAHQDDTERYVLTNLNMGSELLRDPSLGAQFRVHLVKMVILTRPEDAPDITAN 137
Sarcophilus 194 VVGHDVYEYHKEDTERYILTNLNIGAELLRDISIGVPFRVHLIKMIILTEPEAGLNITTN 253
Danio       68  VVGPDVYEVHRQDTERYILTNLNIASELLRDVTLGANIRVHLVRMIILTEPEPDIQISEN 127
```

**p.Y570**

```
Taeniopygia 594 HLCVMGSCRA----FGCDGQMGSRKAMDACKVCGGENSTCTEVSGSYTEG-KAKEYVTFL 648
Gallus      457 HLCVAGSCRA----FGCDGQMNSKRAMDSCKVCGGDNTTCMEVSGSYTEG-KAKEYVTFL 511
Bos         510 RLCVSGSCRT----FGCDGRMDSGQVRDVCQVCGGDNSTCQPQSGSFTAG-RAREYVTFL 564
Ovis        549 SLCVSGSCRT----FGCDGRMDSGQVRDVCQVCGGDSSTCRPQNGSFTAG-RAREYVTFL 603
Gorilla     524 SLCVSGSCRT----FGCDGRMDSQQVWDRCQVCGGDNSTCSPRKGSFTAG-RAREYVTFL 578
Pan         478 SLCVSGSCRT----FGCDGRMDSQQVWDRCQVCGGDNSTCSPRKGSFTAG-RAREYVTFL 532
ADAMTS13    520 SLCVSGSCRT----FGCDGRMDSQQVWDRCQVCGGDNSTCSPRKGSFTAG-RAREYVTFL 574
Nomascus    511 SLCVSGSCRT----FGCDGRMDSQQVQDACQVCGGDNSTCSPQKGSFTAG-RAREYVTFL 565
Pango       548 SLCVSGSCRVRHVHLRCDGRMDSQQVWDACQVCGGDNSTCSPRKGSFHSWQSERKYVTFL 607
Papio       522 SLCVSGSCRT----FGCDGRMDSQQVRDMCQVCGGDNSTCSPRNGSFTAG-RAREYVTFL 576
Callithrix  500 SLCVSGSCRT----FGCDGRMDSQQVWDVCHVCGGDNSTCSPRKGSFTAG-KAGEYVTFL 554
Saimin      485 SLCVSGSCRT----FGCDGRMDSQQVWDACHVCGGDNSTCSPRKGSFTAG-RAGEYVTFL 539
Otolemur    504 SLCVSGSCRT----FGCDGRMDSQQMWDVCQVCGGDNSTCSPQNGSFTDG-RAKEYVTFL 558
Mus         525 SLCLLGSCRT----FGCDGRMDSQKVWDACQVCGGDNSTCSSRNGSFTAG-RAREYVTFL 579
Cricetulus  525 SLCVLGSCRT----FGCDGRMDSQKVWDVCQVCGGDNSTCSSQNGSFTGG-RAREYVTFL 579
Cava        521 SLCVLGSCRM----FGCDGRMDSQQVWDVCQVCGGDNSTCSLQNGSFTGG-AAREYVTFL 575
Canus       671 SLCMLGSCKT----FGCDGRMDSQQVRDVCQVCGGDNSTCSPQNGSFTAG-RAREYVTFL 725
Felis       650 SLCVSGSCRT----FGCDGRMDSQQVRDACQVCGGDNSTCSPRNGSFTAG-RAREYVTFL 704
Ailuropoda  603 SLCVLGSCRT----FGCDGRMDSPQVRDVCQVCGGDNSTCSPRNGSFTAG-RAREYVTFL 657
Equus       512 SLCVSGHCRT----FGCDGRMDSQQVRDVCQVCGGDNSTCSRQSGSFTAG-RAREYVTFL 566
Sarcophilus 623 NLCVMGRCRA----FGCDGGMDSGYVKDVCQVCGGDNTTCSKVSGFYSGG-KAQEYVTFL 677
Danio       496 SACLSGKCQL----FGCDGALHSGKVEDVCGVCGGNGSTCHLISNTYSGG-KAGEYVTFL 550
```

**p.R102**

```
Taeniopygia 166 VAGPDVYLYHREDTERYILANLNIGAELLRDASLGAHFRVHLMQMLVLREPEAEVNITTN 225
Gallus      30  VAGPDVYMYHQEDTERYILTNLNIGAELLRDASLGAHFRVHLMQMLVLREPEVNVNITTN 89
Bos         73  AVGPDVHRTHGEETERYVLTNLNMGSELLRDPSLGAQFRVHLVKMVILTQPEDAPEITAN 132
Ovis        179 AVGPDVQRTHGEETERYVLTNLNMGSELLRDPSLGAQFRVHLVKMVILTQPEDAPKITAN 238
Gorilla     91  AVGPDVFQAHQEDTERYVLTNLNIGAELLRDPSLGAQFRVHLVKMVILTEPEGAPNITAN 150
Pan         91  AVGPDVFQAHQEDTERYVLTNLNIGAELLRDPSLGAQFRVHLVKMVILTEPEGAPNITAN 150
ADAMTS13    87  AVGPDVFQAHQEDTERYVLTNLNIGAELLRDPSLGAQFRVHLVKMVILTEPEGAPNITAN 146
Nomascus    89  AVGLMSFQAHQEDTERYVLTNLNIGAELLRDPSLGAQFRVHLVKMVILTEPEGAPNITAN 148
Pango       87  AVGPDVFQAHQEDTERYVLTNLNIGAELLRDPSLGAQFRVHLVKMVILTEPEGAPNITAN 146
Papio       89  AVGPDVFQAHQEDTERYVLTNLNIGAELLRDPSLGAQFRVHLVKMVILTEPEGAPNITAN 148
Callithrix  85  AVGPDVFQAHQEDTERYVLTNLNIGAELLRDPSLGVQFRVHLVKMVILTEPE-------- 136
Saimin      87  AVGPDVFQAHQEDTERYVLTNLNIGAELLRDPSLGAQFRVHLVKMVILTEPESAPNITAN 146
Otolemur    71  AVGPDVYQAHQEDTERYVLTNLNIGSELLRDPSLGTQFQMHLVKMVILREPQDAPNITAN 130
Mus         89  AVGPDVSRAHQEDTERYVLTNLNIGSELLRNPSLGVQFQVHLVKLITLSDSESTPNITAN 148
Cricetulus  89  AVGPDVYQVHQEDTERYVLTNLNIGSKLLRDPSLGAQFQVHLVKLIILSDSESIPNITTN 148
Cava        87  AVGPDVHQAHQEDTERYVLTNLHIGSDLLRDPSLGVQVQVYLVKLLILTEPEDAPNITAN 146
Canus       237 AVGPDVYQAHQEDTERYVLTNLNMGSELLRDPSLGAQFQVHLVKMVILTQPEDAPNITAN 296
Felis       228 AVGPDVYQAHQEDTERYVLTNLNMGSELLRDPSLGTQFQVHLVKMVTLTQPEDAPNITAN 287
Ailuropoda  182 AVGPDVYQAHQEDTERYVLTNLNTGSELLRDPSLGAQFRVHLVKLVILTQPEDAPNITAN 241
Equus       78  AVGPDVYQAHQDDTERYVLTNLNMGSELLRDPSLGAQFRVHLVKMVILTRPEDAPDITAN 137
Sarcophilus 194 VVGHDVYEYHKEDTERYILTNLNIGAELLRDISIGVPFRVHLIKMIILTEPEAGLNITTN 253
Danio       68  VVGPDVYEVHRQDTERYILTNLNIASELLRDVTLGANIRVHLVRMIILTEPEPDIQISEN 127
```

**Figure 3-4 Alignment of human ADAMTS13 with ADAMTS13 orthologs**

**p.I143**

```
ADAMTS1    295  ------------HPSIRNSVSLVVVKILVIHDEQKGPEVT-SNAALTLRNFCNWQKQ--- 338
ADAMTS4    255  ------------HPSIRNPVSLVVTRLVILGSGEEGPQVG-PSAAQTLRSFCAWQRG--- 298
ADAMTS15   255  ------------HPSILNPINIVVVKVLLLRDRDSGPKVT-GNAALTLRNFCAWQKK--- 298
ADAMTS8    256  ------------HPSIKNSINLMVVKVLIVEDEKWGPEVS-DNGGLTLRNFCNWQRR--- 299
ADAMTS5    304  ------------HASIENHIRLAVVKVVVLGDKDKSLEVS-KNAATTLKNFCKWQHQ--- 347
ADAMTS9    330  ------------DPSIGNLININIVIVNLIVIHNEQDGPSIS-FNAQTTLKNFCQWQHS--- 373
ADAMTS20   296  ------------DPSIGNLIHIVVVKLVMIHREEEGPVIN-FDGATTLKNFCSWQQT--- 339
ADAMTS3    294  ------------DESLGVHINVVLVRMIMLGYAKSISLIERGNPSRSLENVCRWASQ--- 338
ADAMTS14   297  ------------DESLGVHINIALVRLIMVGYRQSLSLIERGNPSRSLEQVCRWAHS--- 341
ADAMTS2    304  ------------DESLGAHINVVLVRIILLSYGKSMSLIEIGNPSQSLENVCRWAYL--- 348
ADAMTS6    288  ------------DSSLGNVVNIIVARLIVLTEDQPNLEIN-HHADKSLDSFCKWQKSILS 334
ADAMTS10   277  ------------DSSLGSTVNILVTRLILLTEDQPTLEIT-HHAGKSLDSFCKWQKSIVN 323
ADAMTS7    280  ------------DPSIGNPIHITIVRLVLLEDEEEDLKIM-HHADNTLKSFCKWQKSINM 326
ADAMTS12   284  ------------NPSIGNAIHIVVVRLILLEEEEQGLKIV-HHAEKTLSSFCKWQKSINP 330
ADAMTS16   328  ------------DGTIGGNINIAIVGLILLEDEQPGLVIS-HHADHTLSSFCQWQSGLMG 374
ADAMTS18   331  ------------DGTIGSDINVVVVSLILLEQEPGGLLIN-HHADQSLNSFCQWQSALIG 377
ADAMTS17   270  ------------HQSLGIKINIQVTKLVLLRQRPAKLSIG-HHGERSLESFCHWQNEEYG 316
ADAMTS19   363  ------------HKSLGVQVNLRVIKLILLHETPPELYIG-HHGEKMLESFCKWQHEEFG 409
ADAMTS13   117  ------------DPSLGAQFRVHLVKMVILTEPEGAPNIT-ANLTSSLLSVCGWSQT--- 160
```

**p.Y570**

```
ADAMTS1    714  ---------------------------------CGVCGGNGSTCKKISGSVTSA--KPGY 738
ADAMTS4    675  ---------------------------------CMVCGGDGSGCSKQSGSFRKF--RYGY 699
ADAMTS15   672  ---------------------------------CGVCGGDNKSCKKVTGLFTKP--MHGY 696
ADAMTS8    679  ---------------------------------CGVCGGKGNSCRKVSGSLTPT--NYGY 703
ADAMTS5    721  ---------------------------------CGVCGGDNSSCTKIVGTFNKK--SKGY 745
ADAMTS9    742  ---------------------------------CGVCGGDNSSCKTVAGTFNTV--HYGY 766
ADAMTS20   710  ---------------------------------CGVCGGDNSSCKTITGVFNSS--HYGY 734
ADAMTS3    702  ---------------------------------CGVCGGDNSHCRTVKGTFTRTPRKLGY 728
ADAMTS14   703  ---------------------------------CGVCGGDNSHCRTVKGTLGKASKQAGA 729
ADAMTS2    712  ---------------------------------CGVCGGDNSHCKVVKGTFTRSPKKHGY 738
ADAMTS6    706  ---------------------------------CRVCGGDGSTCDAIEGFFNDSLPRGGY 732
ADAMTS10   695  ---------------------------------CRVCGGDGSACETIEGVFSPASPGAGY 721
ADAMTS7    687  ---------------------------------CGVCHGNGSTCHTVSGTFEEAE-GLGY 712
ADAMTS12   691  ---------------------------------CGVCLGDGSSCQTVRKMFKQKE-GSGY 716
ADAMTS16   735  ---------------------------------CGVCNGNNSACTIHRGLYTKHHHTNQY 761
ADAMTS18   738  ---------------------------------CGVCKGDNSTCKFYKGLYLNQHKANEY 764
ADAMTS17   689  ---------------------------------CGVCSGDGKTCHLVKGDFS-HARGT-- 712
ADAMTS19   779  ---------------------------------CGVCNGNGKSCKIIKGDFN-HTRGAGY 804
ADAMTS13   545  ---------------------------------CQVCGGDNSTCSPRKGSFTAG-RAREY 570
```

**p.R102**

```
ADAMTS1    256  SHR------------YVETMLVADQSMAEFHG-SGLKHYLLTLFSVAARLYK-------- 294
ADAMTS4    216  LSR------------FVETLVVADDKMAAFHG-AGLKRYLLTVMAAAAKAFK-------- 254
ADAMTS15   216  IPR------------YVETLVVADESMVKFHG-ADLEHYLLTLLATAARLYR-------- 254
ADAMTS8    217  EAR------------FVETLLVADASMAAFYG-ADLQNHILTLMSVAARIYK-------- 255
ADAMTS5    265  RAR------------QVELLLVADASMARLYG-RGLQHYLLTLASIANRLYS-------- 303
ADAMTS9    291  YPR------------FVEVLVVADNRMVSYHG-ENLQHYILTLMSIVASIYK-------- 329
ADAMTS20   257  YPR------------YIEIMVTADAKVVSAHG-SNLQNYILTLMSIVATIYK-------- 295
ADAMTS3    254  NDY------------NIEVLLGVDDSVVRFHGKEHVQNYLLTLMNIVNEIYH-------- 293
ADAMTS14   257  GSY------------SIEVLLVVDDSVVRFHGKEHVQNYVLTLMNIVDEIYH-------- 296
ADAMTS2    264  DDY------------NIEVLLGVDDSVVQFHGKEHVQKYLLTLMNIVNEIYH-------- 303
ADAMTS6    248  IER------------FVETLVVADKMMVGYHGRKDIEHYILSVMNIVAKLYR-------- 287
ADAMTS10   237  RER------------YVETLVVADKMMVAYHGRRDVEQYVLAIMNIVAKLFQ-------- 276
ADAMTS7    240  KEK------------WVETLVVADAKMVEYHGQPQVESYVLTIMNMVAGLFH-------- 279
ADAMTS12   244  KER------------WVETLVVADTKMIEYHGSENVESYILTIMNMVTGLFH-------- 283
ADAMTS16   276  RHKRSLLRSHRNEELNVETLVVVDKKMMQNHGHENITTYVLTILNMVSALFK-------- 327
ADAMTS18   281  RPRRSAGKSQKG--LNVETLVVADKKMVEKHGKGNVTTYILTVMNMVSGLFK-------- 330
ADAMTS17   231  EHT------------VETLVVADADMVQYHGAEAAQRFILTVMNMVYNMFQ-------- 269
ADAMTS19   324  EYN------------IETVVVADPAMVSYHGADAARRFILTILNMVFNLFQ-------- 362
ADAMTS13   78   GILH------------LELLVAVGPDVFQAHQ-EDTERYVLTNLNIGAELLR-------- 116
```

**Figure 3-5 Alignment of human ADAMTS13 with ADAMTS13 paralogs**

The likely effect of the three mutations on ADAMTS13 was analysed using three computational based tools: SNPs3D, Polyphen 2 and SIFT (Table 3-3). The SNPs3D prediction is based on homology analysis and the predicted effect that the amino acid substitutions have on the stability of the protein. A positive score by the SNPs3D database indicates non-deleterious, and a negative score, a deleterious mutation. The Polyphen2 prediction is based upon phylogenetic and structural information. SIFT is a sequence homology based tool, which produces scores ranging from 0 to 1 for each substitution analysed. The amino acid substitution is predicted to be damaging if the score is ≤0.05 and tolerated if the score is >0.05.

The p.R102H and p.I143T mutations were predicted to be harmful by one of the three tools (p.R102H: polyphen2, p.I143T: SIFT). The p.Y570C mutation on the other hand was predicted to be harmful by all three computational tools.

| | | **SNPs3D svm profile** | **Polyphen2** | **SIFT** | |
|---|---|---|---|---|---|
| | | | | Score | Prediction |
| **Mutation** | p.R102H | 1.70 | Probably damaging | 0.28 | Tolerated |
| | p.I143T | 0.67 | Benign | 0.04 | Damaging |
| | p.Y570C | -1.50 | Probably damaging | 0 | Damaging |

**Table 3-3 *In silico* analysis of *ADAMTS13* mutations and polymorphisms**

## 3.3 Site directed mutagenesis

Site directed mutagenesis was used to create three expression vectors, each containing a single different *ADAMTS13* gene mutation. Other missense mutants that were predicted to cause a type 1 deficiency were also created (p.T196I, p.R409W, p.A596V, p.C754R and p.C977F). These mutants were to be analysed in the same way as the other type 1 mutants (p.I143T and p.Y570C). However because of initial problems in the development of some of the experiments, it was decided that it would be better to focus on a smaller number of mutants in more detail. There were initial problems with site directed mutagenesis which was rectified with the use of DMSO. In addition, there were problems with the immunofluorescent staining of ADAMTS13 expressing cells as discussed in the next chapter.

## 3.4 Transient transfection

After site directed mutagenesis, transient transfection of the WT and mutant *ADAMTS13* cDNA was carried out in order to assess the effect of the mutations on the secretion of ADAMTS13 compared to WT. After transient transfection there was some slight variability between experiments. Consequently the results from each experiment were normalised to take into account slight differences in the efficiency of transfection between plated cells. Cells were co-transfected with a plasmid expressing *Renilla* luciferase as described (Chapter 2.3.3).

Initial transient transfection experiments were carried out using electroporation in Milan. In the UK transient transfection was carried out using PEI but the yield from cells expressing WT was lower with PEI (approximately 2-3 fold lower) compared to electroporation.

Levels of expression of both WT and mutant ADAMTS13 protein were compared after transient transfection with either branched chain or linear PEI. Linear PEI appeared to work better, with branched PEI giving approximately 60% of the value obtained with linear PEI.

Preliminary experiments were carried out using an electroporator in another department (using an exponential and square wave method of electrical discharge) however the results were poor. Experiments were carried out using Lipofectamine (Life technologies) (as opposed to PEI) for transfection, but the results were similar to PEI. Linear PEI was therefore used for subsequent experiments.

## 3.5 Western blot analysis of cell lysate and supernatant samples

After transient transfection cell lysate and supernatant samples were harvested and analysed using western blotting. All three mutant proteins were detectable within cell lysate samples using western blotting (Figure 3-6). With the p.R102H mutant, levels were similar to WT. With the p.I143T and p.Y570C mutants, levels were slightly increased compared to WT. Therefore, all the mutants were synthesised within the cell and the mutations did not prevent protein synthesis. The mutant proteins were of

a similar molecular weight to WT ADAMTS13, which showed the expected size (~190kDa).

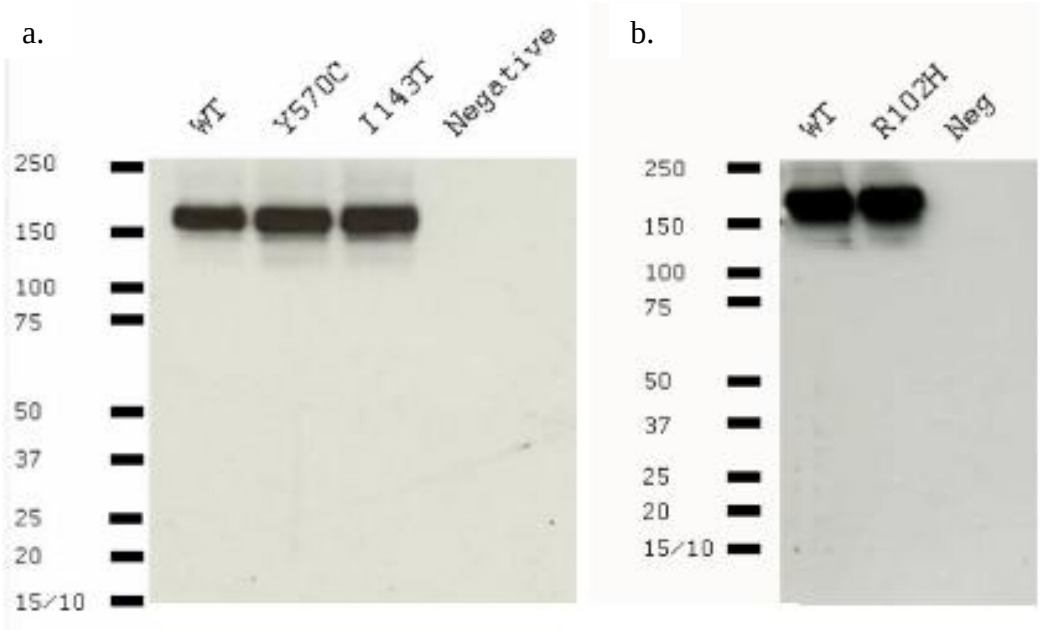


**Figure 3-6 Cell lysate samples harvested after transient transfection of WT and mutant protein**

Samples loaded according to transfection efficiency, representative of n=3. ADAMTS13 expected size ~190kDa.

With the p.I143T and p.Y570C mutants, no ADAMTS13 could be detected using western blotting in supernatant samples (concentrated ~20 fold). On the other hand the p.R102H mutant could be detected in the cell supernatant, but at a reduced level compared to WT (Figure 3-7). Again WT and mutant protein detected in the supernatant were of the expected molecular weight.

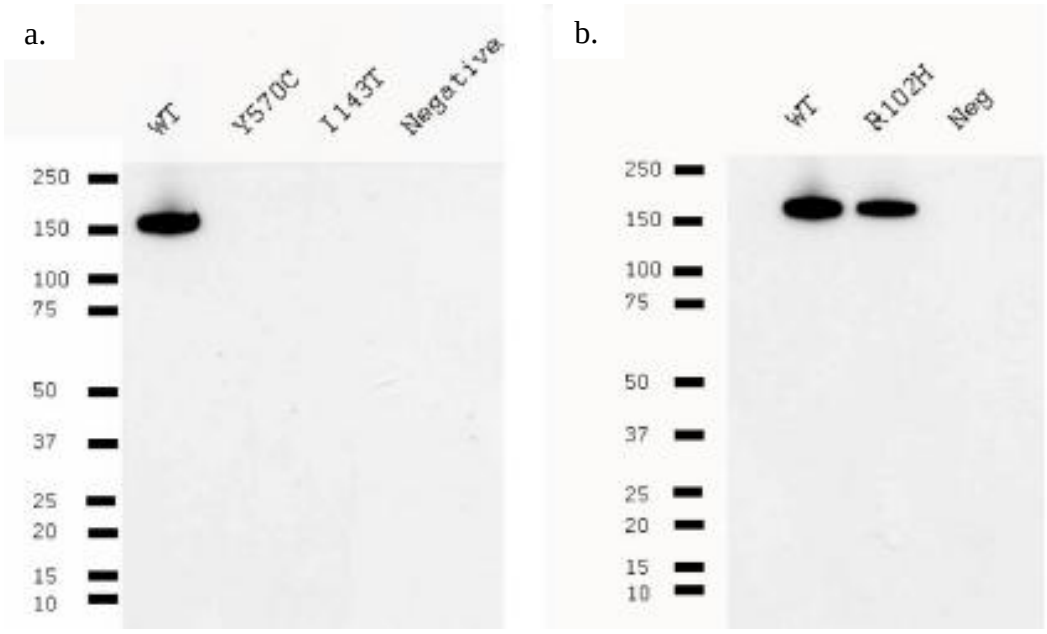


**Figure 3-7 Supernatant samples harvested after transient transfection of WT and mutant protein**

Samples loaded according to transfection efficiency, representative of n=3. ADAMTS13 expected size ~190kDa.

## 3.6 ADAMTS13 antigen and activity in supernatant samples

| Construct | Average ADAMTS13 antigen (% of WT±SD) | Average ADAMTS13 activity (% of WT±SD) | Specific activity (% of WT±SD) |
|---|---|---|---|
| p.I143T | Undetectable | Undetectable | - |
| p.Y570C | Undetectable | Undetectable | - |
| p.R102H | 30±0.016 | 15±0.42 | 50±1.4 |

**Table 3-4 ADAMTS13 antigen and activity in supernatant samples after transient transfection**

Results from n=3 experiments. The specific activity was calculated by dividing the activity levels by antigen levels.

Using an ELISA, ADAMTS13 antigen was undetectable in the p.I143T and p.Y570C mutants and no ADAMTS13 activity could be detected within supernatant samples using FRETS-VWF73 substrate for analysis (detection limit 2.5% of PNP) (Figure 3-4). In contrast the p.R102H mutation led to reduced secretion, with low levels of antigen in the supernatant (30%±0.016 of WT, mean±SD). The quantity of ADAMTS13 antigen in the patient plasma was 42%±5.4 of normal (mean±SD), which is slightly below the normal range. The *in vitro* results show a reduction in the secretion of this mutant similar to that seen in the patient plasma.

## 3.7 Discussion

The three mutations studied affected the secretion of ADAMTS13. The p.I143T and p.Y570C mutations severely affected the secretion whereas the p.R102H mutation partially affected the secretion. The result obtained for the p.R102H mutation is similar to previously published results (Camilleri *et al*, 2012). The specific activity of the p.R102H mutant was on average 50%±1.4 of WT, suggesting that this mutation also affects the activity of ADAMTS13.

The severe defect in secretion observed with the p.I143T and p.Y570C mutations correlated with the undetectable antigen levels in the plasma of patients 1 and 2. The partial defect in secretion observed with the p.R102H mutant correlated with the detectable ADAMTS13 antigen in the plasma of patient 3.

The p.I143T mutation present in patient 1 and the p.R102H mutation present in patient 3 are within the metalloprotease domain of ADAMTS13. The metalloprotease domain is necessary for the cleavage of VWF and contains the catalytic site. Although both mutations were situated within this domain they had different effects on the secretion of ADAMTS13: the p.I143T mutation severely affecting the secretion and the p.R102H mutation partially affecting the secretion. Both of these mutations were also predicted to be damaging by only one of the three computational tools, highlighting the importance of *in vitro* expression in understanding the effect of mutations on the secretion and activity of ADAMTS13.

The isoleucine (I) residue at position p.143 in ADAMTS13 is highly conserved in ADAMTS13 orthologs and partially conserved in ADAMTS13 paralogs. Although ADAMTS proteins have different functions, the N-terminal region of the proteins are similar, (Figure 1-5), all having a signal peptide, propeptide, metalloprotease, disintegrin, TSP1, cysteine-rich and spacer domain. The C-terminal region of these proteins are thought to play an important role in determining function (Huxley-Jones *et al*, 2005). In ADAMTS 1, 4, 5, 8 and 15 the isoleucine (I) 143 residue is replaced with a V (valine) residue, both isoleucine and valine are neutral while the amino acid threonine (T) is polar. Isoleucine and threonine have different properties and so

the replacement of this amino acid with threonine may have a detrimental effect on the overall structure of ADAMTS13.

The p.I143 residue is situated between two glycosylation sites p.N142 and p.N146. The consensus sequence for N glycosylation is N-X-T/S, the amino acid 143 therefore is at position X in the consensus sequence for the p.N142 glycosylation site (Zheng *et al*, 2001). This mutation therefore is unlikely to affect the consensus glycosylation signal. However it may potentially affect the quaternary structure of ADAMTS13 and thus indirectly affect the glycosylation recognition site.

A mutation at the location of amino acid 102 has previously been identified in a patient (Levy *et al*, 2001), where the amino acid arginine (R) was replaced with cysteine (C) and the patient presented during the neonatal period. This is in contrast to patient 3 whose arginine (R) residue was replaced by a histidine (H) residue and presented during adulthood. This particular amino acid is localised in the N terminal region of an alpha helix in the metalloprotease domain of ADAMTS13 (Pozzi *et al*, 2012) and is predicted to stabilise a negative cluster formed by surrounding negatively charged amino acids. The authors proposed that the substitution of the positively charged arginine residue with the neutral cysteine residue would strongly destabilise the metalloprotease domain. In contrast to cysteine, histidine and arginine are positively charged. In some ADAMTS paralogs the R residue at position 102 is replaced by a H residue. The replacement of arginine by histidine in patient 3 at this position may not destabilise the metalloprotease domain to the extent that cysteine is predicted to. Perhaps this could explain the difference in disease onset between patient 3 and the patient reported by Levy *et al* (Levy *et al*, 2001).

The p.Y570C mutation present in patient 2 is located within the spacer domain of ADAMTS13. The crystal structure of the disintegrin, TSP-1, cysteine-rich and spacer domain of ADAMTS13 has been solved (Akiyama *et al*, 2009). The spacer domain plays an important role in VWF binding (Gao *et al*, 2006;Jin *et al*, 2010). Antibody epitopes in some patients with acquired TTP have been analysed and a large proportion of them have antibodies directed towards the spacer domain (Luken *et al*, 2005;Klaus *et al*, 2004). The tyrosine amino acid at position 570 is highly conserved in ADAMTS13 orthologs and paralogs. This amino acid forms part of the surface

aromatic cluster on the outer surface of a β sheet (β2) which is also highly conserved. Cysteine is not an aromatic compound and in fact the spacer domain contains so cysteine residues (Akiyama *et al*, 2009). The properties of Y and C are quite different: Y is neutral, C is polar.

I went on to characterise these mutants further, using different techniques to analyse the type 1a mutants, p.I143T and p.Y570C (Chapters 4-6) and the type 2 mutant (Chapter 7). With the type 1a defects I studied elements of the protein secretion pathway to understand how these mutations affected secretion, analysing the subcellular localisation of WT and mutant protein. With the type 2 the goal was to understand why the secreted protein was not functionally active. This was studied through biochemical characterisation of WT and mutant protein.

# Chapter 4 Immunofluorescence (type 1a mutants)

## 4.1 Introduction

The p.I143T and p.Y570C mutations identified in patients 1 and 2 appeared to cause a severe defect in the secretion of ADAMTS13 (Chapter 3) as no ADAMTS13 antigen was present in the supernatant of cells expressing these proteins (Figure 3-7). I characterised these mutants further in order to understand at which stage of the secretion pathway the defect occurred, by investigating the localisation of the mutant proteins in the ER and Golgi.

### 4.1.1 Protein secretion

The ER consists of an organised network of branching tubules and flattened sacs which extend throughout the cytosol, (Figure 4-1).

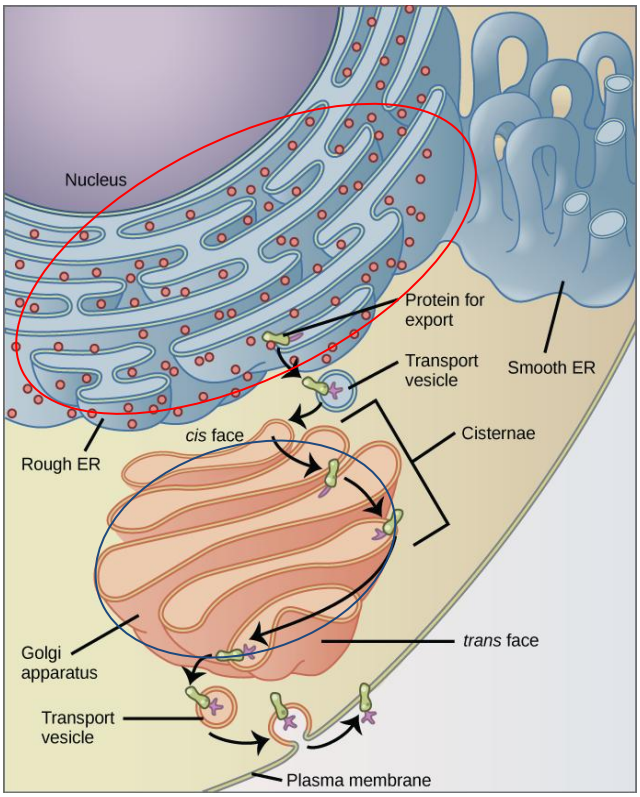


**Figure 4-1 Secreted proteins travel through the ER and Golgi**

Image from (URL: http://cnx.org/content/m45432/latest/?collection=col11551/latest, accessed 17th June 2014). ER is circled in red and the Golgi circled in blue.

Newly synthesised proteins are directed to the ER membrane by a signal sequence (signal peptide region in ADAMTS13) (Figure 1-5) and cross over the ER membrane from the cytosol to enter the ER biosynthetic-secretory pathway. The ribosome responsible for synthesising the protein is directly attached to the ER membrane, these membrane bound ribosomes coat the surface of the ER, creating regions known as the rough ER (Figure 4-1) (Alberts *et al*, 2002).

Within the ER, asparagine (N) linked glycosylation of proteins takes place which involves the transfer of an oligosaccharide to the side chain $NH_2$ group of an asparagine amino acid (Alberts *et al*, 2002). ADAMTS13 has ten potential N-glycosylation sites (N-X-T/S) (Zheng *et al*, 2001), with nine of these identified within plasma and recombinant ADAMTS13 (Sorvillo *et al*, 2014). The N-linked oligosaccharide structures may be further modified during the journey of the protein through the ER.

After transport and modification in the ER, proteins are packaged into small transport vesicles which bud off from the ER and enter the Golgi. The Golgi consists of a collection of flattened, membrane-enclosed cisternae. Each Golgi stack has two distinct faces a *cis* face (entry face) and a *trans* face (exit face). The Golgi acts as a sorting and dispatching centre for products of the ER (Figure 4-1).

Further modification of N-linked oligosaccharides may take place in the Golgi. O-linked glycosylation may also occur in the Golgi which involves the transfer of oligosaccharides to the hydroxyl group on the side-chain of a serine, threonine or hydroxyllysine amino acid (Alberts *et al*, 2002). Seven of the eight TSP repeats of ADAMTS13 contain the consensus sequence CSX(S/T)CG for O-glycosylation (Zheng *et al*, 2001), six of these have been identified within plasma and recombinant ADAMTS13 (Sorvillo *et al*, 2014;Ricketts *et al*, 2007).

C-mannosylation of proteins may also occur which involves the attachment of an alpha-mannosyl group to the C-2 atom of the first W in the consensus sequence WXXW. ADAMTS13 has two putative C-mannosylation sites (Sorvillo *et al*, 2014). Transport vesicles destined for the plasma membrane normally leave the *trans* Golgi through the process of exocytosis.

### 4.1.2 Principles of confocal microscopy

When fluorescent images are viewed with a conventional microscope the entire specimen is bathed with light and the image can be viewed directly by eye. The fluorescence in the specimen away from the region of interest interferes with the resolution of structures in focus. The theoretical resolution of a widefield light microscope is 0.2μm (Paddock, 1999).

The lateral and axial resolution is improved when a confocal microscope is used. Illumination/excitation is achieved by scanning a more focused beam of light (normally from a laser) across the specimen. After the fluorochromes have absorbed the light from the laser they produce fluorescence. A fraction of the emitted fluorescence is collected through the confocal pinhole and imaged onto the detector. The detection pinhole reduces the fluorescence from out of focus planes which causes blurred images when a conventional microscope is used (Paddock, 1999).

## 4.2 Development of immunofluorescence protocol

During the development of the immunofluorescence protocol, cells were stained and viewed using a fluorescence microscope (Zeiss AxioImager A1) to check that the immunofluorescent staining had worked. After the immunofluorescence protocol was successfully set up images were then taken using a confocal microscope. Primary monoclonal antibodies were used whenever possible as opposed to polyclonal antibodies to reduce potential non-specific binding. Antibody dilutions were optimised by testing two or three different dilutions based upon the values recommended by the manufacturer or dilutions previously used (Garagiola *et al*, 2008;Palla *et al*, 2009).

### 4.2.1 Culturing cells

Initially cells were grown on microscope slides and were subsequently fixed and permeabilised. Regions rich in cells were selected for incubation with antibodies for immunofluorescent labelling. However cells were subsequently grown on cover glasses to improve resolution. The optical properties of the cover glasses were matched to the properties of the objective lens of the confocal microscope to

minimise refraction as light passed to and from the samples. Additionally growing the cells on cover glasses increased the specimen depth that could be probed as the cover glasses are much thinner than microscope slides.

### 4.2.2 Mounting media

At first cells were mounted with glycerol after they had been incubated with the relevant antibodies for immunofluorescent labelling. A commercial agent with anti-fading and anti-photobleaching properties (Vectashield) was later used as an alternative mounting media. This enabled the slides to be stored in the fridge for a longer period of time before being viewed and also increased the length of time the immunofluorescent signal could be detected when viewed under the microscope (Florijn *et al*, 1995;Longin *et al*, 1993). This mounting media also contained DAPI which produces blue fluorescence when bound to DNA and excited at the correct wavelength. As a result the nuclei of cells could also be viewed under the microscope which helped to identify the cells.

Cover glasses were sealed with clear nail polish to prevent the appearance of air bubbles in the samples, air drying and prevented the movement of the slide and cover glass during storage as the mounting media Vectashield does not harden.

### 4.2.3 Minimising non-specific background staining

In initial experiments, cells were blocked with 3% BSA overnight. There appeared to be a lot of background staining when the cells were viewed under the microscope. To the blocking buffer 0.3M glycine was added to bind to free aldehyde groups introduced during fixation. Paraformaldehyde reacts and cross links protein molecules but lots of free aldehyde groups remain. This tissue bound free aldehyde will combine with any amino acid group available to them including those of the primary and secondary antibody. Adding glycine to the buffer blocks these free aldehyde groups (Renshaw, 2007). Cells were also incubated for half an hour with goat and rabbit serum before antibody incubation to prevent non-specific binding of the antibodies. The secondary antibodies used were produced in goat (Cy3) and rabbit (FITC).

### 4.2.4 Detection of the ER

Staining for the *cis* Golgi worked well. In early experiments the ER was detected using a mouse monoclonal anti-BiP antibody (BD Biosciences). BiP (binding immunoglobulin protein) is an ER resident protein which aids the movement of proteins post-translationally into the ER. It also acts as a chaperone recognising incorrectly folded proteins that have not yet assembled into their final oligomer complex (Alberts *et al*, 2002). This antibody has been previously used to immunofluorescently label the ER in ADAMTS13 expressing COS cells (Garagiola *et al*, 2008;Palla *et al*, 2009). After attempting immunofluorescent labelling with this antibody, the ER was not visible. The concentration of both this antibody (primary antibody) and the secondary detection antibody was varied (Cy3 antibody) and a new vial of the antibody was also tested but it still didn't work.

An alternative antibody which binds to another ER resident protein, PDI was tested instead. PDI catalyses the oxidation of free sulfhydryl (SH) groups on cysteine amino acids to form disulphide bonds, in proteins (Alberts *et al*, 2002). A mouse polyclonal antibody, TXNDC5 (Abcam) was tested but the ER could still not be detected.

Both of these antibodies were directed towards two different proteins which localise within the ER, but neither appeared to bind to their target protein. Studies have shown that different permeabilisation methods are suitable for different proteins (Melan & Sluder, 1992). Cells had been previously permeabilised with Triton X-100. This permeabilisation technique appeared to work as the *cis* Golgi and ADAMTS13 within the cell could be viewed using immunofluorescence, but not the ER. In order to investigate whether alternative methods of cell permeabilisation could enable the ER to be detected, cells were permeabilised after fixation as follows:

i. 20 minutes in 0.2% saponin

ii. 10 minutes in 0.5% saponin

iii. 4 minutes in 0.1% Triton X-100 and 0.05% SDS

iv. 10 minutes in 0.2% Triton X-100

Cells were permeabilised using one of these methods and were then incubated with one of the following antibodies: i. anti-BiP ER; ii. anti-PDI TXNDC5 ER or iii. anti-GM130 *cis* Golgi primary antibody. Cells were incubated with the anti-GM130 *cis* Golgi antibody as a control as this antibody had worked in previous experiments. Anti-mouse Cy3 conjugated antibody was used as the secondary antibody.

The results are shown in Figure 4-2. Neither of these permeabilisation techniques enabled detection of the ER using immunofluorescence with either the anti-BiP (a) or anti-PDI TXNDC5 antibody (c). The figure demonstrates the inability of the antibodies to detect the ER as the images appear red where the nuclei of the cells are (column two versus column three). The ER should be distinct from the nucleus (Figure 4-1). All three permeabilisation techniques worked successfully in cells incubated with the anti-GM130 *cis* Golgi antibody.

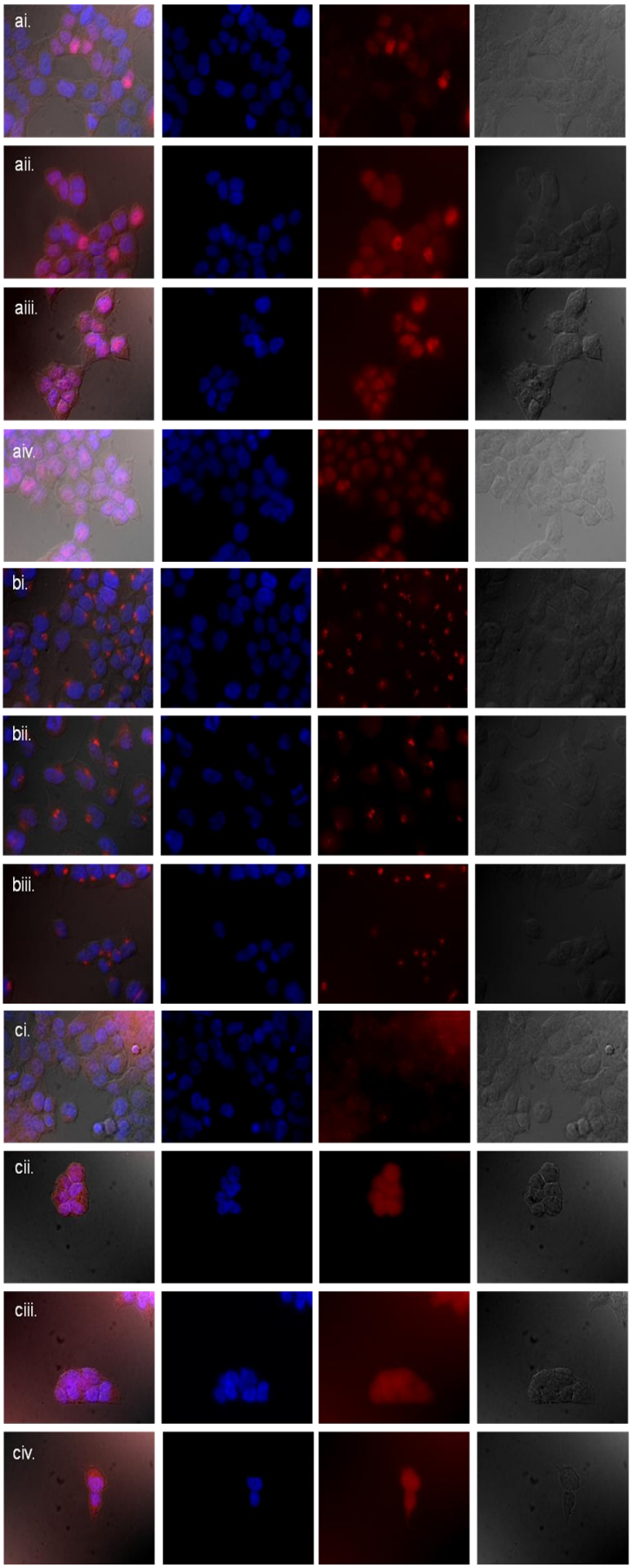
ai.
aii.
aiii.
aiv.
bi.
bii.
biii.
ci.
cii.
ciii.
civ.

**Figure 4-2 Permeabilisation of cells with Triton X-100 or saponin**

HEK 293T cells were stained with either one of three primary antibodies: anti-BiP (a), anti-GM130 (b) or anti-PDI (c). Cells were all fixed with 4% paraformaldehyde and then either permeabilised with 0.2% saponin (i) 0.5% saponin (ii) 0.1% Triton X-100 containing 0.05% SDS (iii) or 0.2% Triton X-100. Cells were permeabilised with 0.2% Triton X-100 (condition iv) for incubation with anti-GM130 antibody. This was successful but images were not taken at the time of the experiment as this permeabilisation technique had been previously used to immunofluorescently label the *cis* Golgi successfully numerous times. The second column shows immunofluorescent labelling of the nuclei, third staining for the ER or Golgi, fourth shows images of the cells taken using differential interference contrast. The first column shows a merged image of the three channels. Cells were viewed using a fluorescent microscope with a 100x oil immersion objective.

In another attempt to detect the ER a different secondary antibody was used to detect both primary antibodies (a goat anti-mouse FITC conjugated antibody, Life Technologies). The ER could still not be detected. Another antibody was used to detect the ER. This antibody was an anti-PDI antibody (RL90, Abcam). This antibody was successfully used to stain the ER. Images are shown in Figure 4-3. Different concentrations of the antibody were used to optimise the quantity to use as shown in the Figure.

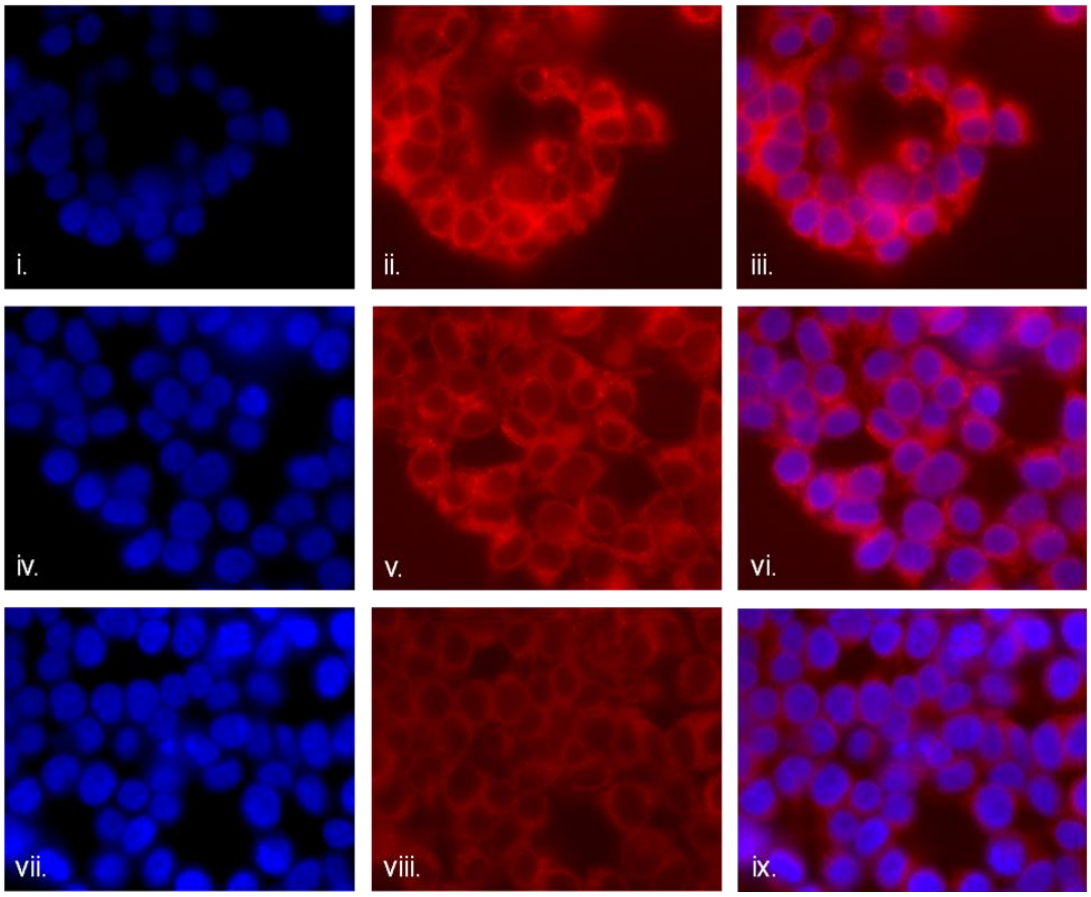


**Figure 4-3 Optimisation of antibody concentrations**

The figure shows immunofluorescent labelling of HEK293T cells with mouse monoclonal RL90 PDI-ER marker. Three different concentrations of the antibody are shown. Top row shows immunofluorescent labelling of the ER with primary antibody RL90 diluted 1/100, second row with primary antibody RL90 diluted 1/200, and bottom row immunofluorescent labelling with RL90 primary antibody diluted 1/400. First column shows immunofluorescent labelling of nuclei, second column labelling using the primary antibody RL90 and the last column a merged image of columns one and two. For all three samples the secondary antibody (Cy3) was diluted 1/200. Cells were viewed with a x100 oil immersion objective using a fluorescent microscope.

The anti-BiP antibody has been previously used to immunofluorescently label the ER (Garagiola *et al*, 2008;Palla *et al*, 2009), however this was carried out in COS cells (not in HEK293T cells) which may explain why it could not be detected in these experiments. The TXNDC5 antibody detects a protein belonging to the PDI family and is an ER associated protein. After using this antibody and finding it was unable to recognise the ER in HEK293T cells, I tried to understand a possible reason for this. I found that although this protein belongs to the PDI family it is not necessarily expressed by all cells (Sullivan *et al*, 2003). So perhaps the protein that the antibody

binds to is not expressed in HEK 293T cells, possibly explaining why it could not be detected.

After the antibody concentrations were optimised for detection of the ER, cells expressing ADAMTS13 were incubated with antibodies directed towards ADAMTS13 and either the ER or *cis* Golgi as described (Chapter 2.8.2). Figure 4-4 shows cells expressing WT ADAMTS13 viewed with a fluorescent microscope stained for the ER or *cis* Golgi and ADAMTS13. An image of the cell was also taken under brightfield light using differential interference contrast (no v). This figure demonstrates that the ER and ADAMTS13 occupy the majority of the cell.

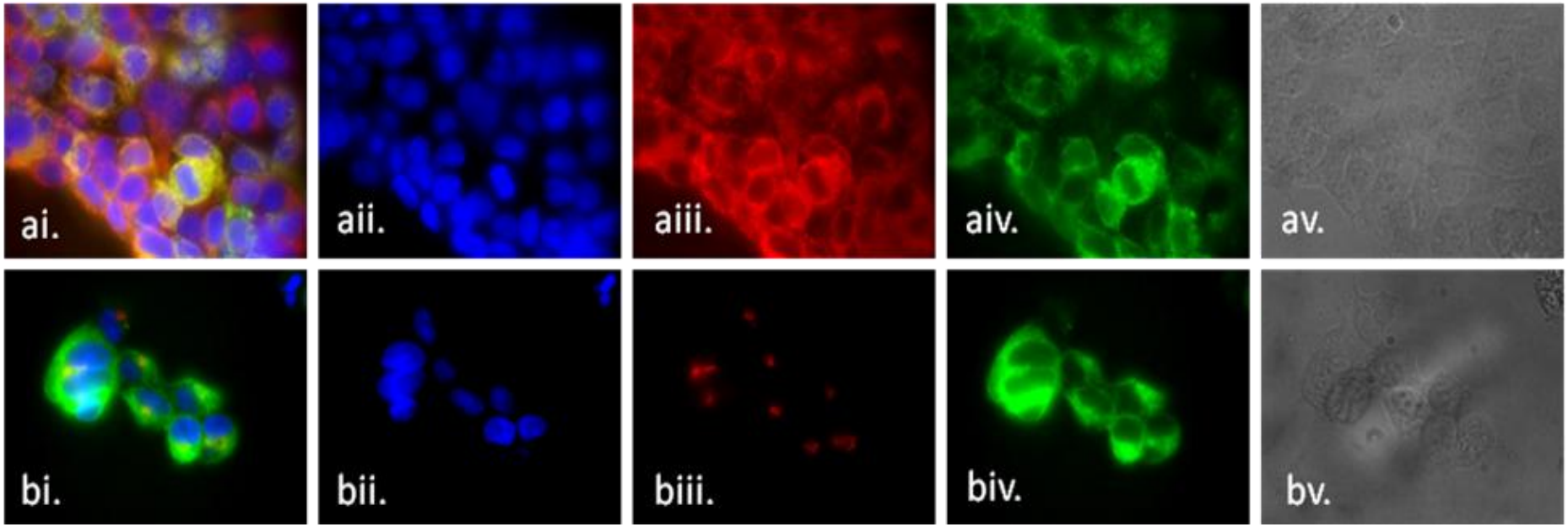


**Figure 4-4 Localisation of ADAMTS13 in the ER and *cis* Golgi**

Images were taken with a fluorescent microscope with a 100x oil immersion objective. Stable line cells expressing WT ADAMTS13 were incubated with an anti-V5 ADAMTS13 antibody and either an anti-ER (using RL90 anti-PDI antibody) (a) or anti-*cis* Golgi antibody (b). Immunofluorescent labelling of nuclei (ii). ER/Golgi (iii), ADAMTS13 (iv) and a merged image of channels ii, ii and iv are shown in i. Images v shows the cells viewed using brightfield differential interference contrast, to demonstrate immunofluorescence labelling in relation to the cell volume.

## 4.3 Localisation in the ER

Confocal microscopy demonstrated that WT ADAMTS13 and both mutants localised within the ER. Representative images are shown in Figure 4-5. Three images from three different experiments are shown for WT and mutant ADAMTS13. WT ADAMTS13 can be seen to localise within the ER throughout the whole of the cell as depicted by the yellow/orange regions (Figure 4-5). The mutants also localised extensively within the ER.

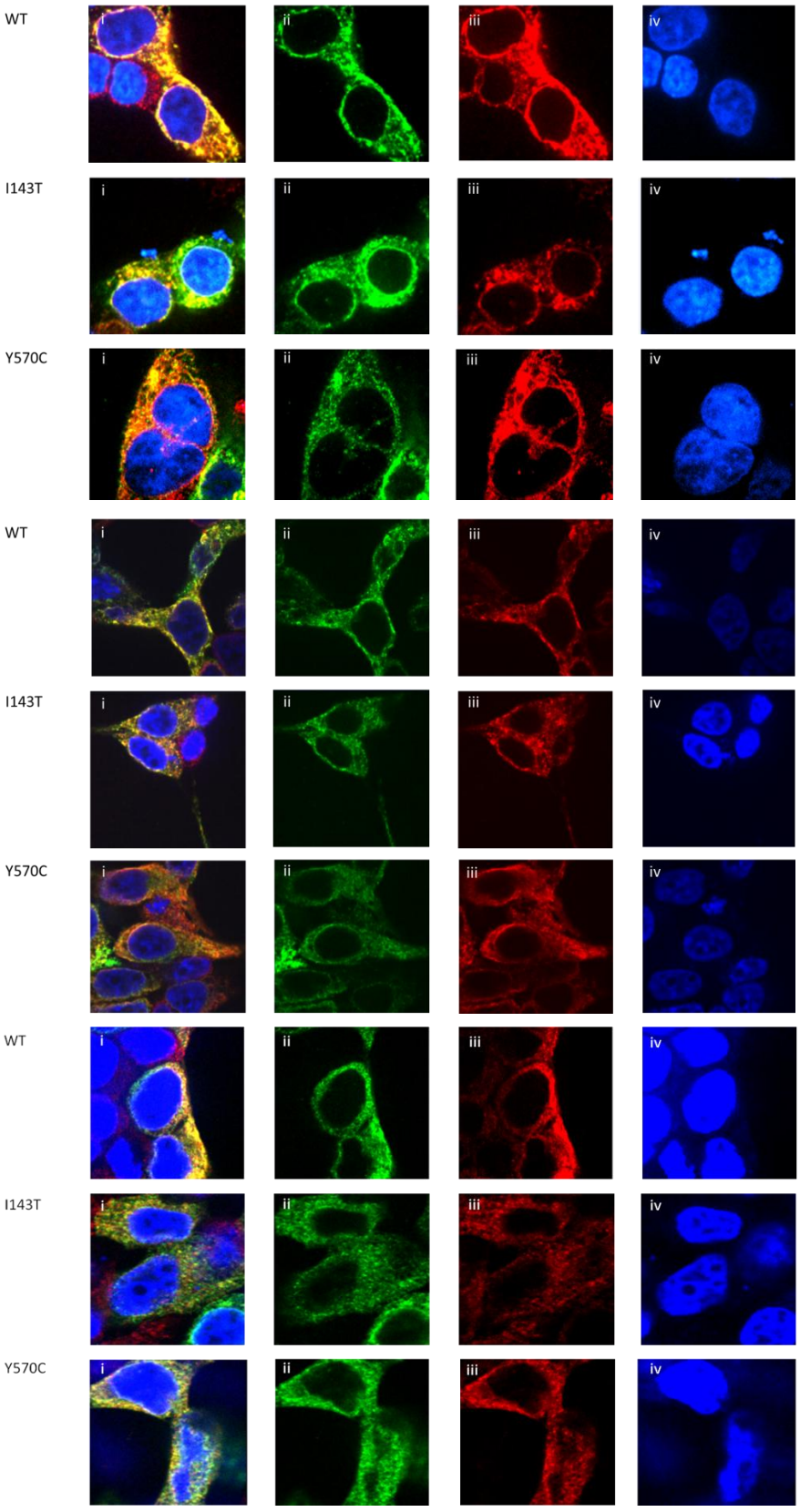


**Figure 4-5 Localisation of WT or mutant (p.I143T, p.Y570C) ADAMTS13 within the ER of the cell**

ADAMTS13 is shown in green (ii), ER in red (iii) nucleus in blue (iv) and a merged image of all channels is shown on the far left to demonstrate colocalisation (i). The image appears yellow/orange where there is colocalisation of ADAMTS13 with the ER. Cells shown in the first panel were viewed

with a magnification of x100 with an oil immersion objective; cells in the second and third panel were viewed with a magnification of x63 with an oil immersion objective. Each panel shows cells from three separate experiments.

## 4.4 Localisation in the *cis* Golgi

Confocal microscopy demonstrated that WT and mutant ADAMTS13 localised within the *cis* Golgi of the cell. Representative images are shown in Figure 4-6. Images from three separate experiments are shown for both WT and mutant ADAMTS13. The mutants appeared to localise less extensively within the *cis* Golgi compared to WT.

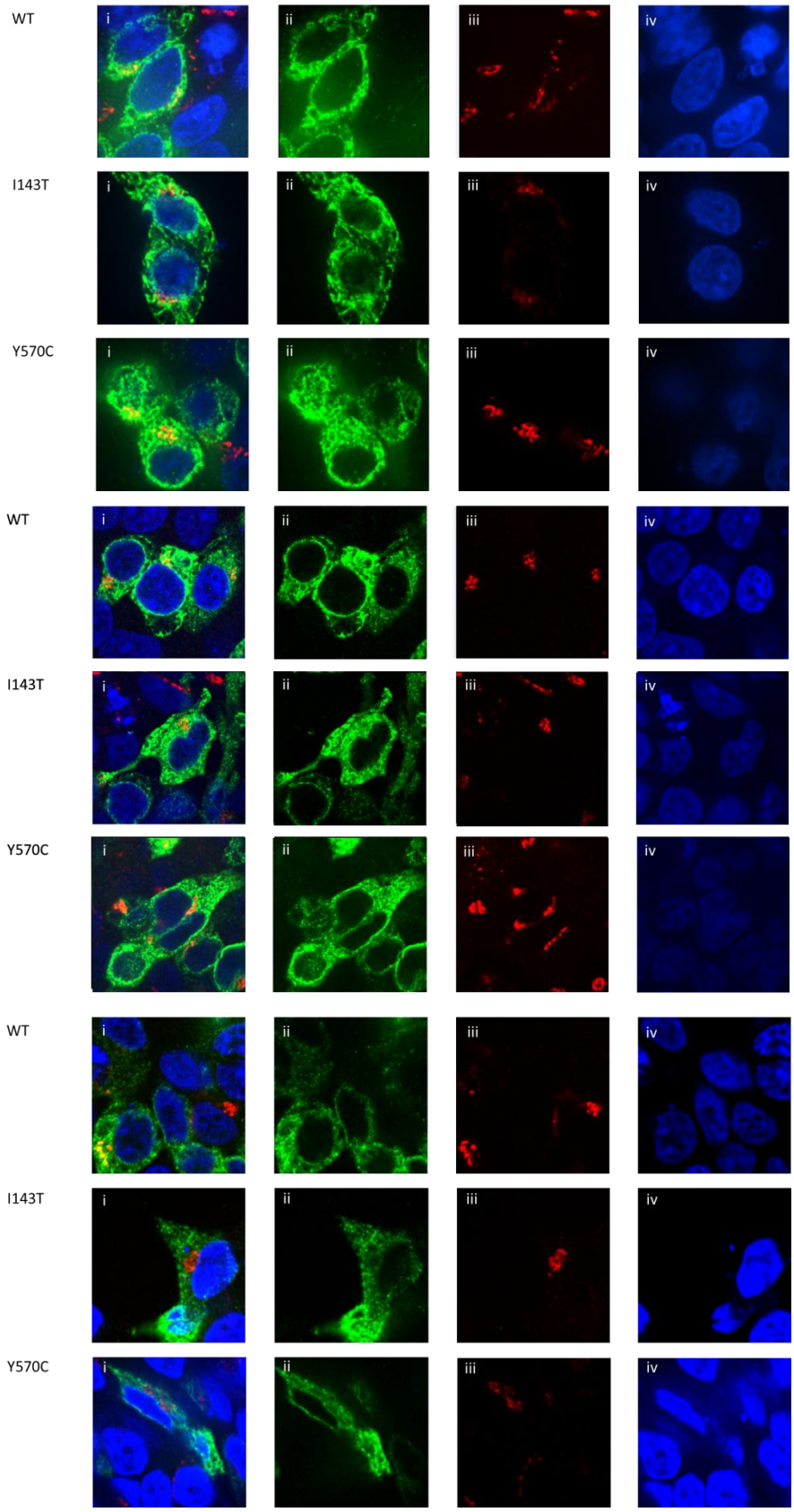


**Figure 4-6 Localisation of WT or mutant (p.I143T, p.Y570C) ADAMTS13 within the *cis* Golgi of the cell**

ADAMTS13 is shown in green (ii), cis Golgi in red (iii) nucleus in blue (iv) and a merged image of all channels is shown on the far left to demonstrate colocalisation (i). The image appears yellow/orange where there is colocalisation of ADAMTS13 with the Golgi. Cells in the first panel were viewed with

a magnification of x100 with an oil immersion objective, cells in the second and third panel with a magnification of x63 with an oil immersion objective. Each panel shows cells from three separate experiments.

## 4.5 Localisation in the *trans* Golgi

As there appeared to be some localisation of the mutants in the *cis* Golgi of the cell I wondered if there was also localisation in the *trans* Golgi of the cell which is the area of exit from the Golgi (Figure 4-1). Cells were stained as described in methods (Chapter 2.8.2) except that the *trans* Golgi antibody (anti-p.230, Abcam) was used. The results from one experiment are shown in Figure 4-7. The localisation of the mutants in the *trans* Golgi appeared to be similar to the localisation of the mutants within the *cis* Golgi.

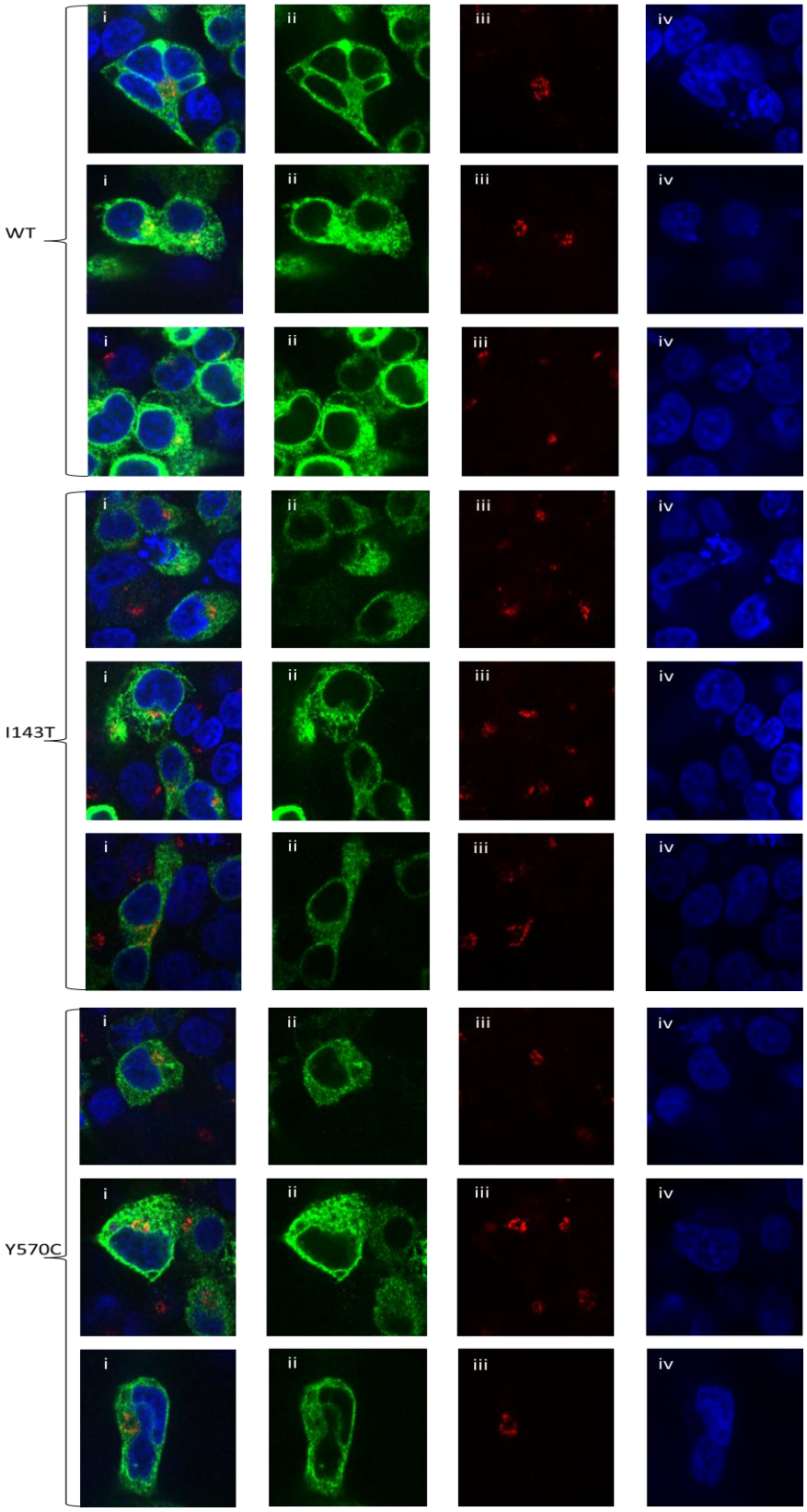


**Figure 4-7 Localisation of WT or mutant (p.I143T, p.Y570C) ADAMTS13 within the *trans* Golgi of the cell**

Three different fields of view from one experiment are shown. ADAMTS13 is shown in green (ii), *trans* Golgi in red (iii) nucleus in blue (iv) and a merged image of all channels is shown on the far left to demonstrate colocalisation (i). The image appears yellow/orange where there is colocalisation of

ADAMTS13 with the *trans* Golgi. Cells shown were viewed with a magnification of x100 with an oil immersion objective.

## 4.6 Quantitation of ADAMTS13 colocalisation in the *cis* Golgi

There appeared to be some localisation of the mutants in the *cis* Golgi, demonstrated by the merged images of these samples (Figure 4-6). The degree of localisation appeared to be different between WT and mutant ADAMTS13. However this was not something that could be easily attained from the images. The degree of colocalisation was quantified using the quantitation tool, which is part of the Volocity software. This software was associated with the confocal microscope that was used to acquire the images.

The presence of yellow/orange regions within a merged image (which is often used to demonstrate colocalisation) is highly dependent upon the relative signal intensities produced by the fluorochromes, collected in both channels. A merged image will only give a reliable representation of colocalisation when both images exhibit similar grey level dynamics (Bolte & Cordelieres, 2006). Image processing can match the fluorescent signal intensities of both fluorochromes; however as a result of this the image produced does not reflect the true stoichiometry of the molecules imaged. The demonstration of colocalisation in the 2D plane (as in Figure 4-5, Figure 4-6 and Figure 4-7) also does not reflect the 3D nature of the sample. Additionally estimating the degree of colocalisation using merged images alone can introduce subjective bias.

### 4.6.1 Images used for analysis

Saturated voxels (voxels which have the maximum value for a given channel) should not be used for quantitation analysis, as these voxels have lost information. Some of the voxels in the images previously taken could not be used for the quantitation analysis as they contained saturated voxels. As a result new transfections were performed and cells were subsequently immunofluorescently labelled for ADAMTS13 and the *cis* Golgi. New images (with unsaturated voxels) were taken; images from three separate experiments were used for quantitation analysis.

Measuring the degree of colocalisation within the whole image captured from a particular field of view would not have accurately measured the degree of colocalisation as not all cells expressed ADAMTS13. Those cells which were not expressing the vector (ADAMTS13) would have stained red for Golgi but not green for ADAMTS13. Therefore, analysis was restricted to regions containing ADAMTS13 expressing cells.

### 4.6.2 Global Pearson Correlation Coefficient

The four main coefficients that are produced by the Volocity quantitation tool after analysis are the thresholded Pearson correlation coefficient (TPCC) the global Pearson correlation coefficient (GPCC), the Manders overlap coefficient 1 ($M_1$) and Manders overlap coefficient 2 ($M_2$).

The use of the PCC to quantify the degree of colocalisation between two signals produced by two different fluorochromes was introduced by Manders *et al* (Manders *et al*, 1992). The formula is shown in Equation 4-1.

$$PCC = \frac{\sum (R_i - R_{aver})(G_i - G_{aver})}{\sqrt{\sum (R_i - R_{aver})^2 . \sum (G_i - G_{aver})^2}}$$

Pearson's correlation coefficient

$R_i$=intensity in red channel

$R_{aver}$=average intensity in red channel

$G_i$=intensity in green channel

$G_{aver}$=average intensity in green channel

**Equation 4-1 Pearson correlation coefficient as described by (Manders *et al*, 1992)**

Image taken from (URL: http://cellularimaging.perkinelmer.com/pdfs/manuals/VolocityuserGuide.pdf Volocity user manual, accessed 17th June 2014). The PCC shown above is the GPCC.

This PCC is the GPCC as it includes all voxels in the analysis regardless of whether these voxels correspond to background or an object. This coefficient is highly dependent upon noise, variation in fluorescence intensities between both channels or heterogeneous colocalisation relationships throughout the sample (Bolte & Cordelieres, 2006). Evaluation of this coefficient alone may therefore be ambiguous.

### 4.6.3 Colocalisation coefficient $M_1$ and $M_2$

Manders *et al* introduced two further coefficients to be used for analysis, the overlap coefficients $M_1$ and $M_2$ (Manders *et al*, 1993). The GPCC gives a value of the correlation between the intensity distributions of the components but the overlap between the intensities can be represented by $M_1$ and $M_2$. The formulas are shown in Equation 4-2 and 3.

$$M_1 = \frac{\sum R_{i,coloc}}{\sum R_i}$$

Overlap coefficient $M_1$

$R_{i,coloc} = R_i$ if $R_i > T_1$ and $G_i > T_2$

Ri = Red intensity if $R_i > T_1$

$R_i$=Pixel intensity of red channel

$G_i$=Pixel intensity of green channel

$T_1$=Threshold for red channel

$T_2$-Threshold for green channel

**Equation 4-2 Manders overlap coefficient $M_1$ (Manders *et al*, 1993)**

Image taken from (URL: http://cellularimaging.perkinelmer.com/pdfs/manuals/VolocityuserGuide.pdf Volocity user manual, accessed 17th June 2014). Manders' original equation has been modified here to include voxels only with values above the threshold.

$$M_2 = \frac{\sum G_{i,coloc}}{\sum G_i}$$

Overlap coefficient $M_2$

$G_{i,coloc} = G_i$ if $G_i > T_2$ and $R_i > T_1$

Gi = Green intensity if $G_i > T_2$

$R_i$=Pixel intensity of red channel

$G_i$=Pixel intensity of green channel

$T_1$=Threshold for red channel

$T_2$-Threshold for green channel

**Equation 4-3 Manders overlap coefficient $M_2$ (Manders *et al*, 1993)**

Image taken from (URL: http://cellularimaging.perkinelmer.com/pdfs/manuals/VolocityuserGuide.pdf Volocity user manual, accessed 17th June 2014). Manders' original equation has been modified here to include voxels only with values above the threshold.

These coefficients provide a measure of the total colocalised intensity of a channel divided by the total intensity for that channel. The coefficients $M_1$ and $M_2$ are not sensitive to differences in signal intensities between different channels (Manders *et al*, 1993), unlike GPCC.

The coefficients shown in Equation 4-2 and Equation 4-3 are modified slightly from Manders original paper (Barlow *et al*, 2010). Manders original equations included all voxels with a value >0 in the analysis. The voxels included in this analysis (and in the Volocity software) are only those voxels with a value above a chosen threshold. This threshold is set to distinguish between voxels representing background and those representing an object of interest. The use of voxels above the threshold to calculate the coefficients $M_1$ and $M_2$ was shown to more accurately describe synthetic and biological data (Barlow *et al*, 2010).

### 4.6.4 Thresholded Pearson Correlation Coefficient

Barlow *et al* proposed that the inclusion of background voxels in the calculation of GPCC generates unrealistically low means, resulting in a disproportionately large number of voxels above the mean and so positive differences from the mean become very large (Barlow *et al*, 2010). The authors introduced TPCC so that only voxels with values above a set threshold were included in the analysis of PCC. GPCC is sensitive to differences in fluorescence intensity but TPCC is not. The authors proposed that $M_1$ and $M_2$ show the extent of correlation but TPCC gives a measurement of the quality of the relationship.

### 4.6.5 Results of analysis

An example scatter plot produced by the software is shown Figure 4-8. Voxels above the threshold in at least one of the channels are plotted on the graph according to the quantity of green ADAMTS13 (x axis) and red Golgi (y axis). Colocalised voxels lie diagonally within the scatter plot.

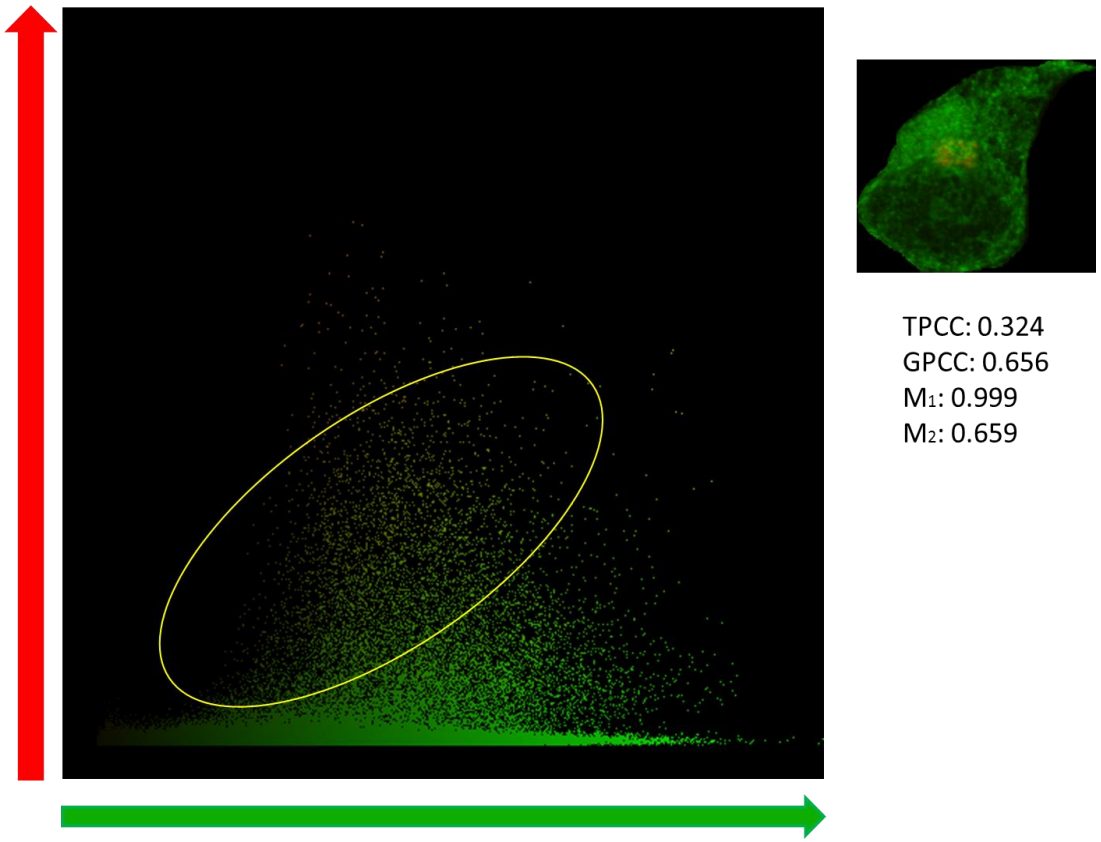


**Figure 4-8 Scatter plot produced by Volocity colocalisation analysis**

An example scatter plot from a WT cell is shown. Voxel values for the green fluorescent protein is plotted along the x axis and voxel values for the red labelled *cis* Golgi is shown along the y axis. Voxels in which there is overlap between the two fluorochromes are circled in yellow. To the right of this an extended view of the cell used for analysis is shown along with the calculated values for TPCC, GPCC, $M_1$ and $M_2$ for that cell.

The data obtained from all the cells analysed are summarised in Figure 4-9. The median values and the 95% CI for these coefficients are shown for both WT and mutant ADAMTS13. The GPCC, TPCC, $M_1$ and $M_2$ values obtained after analysis varied quite a bit for both WT and mutant proteins, as shown by the 95% CI obtained (Figure 4-9). Values for the TPCC and $M_1$ coefficient were lower for both mutants compared to WT. The GPCC and $M_2$ were similar for WT and the p.I143T mutant but slightly higher/lower for the p.Y570C mutant.

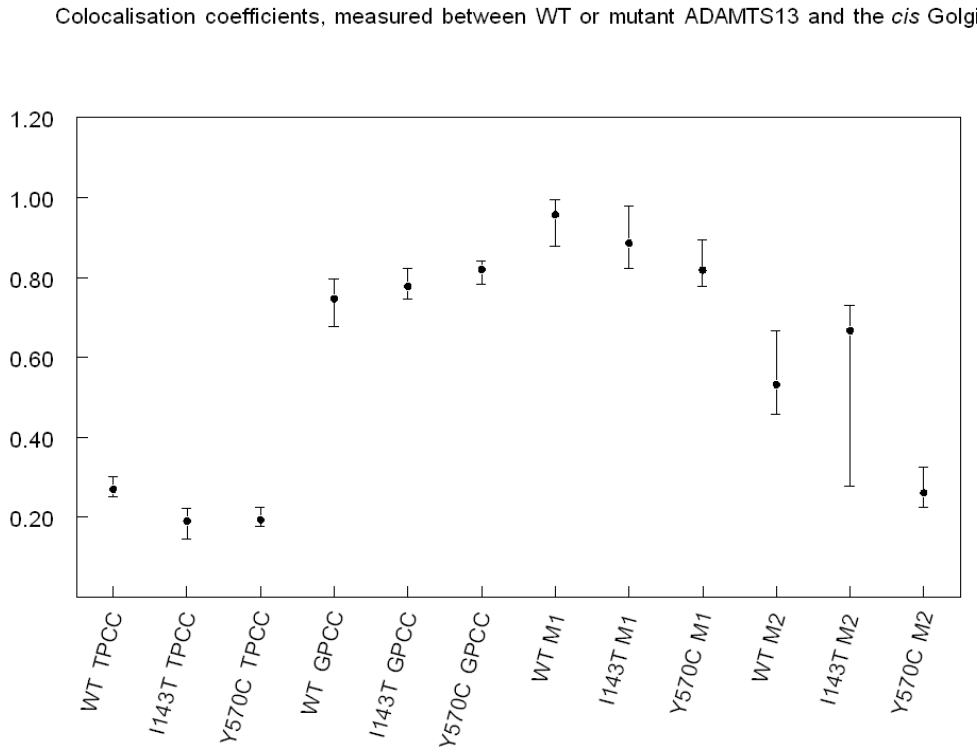


**Figure 4-9 Results obtained after quantitative analysis**

The plot shows median values for the GPCC, TPCC, $M_1$ and $M_2$ coefficients, along with the approximate 95% CI for these coefficients based on the ranked data. The number of cells analysed were: WT (n=35), p.I143T (n=29) and p.Y570C (n=52).

## 4.7 Discussion

### 4.7.1 Summary

ADAMTS13 like other secretory proteins is transported to the ER and Golgi before secretion and has been previously shown to localise within these regions in cells expressing WT ADAMTS13 (Palla *et al*, 2009;Garagiola *et al*, 2008). As the mutant proteins were synthesised in the cells but not secreted, their localisation within the ER and Golgi was investigated in order to determine if these mutants failed to reach either of these regions, preventing their secretion.

Using confocal microscopy, WT and mutant ADAMTS13 were found to localise within the ER. WT and mutant ADAMTS13 also localised within the Golgi. However within the *cis* Golgi mutant ADAMTS13 appeared to localise less extensively than WT. This difference in colocalisation between WT and mutant

ADAMTS13 and the *cis* Golgi was not noticeably apparent from looking at the 2D merged images. Therefore, the degree of colocalisation between WT and mutant ADAMTS13 and the *cis* Golgi was quantified, to confirm that there was a difference.

Colocalisation quantitative analysis showed that less of the total number of red Golgi voxels in the mutants overlapped with the green ADAMTS13 voxels when compared to WT (lower $M_1$ values for the mutant). This was more apparent with the p.Y570C mutant.

With the p.Y570C mutant less of the total green ADAMTS13 voxels overlapped with the red Golgi voxels compared to WT (lower $M_2$ values). The degree of overlap between WT and the p.I143T mutant on the other hand were similar (similar $M_2$ values).

The values obtained for $M_2$ for both WT and mutant ADAMTS13 were lower than those obtained for $M_1$ because the volume of the Golgi is smaller compared to the volume of the cell that ADAMTS13 occupies. Hence a small proportion of the total ADAMTS13 present in the cell will be present in the Golgi (giving a small $M_2$ value) but a large volume of the Golgi is occupied with ADAMTS13 (high $M_1$ value).

The biological implications of the PCC are more difficult to interpret (Manders *et al*, 1993;Bolte & Cordelieres, 2006), but there appeared to be differences between the values for WT and mutant ADAMTS13.

It has been suggested that the GPCC may be affected by a number of factors including differences in fluorochrome intensity and noise (Bolte & Cordelieres, 2006). The proportion of the cell occupied by ADAMTS13 is much greater than the proportion occupied by the Golgi which may affect the GPCC as it has been proposed that differences in the proportion of biological molecules may affect this value (Costes *et al*, 2004). The TPCC seems to be a more reliable value to use (Barlow *et al*, 2010) as it excludes background voxels.

The results for TPCC and GPCC appear to show differing things, in the mutants GPCC is increased whereas with the TPCC this value is decreased. This difference is

due to the inclusion of background pixels in the analysis of GPCC. The values obtained for the TPCC appear to be more sensible than the GPCC. The high values obtained (for both WT and mutant ADAMTS13) for the GPCC suggests that there is a strong correlation between ADAMTS13 and the *cis* Golgi within the cell. However this is not the case as a large amount of the ADAMTS13 is not present in the *cis* Golgi but is present in other regions of the cell such as the ER (Figure 4-5). The lower TPCC values obtained for the mutant compared to WT suggest that although the relationship between ADAMTS13 and the Golgi is weak (low value for WT), it is even weaker for the mutants.

Together these results suggest that less ADAMTS13 occupies the Golgi in cells expressing mutant ADAMTS13 compared to those expressing WT ADAMTS13. This suggests less of the mutant protein is transported to the Golgi compared to WT ADAMTS13.

### 4.7.2 Immunofluorescent staining and imaging

The use of a motorised stage to image multiple random positions would have helped to avoid bias when selecting cells to image. However this process is likely to have taken more time as a motorised stage may select regions which do not contain cells or regions where there are cells not expressing ADAMTS13. The amount of time that the cells were exposed to light was minimised as much as possible to prevent photobleaching.

There are a range of different methods that can be used for fixation and permeabilisation. Inappropriate fixation can cause antigen redistribution and/or reduction in antigenicity. Aldehyde induced fixation can cause changes in the confirmation of proteins and organelles (Neuhaus *et al*, 1998). Glutaraldehyde fixation often reduces antigenicity and increases background autofluorescence (North, 2006) so it is advantageous to fix with paraformaldehyde rather than glutaraldehyde. Fixing with 4% rather than 2% paraformaldehyde in HEK293T and MDCK cells was shown to lead to better protein preservation compared to lower concentrations (Schnell *et al*, 2012).

Methanol, ethanol and acetone are common organic solvents used in immunofluorescent microscopy. They simultaneously fix and permeabilise cells by precipitating proteins and extracting lipids. Fixation with methanol is commonly used for the study of cytoskeletal components, however it can lead cell shrinkage and is not suitable for analysis of soluble proteins (Stadler *et al*, 2010).

Saponin appeared to be able to permeabilise membranes in HEK293T cells successfully (Figure 4-2) to detect the *cis* Golgi but this was not tested with the RL90 ER antibody. Saponin could have been alternatively used as a detergent. Saponin treatment has been shown to produce smaller holes in membranes when compared to Triton -100 exposure (North, 2006).

One of the weaknesses of using transiently transfected cells is that the level of expression in each transfected cell may differ between cells. Both low and high expressing cells were included in the analysis. Low expressing cells can have higher colocalisation (Parmryd *et al*, 2003) possibly because the higher concentrations of fluorescent protein saturate high affinity sites and also occupy sites with lower affinities, whereas lower concentrations are confined to the high affinity sites (Adler *et al*, 2008). Mixed intensity distributions can affect the analysis of the thresholded PCC (Barlow *et al*, 2010). This may explain the variable degree of colocalisation measured between cells in each group (Figure 4-9).

Splitting cells into high and low expressing cells and then analysing them separately may have overcome this problem. Alternatively cells stably expressing the protein could have been used; however stable line cells expressing both of the mutants were not available at the time of analysis.

It has been suggested that live cell imaging should be used in conjunction with the analysis of fixed cells to analyse protein localisation (Schnell *et al*, 2012). With live cell imaging cells are viewed in the '*in vivo*' state and not subject to artefacts which may be introduced in the process of fixation and permeabilisation. However there are also disadvantages of live cell imaging. In live cell imaging, adding a green fluorescent tag to proteins could potentially modify protein function. Phototoxicity and photobleaching are more of a problem in live cell imaging and efforts focus on

keeping the cells alive and behaving in a physiological manner. Approaches to minimise photobleaching in live cell imaging can lead to poorer resolution and reduced signal-to-noise ratios. An issue during time course experiments is focal drift caused by thermal fluctuations in the room. Another challenge is acquiring images fast enough to capture rapid biological events and accurately portray dynamic structures (North, 2006).

The *cis* Golgi was immunofluorescently labelled as this is the site of entry into the Golgi. However it may have been more appropriate to image the whole of the Golgi instead of just the *cis* Golgi. However the results are still valid and show the degree of localisation in the *cis* Golgi.

### 4.7.3 Quantitative analysis

Although quantitative colocalisation analysis tries to overcome some of the problems associated with interpreting merged images, it also has problems associated with it (Bolte & Cordelieres, 2006). Colocalisation can only go as far as indicating that the two proteins are located within close proximity to each other (the same voxel). Due to the limits of resolution, uncertainty about the physical dimensions and location of small objects within the 3D space arise. Fluorochrome distribution may be in the nanometre range whereas the optical microscope's resolution is closer to the micrometre (Bolte & Cordelieres, 2006). A problem that is inherent to all known methods of quantitative colocalisation analysis is that voxels are classified as either colocalised or not colocalised, when in fact voxels are the sum of both colocalised and non-colocalised signals (Costes *et al*, 2004).

The presence of noise within the images can affect colocalisation measurements. This noise may arise during the immunofluorescence labelling procedure and also as a result of image capture. It was found that even in good quality images there was an average discrepancy of about 20% between the measured and corrected colocalisation, due to the presence of noise (Adler *et al*, 2008).

Thresholds for colocalisation analysis were set manually by selecting and cropping cells. This may have introduced bias. However a relatively large number of cells were analysed to try and prevent this bias from affecting the results. Alternatively the

threshold could have been set using automatic thresholding as described by Costes *et al* (Costes *et al*, 2004).

When selecting cells for quantitation the region of interest was selected based upon the ADAMTS13 that was visible. It is possible therefore that the whole cell was not selected but just the regions in which ADAMTS13 was visibly expressed. This region however still encompassed the *cis* Golgi, which is smaller than the total cell volume and the purpose of carrying out the colocalisation, was to measure how much of the ADAMTS13 was within the Golgi. In addition when cells were viewed with the fluorescent microscope in earlier experiments, ADAMTS13 appeared to occupy the majority of the volume of the cell (Figure 4-4).

Alternative methods could have been used to prevent bias in cell selection. A line scan could have been performed in order to identify objects. The limit of an object may be seen as a sudden variation of the voxel intensities. However this method has limitations as structures with a non-uniform fluorescence intensity distribution may lead to an artifactual detection of concentric edges (Bolte & Cordelieres, 2006). Alternatively connexity analysis could have been used (Bolte & Cordelieres, 2006). This process involves the inspection of the neighbouring voxels of the current voxel (reference pixel). All adjacent voxels with intensities above the limit would be considered to be part of the same structure as the reference voxel. Each voxel would then be tagged with a number, with all voxels of the same structure carrying the same tag. A voxel lacking at least one of its neighbours is considered to be at the edge of the structure.

One of the limitations of using PCC for analysis is that it requires that the two populations have a Gaussian distribution which is not required for the Spearman's Rank correlation coefficient (SRC). In addition the PCC is very sensitive to outlying values, whereas those near the mean carry relatively little weight. The SRC is less sensitive to outlying data points and more sensitive to data points closer to the mean (Adler *et al*, 2008). The process of fluorescent image formation and acquisition may include nonlinear components and fluorescent images can have outlying values. When measuring colocalisation in biological samples it was found that the values

reported by the PCC and SRC were broadly similar but some appreciable differences were found (Adler *et al*, 2008).

### 4.7.4 Conclusion

The immunofluorescence and colocalisation analysis results suggested that the p.I143T and p.Y570C mutants localise within the ER and to some extent within the Golgi of the cell. However despite this these mutants are secreted at a severely reduced level (Chapter 3). I went on to investigate whether these mutants were degraded within the cell by either the cell proteasome or lysosomes before they could be secreted (Chapter 5).

# Chapter 5 Proteasome and lysosome inhibition (type 1a mutants)

## 5.1 Introduction

The p.I143T and p.Y570C mutants were synthesised within the cell, localised within the ER and to some extent the Golgi (Chapter 4), but were secreted at a severely reduced level (Chapter 3). I therefore investigated whether these proteins were degraded within the cell either by the cell proteasome or lysosomes.

### 5.1.1 ER quality control mechanisms

The ER provides an environment that is optimised for protein folding and maturation. Within the ER several co-translational and post-translational modifications take place (disulphide bond formation, signal-peptide cleavage and N-linked glycosylation) which are important for correct protein folding (Ellgaard & Helenius, 2003).

The quality control (QC) system operating within the ER recognises and retains unfolded proteins. Consequently folded proteins are not retained by this system and can exit. This recognition relies upon features such as the exposure of hydrophobic regions within the unfolded/misfolded protein, unpaired cysteine residues and the tendency to aggregate. By preventing the premature exit of misfolded proteins, these proteins spend more time within the ER which improves their chances of correct protein maturation. In addition, incompletely folded proteins are prevented from being transferred further within the cell where they could potentially cause damage (Ellgaard & Helenius, 2003).

Cells use molecular chaperones and enzymes to distinguish between folded and unfolded proteins. Molecular chaperones assist in the folding and dispatching of improperly folded proteins for destruction. Enzymes selectively and covalently ‘tag’ misfolded proteins for recognition by the folding and degradation machinery of the

cell. These ‘tags’ include ubiquitin which acts as a signal for degradation (Hershko & Ciechanover, 1998) and glucose which is added to the N-linked glycans of glycoproteins, acting as a signal for retention within the ER (Hammond *et al*, 1994). Chaperoning proteins and enzymes include heat shock proteins, such as BiP; peptidyl-propyl isomerases which catalyse *cis/trans* isomerisation of peptidyl-propyl bonds; calnexin and calreticulin which interact with and assist the folding of proteins carrying monoglucosylated N-linked glycans and thiol-disulphide oxidoreductases, such as PDI, which catalyse the oxidation, isomerisation and reduction of disulphide bonds (Ellgaard & Helenius, 2003).

Abnormal proteins can arise from genetic mutations, errors in transcription, translation and folding or can be induced under stress, including oxidative stress and starvation. Protein misfolding can lead to either reduced or absent functional protein at a required location, due to its degradation or accumulation within the cell in the form of toxic aggregates.

An overload of misfolded or unfolded proteins in the ER can lead to ER stress. This stress, activates the unfolded protein response (UPR) which attenuates protein synthesis to prevent further accumulation of unfolded proteins, induces the transcription and synthesis of ER chaperones to enhance folding capacity and increases the expression of ER associated degradation (ERAD) components to enhance ERAD ability (Wang *et al*, 2008). Prolonged ER stress can eventually trigger apoptosis to safely dispose of cells injured by ER stress (Puthalakath *et al*, 2007). For most polypeptides the interaction with molecular chaperones is transient, once correctly folded these polypeptides no longer represent a substrate for chaperone interaction.

### 5.1.2 Golgi quality control mechanisms

Protein QC within the ER is relatively well characterised. In recent years however it has become apparent that the Golgi complex can also participate in protein QC. The QC protein ERp44 shuttles between the *cis* Golgi (where it engages incorrectly folded proteins) and the ER (where it releases these proteins) in a pH regulated cycle (Vavassori *et al*, 2013). Human ER α1,2-mannosidase a type II transmembrane

protein, capable of initiating the ERAD of numerous misfolded N-glycosylated proteins has been shown to in fact localise within the Golgi (Pan *et al*, 2011), where it is proposed to interact with γCOP, facilitating the retrieval of captured ERAD substrates back to the ER (Pan *et al*, 2013). In addition Golgi alpha1, 2 mannosidase IA, IB and IC play a role in glycoprotein QC (Hosokawa *et al*, 2007). A number of QC proteins therefore also reside in the Golgi where they help to shuttle proteins from the Golgi back to the ER.

### 5.1.3 Ubiquitin-proteasome system

If a misfolded or damaged protein fails to be repaired by chaperone mediated processes, it will be degraded. Disposal of proteins often occurs by ERAD: misfolded proteins are retro-translocated from the ER to the cytosol where they are degraded by proteasomes (Tsai *et al*, 2002) (Figure 5-1).

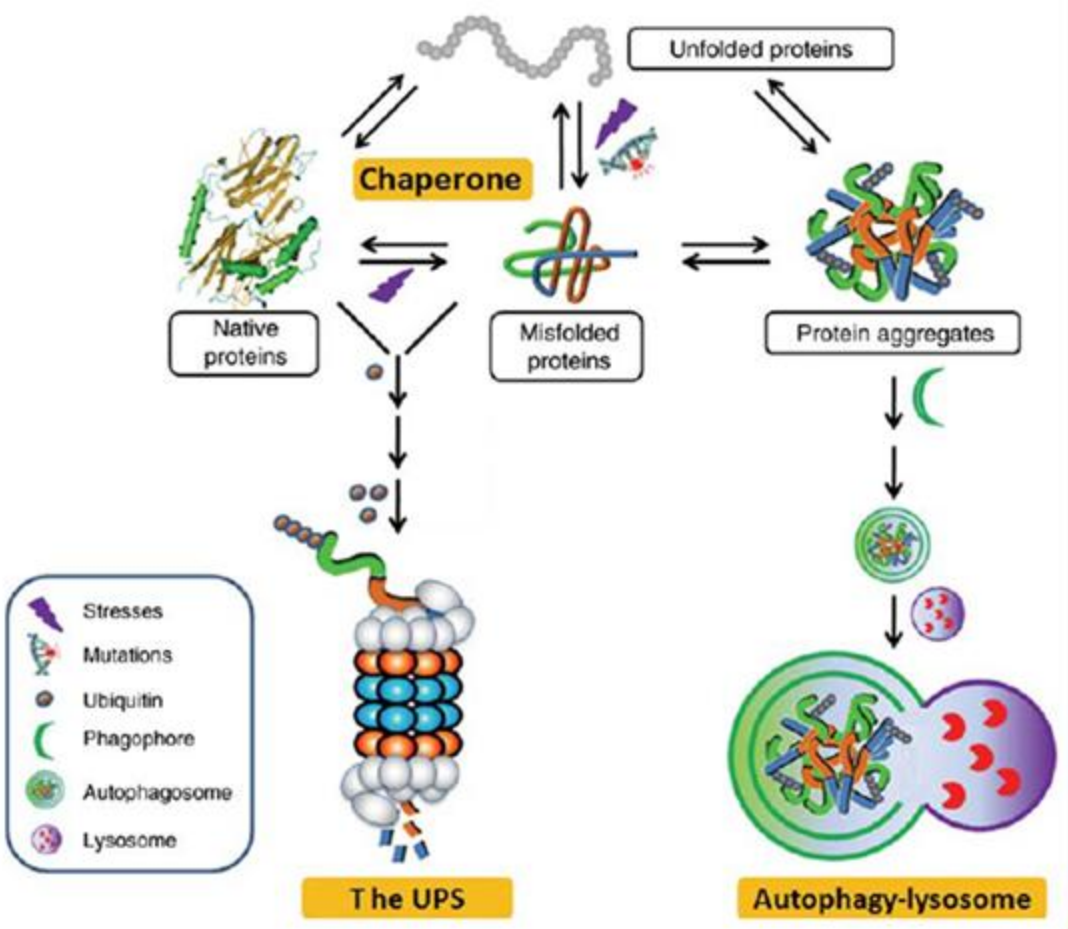


**Figure 5-1 Proteins may be degraded by the cell proteasome or lysosomes**

Image adapted from (Su & Wang, 2010). UPS: ubiquitin-proteasome system.

The ubiquitin-proteasome system (UPS) not only degrades both misfolded/damaged proteins but also degrades native proteins that are no longer required within the cell. This process begins with the ubiquitination of the protein to be degraded, which involves the ATP-dependent covalent attachment of a ubiquitin protein molecule to a lysine residue in a target protein molecule via a cascade of biochemical reactions (Hershko & Ciechanover, 1998). In general the degradation of polyubiquitinated proteins is carried out by the 26S proteasome which consists of a barrel-shaped core particle (the 20S proteasome) and the activation complex (often the 19S proteasome) at one or both ends of the core particle (Stock *et al*, 1996) (Figure 5-2).

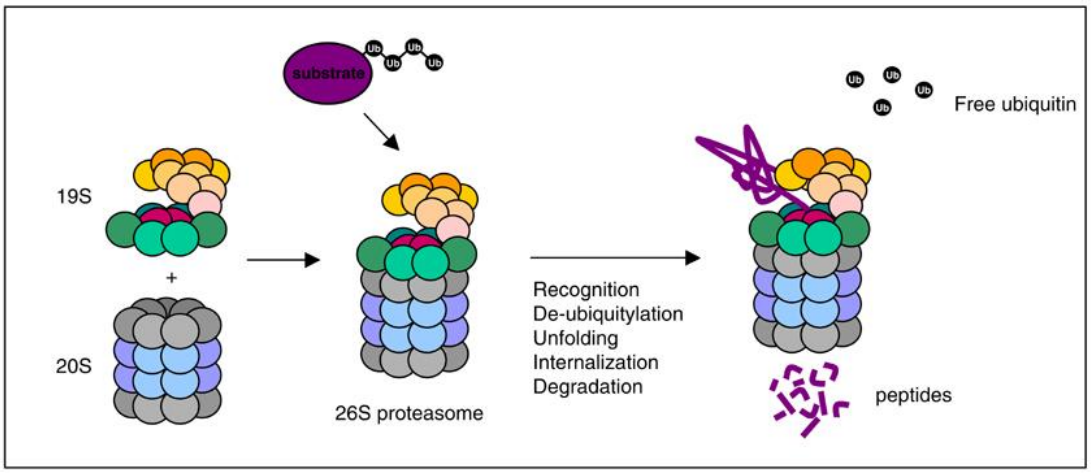


**Figure 5-2 Cell proteasome**

Image from: (Marteijn *et al*, 2006). The 26S proteasome consists of a 20S core unit and 19S unit. The 19S unit unfolds and removes ubiquitin from substrates. The 20S unit is the catalytic unit.

The proteasome mainly degrades ubiquitinated proteins but can also degrade non-ubiquitinated proteins such as ornithine decarboxylase (Ding & Yin, 2008). Misfolded aggregated proteins can impair the proteolytic function of the UPS (Bennett *et al*, 2005) and may instead be degraded by lysosomes.

### 5.1.4 Auto-phagolysosomal system

The autophagy-lysosomal pathway participates in protein QC by helping to remove protein aggregates. Protein aggregates or defective organelles are first segregated by an isolated double membrane (phagophore) to form an autophagosome which later fuses with lysosomes to form an autophagolysosome where the segregated content is degraded by lysosomal hydrolases (Levine & Kroemer, 2008). This type of autophagy is known as macroautophagy.

Macroautophagy can degrade all forms of misfolded proteins whereas proteasome degradation is likely limited to soluble proteins (Ding & Yin, 2008). Macroautophagy may be activated by UPS malfunction and/or aberrant protein aggregation to help remove aggregates (Rubinsztein, 2006). For example a toxic gain-of-function point mutation in alpha1-antitrypsin Z impairs correct protein folding, rendering the protein prone to form aggregated polymers within the hepatocyte ER. WT protein is primarily degraded by the proteasome, but the mutant

is thought to be degraded primarily by macroautophagy (Yorimitsu & Klionsky, 2007).

## 5.2 Cycloheximide chase and proteasome inhibition in WT stable line cells

Many misfolded proteins are unstable within the cell and are rapidly degraded (Waters, 2001). One method by which protein stability can be assessed is by using cycloheximide and performing a cycloheximide chase experiment. Cycloheximide is produced by *S. griseus* and inhibits protein translation by inhibiting peptidyl transferase activity of the 60S ribosomal subunit (Schneider-Poetsch *et al*, 2010). By using cycloheximide to inhibit protein synthesis, the fate of the protein synthesised before inhibition can be analysed.

In order to investigate whether the mutants were rapidly degraded within the cell cycloheximide chase experiments were performed. In preliminary experiments cycloheximide (Sigma, dissolved in DMSO according to the manufacturer's instructions) was first added to confluent stable line cells seeded in six well plates, expressing WT ADAMTS13 at various concentrations (ranging from 0 to 100µg/ml). The concentrations chosen were based upon those previously shown to be optimal for inhibition of protein synthesis (Gorner *et al*, 2004;Canaff *et al*, 2012;Park *et al*, 2012). After 24 hours cell lysates were harvested. This preliminary experiment was carried out to confirm that cycloheximide did inhibit protein synthesis at the concentrations chosen and also that cycloheximide was not toxic at these concentrations. The cells that were incubated with 100µg/ml cycloheximide appeared a lot smaller and 'less healthy' compared to at the other concentrations. Consequently this concentration was omitted in subsequent experiments.

Cell lysate samples are shown in Figure 5-3. The quantity of ADAMTS13 within the cell decreased in the presence of cycloheximide in a dose dependent manner, suggesting that cycloheximide was indeed preventing protein synthesis within the cell at the concentrations chosen.

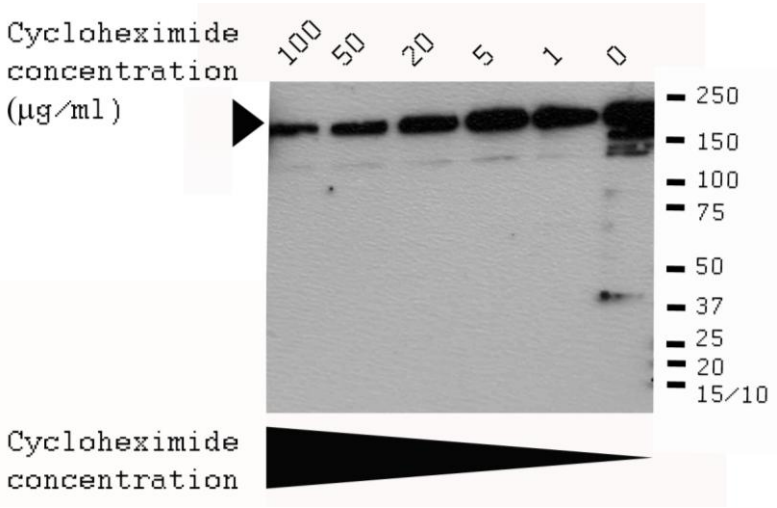


**Figure 5-3 Cycloheximide reduces protein synthesis in cells stably expressing WT ADAMTS13**

Cell lysates are shown of cells stably expressing WT ADAMTS13 incubated with different concentrations of cycloheximide for 24 hours: 100µg/ml, 50µg/ml, 20µg/ml, 5µg/ml, and 1µg/ml and as a control no cycloheximide. Expected size of ADAMTS13 is ~190kDa. Results are from one experiment.

In order to investigate whether the mutants were degraded by the cell proteasome, the proteasome was inhibited using MG132, a peptide aldehyde that blocks the proteolytic activity of the 26S proteasome complex (Lee & Goldberg, 1998). This inhibitor was initially added to cells stably expressing WT ADAMTS13 to understand the effect of this inhibitor on the intracellular levels of WT ADAMTS13 and also how toxic this inhibitor was to the cells. WT ADAMTS13 stable line cells seeded in six well plates were incubated with various concentrations of MG132 varying from 0 to 100µM. The concentrations chosen were based upon those previously shown to be optimal for inhibition of the proteasome (Gorner *et al*, 2004;Canaff *et al*, 2012;Park *et al*, 2012;Jensen *et al*, 1995). Cell lysate samples were harvested 24 hours after incubation with MG132. Examination by light microscopy did not reveal any indication of extreme toxicity at these concentrations (i.e. there was no excessive cell death). However the cells were a lot smaller compared to negative control cells which had not been incubated with MG132. Cell lysate samples are shown in Figure 5-4, lanes 1-6. Although the lanes are heavily loaded, MG132 did not appear to cause a large increase or decrease in ADAMTS13 levels within the cell.

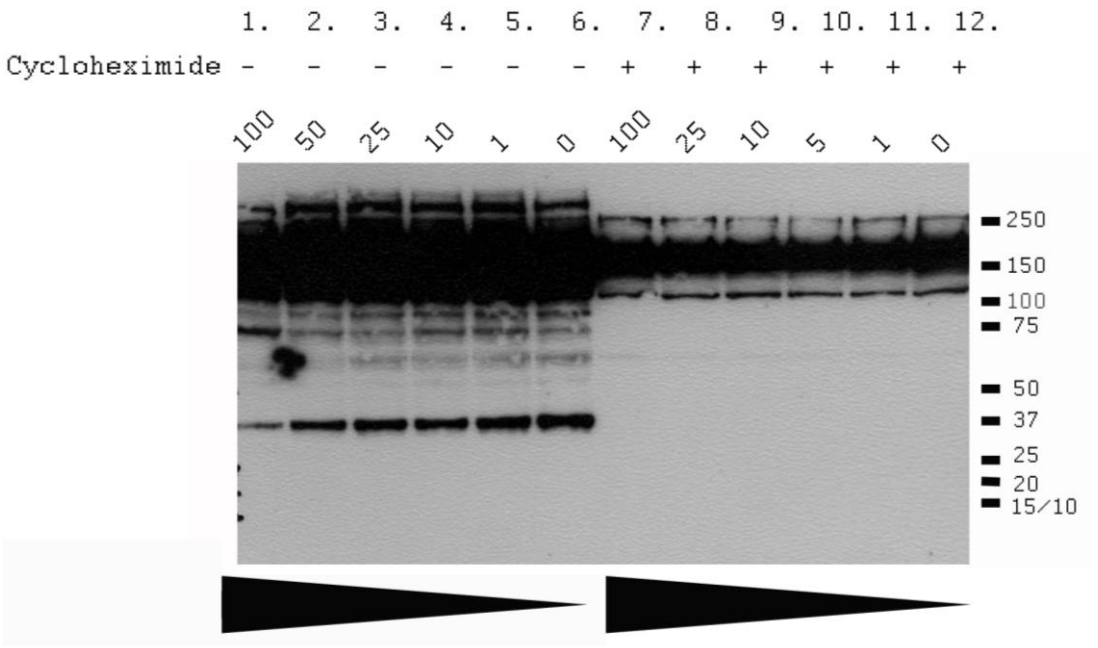


**Figure 5-4 Proteasome inhibition in cells stably expressing WT ADAMTS13**

Cell lysates of cells stably expressing WT ADAMTS13 after 24 hours incubation with various concentrations of MG132: 100µM, 50µM, 25µM, 10µM, 5µM, 1µM or no MG132 and incubated with or without 20µg/ml cycloheximide. Expected size of ADAMTS13 is ~190kDa. Results are from one experiment.

Stable line cells expressing WT ADAMTS13 seeded in six well plates were also incubated with these various concentrations of MG132 in the presence of 20µg/ml cycloheximide to understand if extreme toxicity occurred to the cells in the presence of both of these drugs. Cell lysate samples were harvested after 24 hours and no excessive cell death was observed. Cell lysate samples are shown in Figure 5-4, lanes 7-12.

The quantity of ADAMTS13 within the cell at the various different concentrations of MG132 was similar (Figure 5-4). Levels of ADAMTS13 in lanes 7-12 were lower compared to lanes 1-6 due to the additional presence of cycloheximide in the media of cells shown in lanes 7-12. Protein synthesis was reduced in these samples in agreement with the results from Figure 5-3. Together these results suggest that proteasome inhibition does not have a large effect on the intracellular levels of WT ADAMTS13.

## 5.3 Cycloheximide chase in transiently transfected cells

The experiments described indicated the drug concentrations which may be suitable to use for subsequent experiments. Next it was investigated whether these inhibitors would have the same effect on transiently transfected cells. Stable lines expressing either of the mutants were not available at the time of these experiments so the cycloheximide chase experiments and proteasome inhibition experiments were performed in cells transiently expressing ADAMTS13.

HEK293T cells seeded in T75 flasks were transfected with WT *ADAMTS13* and after 24 hours 50µg/ml cycloheximide was added. Cells were collected before and 24 and 48 hours after cycloheximide addition (Figure 5-5). As with cells stably expressing ADAMTS13 (Figure 5-3) cycloheximide inhibited protein synthesis in cells transiently expressing ADAMTS13.

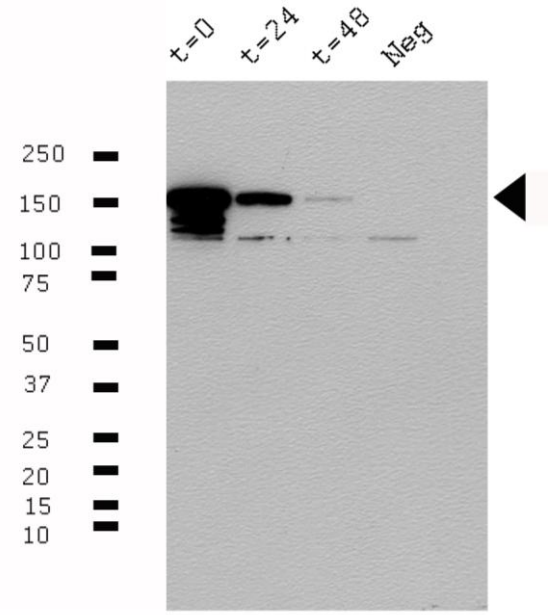


**Figure 5-5 Protein synthesis inhibition in transiently transfected cells**

Cells were incubated with 50µg/ml of cycloheximide for 24 (t=24) and 48 (t=48) hours. Cells were also collected before the addition of cycloheximide (t=0) as a control. Cell lysate samples are shown. Expected size of ADAMTS13 is ~190kDa. Results are from one experiment.

Subsequently the cycloheximide chase experiments were carried out in cells transiently expressing WT or mutant ADAMTS13. HEK 293T cells seeded in six

well plates were transiently transfected with vectors expressing WT or mutant ADAMTS13 (p.I143T and p.Y570C). To the cells 50µg/ml cycloheximide was added. Cell lysate and supernatant samples were collected before and 2, 4, 8, 10 and 24 hours after drug addition (Figure 5-6). These experiments were repeated using longer time intervals of 24 and 48 hours (Figure 5-7).

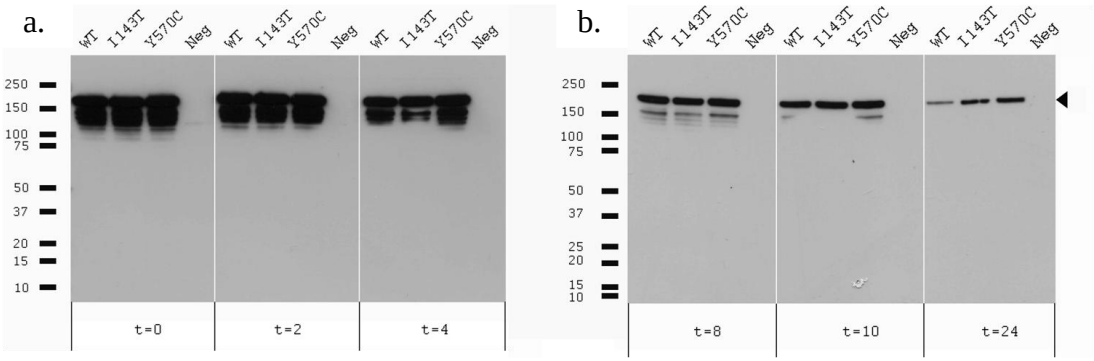


**Figure 5-6 Cycloheximide reduces protein synthesis in transiently transfected cells expressing WT or mutant ADAMTS13 over a 24 hour period**

Cells were incubated with 50µg/ml cycloheximide for 2 (t=2), 4 (t=4), 8 (t=8), 10 (t=10) or 24 (t=24) hours. Cell lysate samples are shown. Expected size of ADAMTS13 is ~190kDa. Results are from one experiment.

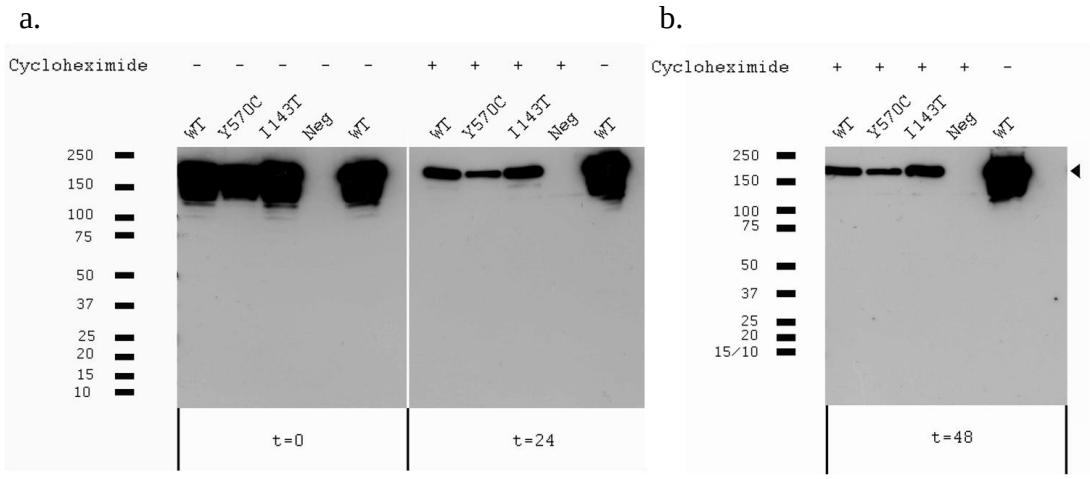


**Figure 5-7 Cycloheximide reduces protein synthesis in transiently transfected cells expressing WT or mutant ADAMTS13 over a 48 hour period**

Cells were incubated with 50µg/ml cycloheximide for 24 (t=24) or 48 (t=48) hours. Cell lysate samples are shown. At each time point cells which had not been incubated with cycloheximide were also harvested as a control. Expected size of ADAMTS13 is ~190kDa. Results are from one experiment.

For both WT and mutant proteins, the levels of ADAMTS13 decreased within the cell over time (Figure 5-6 and Figure 5-7). However it was unclear whether the

mutants decreased faster than WT. In Figure 5-7 levels of the p.Y570C mutant at 24 hours are lower than WT so the mutant appears to decrease quicker than WT. However in Figure 5-6 at the same time point WT levels are lower than the p.Y570C mutant and so WT appears to decrease quicker at 24 hours. Similarly with the p.I143T mutant at 24 hours (Figure 5-6) more of the mutant appears to be present compared to WT, whereas in Figure 5-7 levels are similar. Despite these discrepancies it is clear that the mutants are not degraded rapidly within the cell.

ADAMTS13 antigen was measured in the supernatant of the mutants and was undetectable at all times. Levels of WT ADAMTS13 in the supernatant increased with each time point measured (from 0 to 48 hours).

## 5.4 Proteasome and lysosome inhibition in transiently transfected cells

### 5.4.1 Protein aggregation

As described earlier, misfolded proteins can be degraded by the cellular QC system or can aggregate within the cell. One concern was that the mutants studied were aggregating within the cell and that the method of cell lysis that was used to harvest the cells may not be able to solubilise aggregated protein. This would be important if the mutations caused increased protein aggregation.

A protocol for the crude subcellular lysis of cells was followed (Holden & Horton, 2009), which enabled the extraction of cytosolic proteins (buffer 1), membranous organelles such as ER, Golgi and mitochondria (buffer 2), nuclear membrane and nuclear proteins (buffer 3) and insoluble proteins (buffer 4). Cells were also lysed with *Renilla* luciferase lysis buffer, which had been used in previous experiments and some cells were also lysed with two alternative cell lysis buffers: NP40 (nonidet P-40) and RIPA (radioimmunoprecipitation assay) buffer.

This protocol was tested on cells transiently transfected with WT or one of the mutants (p.I143T). Cells seeded in six well plates were transiently transfected with WT or with the p.I143T mutant. Two days after transfection cell lysate samples were harvested using different lysis buffers. Cells were lysed with a.) *Renilla* luciferase

lysis buffer (prepared as described in methods); b.) NP40 lysis buffer (150mM NaCl, 1% NP40, 50mM Tris pH 8); c.) RIPA buffer (150mM NaCl, 1% NP40, 0.5% sodium deoxycholate, 0.1% SDS, 50mM Tris pH 8); d.) crude subcellular lysis protocol buffer. For the crude subcellular lysis protocol four (i-iv) samples were collected which originated from one well of cells (d).

Buffers 1-4 which were used to collect samples di-div. were prepared as described (Holden & Horton, 2009). Buffer 1 (Digitonin buffer): 150mM NaCl, 50mM HEPES pH 7.4, 25µg/ml digitonin. Buffer 2 (NP40 buffer): 150mM NaCl, 50mM HEPES, pH 7.4, 1% NP40. Buffer 3 (RIPA buffer): 150mM NaCl, 50mM HEPES, pH 7.4, 0.5% sodium deoxycholate, 0.1% SDS, 1U/ml Benzonase. Benzonase was added just before use. Buffer 4 (E-RIPA extraction buffer): 150mM NaCl, 50mM HEPES pH 7.4, 0.5% sodium deoxycholate, 1% SDS, 100mM Dithiothreitol. PMSF was added to buffer 1 and to *Renilla* luciferase, NP40 and RIPA buffer.

For crude subcellular lysis the protocol was followed as described (Holden & Horton, 2009). In brief, media was removed from the cells followed by incubation with trypsin to remove the cells from the surface of the six well plate. Cells were resuspended in 1ml of media and then spun at 100g at 4°C for 5 minutes to pellet the cells. The supernatant was removed and cells were resuspended in 1ml of ice cold PBS to wash the cells, followed by spinning at 100g at 4°C to pellet the cells. PBS was removed and cells were resuspended in 400µl of buffer 1, followed by agitation at 45rpm at 4°C for 10 minutes. Cells were then spun at 2000g for 5 minutes at 4°C. The supernatant from this was harvested and kept (fraction i).

Cells were washed in PBS and then resuspended by vortexing with 400µl of ice cold buffer 2. This was incubated on ice for 30 minutes followed by centrifugation at 7000g to pellet nuclei and cell debris. The supernatant was collected and kept (fraction ii).

Cells were washed in PBS and then resuspended by vortexing with 400µl of ice cold buffer 3. This was incubated for 1 hour at 4°C with shaking at 45rpm. This was then centrifuged at 7000g for 10 minutes. The supernatant was collected and kept (fraction iii).

Cells were again washed in PBS and then resuspended using vortexing and boiling with 400µl of buffer 4. This was spun at 16,000g. The supernatant remaining corresponded to fraction iv.

For NP40 and RIPA lysis, cells were washed two times in cold PBS followed by addition of 250µl buffer to the cells in each well. Cells were incubated with buffer on ice for 10 minutes followed by removal of the cells from the surface of the plate. The cells were spun at 16,000g for 15 minutes at 4°C and the supernatant from this was kept.

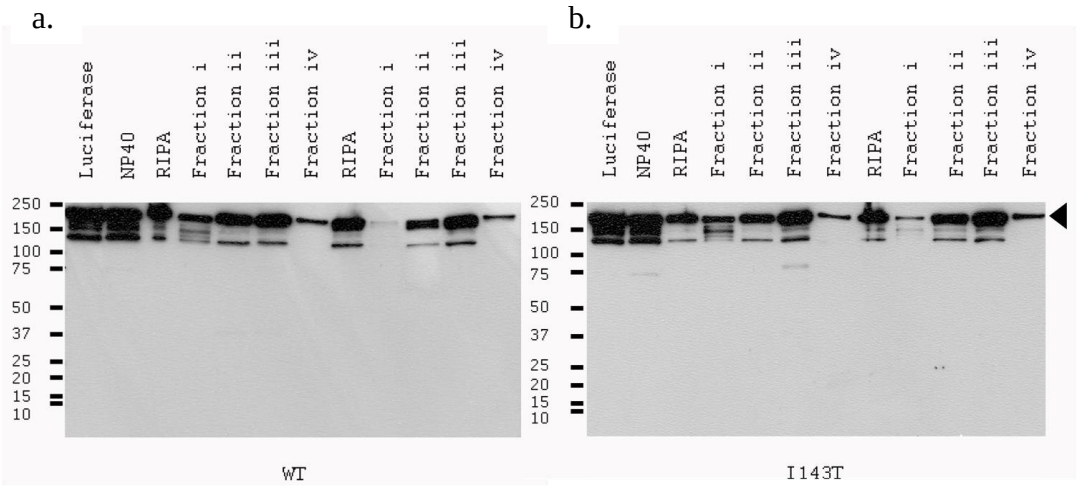


**Figure 5-8 Crude subcellular lysis of cells**

Cells were transiently transfected with WT or p.I143T mutant ADAMTS13. Cells were collected using different lysis methods: *Renilla* luciferase NP40, RIPA and crude subcellular fractionation (buffers i-iv). Expected size of ADAMTS13 is ~190kDa. Results are from one experiment.

Results from the various lysis methods are shown in Figure 5-8. The results after lysis with *Renilla* luciferase lysis buffer and NP40 appear to be similar. Levels of ADAMTS13 within the cell appear to be lower using the RIPA lysis method. This may be because the samples obtained after RIPA extraction were very viscous and difficult to load onto the gel. The levels of protein in fractions i-iv are lower than levels obtained with the *Renilla* luciferase and NP40 lysis buffer. The *Renilla* luciferase and NP40 lysis samples contain 'all proteins' whereas the proteins have been fractionated for samples i-iv.

Most of the protein appears to be within fractions ii and iii, these fractions correspond to membranous organelles such as the ER and Golgi (ii) and nuclear

membrane proteins (iii). The nuclear membrane is continuous with the ER membrane so it is expected that most of the proteins would localise into these fractions.

Buffer iv corresponds to insoluble protein (i.e. aggregated protein). A very small amount was present in WT and the p.I143T mutant ADAMTS13. Additionally the quantity of insoluble protein in WT and mutant appeared to be similar. These results suggest that this mutant protein is not prone to aggregation any more than WT ADAMTS13 and that the method of cell lysis used in previous experiments was sufficient.

### 5.4.2 Proteasome inhibition

With WT ADAMTS13, the decrease in the quantity of ADAMTS13 within the cell over time in the presence of cycloheximide is likely to be due to secretion. This is supported by the finding that increasing levels of ADAMTS13 could be detected in the supernatant of cells expressing WT ADAMTS13 when measured at increasing time points. Levels of the mutant within the cell also decreased over time. However the secretion of the mutants was severely reduced (Chapter 3) and in the cycloheximide chase experiments the mutants could not be detected in the supernatant. One hypothesis was that the decrease in the levels of the mutants within the cell over time was due to degradation of the mutants by the proteasome. Cycloheximide chase experiments in the presence of the proteasome inhibitor MG132 were performed to investigate this, to see if the levels within the cell increased after the addition of this inhibitor.

Cells seeded in six well plates were transiently transfected with vectors expressing either WT or mutant ADAMTS13. After 24 hours 50μg/ml cycloheximide was added to the supernatant of the cells. In addition 100μM MG132 was added to the supernatant of some cells. Cells were collected before and 20, 24, 30 and 48 hours after cycloheximide/MG132 addition. Results are shown in Figure 5-9.

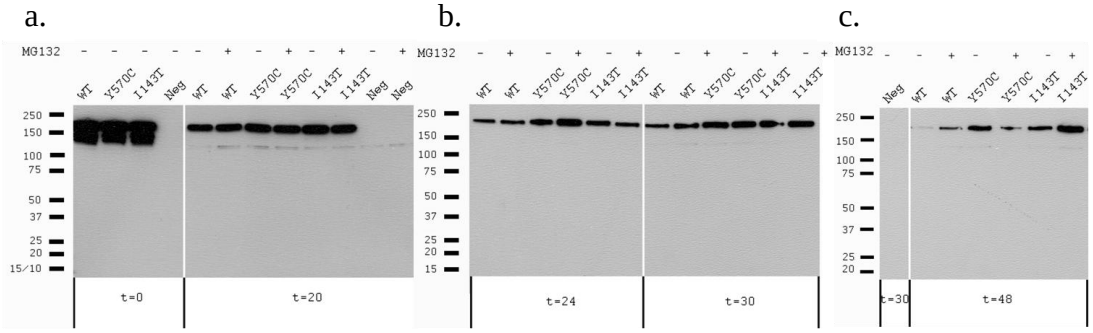


**Figure 5-9 Cycloheximide chase in the presence or absence of MG132**

Transiently transfected cells were incubated with cycloheximide and in some cases with 100µM MG132. Samples were collected at t=20, 24, 30 and 48 hours. Expected size of ADAMTS13 is ~190kDa. Results are from one experiment.

From this experiment no conclusion could be made regarding whether these mutants were degraded by the cell proteasome. At 24 and 30 hours levels of the p.Y570C mutant were greater in the presence of the proteasome inhibitor but not at 48 hours. With the p.I143T mutant levels appeared lower in the presence of the proteasome inhibitor after 24 hours but were increased 30 and 48 hours. The differences may be due to slight differences in the transfection efficiency between plates.

### 5.4.3 Lysosome inhibition

Alternatively the mutants may have been degraded by cell lysosomes. To investigate this preliminary experiments were performed by adding two different lysosome inhibitors (ammonium chloride and Bafilomycin A1), to transiently transfected cells expressing WT or mutant ADAMTS13, to assess which concentration to use. Cells were seeded in six well plates (cycloheximide was not used in these experiments). Ammonium chloride prevents acidification of lysosomes (Gordon *et al*, 1980) and Bafilomycin A1 is a specific inhibitor of vacuolar-type H(+)-ATPase (Bowman *et al*, 1988). The concentrations chosen were previously shown to be optimal for lysosome inhibition (Orenstein *et al*, 2013;Sala *et al*, 2013;Park *et al*, 2012;Yoshimori *et al*, 1991). Bafilomycin A1 concentrations ranged from 0 to 1µM and ammonium chloride from 0 to 16mM. Cell lysate samples were collected 24 hours after lysosome addition.

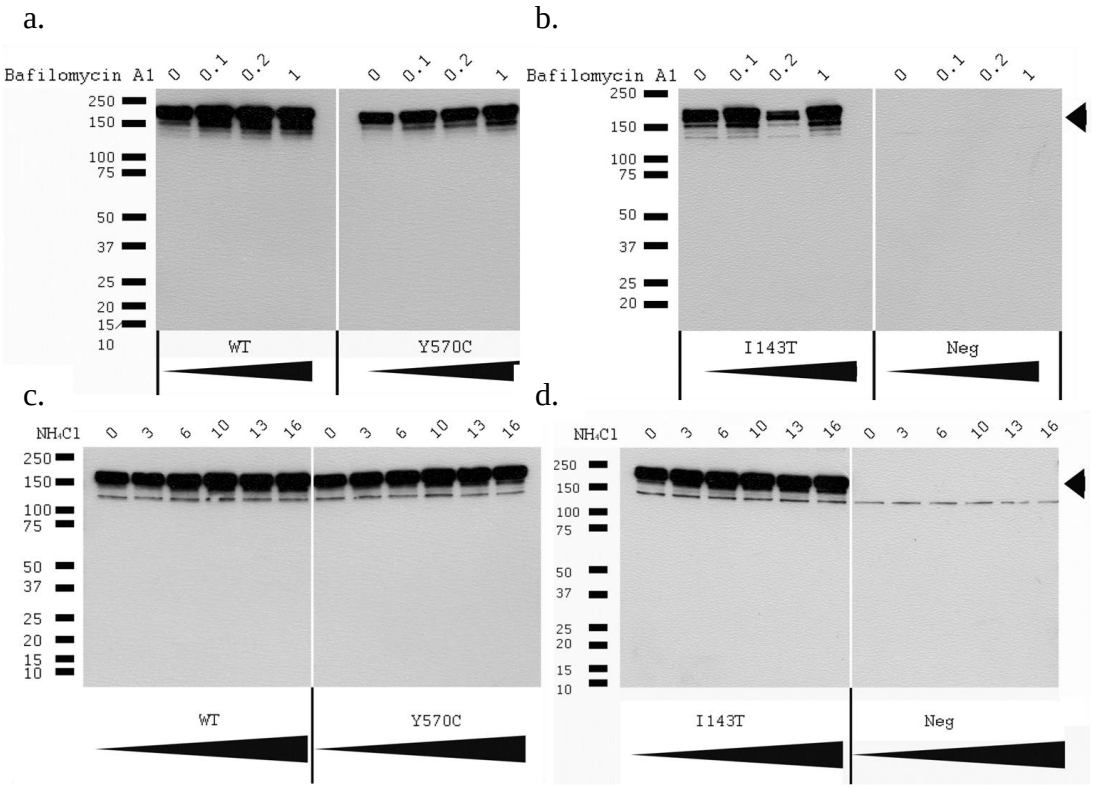


**Figure 5-10 Incubation of transiently transfected cells with lysosome inhibitors**

Cells were incubated with Bafilomycin A1 (a,b) or with ammonium chloride (c,d). Cells were incubated in the absence or presence of 0.1µM, 0.2µM or 1µM Bafilomycin A1. In separate experiments cells were incubated in the absence or presence of 3mM, 6mM, 10mM, 13mM or 16mM ammonium chloride. Cell lysate samples are shown. Expected size of ADAMTS13 is ~190kDa. Results from one experiment.

The cells appeared to tolerate the various concentrations of inhibitors. There appeared to be a slight increase in WT and mutant ADAMTS13 within the cell with increasing concentrations of both inhibitors. However this increase was similar for both WT and mutant. These results suggest that a small proportion of WT and mutant ADAMTS13 is degraded by lysosomes.

### 5.4.4 Normalisation of transfection efficiency

From the earlier cycloheximide chase/proteasome inhibition experiments, it was unclear whether levels of the mutant within the cell were increased in the presence of the proteasome inhibitor. One of the reasons this may have been unclear was because of the transient nature of the experiments. Cycloheximide experiments were carried out in the presence of lysosome and proteasome inhibitors in transiently transfected

cells which were cotransfected with the *Renilla* luciferase vector to normalise the transfection efficiency. Cells were collected before and 22, 28 and 32 hours after drug addition.

The volume of cell lysate added to the gel was normalised either for all time points or for each time point. Western blots were analysed but the results from these experiments were not consistent and unclear (n=3). In retrospect it may not have been valid to use the reporter vector to normalise the results after the addition of cycloheximide or proteasome and lysosome inhibitors, since the reporter may be affected differently to ADAMTS13 in the presence of these inhibitors. Therefore, cells were not cotransfected with *Renilla* luciferase in subsequent experiments.

### 5.4.5 Simultaneous inhibition of proteasome and lysosomes

One possibility is that by blocking the proteasome the cells could be rerouted for degradation by lysosomes. It has been shown that inhibition of the proteasome activates autophagy which is critical for the removal of the polyubiquitinated misfolded proteins (Iwata *et al*, 2005;Ding *et al*, 2007). In earlier experiments cells were incubated for many hours with inhibitors (up to 48 hours). Cycloheximide chase experiments were performed in the presence of both proteasome and lysosome inhibitors. Cells transiently expressing WT or mutant ADAMTS13 seeded in six well plates were incubated with 50μg/ml cycloheximide, 10mM ammonium chloride and 100μM MG132. Cells were collected before and 20, 24, 30, 44 and 48 hours after drug addition. Supernatant was also harvested and concentrated 10-15 fold.

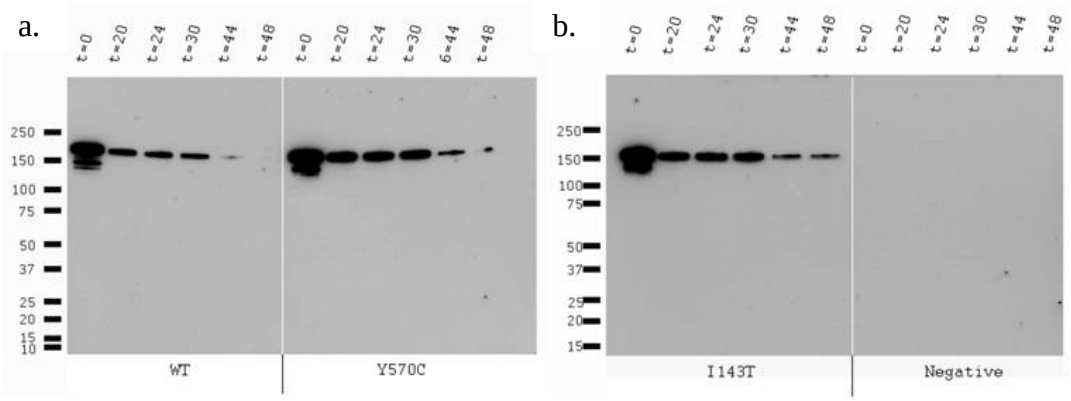


**Figure 5-11 Cycloheximide chase in the presence of both proteasome and lysosome inhibitors**

Transiently transfected cells were incubated with 100µM MG132 (proteasome inhibitor) and 10mM ammonium chloride (lysosome inhibitor) for 24 hours. Cell lysate samples are shown. Expected size of ADAMTS13 is ~190kDa. Results are from one experiment.

For both WT and mutant ADAMTS13 there was a big difference in the levels of protein before and after 20 hours of drug addition. This large difference may be because of the time delay between drug addition and effect. In WT ADAMTS13 between t=20 and t=30 hours there was a slight decrease in levels. On the other hand with the mutants, levels remained similar between these time points. These results suggest that the ADAMTS13 mutants were being degraded by either the proteasome or lysosome.

Between 44 and 48 hours, ADAMTS13 levels greatly decreased for WT and mutant ADAMTS13. This is a long time for the cells to be incubated with the drugs and so perhaps at these time points cells were beginning to die. The mutants were undetectable within the supernatant.

## 5.5 Proteasome inhibition in cells stably expressing ADAMTS13

From the above experiments it was not clear whether the proteasome or lysosome was responsible for protein degradation. This may have been partly due to differences in the transfection efficiency between cells seeded in different petri dishes. Experiments instead were carried out using stable line cells to try and eliminate this problem. Stable line cells were initially not used as it was thought that cells transiently expressing ADAMTS13 would be adequate for analysis and in addition stable line cells expressing either of the mutants had not been created.

During the course of these experiments however a stable line expressing the p.I143T mutant was created.

Cycloheximide was eliminated from these experiments. The addition of cycloheximide to the cells ensured that the effect of the proteasome or lysosome inhibitors on protein already synthesised was under investigation and would control for the possibility that the inhibitors increased/decreased protein synthesis. Cycloheximide was eliminated partly because of the additional toxicity introduced to the cells with its use. In addition if a small amount of mutant protein was secreted after inhibition of the proteasome or lysosome, it was less likely to be detected in the presence of cycloheximide as cycloheximide reduces protein synthesis and so the amount of protein secreted generally would be reduced in the presence of cycloheximide compared to its absence. Furthermore other groups have performed proteasome and lysosome inhibition experiments in secretion defect mutants in the absence of cycloheximide (Hunault *et al*, 1999;Tjeldhorn *et al*, 2011).

Shorter time points were also used to reduce toxicity to the cells. As mentioned before inhibition of the proteasome can lead to autophagy (Iwata *et al*, 2005;Ding *et al*, 2007). Therefore, prolonged incubation of cells with a proteasome inhibitor could trigger autophagy.

Preliminary experiments were performed in six well plates. Stable line cells expressing WT or p.I143T mutant ADAMTS13 were incubated with MG132 or with another proteasome inhibitor ALLN, which inhibits the 20S proteasome, along with calpain I and II, cathepsin B and L and neutral cysteine proteases (Lee & Goldberg, 1998). Concentrations chosen were based on those used by others (Hunault *et al*, 1999;Sidoryk-Wegrzynowicz *et al*, 2010). Cells were incubated with these inhibitors for 5 hours.

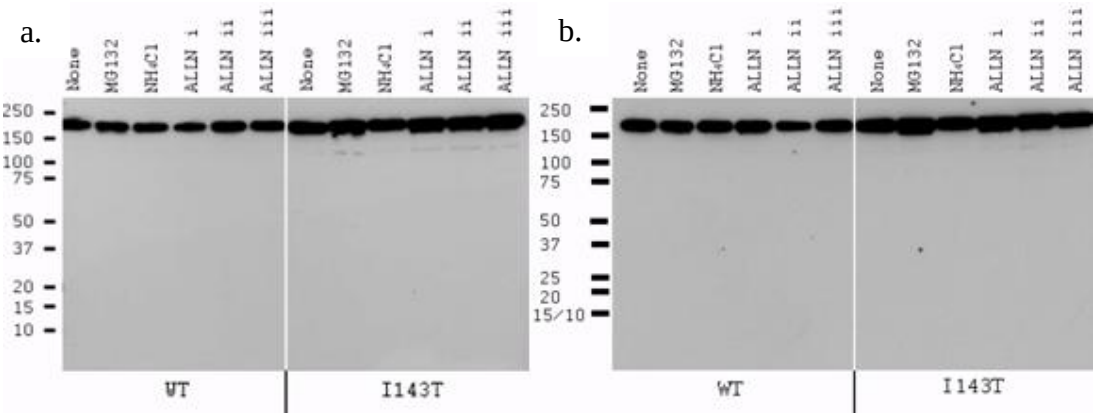


**Figure 5-12 Proteasome and lysosome inhibition in stable line cells**

Cells were incubated with 10µM MG132, 50mM ammonium chloride ($NH_4Cl$), 50µg/ml (i), 10µM (ii) or 6µM (iii) ALLN in duplicate. Cell lysate samples are shown. Expected size of ADAMTS13 is ~190kDa. Results are from one experiment.

Addition of both proteasome inhibitors (MG132 and ALLN) led to an increase in the intracellular levels of the p.I143T mutant ADAMTS13 but not WT ADAMTS13. Within the supernatant no antigen could be detected for the mutant. The addition of ammonium chloride did not appear to increase the intracellular levels of WT or mutant protein.

Experiments were scaled up and instead cells were grown in petri dishes and the supernatant concentrated ~100 fold to increase the chances of detecting antigen in the supernatant of the mutant. Addition of the proteasome inhibitor (MG132) and the proteasome and cathepsin inhibitor (ALLN) to cells stably expressing the p.I143T mutant led to an increase in the intracellular levels of ADAMTS13 (Figure 5-13). This increase was not observed in cells stably expressing WT ADAMTS13 after the addition of either drug. DMSO was added to cells stably expressing WT or mutant ADAMTS13 as a control, as this was the solvent used for both inhibitors (MG132 and ALLN). DMSO caused a slight increase in the intracellular levels of WT ADAMTS13 but not for the mutant.

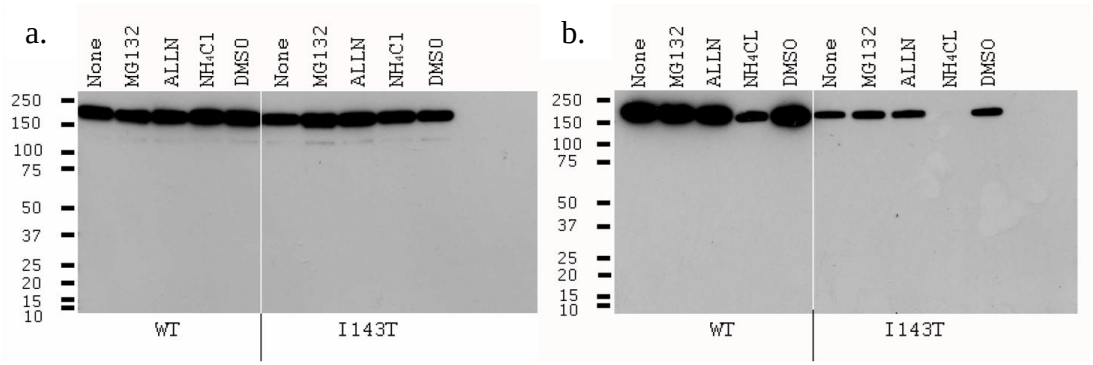


**Figure 5-13 Incubation of WT and p.I143T mutant ADAMTS13 with proteasome and lysosome inhibitors**

Western blotting was used to analyse cell lysate (a) and supernatant (b) samples from cells stably expressing WT or p.I143T mutant ADAMTS13. Cells were incubated with proteasome inhibitors MG132 (10μM) and ALLN (6μM) or the lysosome inhibitor ammonium chloride ($NH_4Cl$ 50mM). Cells were also incubated with DMSO as a negative control. Cells were incubated with these inhibitors for 5 hours and supernatant was concentrated ~100 fold for analysis. Expected size of ADAMTS13 is ~190 kDa. Western blots are representative of 3 experiments.

The quantity of WT and p.I143T mutant ADAMTS13 present in the supernatant of stable line cells in the presence of either proteasome inhibitor was also measured. In these experiments the supernatant was concentrated to a greater degree (~100 fold) compared to the supernatant from transient transfections. At this degree of concentration the p.I143T mutant could be detected in the majority of experiments. The addition of ALLN to stable line cells expressing either WT or mutant ADAMTS13, led to similar/slightly increased levels of ADAMTS13 antigen and activity in the supernatant (Table 5-1). In WT ADAMTS13 the addition of MG132 led to a slight decrease in the quantity and activity of ADAMTS13 measured in the supernatant. With the p.I143T mutant however the opposite occurred, there was a slight increase in the quantity secreted and as a result the activity of the mutant (Table 5-1). The antigen and activity of the mutant measured in the supernatant incubated in the presence of MG132 however was similar to the values obtained after incubation with DMSO, suggesting that the DMSO that MG132 was dissolved in was mainly responsible for the increase in the values obtained. Although the increase in ADAMTS13 activity and antigen observed with DMSO was relatively small (1.3-1.5), it's addition did appear to aid the secretion of ADAMTS13.

| | | Levels relative to no drug (mean±SD) | | | | | |
|---|---|---|---|---|---|---|---|
| | | No drug | MG132 | ALLN | DMSO | Bafilo-mycin A1 | Ammonium chloride |
| **Antigen** | WT | 1 | 0.73±0.18 | 1.2±0.058 | 1.5±0.15 | 0.93±0.32 | 0.19±0.051 |
| | p.I143T | 1 | 1.7±0.89 | 1.5±0.64 | 1.5±0.56 | 0.91±0.031 | 0.31±0.13 |
| **Activity** | WT | 1 | 0.73±0.10 | 1.0±0.18 | 1.3±0.058 | 0.82±0.12 | 0.21±0.032 |
| | p.I143T | 1 | 3.1±3.2[$] | 2.3±2.1[$] | 2.3±1.9[$] | 0.82* | 0.42±0.51[$] |

**Table 5-1 ADAMTS13 antigen and activity in supernatant samples after the addition of proteasome or lysosome inhibitors**

Cells stably expressing WT or p.I143T mutant ADAMTS13 were incubated in the presence of either MG132 (10μM), ALLN (6μM), Bafilomycin A1 (0.1μM) or ammonium chloride (50mM). As controls no inhibitor was added to some cells and DMSO to others. ADAMTS13 antigen and activity were measured and values for each condition were expressed as a proportion of control (no drug) which was given a value of 1. These proportions were calculated for each independent experiment, experiments were repeated three times. Median values are shown, with range in brackets. *In 2 of the Bafilomycin A1 experiments activity was undetectable both in the presence and absence of drug so the value shown in the table is the result from one experiment. Antigen on the other hand was detected in all experiments. [$]In one experiment each for MG132, ALLN, DMSO and ammonium chloride, activity was undetectable in the control (no drug) so the control was assigned a value of 1.25% (half of the detection limit) for the purposes of calculation in this experiment.

## 5.6 Lysosome inhibition in cells stably expressing ADAMTS13

In cells stably expressing WT or mutant ADAMTS13 a higher concentration of ammonium chloride was used (50mM) compared to the concentration used in transiently transfected cells to increase the chances of detecting a difference if a difference did exist. This concentration had been used by other groups in similar experiments (Tjeldhorn *et al*, 2011;Wolins *et al*, 1997;Hunault *et al*, 1999). Addition of ammonium chloride (50mM) to cells stably expressing WT or mutant ADAMTS13 led to severely reduced levels of ADAMTS13 secreted from the cell (Figure 5-13 and Table 5-1). Intracellular levels within the cell increased perhaps slightly but this increase was similar for WT and mutant protein.

Instead a more specific lysosome inhibitor (Bafilomycin A1) was used. Addition of Bafilomycin A1 to both WT and mutant ADAMTS13 did not lead to an increase in the intracellular levels of ADAMTS13 (Figure 5-14) suggesting that no or very little WT or mutant ADAMTS13 is targeted to the lysosome for degradation. Similar/slightly decreased levels of ADAMTS13 antigen was detected in both WT and mutant ADAMTS13 in the supernatant after the addition of Bafilomycin A (Figure 5-14, Table 5-1).

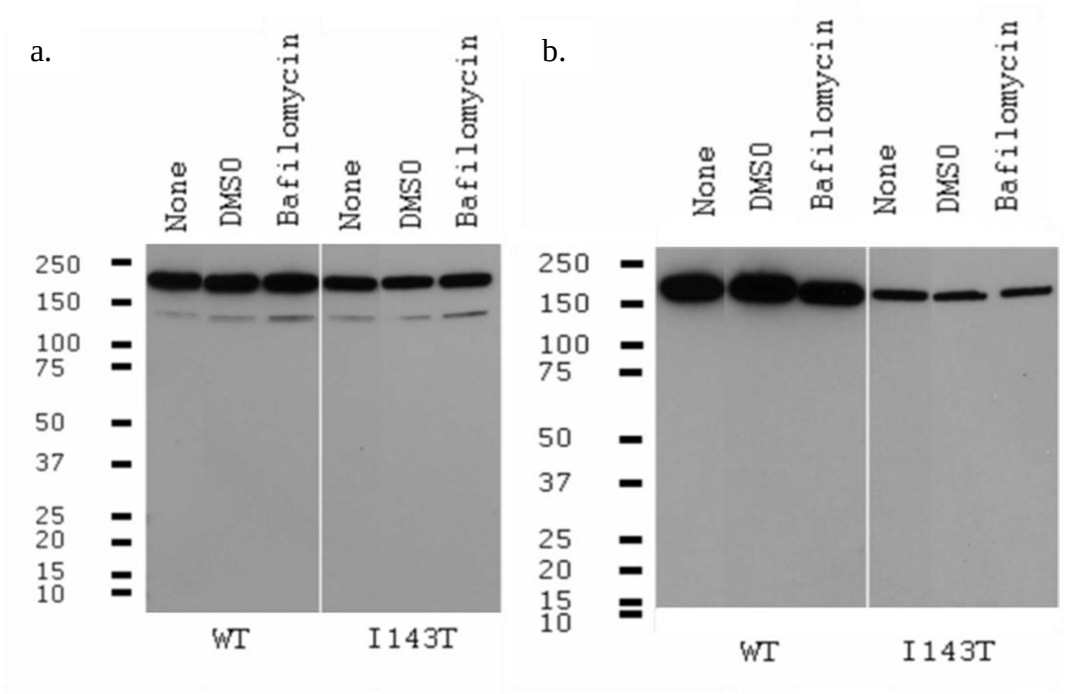


**Figure 5-14 Incubation of WT and p.I143T mutant ADAMTS13 with proteasome and lysosome inhibitors**

Western blotting was used to analyse cell lysate (a) and supernatant (b) samples from cells stably expressing WT or p.I143T mutant ADAMTS13. Cells were incubated in the presence or absence of Bafilomycin A1 (Bafilomycin) or DMSO as a negative control. Cells were incubated for 5 hours and supernatant was concentrated ~100 fold for analysis. Expected size of ADAMTS13 is ~190 kDa. Western blots are representative of 3 experiments.

## 5.7 Discussion

If mutant ADAMTS13 was degraded by either the proteasome or lysosomes, inhibition of these organelles would lead to accumulation of the mutant within the cell as it would no longer be degraded. Initially proteasome and lysosome inhibition experiments were carried out in cells transiently transfected with either WT or mutant ADAMTS13. From these experiments it was not clear if the mutants were

degraded by either of these organelles. This was partly due to slight differences in the efficiency of transfection between cells plated in either six well plates or petri dishes. To try to compensate for this, cells were cotransfected with a reporter vector (*Renilla* luciferase). However the results from this were not consistent. The behaviour of *Renilla* luciferase after proteasome or lysosome inhibition is not known, for example a large proportion of this protein may be degraded by the cell proteasome and so inhibiting the proteasome may lead to a large increase in the levels of the protein within the cell. As a result an increased luminescence may be observed which may be interpreted as a better efficiency of transfection which may not be the case. To overcome this problem cells stably expressing WT or mutant ADAMTS13 were used instead.

Inhibition of the proteasome (with MG132 or ALLN) in cells stably expressing the p.I143T mutant led to increased levels within the cell suggesting that a large proportion of the p.I143T mutant is targeted to the proteasome for degradation. The same effect was not observed with WT ADAMTS13, which is instead secreted. In contrast, inhibition of lysosomes with ammonium chloride or Bafilomycin A1 led to similar/slightly increased levels of both WT and mutant ADAMTS13 within the cell suggesting the mutant was not degraded by lysosomes to a greater extent than WT ADAMTS13.

When supernatant samples were concentrated ~100 fold the p.I143T mutant could be detected within the supernatant using both an ELISA and Western blotting, (Figure 5-13, Figure 5-14, Table 5-1). After proteasome inhibition there was a slight increase in the levels of the p.I143T mutant ADAMTS13 secreted into the supernatant. These increased levels however were similar to the levels observed in the presence of DMSO (Table 5-1); MG132 was dissolved in DMSO suggesting that this was probably responsible for the increased levels of ADAMTS13 antigen measured in the supernatant. It should be noted that the levels of antigen and activity in these experiments varied from undetectable to 48ng/ml and undetectable to 10.4% respectively, and at these lower levels the assay CVs were relatively high (Chapter 2.6 and 2.7).

As stated DMSO caused an increase in the quantity of WT and mutant ADAMTS13 secreted (Table 5-1). DMSO has been shown to act as a chemical chaperone aiding the folding and secretion of some proteins (Brown *et al*, 1996;Tamarappoo *et al*, 1999;Robben *et al*, 2006). Although there was an increase, the magnitude of the change was relatively small perhaps because a relatively small amount of DMSO was added to the cells (0.1%, which was equal to the greatest quantity of drug added). The concentrations of DMSO used in previous experiments and shown to have a chaperoning effect was higher than this (1-2%). Perhaps if higher concentrations of DMSO were used, similar to those in previous experiments (Robben *et al*, 2006;Tamarappoo & Verkman, 1998;Bebok *et al*, 1998), a larger increase may have been observed. Another possibility is that the higher levels detected could be as a consequence of the high CV associated with the assays used to measure low levels of ADAMTS13 activity and antigen. However ADAMTS13 activity and antigen was consistently increased in the presence of DMSO, in all three experiments.

The proteasome inhibitor MG132 can be toxic to cells initiating apoptosis (Park *et al*, 2011) which may explain why in WT ADAMTS13, decreased antigen and activity was measured in the presence of MG132 (Table 5-1). MG132 would also be toxic for the cells expressing the p.I143T mutant protein however this may have been offset by the beneficial effect of the DMSO solvent which aided the secretion of the mutant.

After the addition of Bafilomycin A1, ADAMTS13 antigen levels within the supernatant were similar to those observed in its absence. The addition of ammonium chloride on the other hand, which also inhibits lysosomes, severely reduced the secretion of ADAMTS13. Bafilomycin A1 is a more specific lysosome inhibitor compared to ammonium chloride. Ammonium chloride may have affected other processes within the cell which may have led to the reduced levels of ADAMTS13 measured in the supernatant.

An additional way to analyse the effect of these inhibitors could have been through the use of pulse chase experiments. This method would have enabled the protein to be tracked inside and outside the cell after proteasome and lysosome inhibition. This

was not performed because of time constraints but may be something worth carrying out in the future.

The behaviour of the protein within the cell was initially studied in transiently transfected cells using cycloheximide chase experiments. Cycloheximide was not used in subsequent experiments with stable line cells in order to reduce toxicity to the cells. Additionally other groups have performed these types of experiments (lysosome/proteasome inhibition) in the absence of cycloheximide (Hunault *et al*, 1999;Tjeldhorn *et al*, 2011). The cycloheximide experiments did demonstrate however that the mutants were not unstable within the cell or rapidly degraded.

It may have been useful to carry out the cycloheximide chase experiments in the presence of these inhibitors using stable line cells, to be sure that the inhibitors did not increase the synthesis of the proteins. This is unlikely to have occurred however because addition of the inhibitors (MG132, Bafilomycin A1, ammonium chloride) to WT ADAMTS13 did not lead to an increase in levels, in fact levels decreased.

Furthermore, cycloheximide has been shown to inhibit macroautophagy (Watanabe-Asano *et al*, 2014). Therefore, adding lysosome inhibitors to cycloheximide treated cells may not have been informative as the cycloheximide may have already inhibited the lysosomes in these cells.

In initial experiments, relatively long time points were used. This was to increase the chance of detecting protein in the supernatant and in case shorter time points would not be long enough to detect changes in the cell (<20 hours). However shorter time points were later used to reduce the toxicity associated with these inhibitors.

In pulse labelled experiments in HeLa cells (Majerus *et al*, 2003), ADAMTS13 appeared in the media within 3 hours of chase with a half-life of secretion of ~7 hours. After 35 hours no radiolabelled ADAMTS13 could be detected in the cell. Similarly in HEK 293 cells, radiolabelled ADAMTS13 within the cell started to decrease after 7 hours (Palla *et al*, 2009), was barely detectable at 3 hours and reached the maximum concentration at 24 hours. Looking at Figure 5-6 the results appear to broadly agree with these estimates of the half-life, at 8 hours levels of

ADAMTS13 in WT and mutant appear to be approximately half of the level before drug addition. ADAMTS13 appears to have a relatively long half-life within the cell; 30-75% of proteins that are synthesised are degraded within 20 minutes (Ellgaard & Helenius, 2003).

Inhibition of the proteasome led to the accumulation of the p.I143T mutant within the cell. The proteasome inhibitor, MG132 has been shown to activate the UPR leading to up regulation of chaperones and folding enzymes that can enhance the folding efficiency of mutant enzymes (Engin & Hotamisligil, 2010). However inhibition of the proteasome did not appear to enhance secretion of the mutant in three experiments. Although slightly increased levels were found in the supernatant this appeared to be due to the DMSO solvent, MG132 was dissolved in. I went on to investigate whether the addition of the chemical chaperone betaine could enhance the secretion of the misfolded protein (Chapter 6).

# Chapter 6 Betaine experiments (type 1a mutants)

## 6.1 Introduction

The p.I143T *ADAMTS13* mutation appeared to cause misfolding of the ADAMTS13 enzyme, which was recognised by the cells QC system and degraded by the cell proteasome (Chapter 5). Consequently, little or no ADAMTS13 was secreted (Chapter 3). I aimed to investigate whether it was possible to prevent the degradation of this mutant within the cell, thus promoting its secretion.

In the previous chapter (Chapter 5), it was shown that after inhibition of the proteasome in cells stably expressing the p.I143T mutant, levels of ADAMTS13 antigen in the supernatant increased. However this affect appeared to be due to the solvent that the inhibitor was dissolved in (DMSO) rather than the inhibitor itself. DMSO is a chemical chaperone and has been shown to aid the secretion of some proteins. I investigated whether another chemical chaperone, betaine (which is approved for the treatment of homocystinuria) (Lawson-Yuen & Levy, 2006), could alternatively help promote the folding and subsequent secretion of this mutant.

### 6.1.1 Chemical chaperones

As described in Chapter 5 cells synthesise and produce a number of chaperone proteins which aid the correct folding of proteins. These molecular chaperones recognise particular regions of unfolded proteins. Chemical chaperones are molecules which can be acquired from the environment (sometimes synthesised in the cell) that exert a non-specific effect (unlike molecular chaperones), facilitating correct protein folding, by stabilising native or native-like states or by reducing aggregation (Ellgaard & Helenius, 2003). These molecules are normally osmolytes, small solutes which can equilibrate cellular osmotic pressure. There are three main classes of osmolytes including, amino acid derivatives, carbohydrates and methylamines (Table 6-1).

| I. Amino acids & derivatives | II. Carbohydrates | III. Methylamines |
|---|---|---|
| Alanine | Arabitol | Betaine |
| Glutamic acid | Glycerol | Glycerophosphorylcholine |
| Proline | Mannitol | Sarcosine |
| γ-Aminobutyric acid | Mannose | Trimethylamine N-oxide |
| Taurine | Sorbitol | |
| Sucrose | | |
| Trehalose | | |
| Myo-inositol | | |

**Table 6-1 Osmolyte classes**

Taken from (Welch & Brown, 1996).

### 6.1.2 Osmolytes in organisms

Osmolytes accumulate in the cytoplasm of cells exposed to water stress and protect the cells from osmotic pressure (Yancey, 2005). A number of experiments have shown that to varying degrees organic osmolytes have the ability to stabilise and protect intracellular proteins against commonly occurring denaturing environmental stresses (Yancey *et al*, 1982;Yancey & Somero, 1979;Somero, 1986). These osmolytes do not interfere with cellular function or protein structure (Lee & Timasheff, 1981;Arakawa & Timasheff, 1983;Arakawa & Timasheff, 1985).

During osmotic stress for example, yeast increase their intracellular levels of glycerol (Reed *et al*, 1987) and elasmobranchs (sharks) increase levels of TMAO (Trimethylamine N-oxide) (Forster & Goldstein, 1976). Urea is an osmolyte, but unlike other osmolytes it does not protect cellular proteins. While protective osmolytes push the equilibrium of protein folding towards the native form denaturing osmolytes such as urea push the equilibrium towards the unfolded state. Urea accumulates in renal medulla cells but these cells contain ‘counteracting osmolytes’ to offset the protein denaturing effects of urea. In the kidney, osmolytes such as sorbitol and glycerophosphorylcholine are produced by *de novo* synthesis. Others such as betaine and taurine are taken up from the extracellular media via the action of specific transporters present in the plasma membrane (Welch & Brown, 1996).

### 6.1.3 Chemical chaperones

A number of groups have analysed the effect of chemical chaperones on the folding of mutant proteins. A variety of chemical chaperones have been tested in a variety of different proteins associated with various different diseases. Some of these are shown in Table 6-2. These chemicals have been able to rescue defects in protein function caused by mutations, to various degrees.

These molecules have been an attractive therapeutic option in some diseases, with some of the molecules being tested in clinical trials. For example approximately 90% of patients with cystic fibrosis have a common deletion mutation (ΔF508) in the cystic fibrosis transmembrane receptor (CFTR). This mutation leads to misfolding and subsequent degradation of the chloride ion channel (Loo & Clarke, 2007). Chemical chaperones have been able to 'rescue' this mutant, enabling it to traffic to the plasma membrane and perform its function. Rescuing this mutant is clinically relevant as a large number of patients could be potentially treated with the same drug. In fact one of these chaperones 4-phenylbutyric acid (4PBA) has been tested in clinical trials and is approved for the use of cystic fibrosis.

As well as rescuing misfolded mutants which are degraded by the cells QC system, these chemicals have been able to 'rescue' aggregated proteins. Tatzelt *et al* incubated scrapie infected mouse neuroblastoma cell lines with 1M glycerol, 100mM DMSO or 100mM TMAO which all reduced the amount of insoluble prion protein (Tatzelt *et al*, 1996). Administration of 4PBA to mice in a Parkinson's like disease mouse model prevented neurodegeneration (Inden *et al*, 2007). Oral administration of trehalose decreased polyglutamine aggregates in the cerebrum and liver, improved motor dysfunction and extended lifespan in a transgenic model of Huntington disease (Tanaka *et al*, 2004).

| Disease | Protein | Function | Chemical chaperone | References | Clinical trial/mice |
|---|---|---|---|---|---|
| Cystic fibrosis | CFTR | Membrane channel | Glycerol, DMSO, TMAO, Glycerophosphorylcholine, Myoinositol, Sorbitol, Taurine, betaine(10mM), 4PBA | (Sato *et al*, 1996;Brown *et al*, 1996;Rubenstein *et al*, 1997;Bebok *et al*, 1998;Zhang *et al*, 2003) | 4PBA Phase I/II (Zeitlin *et al*, 2002) |
| Emphysema and liver disease | $\alpha_1$-antitrypsin | Secreted protein | Glycerol, 4PBA | (Burrows *et al*, 2000) | 4PBA mice (Burrows *et al*, 2000) Phase I/II (Teckman, 2004) |
| NDI | Aquaporin-2 | Membrane channel | Glycerol, TMAO, DMSO | (Tamarappoo *et al*, 1999;Tamarappoo & Verkman, 1998) | - |
| NDI | Vasopressin $V_2$ receptor | Membrane receptor | Glycerol, DMSO | (Robben *et al*, 2006) | - |
| Haemophilia A | FVIII | Secreted protein | Betaine (25-100mM) | (Roth *et al*, 2012) | Betaine mice (Roth *et al*, 2012) |
| Machado-Joseph disease | Ataxin-3 | Nuclear and cytoplasmic | DMSO, glycerol, TMAO, Ectoine, 10mM betaine | (Yoshida *et al*, 2002;Furusho *et al*, 2005) | - |
| Primary hyperoxaluria type I | alanine: glyoxylate aminotransferase | Peroxisome enzyme | Betaine (75-100mM), Glycerol, DMSO, TMAO, 4PBA | (Santana *et al*, 2003) | Betaine Phase II NCT00283387 |
| Homocystinuria | Cystathionine beta synthase | Cytoplasmic and nuclear enzyme | Betaine (100mM), delta-ALA, Glycerol, TMAO, DMSO, proline, sorbitol | (Singh *et al*, 2007;Kopecka *et al*, 2011) | - |
| Branched chain ketoaciduria | Branched chain α-ketoacid dehydrogenase | Mitochondrial enzyme | TMAO | (Song & Chuang, 2001) | - |
| Long QT syndrome | HERG channel | Membrane channel | Glycerol | (Zhou *et al*, 1999) | - |
| Cataracts | αA-crystallin | Intracellular protein | TMAO | (Gong *et al*, 2009) | - |
| Cataracts | CRYGD | Intracellular protein | 4PBA | (Gong *et al*, 2010) | - |
| Retinitis pigmentosa | Carbonic anhydrase | Intracellular enzyme | 4PBA | (Bonapace *et al*, 2004) | - |
| Zellweger spectrum disorder | Peroxin 1/6/12 | Peroxisome enzyme | TMAO, glycerol Betaine (100mM), Arginine | (Zhang *et al*, 2010;Berendse *et al*, 2013) | Betaine Phase III NCT01838941 |
| Interstitial lung disease | Surfactant protein C | Secreted protein | 4PBA | (Stewart *et al*, 2012) | - |
| Parkinson Disease | PaeI-R | Membrane protein | 4PBA | (Kubota *et al*, 2006) | - |
| Intrahepatic cholestasis type 2 | BSEP E297G | Membrane protein | 4PBA | (Hayashi & Sugiyama, 2007) | - |
| Dystrophic mineralisation | ABCC6 | Membrane protein | 4PBA | (Le *et al*, 2011) | - |
| Nephritic syndrome | Nephrin | Membrane protein | 4PBA | (Liu *et al*, 2004) | - |
| Neurodegenerative disease | Insulin Amyloid | Intracellular protein | Trehalose Ectoine Betaine (300mM), | (Arora *et al*, 2004) | Trehalose mice (Perucho *et al*, 2012) |
| Oculopharyngeal muscular dystrophy | PABPN1 | Nuclear protein | Trehalose | (Davies *et al*, 2006) | Trehalose mice (Davies *et al*, 2006) |

**Table 6-2 Chemical chaperones *in vitro* and *in vivo***

4PBA: 4-phenylbutyric acid, CFTR: cystic fibrosis transmembrane receptor. NDI: Nephrogenic diabetes insipidus. Herg: Human ether-a-go-go-related gene. CRYGD: GammaD-crystallin. PaeI-R: Parkin-associated endothelin-receptor-like receptor. BSEP: Bile salt export pump, ABCC6: ATP-binding cassette sub-family c membrane 6. PABPN1: Polyadenylate-binding nuclear protein 1. Clinical trial numbers obtained from URL: https://clinicaltrials.gov/, accessed 17th June 2014.

### 6.1.4 Pharmacological chaperones

Some groups have subsequently developed pharmacological chaperones. These chaperones are small molecules, generally a ligand, antagonists (receptors) or competitive inhibitors (enzymes), that reversibly bind and stabilise the protein rather than assisting the general folding properties (Engin & Hotamisligil, 2010). They are more specific than chemical chaperones which can be advantageous as only the protein of interest is 'rescued'. Some of these chaperones are shown in Table 6-3.

| Disease | Protein | Protein function | Pharmacological chaperone references | Tested in clinical trial |
|---|---|---|---|---|
| Cystic fibrosis | CFTR | Membrane channel | (Wang *et al*, 2006;Pedemonte *et al*, 2005;Van *et al*, 2006) | VX-809, NCT00865904 Phase II (Clancy *et al*, 2012) |
| NDI | Vasopressin $V_2$ receptor | Membrane Receptor | (Morello *et al*, 2000;Tan *et al*, 2003;Bernier *et al*, 2006) | - |
| ND1 | Aquaporin-2 | Membrane receptor | (Bouley *et al*, 2005;Bouley *et al*, 2011) | Calcitonin, sildenafil, Phase II NCT00478335 |
| Fabry | α-Galactosidase A | Lysosome Enzyme | (Okumiya *et al*, 1995;Fan *et al*, 1999;Ishii *et al*, 2007;Shin *et al*, 2008;Wu *et al*, 2011;Frustaci *et al*, 2001) | AT1001, Phase III NCT00925301, NCT01458119, NCT01218659 |
| $G_{M1}$-gangliosidosis & Morquio B disease | β-Galactosidase | Lysosome Enzyme | (Matsuda *et al*, 2003) | - |
| Tay-Sachs & Sandhoff | β-hexosaminidase A (αβ) | Lysosome Enzyme | (Tropak *et al*, 2004;Maegawa *et al*, 2007;Rountree *et al*, 2009) | Pyrimethamine, Phase I/II, NCT01102686 |
| Pompe disease | α-glucosidase | Lysosome Enzyme | (Okumiya *et al*, 2007;Parenti *et al*, 2007) | AT2220, Phase II NCT00688597 |
| Gaucher disease | β-glucosidase | Lysosome Enzyme | (Benito *et al*, 2011) | AT2101, Phase 2 NCT00433147, NCT00813865, NCT00446550 Miglustat, Phase III NCT00319046, ISU302, Phase II NCT02053896 |
| Phenylketonuria | Phenylalanine hydroxylase | Cytosol Enzyme | (Pey *et al*, 2008;Santos-Sierra *et al*, 2012) | Yes on market |
| Hypogonadotropic hypogonadism | GNRHR | Membrane Receptor | (Janovick *et al*, 2002;Leanos-Miranda *et al*, 2002) | - |
| Long QT syndrome | HERG | Membrane channel | (Zhou *et al*, 1999) | - |
| Retinitis pigmentosa | Rhodopsin | Membrane receptor | (Krebs *et al*, 2010), (Ohgane *et al*, 2010) | - |
| Retinitis pigmentosa | Opsin | Membrane receptor | (Noorwez *et al*, 2003;Noorwez *et al*, 2004) | - |
| Metabolic disorders | hMCHR1 | Membrane receptor | (Fan *et al*, 2005) | - |
| Obesity | Melanocortin-4 | Membrane receptor | (Fan & Tao, 2009;Rene *et al*, 2010) | RM-493, Phase II NCT02041195 |
| Mucopolysaccharidosis III Type C | HGSNAT | Lysosomal enzyme | (Feldhammer *et al*, 2009) | - |
| Krabbe disease | Galactocerebrosidase | Lysosomal enzyme | (Lee *et al*, 2010;Berardi *et al*, 2014) | - |
| Long QT syndrome | Kv11.1 channel | Membrane channel | (Smith *et al*, 2013) | - |
| Intrahepatic cholestasis type 2 | BSEP E297G | Membrane protein | (Misawa *et al*, 2012) | - |

**Table 6-3 Pharmacological chaperones**

CFTR: cystic fibrosis transmembrane receptor, NDI: Nephrogenic diabetes insipidus, GNRHR: Gonadotropin-releasing hormone receptor, HERG: Human ether-a-go-go-related gene, hMCHR1: human melanin concentrating hormone receptor 1, HGSNAT: Heparan sulphate acetyl-coA: α-glucosaminide N-acetyltransferase, BSEP: Bile salt export pump. Clinical trial numbers obtained from URL: https://clinicaltrials.gov/, accessed 17th June 2014.

## 6.2 Addition of betaine to transiently transfected cells

The effect of the chemical chaperone betaine on the secretion of secretion defect mutants (p.I143T and p.Y570C) was investigated. Betaine was chosen as it has been previously shown to aid the secretion of a haemophilia A Factor VIII mutant *in vitro* and *in vivo* (Roth *et al*, 2012). Additionally it can be used safely in humans as it is approved for the treatment of homocystinuria where it acts as a methyl donor, lowering homocystinuria by remethylating methionine (Lawson-Yuen & Levy, 2006).

Initially betaine was added to cells transiently expressing ADAMTS13. Cells seeded in six well plates were incubated with various concentrations of betaine (0-150mM). Betaine was added 24 hours after transfection and 72 hours after incubation, cell lysate and supernatant were harvested. Supernatant was concentrated approximately 15 fold for analysis. Results are shown in Figure 6-1 and Table 6-4.

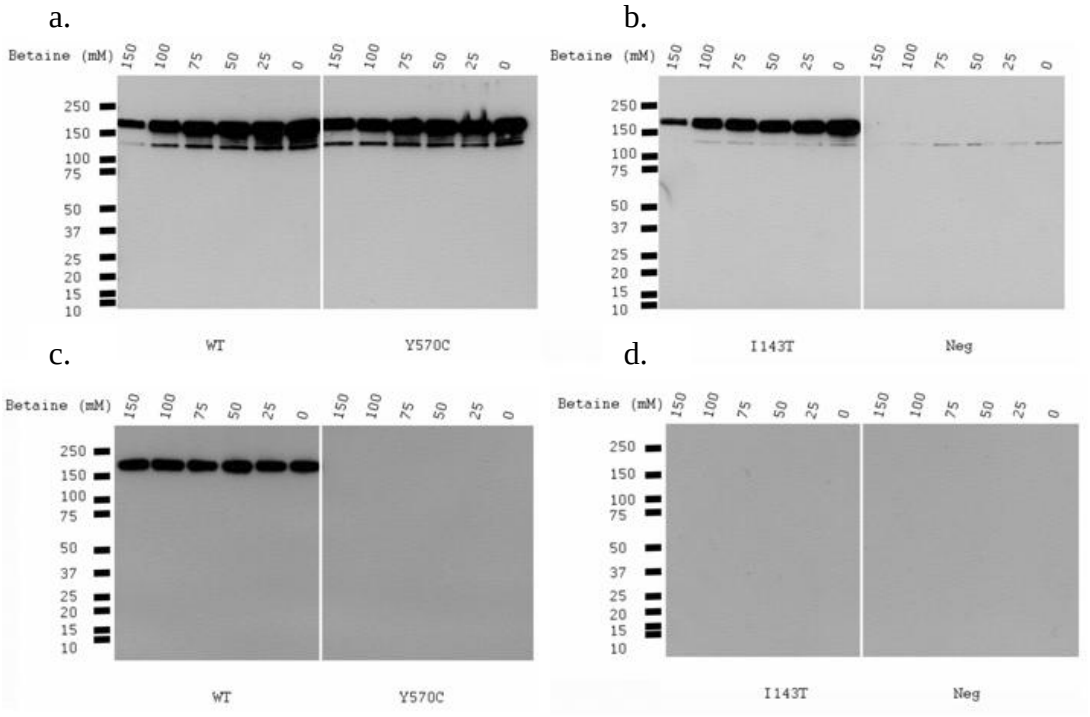


**Figure 6-1 Incubation of transiently transfected cells with betaine**

Cells transiently expressing WT or mutant (p.I143T, p.Y570C) ADAMTS13 were incubated with various concentrations of betaine (150mM, 100mM, 75mM, 50mM, 25mM and none) 24 hours after transfection. Cell lysate (a, b) and supernatant (c, d) were harvested after three days. Results are from one experiment. Expected size of ADAMTS13 is ~190kDa.

| | Concentration of betaine (mM) | | | | | |
|---|---|---|---|---|---|---|
| | 150 | 100 | 75 | 50 | 25 | 0 |
| **WT antigen** | 0.8 | 0.9 | 0.8 | 0.9 | 0.9 | 1 |

**Table 6-4 ADAMTS13 antigen in supernatant samples from cells transiently transfected with WT ADAMTS13 and incubated with betaine for three days**

ADAMTS13 antigen was undetectable in the supernatant of both mutants after incubation with betaine. Results are from one experiment. Antigen levels are expressed relative to no betaine (1).

In cell lysate samples the quantity of ADAMTS13 within the cell of both WT and mutant ADAMTS13 decreased with increasing concentrations of betaine. WT ADAMTS13 could be detected in the supernatant (Figure 6-1 and Table 6-4). Levels were similar/slightly decreased with increasing concentrations of betaine. In the mutants, no ADAMTS13 could be detected in the supernatant, regardless of the concentration of betaine used during incubation (Figure 6-1). The level of WT ADAMTS13 detected in the supernatant was relatively low (6.5→8.3% of PNP) as the cells were grown in six well plates, so the effect of betaine on the secretion of the mutants (if any) may have been too low to be detected.

## 6.3 Addition of varying concentrations of betaine to cells stably expressing ADAMTS13

The results from the transient transfection experiments demonstrated that betaine had an effect on ADAMTS13. Subsequent experiments were carried out using cells stably expressing ADAMTS13 to try and overcome the potential problems that may have been encountered if transiently transfected cells had been used (i.e. difference in transfection efficiency). At the time of these experiments a stable line expressing the p.Y570C mutant was also not available so the effect of betaine was investigated with only the p.I143T mutant.

Cells stably expressing WT or p.I143T mutant ADAMTS13 seeded in petri dishes were incubated with various concentrations of betaine (ranging from 0 to 150mM). After three days supernatant and cell lysate samples were harvested. Supernatant was concentrated ~100 fold. Results are shown in Figure 6-2 and Figure 6-4.

.

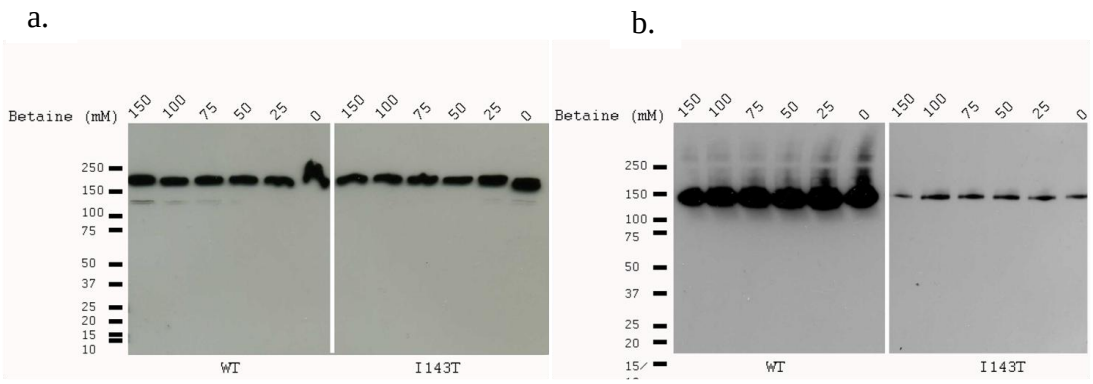


**Figure 6-2 Incubation of cells stably expressing WT or mutant p.I143T ADAMTS13 with betaine**

Cells stably expressing either WT or p.I143T mutant ADAMTS13 were incubated with various concentrations of betaine (150mM, 100mM, 75mM, 50mM, 25mM or 0), for three days. Cell lysate (a) and supernatant (b) samples are shown. Results from 1 of 2 experiments are shown. Expected size of ADAMTS13 is ~190kDa.

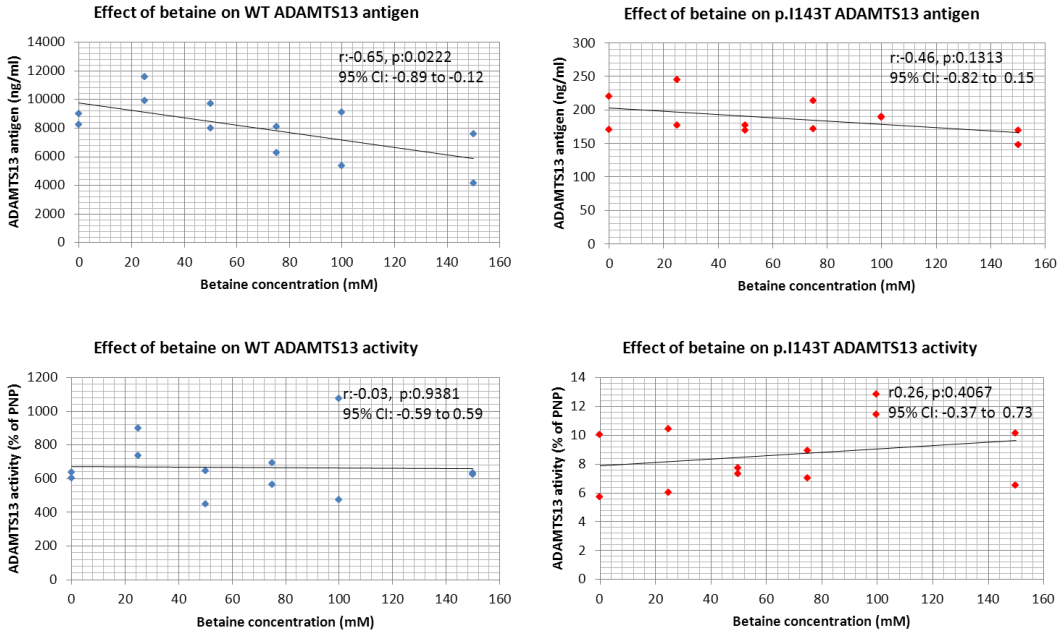


**Figure 6-3 ADAMTS13 antigen and activity measured in the supernatant of cells stably expressing either WT or p.I143T mutant ADAMTS13 after incubation with betaine**

The results shown are from two experiments. The value r represents the Pearson correlation coefficient, the 95% CI are also shown.

Following the addition of betaine there appeared to be similar/slightly reduced levels of WT ADAMTS13 within the supernatant. With the mutant there appeared to be a partial increase in the activity at a concentration of 100mM. The results from the two

experiments were not always consistent at the different concentrations and so instead in subsequent experiments one concentration of betaine (100mM) was added to the cells (as opposed to a number of different concentrations). For each independent experiment this concentration of betaine was tested in triplicate (cells seeded in three different plates). A concentration of 100mM betaine was chosen as this concentration appeared to lead to an average increase in the activity measured in the supernatant of the mutant.

## 6.4 Addition of 100mM betaine to cells stably expressing ADAMTS13

Betaine was added to the cells as described in the methods (Chapter 2.11). Results are shown in Figure 6-4.

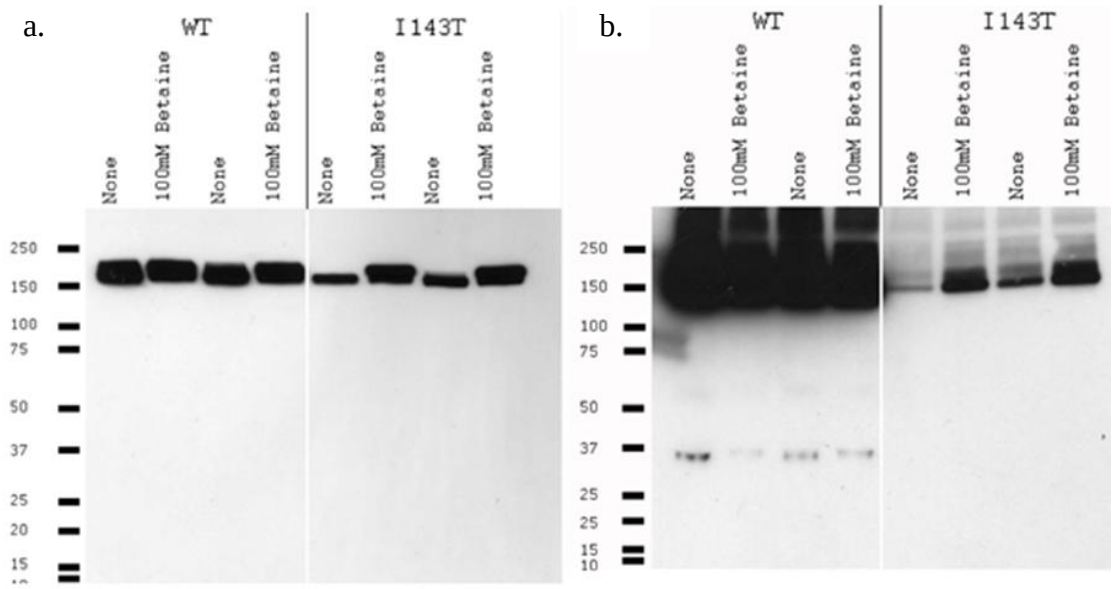


**Figure 6-4 Incubation of WT and p.I143T mutant ADAMTS13 with betaine**

Western blotting was used to analyse cell lysate (a) and supernatant (b) samples from cells stably expressing WT or p.I143T mutant ADAMTS13. Cells were incubated in the absence or presence of 100mM betaine for 96 hours. Supernatant was concentrated ~100 fold for analysis. Expected size of ADAMTS13 is ~190kDa. Western blots are representative of n=4 experiments.

The addition of betaine led to a slight decrease in the quantity and activity of WT ADAMTS13 detected in the supernatant (measured using an ADAMTS13 antigen ELISA). After 12 experiments the median WT ADAMTS13 antigen in the

supernatant in the presence of betaine was 0.9 of the value obtained in the absence of betaine (i.e. 0.1 fold decrease, compared to in the absence of betaine). The median ADAMTS13 activity in the presence of betaine was slightly decreased, 0.9 of the value obtained in its absence.

After the addition of betaine to cells expressing the p.I143T mutant there was a median 1.8 fold increase in ADAMTS13 antigen in the supernatant compared to in the absence of betaine. In cells stably expressing the p.I143T mutant, antigen could be detected in the supernatant in all (11/11) experiments carried out in the presence of betaine and in 9/11 of the experiments in the absence of betaine. In these two experiments for the purpose of calculating the effect of betaine on antigen levels, a value of 5ng/ml was assigned (half the detection limit for the ELISA). The median antigen value obtained in the absence of betaine was 17ng/ml, (range :< 10-197ng/ml), median values in the presence of betaine on the other hand was 28ng/ml (12- 354ng/ml). In 7/9 experiments in which antigen could be detected in both the absence and presence of betaine, antigen was increased in the presence of betaine. However in two of these experiments, antigen did not appear to increase in the presence of betaine. The antigen values were low (<15ng/ml) in these experiments and therefore differences may not have been observed so easily.

For the p.I143T mutant, activity in the absence of betaine was undetectable (<2.5% of PNP) in all experiments, but could be detected in 6/11 experiments in the presence of betaine. Activity was not detected in the remaining 5 experiments because smaller amounts of protein were secreted in these experiments. In the six experiments in which activity could be detected in the presence of betaine, there was a several fold increase in the activity of the mutant in the presence of betaine. The median activity of the mutant in the presence of betaine for these six experiments was: 5.5% of PNP, ranging from 2.7%-7.1% of PNP.

In order to test that the betaine within the supernatant was not directly affecting the measurement of ADAMTS13 activity betaine was added to supernatant collected from WT stable line cells which had not been incubated with betaine during culture. The activity in this supernatant (+ betaine) was then compared to the activity measured in the supernatant of cells which had not been incubated with betaine. The

results were similar. Together these results suggest that betaine aids the folding of the p.I143T mutant within the cell enabling its subsequent secretion by the cell.

## 6.5 Endoglycosidase H and PNGase F digestion

The band which was produced from cell lysate samples after western blotting appeared to consist of two bands merged together (Figure 6-4). These western blots were run on 4-12% gels. Samples were subsequently run on 3-8% Tris-Acetate gels (also under reducing conditions) to enable better separation, and it became apparent that two bands were present (Figure 6-5). The upper band appeared to be more prominent in the stable line cells that had been incubated with betaine (for both WT and mutant ADAMTS13). The presence of two bands was also evident in repeated experiments.

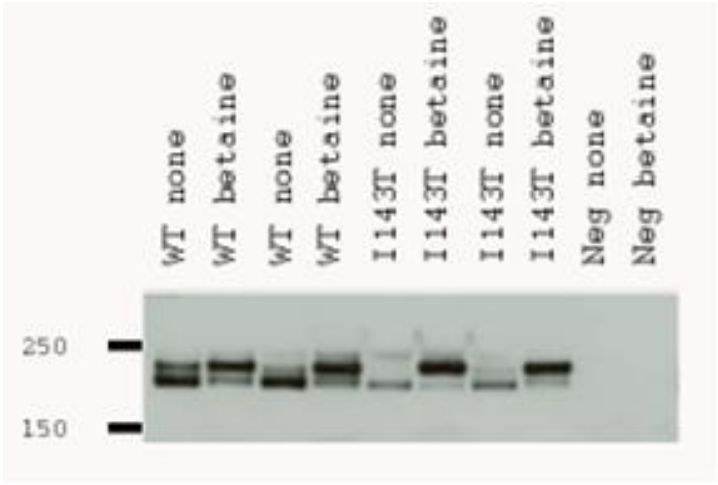


**Figure 6-5 Cell lysate samples run on a 3-8% Tris-Acetate gel**

Cell lysate samples harvested from stable line cells incubated in the presence or absence of 100mM betaine underwent electrophoresis on 3-8% Tris-Acetate gels, demonstrating the appearance of two bands in cell lysate samples. Expected size of ADAMTS13 ~190kDa.

To investigate whether these bands represented different glycosylated forms of ADAMTS13, cell lysate samples were digested with Endoglycosidase H which cleaves high mannose and some hybrid oligosaccharides from N-linked glycoproteins but not complex glycans. The addition of Endoglycosidase H to cell lysates harvested from both WT and the p.I143T mutant stable line cells led to the appearance of just one band (Figure 6-6). This occurred regardless of whether the cells had been previously incubated in the absence or presence of 100mM betaine

(Figure 6-6) and all bands were approximately the same molecular weight. This band was approximately the same weight as the lower band which had been observed in the cell lysate samples before Endoglycosidase H digestion (WT lower band). The addition of Endoglycosidase H therefore led to the disappearance of the upper band present in cell lysate samples, this band had been more prominent in those cells that had been incubated with betaine. The lower band present in cell lysate samples however did not appear to be sensitive to Endoglycosidase H, as after digestion the band appeared to be of the same size.

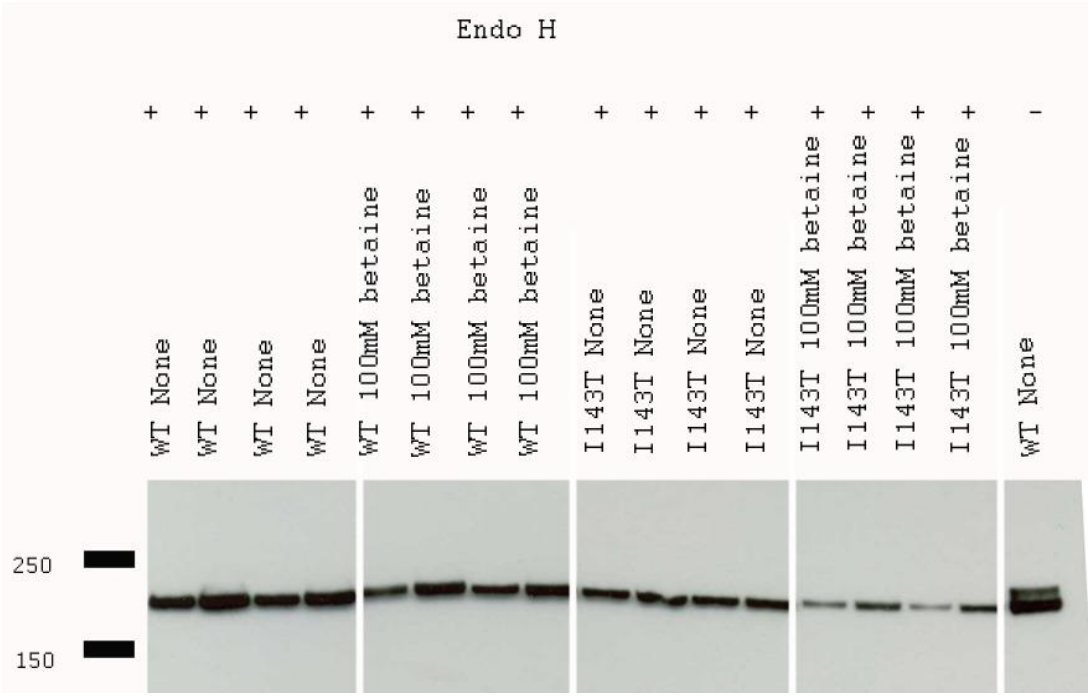


**Figure 6-6 Endoglycosidase H digestion of cell lysate samples**

Cell lysate samples harvested from stable line cells incubated in the presence or absence of 100mM betaine underwent deglycosylation with Endoglycosidase H, followed by electrophoresis on 3-8% Tris-Acetate gels. Expected size of ADAMTS13 ~190kDa.

Digestion of the cell lysate samples with PNGase F which unlike Endoglycosidase H can cleave complex glycans led to the appearance of one band within all cell lysate samples, similar to the results obtained with Endoglycosidase H (Figure 6-7). This band was of approximately the same molecular weight as the lower band present in undigested cell lysate samples.

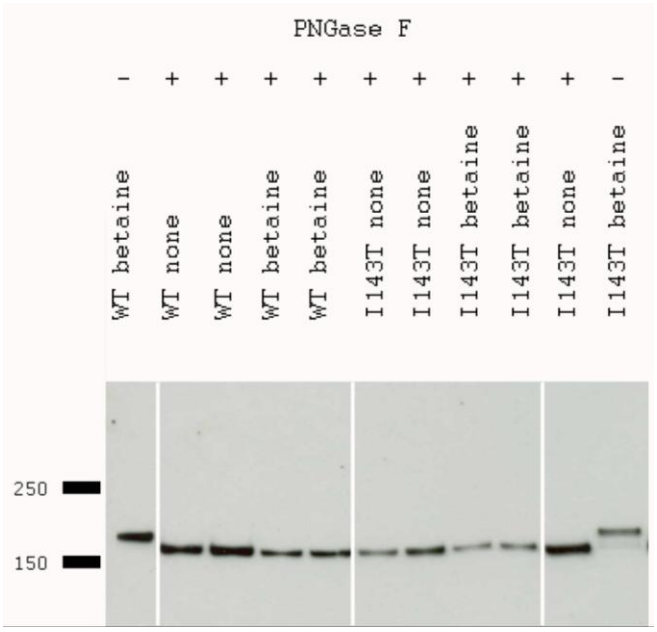


**Figure 6-7 PNGase F digestion of cell lysate samples**

Cell lysate samples harvested from stable line cells incubated in the presence or absence of 100mM betaine underwent deglycosylation with PNGase F followed by electrophoresis on 3-8% Tris-Acetate gels. Expected size of ADAMTS13 ~190kDa.

In the supernatant samples only one band was present after running the samples on 3-8% Tris-Acetate gels and this protein was resistant to Endoglycosidase H digestion as expected (Figure 6-8).

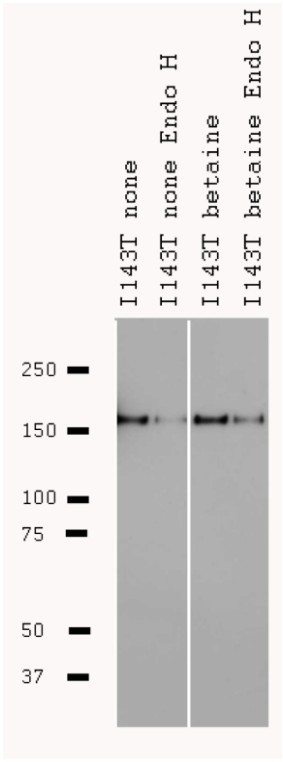


**Figure 6-8 Endoglycosidase H digestion of supernatant samples**

Supernatant samples harvested from stable line cells incubated in the presence or absence of betaine underwent deglycosylation with Endoglycosidase H followed by electrophoresis on 3-8% Tris-Acetate gels. Expected size of ADAMTS13 ~190kDa. Endo H: Endoglycosidase H.

Some of the cell lysate samples from the transient transfection experiments described in Chapter 3 (harvested ~96 hours after the cells were confluent) and the cell lysate samples from stable line cells incubated with proteasome and lysosome inhibitors (Chapter 5), (harvested ~5 hours after confluent) were also loaded onto 3-8% Tris-Acetate gels to see if two bands were also present in these samples (Figure 6-9). Two bands were present in the cell lysate samples from transiently transfected cells but only one band, corresponding to the upper band was present in the stable line cells harvested from the drug experiments.

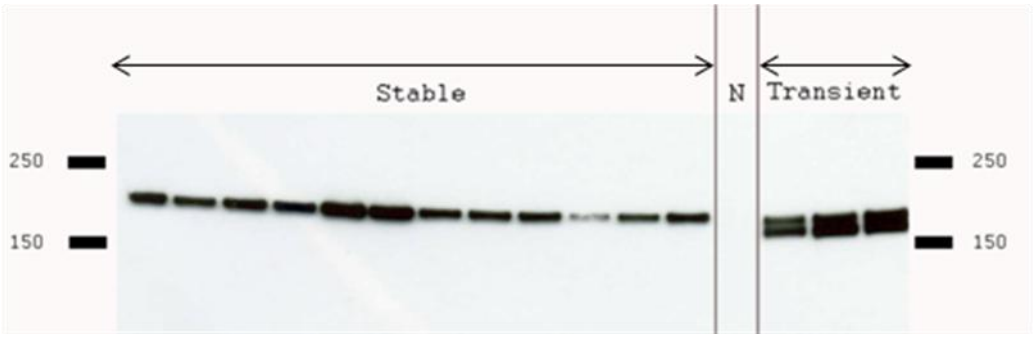


**Figure 6-9 Transiently transfected and stable line cell lysate samples run on 3-8% Tris-Acetate gels**

Cell lysate samples harvested from transiently transfected cells (collected ~96 hours after confluency) and from stable line cells (collected ~5 hours after confluency) were run on 3-8% Tris-Acetate gels.N: negative control. Expected size of ADAMTS13 ~190kDa.

## 6.6 Discussion

### 6.6.1 Betaine results

The addition of betaine to cells stably expressing the p.I143T mutant increased the secretion approximately two fold and led to detectable ADAMTS13 activity in the supernatant. The increase in activity detected fits with the increase in secretion observed in the presence of betaine. It should be noted however that the intra and inter assay CVs are relatively high at the low levels measured in these experiments (Chapter 2.6 and 2.7).

One might argue that the increase in secretion of the p.I143T mutant in the presence of betaine could be due to increased cell division and subsequently increased protein secretion. Although this was not tested it seems unlikely because WT ADAMTS13 levels did not increase in the presence of betaine. In fact there was a slight decrease in antigen and activity. This may have been due to toxicity of betaine to the cells. Despite this apparent slight toxicity increased levels of the mutant were still detected in the supernatant after betaine treatment.

### 6.6.2 Deglycosylation experiments

In cell lysate samples, two distinct bands were present, with the upper band more prominent in cells treated with betaine. This band was sensitive to Endoglycosidase

H digestion, which cleaves most N-linked glycans except for complex glycans. Complex glycans are formed in the Golgi so ER associated proteins are sensitive to Endoglycosidase H digestion, suggesting that the upper band that was present in cell lysate samples corresponded to ER associated ADAMTS13.

The lower band did not appear to be sensitive to Endoglycosidase H digestion as the band which remained after digestion appeared to be approximately the same size as the band before digestion. This band could therefore correspond to glycosylated ADAMTS13 present in the Golgi of the cell (resistant to Endoglycosidase H digestion) or unglycosylated protein. It seems more likely to be unglycosylated protein because of its lower molecular weight. Glycosylation increases the molecular weight of a protein causing it to run slower on an SDS-gel and hence lies closer to the top of the gel. If this lower band did correspond to glycosylated protein present in the Golgi of the cell then it would be sensitive to PNGase F digestion as this enzyme can cleave complex glycans. After PNGase digestion one band remained and again this was approximately the same size as the lower band present before digestion. This suggests that the lower band in the undigested samples corresponds to unglycosylated protein as opposed to glycosylated protein present within the Golgi.

The appearance of the lower unglycosylated band appeared to be time dependent, being present in cells that that were confluent ~96 (cell lysate samples from transiently transfected cells) hours but not ~5 hours (cell lysate samples from proteasome/lysosome inhibition experiments). Majerus *et al* found that intracellular ADAMTS13 is predominantly located in compartments of the secretory pathway prior to the cis-Golgi (Majerus *et al*, 2003) suggesting that the rate limiting step for ADAMTS13 synthesis is folding in the ER. Perhaps after 96 hours there is more protein 'waiting' to be glycosylated, leading to more unglycosylated protein present in the cell (lower band). Betaine was associated with a higher proportion of glycosylated compared to unglycosylated protein. This fits with the role of betaine acting as a chaperone within the cell to aid folding. The ability of betaine to aid folding of ADAMTS13 appears to promote glycosylation of the protein, in turn leading to a greater proportion of glycosylated compared to unglycosylated protein within the ER of the cell. This in turn promotes the secretion of the protein.

Glycosylated and unglycosylated forms of other proteins have been demonstrated in cell lysate samples (cystic fibrosis, Long QT syndrome), with misfolded mutants having more of the unglycosylated compared to glycosylated forms present within the cell. When cells were incubated with chaperones an increase in the glycosylated form could be detected in the cell (Zhou *et al*, 1999;Brown *et al*, 1996).

Looking back at Figure 6-1 it appeared that with increasing concentrations of betaine there was less ADAMTS13 within the cell. In the experiments described above (with 100mM betaine), this was not always the case (Figure 6-4, more total ADAMTS13 in the presence of betaine). However in the presence of betaine the upper band was always more prominent. This band corresponded to glycosylated protein. The cell lysate samples from Figure 6-1 were not run on 3-8% gels but looking at the cell lysate samples at 150mM, although there appears to be less total ADAMTS13, the ADAMTS13 that is present does appear to be of a higher molecular weight. In Figure 6-2 looking at the p.I143T mutant in the absence of betaine compared to the presence, the band in the absence of betaine appears to have a lower molecular weight than the others. Similarly comparing the WT 150mM band with the 100mM band, the 150mM band appears to be slightly higher.

### 6.6.3 Protein folding and the osmophobic effect

The hydrophobic effect is one of the important determinants of protein folding. Osmolytes are thought to produce an additional force, the osmophobic effect, for protein folding. The mechanism behind the stabilisation of proteins in the presence of osmolytes was first investigated by Lee and Timasheff (Lee & Timasheff, 1981). The authors studied the thermal transition of three proteins in the presence of an osmolyte, sucrose and found that sucrose was preferentially excluded from the vicinity of the protein, with an increase in the Gibbs free energy (more negative value). The presence of sucrose did not significantly change the confirmation of the the proteins studied.

This preferential exclusion phenomena has been subsequently found for other naturally occurring osmolytes (Arakawa & Timasheff, 1983;Arakawa & Timasheff, 1985), including betaine (Arakawa & Timasheff, 1983). This increase in negative

Gibbs free energy enhances the thermodynamic stability of proteins, thereby enhancing protein folding.

It has been shown that an unfavourable interaction exists between an osmolyte and the peptide backbone (Qu *et al*, 1998). On the other hand a favourable interaction occurs between amino acid side chains. The unfavourable interaction of the peptide backbone with an osmolyte, however, is the thermodynamic force responsible for raising the chemical potential of both the native and unfolded states upon their transfer from water to osmolyte solution. The unfavourable interaction causes a preferential exclusion of the osmolyte (Qu *et al*, 1998). Relative to the native state, a denatured protein exposes much more of the protein fabric to the solvent. Thus the denatured state of the protein is more solvophobic (has a greater preferential exclusion) toward osmolyte than the native state. By focusing the solvophobic effect force on the denatured state, the native state is left free to function relatively unaffected by the presence of osmolyte.

### 6.6.4 Therapeutic use of chaperones

Betaine could potentially be a good candidate for therapy. It is present in various organisms including animals and plants (Yancey *et al*, 1982) and is used in the treatment of homocystinuria (Lawson-Yuen & Levy, 2006). It is used as a food supplement (Zeisel *et al*, 2003) and can be taken orally. The activity of many enzymes *in vitro* was shown not to be affected by high concentrations of betaine (up to 1M) (Pollard & Wyn Jones, 1979).

Betaine could be potentially administered to patients prophylactically and would be a more practical method of prophylaxis than plasma infusion. It could also be administered orally. This would have its advantages over plasma infusion which is an invasive procedure.

Organic solutes such as betaine can be transported into cells via sodium and chloride-coupled cotransporters. Betaine can be transported by the betaine/GABA cotransporter (BGT-1). These cotransporters are present in many cells including the kidney, brain, liver, heart, muscle and placenta (Borden *et al*, 1995;Rasola *et al*, 1995).

The use of betaine or other chemical chaperones or the development of pharmacological chaperones may be something worth considering in the treatment of TTP, particularly as the majority of mutations in *ADAMTS13* which have been identified and investigated *in vitro* have been shown to reduce its secretion.

Besides Haemophilia A, the use of chaperones to rescue mutant proteins in other haematological disorders has not been investigated *in vitro* or *in vivo*. The results summarised in Table 6-2 and Table 6-3 demonstrate that a variety of proteins (nuclear, cytoplasmic, plasma membrane and secreted proteins) can be rescued by chemical or pharmacological chaperones, although sometimes the effect of these chaperones is mutation dependent. Chemical or pharmacological chaperones may have the potential therefore to rescue mutant proteins defective in other haematological disorders, i.e. not just secretory proteins such as ADAMTS13 and FVIII.

It is important to consider also that the concentrations of chemical chaperones that were shown to have an effect *in vitro* may not be achievable in humans. The concentrations of glycerol and TMAO needed for chaperone-like effects in cell culture have been in the range of 0.5-1.2M and 50-100mM, respectively. Studies in mice administered glycerol or TMAO have indicated that it is possible to achieve these concentrations for TMAO but not for glycerol *in vivo* (Bai *et al*, 1998).

Pharmacological rather than chemical chaperones may have a broader and more potent effect than chemical chaperones for the protein of interest. For example Robben *et al* added various pharmacological and chemical chaperones to mutant vasopressin $V_2$ receptors. Chemical chaperones could rescue 1 of 9 mutants, whereas pharmacological chaperones rescued 2 of 9 of these mutants (Robben *et al*, 2006). Additionally higher concentrations of chemical chaperones are generally required than pharmacological chaperones. In Gaucher disease the development of new generations of pharmacological chaperones has increased the number of mutations that can be treated with these chaperones (Benito *et al*, 2011). As pharmacological chaperones are more specific they would also reduce the risk of possible side effects.

Chemical/pharmacological chaperone treatment in combination with enzyme/factor replacement strategies could improve their efficacy. Incubation of fibroblasts from patients with Fabry disease with the pharmacological chaperone DGJ and recombinant α-Galactose A resulted in up to 4 fold higher enzyme levels than enzyme alone. Coadministration in rats led to an increase in the circulating half-life of recombinant α-Galactose A by >2.5 fold and in *α-Galactose A* KO mice up to 5 fold (Benjamin *et al*, 2012). This strategy of co-administration of a pharmacological chaperone with enzyme replacement therapy is currently being tested in a Phase III clinical trial in patients with Fabry disease (NCT01218659, URL: www.clinicaltrials.gov, accessed 17th June 2014).

### 6.6.5 Osmolytes and the kidney

As explained earlier kidney cells contain urea which denatures protein. To offset this cells produce/acquire osmolytes to counteract the effect of urea. It is interesting that the kidney (which produces ADAMTS13) is generally unaffected in patients with TTP. ADAMTS13 is produced by podocytes in the renal cortex (Manea *et al*, 2007a) and is also expressed in glomerular endothelial cells, microvascular endothelial cells (Tati *et al*, 2011) and in renal cortex tubular endothelial cells (Manea *et al*, 2010).

Similarly the CFTR protein which is defective in patients with cystic fibrosis is expressed at high levels in the kidney but patients have little or no apparent kidney dysfunction. Howard *et al* found that hyperosmotic stress in kidney cells cultured *in vitro* expressing a CFTR mutant, increased levels of different osmolytes within the cell and additionally promoted the correct maturation of the CFTR mutant (Howard *et al*, 2003).

### 6.6.6 Weaknesses

It should be noted that the supernatant samples analysed in these experiments were highly concentrated ~100 fold for analysis. Therefore, in unconcentrated media it is likely that there would only be a small increase in secretion and activity of the mutant in the presence of betaine. If betaine was to be used *in vivo* its effects on ADAMTS13 secretion may appear to be small or may not be easily detectable. However, *in vivo* it has been shown that residual ADAMTS13 activity (undetectable

by assays currently used to measure ADAMTS13 activity in patient plasma) is associated with disease severity (Lotta *et al*, 2012). Therefore. even a small increase in ADAMTS13 activity may be beneficial and change significantly the picture of clinical severity of congenital TTP patients.

### 6.6.7 Future work

In the future it would be interesting to express the mutant in different cells types such as hepatic stellate cells and to analyse whether betaine or other osmolytes have the same effect on the secretion of the mutant. Furthermore expression of the mutant in transgenic mice administered betaine would help to understand whether betaine is likely to have an effect *in vivo*.

### 6.6.8 Conclusion

The p.I143T mutant severely affected the secretion of ADAMTS13. This mutant is degraded by the cell proteasome. The use of a chemical chaperone (betaine) led to increased secretion and as a result increased activity of the mutant. Betaine appears to aid the folding of the mutant within the cell (preventing its degradation by the proteasome) thereby promoting its secretion.

# Chapter 7 ADAMTS13 catalytic characterisation (type 2 mutant)

## 7.1 Introduction

When the p.R102H mutant was expressed *in vitro* it led to reduced secretion of ADAMTS13 (on average 30% of WT ADAMTS13) (Chapter 3). The activity of the mutant was also reduced. I aimed to characterise further how this mutation affected the enzyme activity using purified protein.

### 7.1.1 Order of reaction

The rate of catalysis of an enzyme can often be calculated by measuring product formation or substrate depletion over time. The velocity of an enzymatic reaction may or may not depend on the concentration of a particular reactant. The relationship between the initial concentration of a substrate and the rate of a reaction can be described by the order of the reaction. A reaction can be described as zero order with respect to substrate, if substrate concentration decreases and product formation increases in a linear fashion over time (Figure 7-1). In a zero order reaction the rate of the reaction is independent of substrate concentration.

In a first order reaction the rate of the reaction is proportional to substrate concentration. The relationship between substrate concentration and time is not linear because during the course of the reaction the concentration of substrate decreases which affects the rate of the reaction (Figure 7-1). If a reaction is second order with respect to a substrate the rate of reaction is proportional to the square of the substrate concentration.

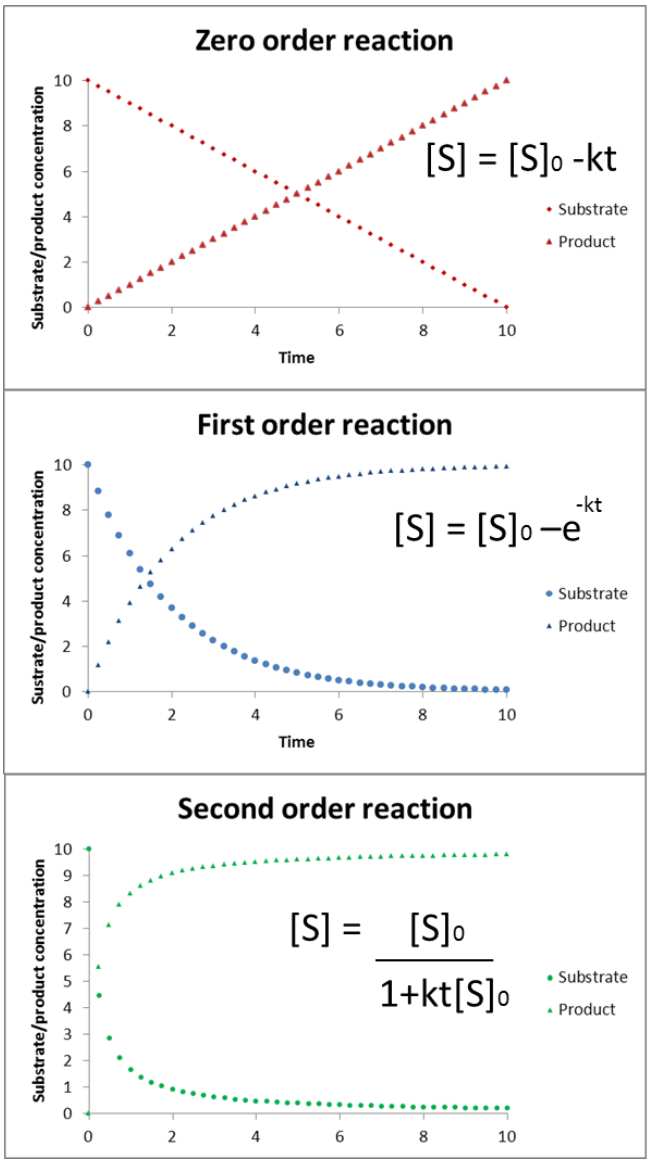


$$-\frac{d[S]_0}{dt} = \text{rate} = k$$

$$-\frac{d[S]_0}{dt} = \text{rate} = k\,[S]$$

$$-\frac{d[S]_0}{dt} = \text{rate} = k\,[S]^2$$

**Figure 7-1 Changes in substrate and product concentration in zero, first and second order reactions**

The graphs show the relationship between substrate concentration and product concentration over time in zero, first and second order reactions. The relationship between substrate concentration and time is represented by the equation within each plot. The rate of reaction or velocity in relation to a particular substrate is shown on the far right hand side. In a zero order reaction, the reaction does not depend on substrate concentration, but on the rate constant (k). In a first order reaction it depends upon the concentration of substrate and k, whereas in a second order reaction it depends on the square of the substrate concentration and k. The constant k is a specific constant for a given reaction (Segel, 1993). [S]: substrate concentration, $[S]_0$: substrate concentration at time 0.

### 7.1.2 Michaelis-Menten kinetics

The relationship between an enzyme, its substrate(s) and product(s) can be thought to follow the scheme shown in Figure 7-2. Enzyme combines with substrate to form an enzyme/substrate complex which is dependent upon the rate constant ($k_1$). This can

lead to product formation with separation of the product from the enzyme (rate of which depends upon the rate constant $k_2$) or alternatively the enzyme and substrate can seperate without catalysis occuring (rate of which depends upon the rate constant $k_{-1}$). The enzyme and product can sometimes revert back to form the enzyme substrate complex (the rate of this is dependent upon the rate constant $k_{-2}$).

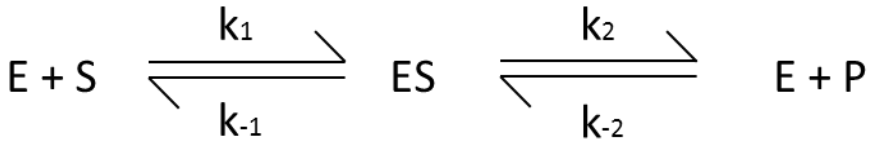


**Figure 7-2 Enzyme catalysis**

Where E is enzyme, S is substrate, P is product, and ES is enzyme/substrate complex. The terms $k_1$, $k_{-1}$, $k_2$ and $k_{-2}$ represent rate constants (Berg *et al*, 2002).

Reaction rates ($\upsilon$) are often defined as the rate of increase in product, when product concentrations are low, at times close to 0. The reaction rate is almost linearly proportional to substrate concentration when substrate concentration is low (first order kinetics). Under these conditions the reaction is said to behave like a pseudo first order reaction (Segel, 1993).

The rate of a reaction is almost independent of substrate concentration when substrate concentration is large (zero order kinetics) (Figure 7-3). As substrate concentration increases the velocity plateaus and approaches the maximum velocity of the enzyme. Michaelis and Menten proposed a model to explain these kinetics (Equation 7-1).

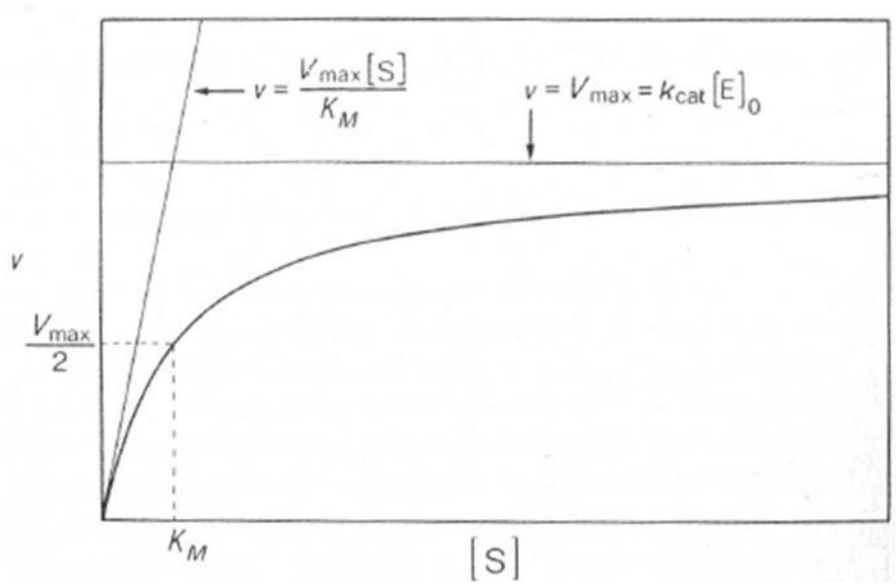


**Figure 7-3 Michaelis-Menten kinetics**

The reaction rate (y axis) is plotted against substrate concentration (x axis) for a reaction obeying Michaelis-Menten kinetics. Where v is the rate of catalysis, $V_{max}$ is the maximum rate of a reaction, [S] is substrate concentration, $K_M$ is the Michaelis constant, $k_{cat}$ is the catalytic concentration, $[E]_0$ is the initial enzyme concentration. Image from: (Fersht, 1985).

$$\upsilon = \frac{k_{cat}[S][E]_0}{K_m + [S]} \quad \text{or} \quad \upsilon = \frac{V_{max}[S]}{K_m + [S]} \quad \text{as} \quad V_{max} = k_{cat}[E]_0$$

**Equation 7-1 Michaelis-Menten equation**

Where $\upsilon$ is the initial rate of reaction, $[E]_0$ is the initial enzyme concentration, [S] is the substrate concentration, $K_m$ is the Michaelis constant and $k_{cat}$ is the catalytic constant. The $k_{cat}$ is the same constant as $k_2$ shown in Figure 7-2 and Figure 7-4 (Berg *et al*, 2002).

The Michaelis-Menten equation assumes that none of the product reverts back to the original product (substrate) (Figure 7-4). This condition holds for the initial stage of a reaction, where products have not significantly accumulated and substrates have not been significantly depleted. This equation also assumes that the concentration of substrate is in excess of enzyme (Berg *et al*, 2002).


**Figure 7-4 Enzyme catalysis according to the Michaelis-Menten equation**

Where E is enzyme, S is substrate, P is product, and ES is enzyme/substrate complex. The symbols $k_1$, $k_{-1}$ and $k_2$ represent rate constants (Berg *et al*, 2002).

### 7.1.3 Michaelis constant ($K_m$)

The Michaelis-Menten equation (Equation 7-1) includes the term $K_m$, the Michaelis-Menten constant. This constant (Equation 7-2) is an important characteristic of enzyme-substrate interactions and is independent of enzyme and substrate concentrations. This constant is equal to the substrate concentration at which the reaction rate is half of its maximal value (Figure 7-3 and Equation 7-2). It therefore provides a measure of the substrate concentration required for significant catalysis to occur. For many enzymes, experimental evidence suggests that $K_m$ provides an approximation of substrate concentration *in vivo* (Berg *et al*, 2002).

$K_m$ also equals the dissociation constant of the ES complex (ES→E+S) if the constant $k_2$ is much smaller than $k_{-1}$. If this condition is met then it can be a measure of the strength of the ES complex, a high $K_m$ indicates weak binding, a low $K_m$ indicates strong binding.

$$K_m = \frac{k_{-1} + k_2}{k_1} \qquad \& \qquad K_m = \frac{V_{max}}{2}$$

**Equation 7-2 Michaelis constant**

The Michaelis constant can be expressed by the two equations above. Where $K_m$ is the Michaelis constant, $V_{max}$ is the maximum velocity and $k_1$, $k_{-1}$ and $k_2$ and rate constants (Berg *et al*, 2002).

### 7.1.4 Kinetic constant ($k_{cat}$)

The maximal rate of a reaction ($V_{max}$) describes the turnover number of an enzyme which is the number of substrate molecules converted into product by an enzyme molecule per unit time when the enzyme is fully saturated with substrate. It depends on the enzyme concentration and the constant $k_2$. The constant $k_2$ is also known as the $k_{cat}$ (Figure 7-2).

### 7.1.5 Catalytic efficiency ($k_{cat}/K_m$)

The ratio $k_{cat}/K_m$ also known as the catalytic efficiency is often used to characterise an enzyme. It depends upon the enzymes ability to bind substrate and then subsequently catalyse the reaction. When the concentration of a substrate is much lower than the $K_m$, of the enzyme then the velocity depends upon $k_{cat}/K_m$, [S] and [E] as shown in Equation 7-3. This can be used to measure the $k_{cat}/K_m$ of the enzyme.

$$\upsilon = \frac{k_{cat}}{K_m}[S][E]_0$$

**Equation 7-3 Michaelis-Menten equation when substrate concentration is lower than $K_m$**

When substrate concentration is much lower than the $K_m$, $\upsilon$ in Equation 7-1 can be expressed as shown above. Where $\upsilon$ is the initial rate of the reaction, $k_{cat}$ is the catalytic constant, $K_m$ is the Michaelis constant, [S] is the substrate concentration and $[E]_0$ is the initial enzyme concentration (Berg *et al*, 2002).

### 7.1.6 Assays to measure ADAMTS13 activity

A variety of assays have been developed to measure ADAMTS13 activity in routine laboratories. These assays vary in terms of the substrate used (full length VWF multimers vs recombinant VWF peptides) and the method of detection (direct or indirect detection of VWF products) (Peyvandi *et al*, 2010). The VWF cleaved products can be detected using electrophoresis, measuring platelet aggregation, measuring FRET or using immunobinding (Peyvandi *et al*, 2010).

The sensitivity of these methods varies. Assays using multimeric VWF can detect activities as low as 3-6% of normal, whereas VWF peptide assays are more sensitive, with the ability to detect activity 1-3% of normal. Assays based on the analysis of full length VWF multimers are time consuming (2-3 days) and are performed with the use of denaturing agents. On the other hand VWF peptide based assays are rapid (1-4 hours) and are performed in the absence of denaturing agents; however these assays use non-physiological VWF as a substrate (Peyvandi *et al*, 2010). There are advantages and disadvantages therefore of the various methods to detect ADAMTS13 activity.

### 7.1.7 *ADAMTS13* polymorphisms

Polymorphisms and mutations are genetic changes which can lead to amino acid changes such as missense mutations and deletions, but are distinguished based upon the frequency of occurrence of these genetic changes in the 'normal' population. Single nucleotide polymorphisms are defined here as single nucleotide variations with a minor allele frequency (MAF) >0.01 in the population, whereas mutations are defined as having a MAF<0.01. *ADAMTS13* polymorphisms are shown in Figure 7-5.

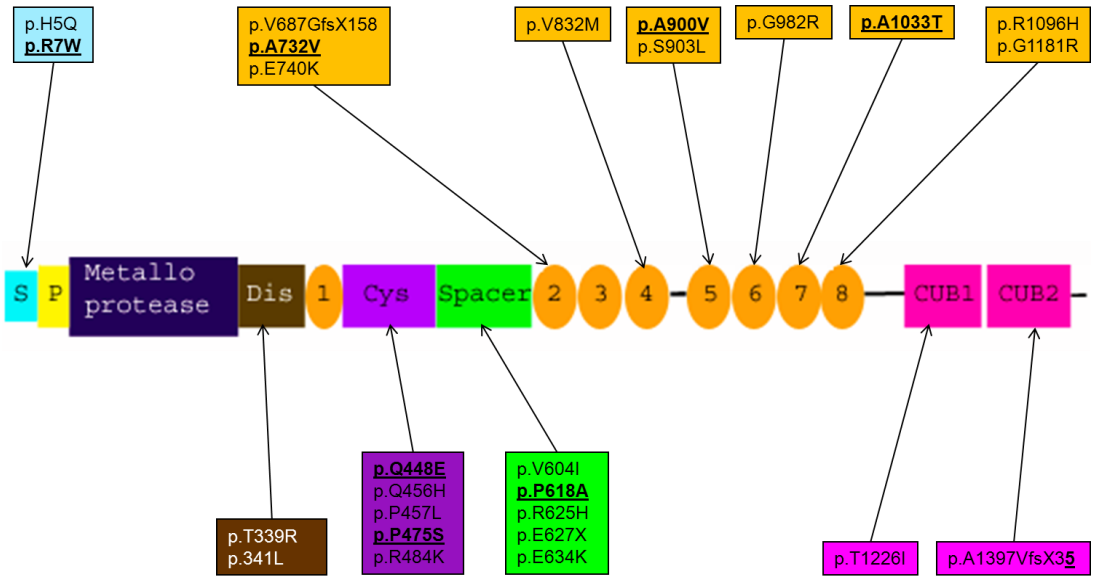


**Figure 7-5 *ADAMTS13* polymorphisms**

*ADAMTS13* polymorphisms as described by (Lotta *et al*, 2010) and (Tseng & Kimchi-Sarfaty, 2011). Polymorphisms which have been expressed *in vitro* are shown underlined and in bold.

Patient 3, a Caucasian patient, was homozygous for the mutation p.R102H and three polymorphisms: p.Q448E (cysteine-rich region), p.P618A (spacer domain) and p.A900V (TSP-1:5 domain) (Figure 7-6).

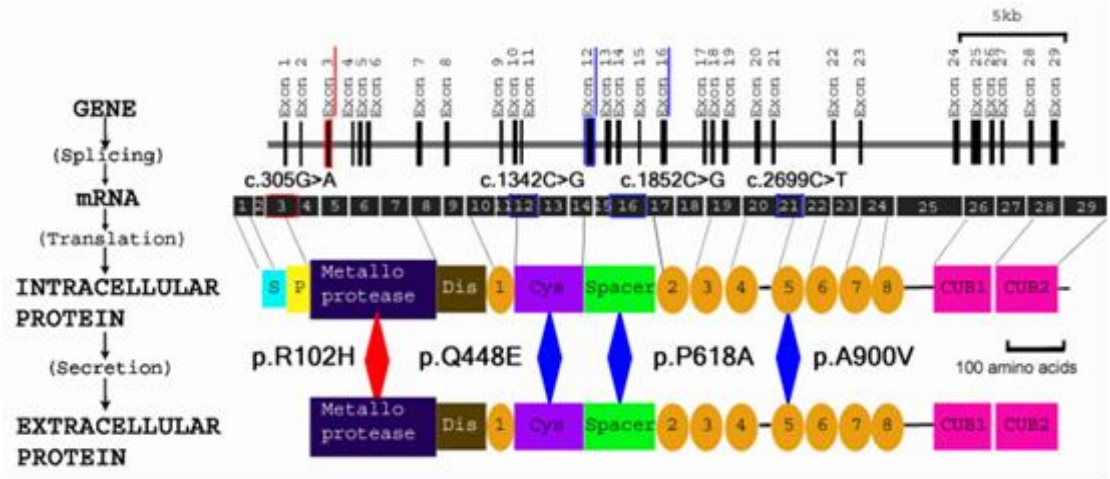


**Figure 7-6 Location of *ADAMTS13* mutation and polymorphisms in the *ADAMTS13* gene, mRNA and protein in patient 3**

Image adapted from (Zheng *et al*, 2001). Mutations are shown in red and polymorphisms in blue.

Analysis of the crystal structure of ADAMTS13 has shown that the amino acid p.Q448 is located within an α-helix in the N-terminal region of the cysteine-rich domain (Akiyama *et al*, 2009). The amino acid p.P618 is located in a loop proximal to the N-terminal cysteine-rich region, following a β6 sheet in the spacer domain. This loop which lies between β6 and β7 sheets plays a pivotal role in the interaction between the spacer domain and the N-terminal cysteine-rich domain (Akiyama *et al*, 2009). Comparative modelling of ADAMTS13 with similar structures has suggested that the p.A900V polymorphism lies within a beta sheet (Edwards *et al*, 2012).

The frequency of the two alleles of the polymorphic amino acids identified in patient 3 is shown in Table 7-1. The reported frequencies are based upon results from phase I of the 1000 genomes project, which are reported in Ensembl (URL: www.Ensembl.org, accessed 17th June 2014).

As shown in Table 7-1, in Caucasians (and in the total number of individuals studied), the MAF of these three polymorphisms is >0.01. The p.Q448E polymorphism in Caucasians appears to be the most common polymorphism (studied here), whereas the p.P618A polymorphism appears to be less common. In other ethnic groups some of these polymorphisms have a MAF<0.01 (African: p.P618A and Eastern Asians: p.A900V).

| rs number | cDNA change | Protein change | Allele Frequency | | | | | | | | | |
|---|---|---|---|---|---|---|---|---|---|---|---|---|
| | | | ALL | | AFR | | AMR | | ASN | | EUR | |
| rs2301612 | c.1342C>G | p.Q448E | CAA | GAA | CAA | GAA | CAA | GAA | CAA | GAA | **CAA** | **GAA** |
| | | | 0.725 | 0.275 | 0.943 | 0.057 | 0.635 | 0.365 | 0.811 | 0.189 | **0.562** | **0.438** |
| rs28647808 | c.1852C>G | p.P618A | CCC | GCC | CCC | GCC | CCC | GCC | CCC | GCC | **CCC** | **GCC** |
| | | | 0.956 | 0.044 | 0.994 | 0.006 | 0.961 | 0.039 | 0.979 | 0.021 | **0.912** | **0.088** |
| rs685523 | c.2699C>T | p.A900V | GCG | GTG | GCG | GTG | GCG | GTG | GCG | GTG | **GCG** | **GTG** |
| | | | 0.914 | 0.086 | 0.839 | 0.161 | 0.914 | 0.086 | 1 | 0 | **0.897** | **0.103** |

**Table 7-1 Allele frequency of *ADAMTS13* polymorphisms within different populations included in the 1000 genomes project**

ALL-all individuals studied, AFR-African, AMR-American, ASN-Eastern Asian, EUR-European individuals from phase I of the 1000 genome project. African sub-populations included Americans of African ancestry in South-Western USA, Luhya in Webuye, Kenya and Yoruba in Ibadan Nigeria. American sub-populations included Columbian from Medellin, Columbia, Mexican ancestry from Los Angeles, USA and Puerto Ricans from Puerto Rica. Asian sub-populations included Han Chinese in Beijing, Southern Han Chinese and Japanese in Tokyo, Japan. Europeans included Utah residents with Northern and Western European ancestry, Finnish in Finland, British in England and Scotland, Iberian population in Spain and Toscani in Italy. The nucleotide which differs between the two amino acids is shown underlined. The allele which is less common is highlighted in pink. Information from Ensembl (URL: http://www.ensembl.org/index.html, accessed 17th June 2014).

## 7.2 Purification of WT and p.R102H mutant ADAMTS13

A stable line of WT and p.R102H mutant ADAMTS13 was produced to stably express large quantities of protein for catalytic analysis. WT and p.R102H mutant ADAMTS13 were purified as described in methods (Chapter 2.12). After purification of WT and p.R102H mutant recombinant ADAMTS13, samples of the purified material were viewed using a Coomassie stain (Figure 7-7), which non-specifically stains proteins, to assess the purity of the samples. Along with the purified WT and p.R102H mutant ADAMTS13 samples, unpurified material and some of the flow through obtained after the purification procedure were also run.

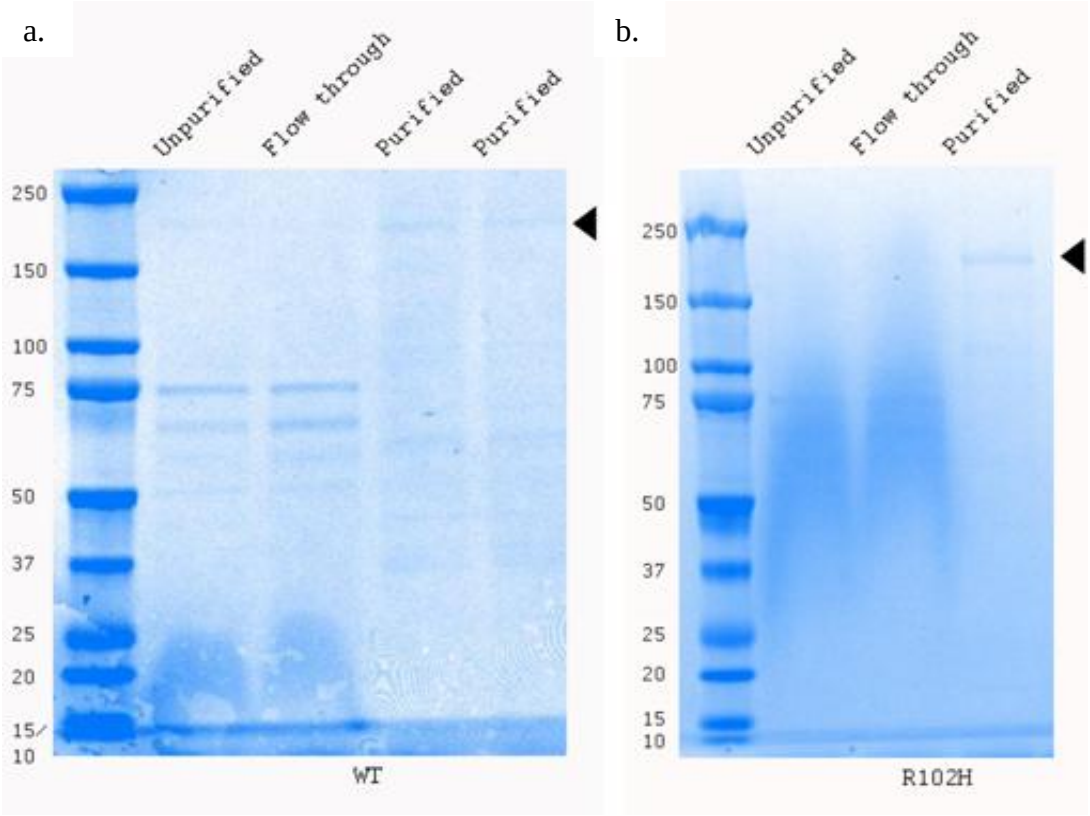


**Figure 7-7 Coomassie staining**

Unpurified, purified and the flow through obtained after purification of WT and p.R102H mutant ADAMTS13 were analysed using Coomassie staining. Expected molecular weight of ADAMTS13 ~190kDa.

Multiple bands could be observed in the unpurified supernatant from WT and p.R102H mutant ADAMTS13 (Figure 7-7). A number of bands could be observed in the flow through also (particularly between 75 and 50kDa). Within the purified material a band could be seen at the expected molecular weight of ADAMTS13

(~190kDa). A faint band of the same size could be observed in the unpurified material from WT but not in the flow through. The band corresponding to ADAMTS13 was clearly visible in the purified, as opposed to the unpurified material as the purified material was more concentrated.

Western blotting was additionally carried out on the samples. This method is more sensitive and specific in its ability to detect the protein of interest (i.e. ADAMTS13). As shown in Figure 7-8 a band corresponding to ADAMTS13 was present at the expected molecular weight, confirming that the band visible in the Coomassie stain was ADAMTS13.

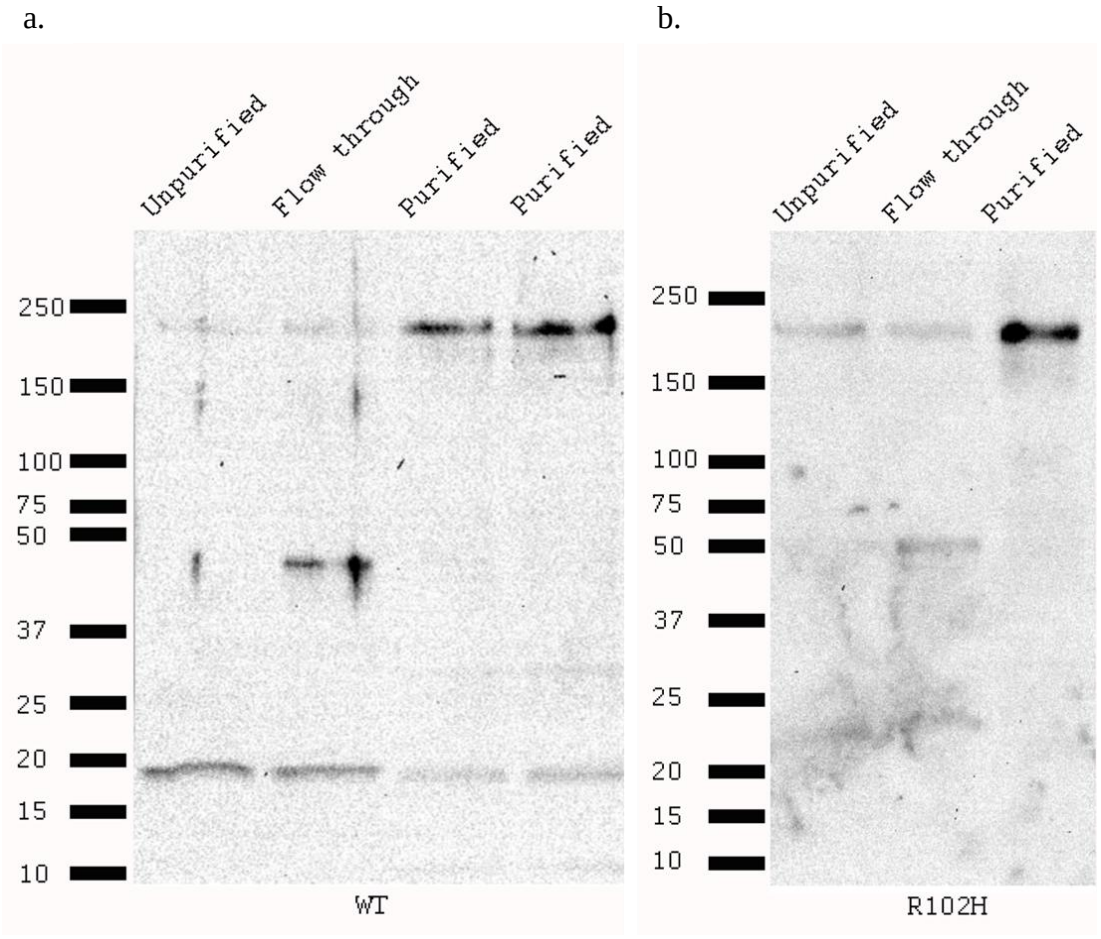


**Figure 7-8 Purified and unpurified ADAMTS13**

Unpurified, purified and the flow through obtained after purification of WT and p.R102H mutant ADAMTS13 were analysed using western blotting. Expected size of ADAMTS13~190kDa.

In WT ADAMTS13 a lower molecular weight band, approximately 20kDa was present. The purified samples were later concentrated using an Amicon centrifugal device with a 100kDa cut-off, which would have removed these lower molecular weight bands. WT protein was produced and analysed using Coomassie staining and western blotting first. Consequently the purified p.R102H mutant was concentrated before Coomassie staining and western blotting was carried out and as shown these lower molecular weight bands are not present in this sample

## 7.3 Calculating the catalytic efficiency ($k_{cat}/K_m$)

Time course experiments were set up to assess the catalytic efficiency ($k_{cat}/K_m$) of WT and p.R102H mutant ADAMTS13. In order to assess this ADAMTS13 was incubated with FRETS-VWF73 substrate and fluorescence was measured, as a measure of product formation over time as shown in Figure 7-9.

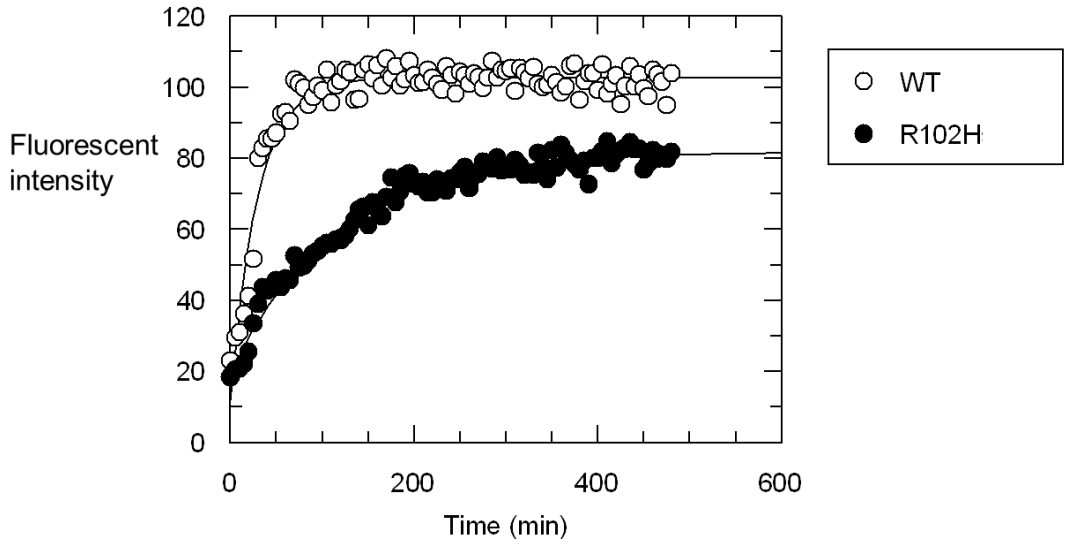


**Figure 7-9 Time course experiment**

Initial reaction values were used to calculate $k_{cat}/K_m$.

The reaction was set up under pseudo first order conditions, so that the concentration of VWF (2μM) was smaller than the $K_m$ of FRETS-VWF73. Anderson *et al* found that ADAMTS13 cleaved FRETS-VWF73 with a $K_{m\ app}$ of 3.2±1.1μM, Di Stasio *et al* measured a $K_m$ of 4.5±0.5μM and Feys et al 2010 measured a $K_m$ of 2.3±0.3μM (Anderson *et al*, 2006;Di Stasio *et al*, 2008;Feys *et al*, 2009b). Under these pseudo first order conditions the rate of reaction should be proportional to the substrate

concentration, υ=k[S] (Figure 7-1). Equation 7-3 shows the value of υ when substrate concentrations are low so substituting υ=k[S] into this equation gives the equation shown in Equation 7-4. The $k_{cat}/K_m$ can then be calculated from this. The observed value of k ($k_{obs}$) was derived from the curve obtained after fluorescence production.

$$k = \frac{[E]_0 k_{cat}}{K_M} \quad \text{or} \quad \frac{k_{cat}}{K_M} = \frac{k}{[E]_0}$$

**Equation 7-4 Experimental determination of $k_{cat}/K_m$**

Where $E_0$ is the enzyme concentration (Fersht, 1985).

The $k_{cat}/K_m$ for WT was 2.8 x $10^5$ $M^{-1}sec^{-1}$ and for the p.R102H mutant this value was 0.75 x $10^5$ $M^{-1}sec^{-1}$, so there was an approximate 4 fold difference between the two.

## 7.4 VWF multimer analysis

The activity of WT and p.R102H mutant ADAMTS13 was analysed further using VWF multimer analysis. Equal quantities of WT or p.R102H mutant ADAMTS13 was incubated with full length VWF and VWF multimeric pattern was analysed over time (Figure 7-10). At 30 minutes there appeared to be a slight difference between WT and p.R102H mutant ADAMTS13, with more of the intermediate molecular weight multimers present in the mutant. However at the remaining time points there did not appear to be a noticeable difference between the two.

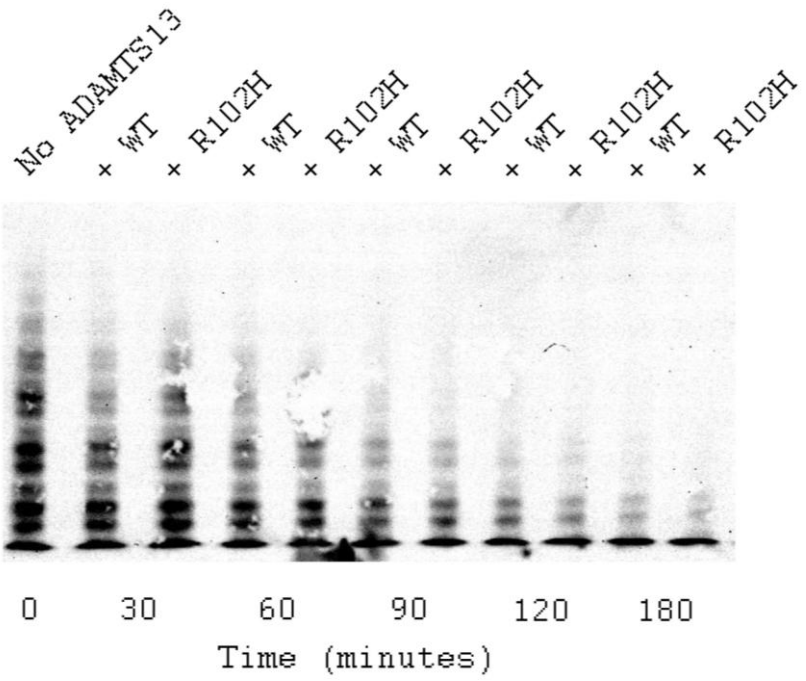


**Figure 7-10 VWF multimer analysis**

Equal quantities of WT and p.R102H mutant ADAMTS13 were incubated with full length VWF and VWF multimeric pattern over time was analysed using electrophoresis. Representative of n=2.

## 7.5 *In silico* analysis of polymorphisms

The p.R102H mutation affected the secretion and activity of ADAMTS13. However the activity of the p.R102H mutant was not as severely affected as hypothesised based upon the undetectable ADAMTS13 activity measured in the patient plasma. The patient with the p.R102H mutation was also homozygous for three ADAMTS13 polymorphisms (p.Q448E, p.P618A and p.A900V). The effect of these polymorphisms in combination with the p.R102H mutation was investigated to understand whether they could further affect the activity of ADAMTS13.

The predicted effects of the polymorphisms present in patient 3 on ADAMTS13 was analysed using three computational tools: SNPs3D, Polyphen2 and SIFT (Table 7-2). All three polymorphisms appeared to be tolerated as predicted by SIFT, although the p.P618A polymorphism had the lowest score. The p.Q448E and p.A900V polymorphisms were not predicted to be deleterious by SNPs3D are were predicted to be benign by Polyphen2, whereas the p.P618A polymorphism was predicted to be probably damaging by Polyphen2 and had a negative score by SNPs3D, indicating

that it may be deleterious. Of the three polymorphisms, the p.P618A polymorphism appeared to be the most likely to have an effect *in vivo* and *in vitro*.

| | **SNPs3D** svm profile | **Polyphen2** | **SIFT** | |
|---|---|---|---|---|
| | | | Score | Prediction |
| p.Q448E | 1.35 | Benign | 1 | Tolerated |
| p.P618A | -1.09 | Probably damaging | 0.14 | Tolerated |
| p.A900V | 0.33 | Benign | 0.29 | Tolerated |

**Table 7-2 *In silico* prediction of the effect of *ADAMTS13* polymorphisms**

Positive SNPs3D score indicated to be non-deleterious whereas a negative score deleterious. Accuracy is significantly increased with scores above 0.5 and below -0.5. Scores >0.05 are predicted to be tolerated by SIFT.

The conservation of the amino acids affected by polymorphisms in patient 3 was investigated by aligning the protein sequence of human ADAMTS13 with either the protein sequence of ADAMTS13 in other animals (ADAMTS13 orthologs) or with the protein sequence of other human ADAMTS proteins (ADAMTS13 paralogs). Results of this analysis in the region of the amino acids affected by these polymorphisms are shown in Figure 7-11 and Figure 7-12. The polymorphic amino acids in the patient are highlighted in yellow.

In 20/21 ADAMTS13 orthologs studied (Figure 7-11) the glutamine (Q) at position 448 was replaced with glutamic acid (E). This suggests that the polymorphism may have little or no effect on the structure or activity of ADAMTS13. Glutamic acid (E) and glutamine (Q) are both surface exposed polar molecules, glutamic acid however is negatively charged whereas glutamine is neutral.

In 20/21 ADAMTS13 orthologs studied (Figure 7-11) there was a proline residue (P) at position 618 whereas in 1/21 there was an alanine (A) residue at this position. This amino acid therefore (p.P618) is more highly conserved in ADAMTS13 orthologs in comparison to p.Q448, suggesting it may be important to have a proline (P) residue at position 618. Proline (P) and alanine (A) are hydrophobic and neutral amino acids;

proline (P) is normally a surface exposed amino acid, whereas the amino acid alanine (A) is normally buried within a protein.

The amino acid at position 900 was more variable in terms of conservation (Figure 7-11). In 2/21 orthologs studied there was an alanine (A) at this position and in 7/21 there was a valine (V) at this position. Therefore, in 12/21 orthologs an amino acid other than alanine (A) or (V) was present. Alanine and valine are hydrophobic, buried and neutral amino acids.

These amino acids are not so well conserved in ADAMTS paralogs (Figure 7-12). In paralogs glutamine (Q) was present in 5/18 ADAMTS proteins and a glutamic acid (E) was present in 6/18 paralogs at position 448. In ADAMTS paralogs there was neither a proline (P) nor alanine (A) present at the position corresponding to amino acid 618. Polymorphisms p.Q448E and p.P618A are present in the cysteine and spacer domains of ADAMTS13 respectively. These domains within ADAMTS proteins are thought to confer substrate specificity to the ADAMTS proteins (Apte, 2004). Therefore, the functions of these domains are slightly different in different ADAMTS proteins and so it is not surprising that they are not so well conserved.

The amino acid at position 900 in ADAMTS13 is present in the TSP-5 domain of ADAMTS13. The number of TSP repeats within ADAMTS proteins is variable (Apte, 2004) which is evident in Figure 7-12. This region is absent from many ADAMTS paralogs.

**p.Q448**

```
Taeniopygia 481 RQRFCNNPRPAFGGQECHGASMQAEMCNTQACLMTQQDFMAEQCAATNLKPLYLDVET-P 539
Gallus      345 RQRFCNNPRPAFGGKECQGASIQAEMCNTQACLMTQLDFMAEQCAATNLKPLYLTVGV-P 403
Bos         396 RRRRCNNPRPAFGGRTCVGSDLQAEMCNTQACEKTQLEFMSEQCAQTDSEPLRLSPGGST 455
Ovis        435 RRRRCDNPRPAFGGRACVGSDLQAEMCNTQACETTQLEFMSEQCAQTDGEPLHLSPGGST 494
Gorilla     411 RRRQCNNPRPAFGGRACVGADLQAEMCNTQACEKTQLEFMSEQCARTDGQPLRSSPGG-A 469
Pan         365 RRRQCNNPRPAFGGRACVGADLQAEMCNTQACEKTQLEFMSEQCARTDGQPLRSSPGG-A 423
ADAMTS13    407 RRRQCNNPRPAFGGRACVGADLQAEMCNTQACEKTQLEFMSQQCARTDGQPLRSSPGG-A 465
Nomascus    401 ---QGGIPVPAFGGRACVGADLQAEMCNTQACEKTQLEFMSEQCARTDGQPLHSSPGG-A 456
Pango       429 RRRQCNNPRPAFGGRACVGADLQAEMCNTQACEKTQLEFMSEQCARTDGQPLRSSPAG-A 487
Papio       409 RRRQCNNPRPAFGGRACVGADLQAEMCNTQACEKTQLEFMSEQCARTDGQPLHSSPGG-A 467
Callithrix  387 RRRQCSNPRPAFGGRVCVGADLQAEMCNTQACEKTQLEFMSEQCARTDGQPLPSSPGG-T 445
Saimin      372 RRRQCSNPRPAFGGRACVGADLQAEMCNTQACEKTQLEFMSEQCSRTDGQPLHSSPGG-T 430
Otolemur    391 RRRWCNNPRPAFGGRACVGADLQAEMCNTQACDKTQLEFMSEQCAETDDQPLHLSPGS-R 449
Mus         412 RRRWCNNPRPAFGGRACVGEDLQAKMCNTQACEKTQLEFMSEQCAQTDRQPLQLSQGT-A 470
Cricetulus  412 RRRWCNNPRPAFGGRTCVGEDLQAKMCNTQACEKTQLEFMTEQCAQTDSQPLHLPQGG-A 470
Cava        408 RRRRCDNPRPAFGGRACAGADLQAEMCNTQACEKTQLEFMSEQCAQTDRQPLSLSLGG-T 466
Canus       558 RRRHCNNPRPAFGGHVCVGADLQAEMCNTQACEKTQLEFMSEQCSQTDRKPLYLTPGN-A 616
Felis       537 RRRQCSNPRPAFGGRACVGDDLQAEMCNTQACEKTQLDFMSEQCSRTDRKPLHLSPGH-A 595
Ailuropoda  490 RRRQCNNPRPAFGGRACVGADLQAEMCNTQACEKTQLEFMSEQCSQTDRKPLHLSPGN-A 548
Equus       399 RRRQCNNPRPAFGGRACVGADLQAEMCNTQACEKTQLEFMSEQCAETNGKPLSLSPGS-T 457
Sarcophilus 510 RRRHCNNPRPAFGGRDCVGADLKAELCNTQACGKTQLEFMSEQCAATDGKPLYLTPGI-P 568
Danio       383 RRRQCNNPRSAFGGTICKGQNTEAELCNLQLCDSTQLEFMARQCSATDQQPLSVSTDS-K 441
```

**p.P618**

```
Taeniopygia 649 SLPYNTTSAH-VTNRRPLFTHLAVKVKGEYVVAGKGKISLNVTYPSVLEDNQ-IKYQVFL 706
Gallus      512 SLPYNATSVH-VINQRPLFTHLAVKVKGEYVVAGKGKISLNVTYPSVLEDRQ-IEYKVFL 569
Bos         565 TVTPNLTSIY-IINRRPLFTHLAVRVRGRYVVAGNGSASASTSYPSLLEDNR-VEYRVTL 622
Ovis        604 TVTPNLTSIS-VINRRPLFTHLGELARRSRLPNAGCRAVLLASFAAQIETQIPRSCSGPL 662
Gorilla     579 TVTPNLTSVY-IANHRPLFTHLAVRIGGRYVVAGKMSISPNTTYPSLLEDGR-VEYRVAL 636
Pan         533 TVTPNLTSVY-IANHRPLFTHLAVRIGGRYVVAGKMSISPNTTYPSLLEDGR-VEYRVAL 590
ADAMTS13    575 TVTPNLTSVY-IANHRPLFTHLAVRIGGRYVVAGKMSISPNTTYPSLLEDGR-VEYRVAL 632
Nomascus    566 TVTPNLTSVY-IANHRPLFTHLAVRIGGRYVVAGKTSISPNTTYPSLLEDGR-VEYRVAL 623
Pango       608 TVTPSLTSVYXXPTHRPLFTHLAVRLGGRYVVAGKTSISPNTTYPSLLEDGR-IEYRVAL 666
Papio       577 TVTPNLTSVY-IANHRPLFTHLAVRIGGRYVVAGKTSISSNTTYPSLLEDGR-VEYRVAL 634
Callithrix  555 TVTPNLTSVY-VANHRPLFTHLAVRIGARYVVAGKSSISPSTTYPSLLEDGR-VEYRVTL 612
Saimin      540 TVTPNLTSVY-VANHRPLFTHLAVRIGARYVVAGKSSISPSTTYPSLLEDGR-VEYRVAL 597
Otolemur    559 TVTPNLTSVY-IANHRPLFSHLAVKVGGRYVVAGKASISPSTIFPSLLEDSR-VEYRVAL 616
Mus         580 IVTPNMTNAH-IVNRRPLFTHLAVRIQGHYIVAGKTSISPNTTYPSLLEDYR-VEYRVTL 637
Cricetulus  580 TVTPNMTSVH-IVNRRPLFTHLAVRIQGHYIVAGKTSISPSIMYPSLLEDCR-VEYRVTL 637
Cava        576 TVTPNMTSVH-IVNRRPLFTHLAVKIGGRYVVAGEAGLAPSTTHPSLLEDSR-VEYRVAL 633
Canus       726 TVTRNLTSVH-ITNRRPLFTHLAVRIRGHYIVAGNSSISPSTTYPSLLEDSR-VEYRVTL 783
Felis       705 TVTRNLTSIY-VTNQRPLFTHLAVRIGGRYIVAGNSSISPSTTYPSLLEDSR-VEYRVTL 762
Ailuropoda  658 TVTRNLTSVH-ITNRRPLFTHLAVRIRGRYVVAGNSSISPSTTYPSLLEDSR-VEYRVAL 715
Equus       567 TVTPNLTSIY-VANQRPLFTHLAVRIRGRYVVAGNSSISPSTTYPSLLEDSR-VEYKVTL 624
Sarcophilus 678 TIPPNFTTVH-ITNQKPLFTHLAVKVRGQYVVSGKKSISFNTTYPSVLEDNQ-IEYKVFL 735
Danio       551 TLPLNASQVH-VFNTRSIFTHLAVLLNDKYVVSGNGKPGLSNTYPSPLEKSL-ITYKLYL 608
```

**p.A900**

```
Taeniopygia 908 SPVAGECSVSCGRGKTQLHY---------------------------------------- 927
Gallus      772 SPLPGECSVSCGRGKTQIQWH-------------------------------------- 792
Bos         883 TPLAGPCSVSCGQGLVELRFVCMDTALRTPVREELCDLASKPGSRREACQAAPCPARWR- 941
Ovis        917 TPLAGPCSASCGQGLAELHFVCMDPALRTPVREELCDLASKPGSRREACQAAPCPARWR- 975
Gorilla     902 TPAAGSCSVSCGRGLMELRFLCMDSALRVPVQEELCGLASKPGSRQEVCQAVPCPARWR- 960
Pan         856 TPAAGSCSVSCGRGLMELRFLCMDSALRVPVQEELCGLASKPGSRREVCQAVPCPARWR- 914
ADAMTS13    898 TPAAGSCSVSCGRGLMELRFLCMDSALRVPVQEELCGLASKPGSRREVCQAVPCPARWQ- 956
Nomascus    889 TPVAGPCSVSCGRGLMELRFLCMDSALRVPVQEELCGLASKPGSRREVCQAVPCPARWR- 947
Pango       932 TPVAGPCSVSCGRGLMELRFVCTDSALRVPVQEELCGLASKPGSRREVCQAVLCPAEWR- 990
Papio       980 TPLAGPCSVSCGRGLMELRFLCMDSALRVPVQEELCGLASKPGSRWEVCQAVPCPARWQ- 958
Callithrix  877 TPVAGLCSVSCGRGLMELRFLCMDSALRVPAQEELCGLANKPGSRWEVCQAVPCPARWR- 935
Saimin      804 TPLAGPCSVSCGRGLMKLRFLCMDSALRVPAQEELCGLASKPGSRWEVCQAVPCPARWR- 862
Otolemur    807 TPLVGPCSVSCGRGLMELWFLCTDSALRVPVEEVLCDLAGKPGSRWMVCQADPCPAQWR- 865
Mus         905 TPLVGLCSISCGRGLKELYFLCMDSVLKMPVQEELCGLASKPPSRWEVCRARPCPARWET 964
Cricetulus  902 TPVTGLCSTSCGRGLMELHFLCMDSVLKMPVQEELCDLASKPSSRWEVCRAGPCPARWET 961
Cava        864 TPVPGLCSVSCGQGLVELRSLCVDPVLRTPVQEKLCNLASRPGSRWEVCWAGPCPAHWEA 923
Canus       987 TPLAGPCSASCGQGLTELNFMCMDSALGTPVREELCDLESKPGSRQEVCQAAPCPAWWR- 1045
Felis       965 TPVAGPCSVSCSRGLKELHFVCVDSVLGTPVQEELCDLGSKPGSRREVCQAAPCPAWWQ- 1023
Ailuropoda  978 TPLAGPCSASCGRGLMELHFVCMDSALGTSVREELCDLESKPGSRQEACQAAPCPAGWR- 1036
Equus          ------------------------------------------------------------
Sarcophilus 999 SPLVGECSVSCGTGLRELRYVCLDFASRKEVQEEKCNPVNPPANQMMVCHAAACPPRWR- 1057
Danio       813 SPRTGECSKTCGNGSQQVQFSCVDHKSRLEVPETLCDPTTKPAQDTQPCRISLCLPIWR- 871
```

**Figure 7-11 Alignment of human ADAMTS13 with ADAMTS13 orthologs**

**p.Q448**

```
ADAMTS1    603  VRYRSCNLEDCPD-NNGKTFREEQCEAHNEFSKASFGSGPAVEWIPKYAGVS-PKDRCKL 660
ADAMTS4    564  TRFRSCNTEDCPT-GSALTFREEQCAAYNHRTDLFKSFPGPMDWVPRYTGVA-PQDQCKL 621
ADAMTS15   560  VKYRSCNLEPCPSSASGKSFREEQCEAFNGYNHSTNRLTLAVAWVPKYSGVS-PRDKCKL 618
ADAMTS8    570  AKYQSCHTEECPP--DGKSFREQQCEKYNAYNYTDMDGN-LLQWVPKYAGVS-PRDRCKL 625
ADAMTS5    611  AIYRSCSLMPCPP--NGKSFRHEQCEAKNGYQSDAKGVKTFVEWVPKYAGVL-PADVCKL 667
ADAMTS9    632  MKFKSCNTEPCLK--QKRDFRDEQCAHFDGKHFNINGLLPNVRWVPKYSGIL-MKDRCKL 688
ADAMTS20   600  MKFRSCNTDSCPK--GTQDFREKQCSDFNGKHLDISGIPSNVRWLPRYSGVG-TKDRCKL 656
ADAMTS3    595  FEYQLCNTEECQK--HFEDFRAQQCQQRNSHFEYQNTKHHWLPYEHPDP-----KKRCHL 647
ADAMTS14   596  FEYQVCNSEECPG--TYEDFRAQQCAKRNSYYVHQNAKHSWVPYEPDDD-----AQKCEL 648
ADAMTS2    605  YDFQLCSRQDCPD--SLADFREEQCRQWDLYFEHGDAQHHWLPHEHRDA-----KERCHL 657
ADAMTS6    602  KRYRSCNTDPCPL--GSRDFREKQCADFDNMPFRGKYYN-----WKPYTGG--GVKPCAL 652
ADAMTS10   591  RRHRSCNTDDCPP--GSQDFREVQCSEFDSIPFRGKFYK-----WKTYRGG--GVKACSL 641
ADAMTS7    582  KRFRLCNLQACPA--GRPSFRHVQCSHFDAMLYKGQLHT-----WVPVVN---DVNPCEL 631
ADAMTS12   586  KRYRLCNVHPCRS--EAPTFRQMQCSEFDTVPYKNELYH-----WFPIFN---PAHPCEL 635
ADAMTS16   630  RTLKLCNSQKCPR--DSVDFRAAQCAEHNSRRFRGRHYK-----WKPYTQVE-DQDLCKL 681
ADAMTS18   633  RIYQLCNINPCNE--NSLDFRAQQCAEYNSKPFRGWFYQ-----WKPYTKVE-EEDRCKL 684
ADAMTS17   587  VEHAVCENLPCPK--GLPSFRDQQCQAHDR--LSPKKKG-----LLTAVVV--DDKPCEL 635
ADAMTS19   675  KQYRICENPPCPA--GLPGFRDWQCQAYSVRTSSPKHIL-----QWQAVLD--EEKPCAL 725
ADAMTS13   428  LQAEMCNTQACEK--TQLEFMSQQCARTDGQPLRSSPGGASFYHWGAAVPHSQGDALCRH 485
```

**p.P618**

```
ADAMTS1    739  HDIITIPTGATNIEVKQRNQRGSRNNGSFLAIKAADGTYILNGDYTLSTLEQDIMYKG-V 797
ADAMTS4    700  NNVVTIPAGATHILVRQQGNPGHRS--IYLALKLPDGSYALNGEYTLMPSPTDVVLPGAV 757
ADAMTS15   697  NFVVAIPAGASSIDIRQRGYKGLIGDDNYLALKNSQGKYLLNGHFVVSAVERDLVVKG-S 755
ADAMTS8    704  NDIVTIPAGATNIDVKQRSHPGVQNDGNYLALKTADGQYLLNGNLAISAIEQDILVKG-T 762
ADAMTS5    746  TDVVRIPEGATHIKVRQFKAKDQTRFTAYLALKKKNGEYLINGKYMISTSETIIDING-T 804
ADAMTS9    767  NTVVRIPAGATNIDVRQHSFSGETDDDNYLALSSSKGEFLLNGNFVVTMAKREIRIGN-A 825
ADAMTS20   735  NVVVKIPAGATNVDIRQYSYSGQPDD-SYLALSDAEGNFLFNGNFLLSTSKKEINVQG-T 792
ADAMTS3    729  LKMFDIPPGARHVLIQED----EASPHILAIKNQATGHYILNGKG-EEAKSRTFIDLG-- 781
ADAMTS14   730  LKLVQIPAGARHIQIEAL----EKSPHRIVVKNQVTGSFILNPKG-KEATSRTFTAMG-- 782
ADAMTS2    739  IKMFEIPAGARHLLIQEV----DATSHHLAVKNLETGKFILNEENDVDASSKTFIAMG-- 792
ADAMTS6    733  MEVVQIPRGSVHIEVREV-----AMSKNYIALKSEG-DDYYINGAWTIDWPRKFDVAG-T 785
ADAMTS10   722  EDVVWIPKGSVHIFIQDL-----NLSLSHLALKGDQ-ESLLLEGLPGTPQPHRLPLAG-T 774
ADAMTS7    713  VDVGLIPAGAREIRIQEV-----AEAANFLALRSEDPEKYFLNGGWTIQWNGDYQVAG-T 766
ADAMTS12   717  VDIGLIPKGARDIRVMEI-----EGAGNFLAIRSEDPEKYYLNGGFIIQWNGNYKLAG-T 770
ADAMTS16   762  YHMVTIPSGARSIRIYEM-----NVSTSYISVRNAL-RRYYLNGHWTVDWPGRYKFSG-T 814
ADAMTS18   765  YPVVLIPAGARSIEIQEL-----QVSSSYLAVRSLS-QKYYLTGGWSIDWPGEFPFAG-T 817
ADAMTS17   713  ------------------------------ALKDSG--KGSINSDWKIELPGEFQIAG-T 739
ADAMTS19   805  VEVLVIPAGARRIKVVEE-----KPAHSYLALRDAG--KQSINSDWKIEHSGAFNLAG-T 856
ADAMTS13   571  VTFLTVTPNLTSVYIANHRPLFTHLAVRIGGRYVVAGKMSISPNTTYPSLLEDGRVEYRV 630
```

**p.A900**

```
ADAMTS1           ------------------------------------------------------------
ADAMTS4           ------------------------------------------------------------
ADAMTS15          ------------------------------------------------------------
ADAMTS8           ------------------------------------------------------------
ADAMTS5           ------------------------------------------------------------
ADAMTS9           ------------------------------------------------------------
ADAMTS20          ------------------------------------------------------------
ADAMTS3           ------------------------------------------------------------
ADAMTS14          ------------------------------------------------------------
ADAMTS2           ------------------------------------------------------------
ADAMTS6    989    ----------------------------------------SDLSKTFPA---------- 997
ADAMTS10   974    ----------------------------------------ADHRATLPP---------- 982
ADAMTS7    1379 WDSPANSHRVPETQPLAPSLAEAGPPADPLVVRNAGWQAGNWSECSTTCGLGAVWRPVRC 1438
ADAMTS12   1285 LTEEDATSLITEGFLLNASNYKQLTNGH----GSAHWIVGNWSECSTTCGLGAYWRRVEC 1340
ADAMTS16   1019 ----------------------------------------SARAQLLPD---------- 1027
ADAMTS18   1022 --------------------------------------------AAETLPE---------- 1028
ADAMTS17          ------------------------------------------------------------
ADAMTS19          ------------------------------------------------------------
ADAMTS13   868  -WGHLDATSAGEKAPSPWGSIRTGAQAAHVWTPAAGSCSVSCGRGLMELRFLCMDSALRV 926
```

**Figure 7-12 Alignment of human ADAMTS13 with ADAMTS13 paralogs**

## 7.6 Creation of vectors expressing polymorphisms

Site directed mutagenesis was used to add the three polymorphisms (p.Q448E, p.P618A and p.A900V) to either WT or p.R102H mutant ADAMTS13. The following constructs were created:

i. p.R102H+p.Q448E+p.P618A+p.A900V

ii. WT+p.Q448E

iii. WT+p.P618A

iv. WT+p.A900V

v. WT+p.Q448E+p.P618A+p.A900V

Construct i. was created to mimic the genotype of patient 3. Constructs ii-iv were created to investigate the effect of each individual polymorphism on WT ADAMTS13. Construct v. was created to investigate the effect of the three polymorphisms expressed together, in the absence of p.R102H. The three polymorphisms added to constructs i. and v. were added sequentially in separate site directed mutagenesis reactions. Constructs i-iv were created first followed by expression *in vitro*. Western blotting is shown in Figure 7-13.

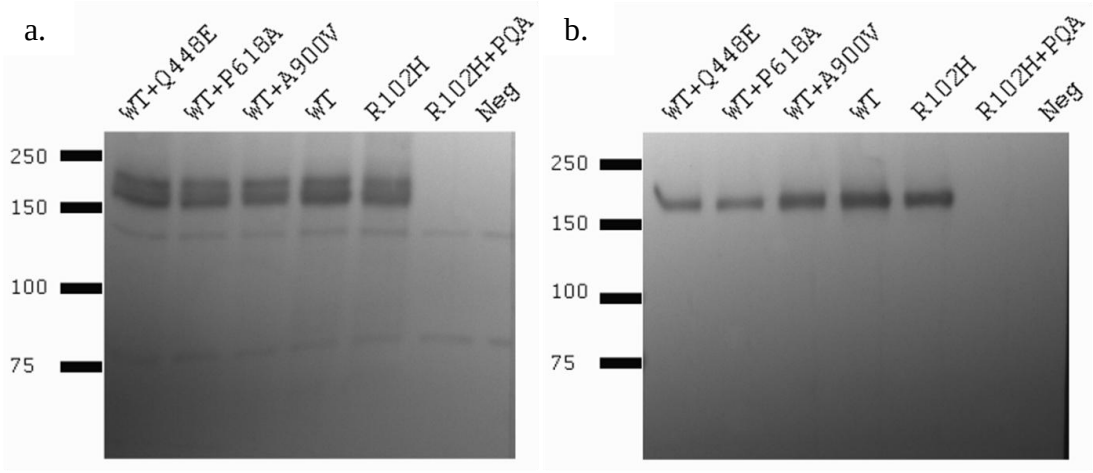


**Figure 7-13 *In vitro* expression of *ADAMTS13* polymorphisms**

This western blot was developed using a colorimetric detection kit, (Bio-Rad 170-8235, Opti 4CN substrate), as described by the manufacturer. Images were captured using Genesnap software (Gbox, Syngene). Cell lysate samples are shown on the left and supernatant on the right.

All proteins except the p.R102H+p.Q448E+p.P618A+p.A900V mutant could be detected by western blotting within cell lysate samples. The results suggested that either something went wrong during the transfection procedure and the vector was not taken up by the transfected cells or the mRNA of this recombinant protein was recognised as abnormal and degraded within the cell before protein synthesis could take place. It was unlikely to be the first problem (i.e. a problem with the transfection) as all the other transfections worked well and nothing abnormal occurred during the transfection procedure. A problem at the mRNA level was unexpected because when these polymorphisms were expressed separately *in vitro* as shown in Figure 7-13, protein synthesis was not abolished. It was hypothesised that the problem was likely to be with the vector that was used to express this mutant.

The whole of the *ADAMTS13* gene within the vector expressing the p.R102H+p.Q448E+p.P618A+p.A900V construct was sequenced to check for any abnormalities. A deletion within the *ADAMTS13* gene in the vector was found which led to the presence of a premature stop codon. After sequencing the constructs that had been used to create this vector (i.e. p.R102H+p.P618A and p.R102H+p.P618A+p.Q448E), within the same region, it was found that the deletion had been introduced after the addition of the second polymorphism (p.Q448E) to the vector.

Consequently the polymorphisms were reintroduced into the vector expressing the p.R102H mutant. Different primers were used to introduce the p.Q448E polymorphism. After the addition of all three polymorphisms the whole of the *ADAMTS13* sequence within the vector was sequenced to make sure that there were no deletions/insertions or amino acid substitutions and there were no problems with this vector. Additionally the whole of the *ADAMTS13* region in other vectors created earlier were retrospectively sequenced (p.I143T, p.Y570C, WT+p.Q448E, WT+p.P618A, WT+p.A900V) and subsequent vectors created (WT+p.Q448E+p.P618A+p.A900V) to make sure that there were not any similar problems. There were no problems in these vectors.

## 7.7 *In vitro* expression of *ADAMTS13* polymorphisms

After constructs i-v were created they were expressed transiently *in vitro*. Results are shown in Table 7-3 and Figure 7-14. These results have not been normalised and are representative of n=2 experiments.

| Construct | Mean antigen (% of WT±SD) (n=2) | Mean activity (% of WT±SD) (n=2) | Specific activity |
|---|---|---|---|
| **WT** | 100 | 100 | 100 |
| **W+PQA** | 54±5.6 | 34±14 | 63±32 |
| **R102H** | 46±0.6 | 10±0.1 | 22±0.51 |
| **R+PQA** | 6±2.0 | - | - |
| **W+P** | 9±3.0 | 10±6.3 | 111±86 |
| **W+Q** | 72±7.5 | 80±14 | 111±25 |
| **W+A** | 129±1.9 | 86±11 | 67±21 |

**Table 7-3 ADAMTS13 antigen and activity measured in the supernatant of transiently transfected cells**

Mean antigen and activity from n=2 experiments are shown. The specific activity was calculated by dividing the activity levels by antigen levels.

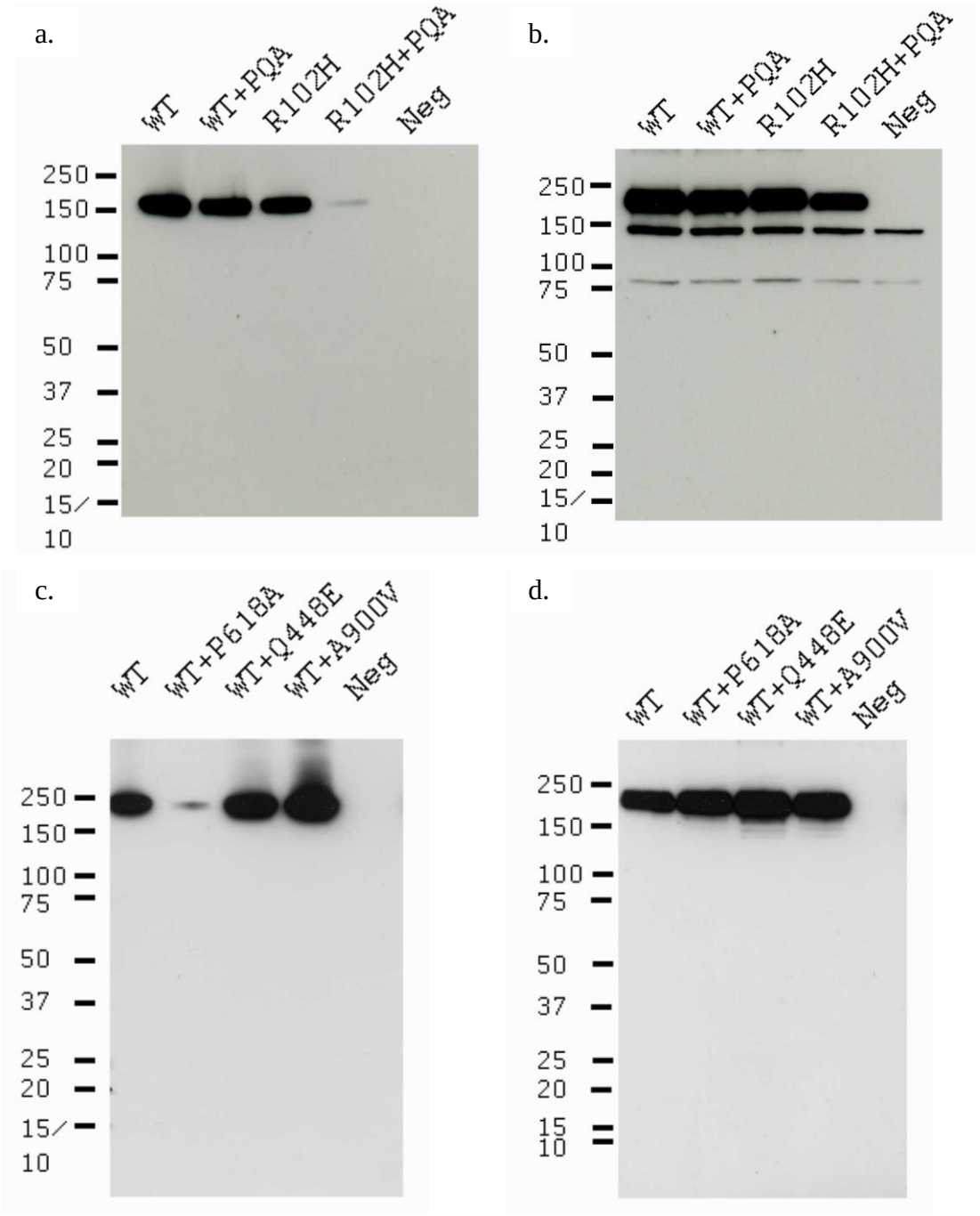


**Figure 7-14 Supernatant and cell lysate samples harvested after transient transfection of *ADAMTS13* polymorphisms**

Supernatant samples are shown in a and c. Cell lysate samples are shown in b and d. PQA: P618A+Q448E+A900V. Representative of n=2 experiments.

When expressed separately, the p.P618A polymorphism had the greatest effect on the secretion of ADAMTS13, reducing the secretion of ADAMTS13 more than the p.R102H mutant. The p.Q448E polymorphism appeared to slightly decrease the secretion of ADAMTS13, whereas the p.A900V polymorphism increased it. When all three polymorphism were expressed in WT ADAMTS13 or in combination with the p.R102H mutant they reduced the secretion of both molecular forms of ADAMTS13, when compared to WT or p.R102H alone.

The p.Q448E and p.P618A polymorphisms did not appear to additionally affect the activity of ADAMTS13, whereas the p.A900V polymorphism did. The specific activity of WT and p.R102H mutant with all three polymorphisms was also reduced. No activity could be detected in the p.R102H+p.Q448E+p.P618A+p.A900V construct. The quantity of WT ADAMTS13 in these experiments was ~160% of that in PNP.

A stable line of the p.R102H+p.Q448E+p.P618A+p.A900V mutant has been created. The various clones have been collected and in the future they will be analysed for further experiments.

## 7.8 Discussion

The results from the time course experiments, using FRETS-VWF73 as a substrate, demonstrated that the p.R102H mutation affects the $k_{cat}/K_m$ of ADAMTS13 with the mutant having an approximately 4 fold reduction in its catalytic efficiency (WT: 2.8 x $10^5$ $M^{-1}sec^{-1}$, p.R102H mutant: 0.75 x $10^5$ $M^{-1}sec^{-1}$). The mutation may affect the turnover number ($k_{cat}$) or $K_m$ of the enzyme or both. In the circulation this mutant is likely to be less efficient at cleaving VWF than WT.

When degradation of full length VWF was carried out using equal quantities of either WT or p.R102H mutant ADAMTS13, there was no obvious difference between the two at later time points. Assays using full length VWF as a substrate have a lower sensitivity and poorer precision compared to those using a peptide substrate (Peyvandi *et al*, 2010). Together these results suggest that although there was a difference between WT and the p.R102H mutant, the mutant's activity was not

severely reduced as expected based upon the undetectable activity measured in the patient plasma. It is true that the mutant is secreted at a reduced level (Chapter 3) which would also impact on the activity measured in the patient plasma but this was still not enough to severely reduce the activity measured in the supernatant.

A stable line of WT and p.R102H mutant ADAMTS13 was created to produce large quantities of ADAMTS13 protein to be purified. The purified protein was eluted in a buffer with a composition closer to physiological conditions (150mM NaCl, 20mM HEPES, pH7.4). The unpurified protein was present in OptiMEM media which had been collected after incubation with respiring cells. The media is likely to have been slightly acidic due to the $CO_2$ dissolved in it. ADAMTS13 has been shown to be affected by pH (Di Stasio *et al*, 2008), therefore the measured activity may have been slightly higher in a lower pH. This is one of the reasons it is important to purify and change the media of the buffer the protein is in. Additionally the purification of ADAMTS13 removed other proteins which may have also been present in the media and potentially interfered with the measured activity.

The $k_{cat}/K_m$ was calculated by measuring product formation with a peptide fragment, as it is quicker and easier to carry out the analysis with this substrate compared to full length VWF. In addition measuring ADAMTS13 activity using FRETS-VWF73 as a substrate may be a more relevant assay to measure ADAMTS13 activity (Tripodi *et al*, 2008;Mancini *et al*, 2014).

The $k_{cat}/K_m$ values reported by others for WT using FRETS-VWF73 as a substrate varied from 0.30-1.2x$10^6 M^{-1}s^{-1}$ (Anderson *et al*, 2006;Di Stasio *et al*, 2008;Feys *et al*, 2009b). My results agree with these values as I obtained a value of 2.8x$10^5 M^{-1}s^{-1}$ (or 0.28x$10^6 M^{-1}s^{-1}$) for WT ADAMTS13.

The $k_{cat}/K_m$ value measured depends upon the substrate used. The $k_{cat}/K_m$ using VWF74 peptide (with Cys1669 replaced with alanine) gave values ranging from 0.31-1.24x$10^5 M^{-1}s^{-1}$ (Lancellotti *et al*, 2010). The $k_{cat}/K_m$ using VWF115 (1554-1668) varied from 7.5-8.7x$10^4 M^{-1}s^{-1}$ (Zanardelli *et al*, 2006;Lam *et al*, 2007;Xiang *et al*, 2011). The $k_{cat}/K_m$ using guanidine HCl treated multimeric VWF was 0.92x106M-1s-1 (Anderson *et al*, 2006). The $k_{cat}/K_m$ using urea treated multimeric

VWF in the presence of 150mM NaCl was $0.34x10^4M^{-1}s^{-1}$ (De Cristofaro *et al*, 2005). These differences probably exist because of the different subsites available for interaction in the different VWF fragments (Anderson *et al*, 2006).

The p.S119F ADAMTS13 mutant was found to cause an approximate 2 fold reduction in the $k_{cat}/K_m$ of ADAMTS13 compared to WT (Feys *et al*, 2009b). The authors also measured activity using FRETS-VWF73 substrate. However the secretion of the p.S119F mutant was more severely reduced compared to the p.R102H mutant studied here. The p.S119F could be detected using western blotting but not quantified with an antigen ELISA (below the detection limit) (personal communication). So the severe defect introduced by the p.S119F mutation was likely responsible for the undetectable activity measured in the patient plasma.

Analysis of ADAMTS13 activity using full length VWF requires unfolding of VWF to enable exposure of the A2 cleavage site, which is buried in its globular form. Urea is commonly used as a denaturant for multimer analysis; guanidine chloride may also be used for analysis. Ristocetin was used in these experiments to denature VWF; this has been used by other groups to measure ADAMTS13 activity (De Cristofaro *et al*, 2005;Lancellotti *et al*, 2010;Chen *et al*, 2012).

Ristocetin is commonly used to assess the functional state of VWF, by inducing the interaction of VWF and the platelet glycoprotein (GP) Ib-IX-V complex in the absence of shear stress or VWF immobilisation. It induces an allosteric change in VWF that exposes the binding site for glycoprotein Ibα (GPIbα) (Kang *et al*, 2008). Two binding sites for ristocetin have been identified within VWF flanking the platelet-binding A1 domain (Girma *et al*, 1990;Berndt *et al*, 1992;Azuma *et al*, 1993).

Chen *et al* found that when ristocetin (1mg/ml) was added to plasma, it could enhance the ability of endogenous ADAMTS13 to cleave VWF in a manner similar to 1.5mol/L urea (Chen *et al*, 2012). De Cristofaro *et al* demonstrated that the conformational change induced by urea in VWF appears to be different from that induced by ristocetin (De Cristofaro *et al*, 2005).

Ristocetin may be a more specific reagent than chaotropic agents such as urea, to evaluate the ability of ADAMTS13 to cleave multimeric VWF *in vitro* (Chen *et al*, 2012). Urea unfolds VWF whereas ristocetin causes a conformational change in VWF, holding it in a GPIb bound like state. Furthermore as urea non-specifically affects protein folding, it may also alter the folding of ADAMTS13.

The various assays used to measure ADAMTS13 activity in patient plasma generally give similar results; however there can be discrepancies between the assays (Palla *et al*, 2011;Mackie *et al*, 2013). Consequently I analysed ADAMTS13 activity using both a VWF peptide substrate and full length VWF.

The ADAMTS13 activity assays used routinely are performed under static conditions but *in vivo* ADAMTS13 cleaves VWF under conditions of flow, shear stress aids the unfolding of VWF and exposes the ADAMTS13 cleavage site. Static assays require denaturation to unfold full length VWF or the assays use a VWF peptide in which the cleavage site is already exposed. Flow based assays are not practical in routine laboratories and are technically difficult to set up.

Activity of the mutants was not assessed using a flow based assay system but this is something planned for the future. I hypothesise that the flow based assays would show similar results, i.e. a small difference in the activity of WT and p.R102H mutant ADAMTS13. Investigation of ADAMTS13 activity in C-terminal mutants would be particularly important under flow because the C-terminal regions appear to be dispensable for ADAMTS13 activity under static conditions but important under conditions of flow (Soejima *et al*, 2003;Zheng *et al*, 2003;Zhang *et al*, 2007;Zhou *et al*, 2007;De Maeyer *et al*, 2010). Subsequent research has shown that the C-terminal region binds to VWF in its globular state, so the C-terminal region may be important for localisation of ADAMTS13 to the site of thrombus formation (Zanardelli *et al*, 2009;Feys *et al*, 2009a). The p.R102H mutation however is within the N-terminal region. Although it will be important to measure the activity of this mutant under flow, I hypothesise that the results will not disagree with the above results, but will complement them.

As the p.R102H mutation did not severely affect the activity of ADAMTS13 to the effect predicted, the effect of polymorphisms in combination with this mutation was investigated. *In vitro* expression of the p.R102H mutant, present in patient 3 along with the three *ADAMTS13* polymorphisms also present in this patient (p.Q448E, p.P618A, p.A900V) led to a further reduction in the secretion and consequently activity of the p.R102H mutant. No ADAMTS13 activity could be detected in the supernatant of cells expressing the mutant with polymorphisms. This is in contrast to the mutant alone in which activity could be detected, on average 10% of WT ADAMTS13. The patient had undetectable (<5%) activity in her plasma and so these results suggest that the polymorphisms in combination with the mutation as opposed to the mutation alone was responsible for the undetectable activity measured in the patient plasma.

Due to the small amount of protein secreted in the mutant with polymorphisms (6%) and the observation that the p.R102H mutation itself leads to a decrease in ADAMTS13 specific activity, it is difficult to conclude whether the polymorphisms reduce the specific activity of the mutant further. In the future purified ADAMTS13 mutant plus polymorphisms will be used to investigate whether and how the polymorphisms further affect the activity of ADAMTS13.

When the three polymorphisms were expressed with WT ADAMTS13 there was similarly a reduction in the antigen and activity of ADAMTS13. However although activity was reduced (34%), it was still much greater that 5%, so these polymorphisms alone are not responsible for the reduced activity (<5%) measured in the patient plasma. This further suggests that the combination of the mutation with the three polymorphisms is responsible for the reduced activity in the patient plasma (i.e. not the polymorphisms alone).

In these experiments WT ADAMTS13 antigen was on average 150% of PNP and therefore the proteins detected using this transiently transfected system were at a level similar to quantities we would expect to find in plasma.

The effect of polymorphisms in combination with a mutation was studied also by Plaimauer *et al* (Plaimauer *et al*, 2006). The authors studied the combination of a

mutation (p.R1336W) with 4 different polymorphisms which were identified in two brothers. One brother was heterozygous for the mutation and three polymorphisms and the other brother was heterozygous for this mutation and four polymorphisms (p.R7W, p.Q448E, p.P618A, p.A732V). Antigen in the supernatant of the p.R1336W mutant alone was 23%±3 and activity was 12%±1 of PNP. When the mutant was expressed with the 4 polymorphisms, ADAMTS13 antigen and activity were undetectable. Similar to my results when WT ADAMTS13 was expressed with the 4 polymorphisms ADAMTS13 antigen and activity were reduced (80% and 40% respectively), but this was not enough to severely reduce the antigen and activity alone.

The patients studied by Plaimauer were heterozygous for four (or three) of the *ADAMTS13* polymorphisms and were heterozygous for the p.R1336W mutation (Plaimauer *et al*, 2006). The authors did not analyse whether the polymorphisms were on the same *ADAMTS13* allele and the patients were also heterozygous for another *ADAMTS13* mutation p.Q449X, which would have also contributed to the undetectable ADAMTS13 activity measured in the patient plasma. The p.Q449X mutation leads to a protein with undetectable ADAMTS13 activity (Kokame *et al*, 2002;Plaimauer *et al*, 2006). Therefore, in these patients it is difficult to determine whether the p.R1336W mutation was sufficient (in the absence of polymorphisms) to lead to the reduced activity measured in the patient plasma, as the contribution of the p.Q449X protein also has to be considered.

The patient studied here was homozygous for the p.R102H mutation and the three polymorphisms. Therefore, this was the only *ADAMTS13* mutation present in this patient and it can be clearly seen in this patient that the 3 polymorphisms along with the mutation are necessary to reduce the activity of ADAMTS13 to levels comparable to those measured in the patient plasma.

The ADAMTS13 antigen measured in the supernatant of the mutant with polymorphisms was approximately 6% of WT. In patient 3 (in which the mutations and polymorphisms were identified), ADAMTS13 antigen was higher, 42%±5.4 (mean±SD), of PNP. It is unclear why these differences exist. This patient was also homozygous for a number of synonymous *ADAMTS13* polymorphisms (p.P118P,

p.140A, p.G194G, p.1407T) which may have modulated the secretion (or even activity) of ADAMTS13 further. Edwards *et al* showed that non-synonymous polymorphisms can modulate the secretion and activity of ADAMTS13 (Edwards *et al*, 2012). The authors studied three of the silent polymorphisms present in patient 3 (p.P118P, p.A40A and p.T1407T), *in vitro*. ADAMTS13 antigen and specific activity of these silent polymorphisms were as follows: p.P118P (antigen 137%, specific activity 208%), p.A140A (antigen 120%, specific activity 169%), p.T1470T (antigen 63%, specific activity 88%). Silent polymorphisms therefore appear to have a significant effect on the secretion and activity of ADAMTS13.

When the three polymorphisms were expressed separately in WT ADAMTS13 they had different effects on ADAMTS13 secretion and activity. These polymorphisms have been expressed *in vitro* by other groups. In the supernatant of WT ADAMTS13 expressing the p.Q448E *ADAMTS13* polymorphism, the mean antigen was 72%±7.5 and the activity was 80%±14 of WT ADAMTS13. Others have found reduced ADAMTS13 antigen with this polymorphism (95-99%) (Plaimauer *et al*, 2006;Edwards *et al*, 2012;Rurali *et al*, 2013). Levels of ADAMTS13 antigen in the experiments described here are slightly lower than these values. However the results need to be repeated and normalised to take into account differences in the transfection efficiency between experiments. The specific activity of this mutant appears to be greater than 100% which agrees with the results of Rurali *et al* and Edwards *et al* but disagrees with the results of Plaimauer *et al*.

Plaimauer *et al* found that p.Q448E was a positive modifier in the context of p.P618A but could not rescue the severely reduced specific activity conferred by p.P618A. In contrast when expressed with the p.R1336W mutant and p.R7W, another positive modifier, the polymorphisms enhanced the detrimental effect of the p.R1336W mutation (Plaimauer *et al*, 2006). The p.Q448E polymorphism therefore may act to increase or decrease ADAMTS13 activity, when expressed with the p.R102H mutation, along with the other two polymorphisms.

In the supernatant of WT ADAMTS13 expressing the p.P618A polymorphism the average antigen was 9%±3 and activity was 10±6.3. This is slightly lower than the antigen levels measured by others (27-75%) (Plaimauer *et al*, 2006;Edwards *et al*,

2012;Rurali *et al*, 2013). In the experiments described here polymorphism did not appear to affect the activity of ADAMTS13; others have found that this mutant also has reduced specific activity (49-68%) (Plaimauer *et al*, 2006;Edwards *et al*, 2012;Rurali *et al*, 2013). A reduction in activity may not have been detected here as a small amount of protein was secreted and a small number of experiments performed.

In the supernatant of WT expressing the p.A900V polymorphism the average antigen was 129%±1.9 and the activity was 86±11. Others have found reduced levels (86%, 95%, (Rurali *et al*, 2013;Edwards *et al*, 2012)). The specific activity measured by others was similar or slightly reduced (Rurali *et al*, 2013;Edwards *et al*, 2012)(100%, 73%, respectively). Similar to Edwards *et al*, a reduced specific activity in WT ADAMTS13 expressing this polymorphism was found.

The differences in antigen and activity obtained here after expression of each polymorphism in WT ADAMTS13, may be partly because a small number of experiments were performed (n=2) and also because the results have not been normalised to take into account differences in the transfection efficiency. This may also explain why levels of antigen in the p.R102H mutant measured and shown in

Table 7-3, are slightly higher than those reported in Chapter 3. Also different cell lines, methods of transfection and measurement of ADAMTS13 antigen and activity have been used in the experiments described here and by others, which may also account for some of these differences. For example quantities of the p.P618A antigen measured in the supernatant *in vitro* by others are quite variable, ranging from 27-75% of WT (Plaimauer *et al*, 2006;Edwards *et al*, 2012;Rurali *et al*, 2013).

*In vivo* ADAMTS13 activity in the Japanese population heterozygous and homozygous for p.E448 was slightly but significantly higher than those homozygous for p.Q448 (97%±25 vs 91%±24 in men and 111%±28 vs 104%±26 in women, mean±sd). These results suggest that the p.E448 amino acid increases ADAMTS13 activity (Kokame *et al*, 2011), which is in contrast to the results obtained *in vitro* and also obtained by Plaimauer *et al*, but agrees with the results obtained by Edwards *et al*.

In diabetic patient's serum ADAMTS13 activity was found to be significantly lower in alanine carriers than in proline carriers (77.8 vs 68%)(Rurali *et al*, 2013). In addition there were significant differences in 102 healthy subjects in terms of ADAMTS13 activity in patients with PP genotype compared to AA genotype. These results agree with the *in vitro* results obtained here and the results obtained by others (Plaimauer *et al*, 2006;Edwards *et al*, 2012;Rurali *et al*, 2013). In contrast in another study the p.P618A polymorphism was not associated with changes in plasma activity (Kokame *et al*, 2011). However the MAF for p.A618 in this population was 0.027 in 346 patients and so the number of patients may have been too small to detect a difference. This MAF is smaller than the MAF of p.E448 in this study (0.192) in which they found an association.

The amino acids affected by polymorphisms within ADAMTS13 orthologs do not appear to be as conserved as the amino acids affected by mutations and studied here (Chapter 3). This is consistent with these variants being polymorphisms as opposed to mutations. Conservation of these amino acids within paralogs may not be as informative as conservation within orthologs as these domains (cysteine-rich, spacer, TSP-1) may have a different function in other ADAMTS proteins, as the substrate they recognise differs (Nicholson *et al*, 2005;Gao *et al*, 2008).

The tyrosine (Y) residue at position p.570, present in patient 1, (Chapter 3), lies within a β2 sheet whereas the glutamine (Q) at position 448 lies within an α helix and the proline (P) at position 618 lies in a loop after the β6 sheet (Akiyama *et al*, 2009). In terms of location within ADAMTS13 it can be seen why the p.Y570C mutation appears to cause a severe defect in the secretion and activity of ADAMTS13 *in vitro* (Chapter 3), which is in contrast to the polymorphisms (p.Q448E and p.P618A). Beta-sheets are generally thermodynamically more stable than α helices and hence their impact on protein-folding/stability is greater. Therefore, variants in beta-sheets are expected to produce a greater impact on protein folding (Henzler Wildman *et al*, 2002).

Proline in p.P618 adopts a *cis* conformation and therefore substitution by non proline residues could cause structural differences (Akiyama *et al*, 2009). The loop that the p.P618 amino acid lies in plays a pivotal role in the interaction between the N-

terminal cysteine-rich region and the spacer domain (Akiyama *et al*, 2009). This may explain why this polymorphism has a large effect on ADAMTS13 in terms of secretion.

In the future I hope to produce and purify large amounts of the p.R102H+p.Q448E+p.P618A+p.A900V mutant and to analyse it under flow along with the p.R102H mutant. It will be particularly interesting to compare the activity of the mutant with polymorphisms under flow and static conditions because the C-terminal region of ADAMTS13 appears to be important under conditions of flow but not static conditions (Soejima *et al*, 2003;Zheng *et al*, 2003;Zhang *et al*, 2007;Zhou *et al*, 2007;De Maeyer *et al*, 2010). The p.A900V polymorphism is located in the C-terminal region of ADAMTS13.

*ADAMTS13* polymorphisms may also have an important role other than in TTP. In 1,163 type 2 diabetic patients interactions between p.P618A and ACE inhibitors was significant in predicting both renal and combined renal and cardiovascular events increasing in risk in the order alanine (A) carriers on ACE inhibitors→proline (P) homozygotes not on ACE inhibitors→ proline (P) homozygotes on ACE inhibitors→alanine carriers not on ACE inhibitors (Rurali *et al*, 2013). Alanine (A) carriers therefore had a higher risk of chronic complications and responded better to ACE inhibitors (Rurali *et al*, 2013). Furthermore serum ADAMTS13 activity was significantly lower in alanine carriers than in proline homozygotes (77.8 vs 68%) and in case subjects with renal, cardiovascular or combined events than in diabetic control subjects without events (Rurali *et al*, 2013).

A significant association was observed between the *ADAMTS13* p.A900V polymorphism and risk of death from cardiac causes (OR: 2.67, CI: 1.59-4.49, p=0.0009) in 559 patients with coronary artery disease (Schettert *et al*, 2010). This association was not found with p.Q448E or p.P618A. In this study there was only 6 patients homozygous for the p.A900V polymorphism and so heterozygous and homozygous patients were grouped together (464 patients homozygous for alanine [A] vs 95 patients heterozygous or homozygous for valine [V]). The relatively small number of patients with the valine amino acid suggests that there may be some false positive results. Additionally cholesterol levels (p=0.02) were lower in individuals

with the valine amino acid which may have contributed to these results. Furthermore the authors did not measure ADAMTS13 activity or antigen levels in the patients. This study suggests that there could potentially be an association but this is unclear.

The combination of the p.R102H mutation present in patient 3 with the three *ADAMTS13* polymorphisms also present appears to lead to the reduced activity measured *in vivo*. The p.R102H mutation by itself or the three polymorphisms expressed together in WT ADAMTS13 was not enough to cause this reduction. This study demonstrates firstly the importance of *in vitro* expression as before expression it was hypothesised that the mutation was responsible for the disease phenotype. However *in vitro* expression showed that the mutation was not enough to lead to the reduced activity levels measured in the patient plasma. Secondly this study demonstrates the importance of polymorphisms. Expression of the mutant with the three polymorphisms also present in the patient, highlighted the importance and contribution of these polymorphisms to the decreased activity measured in the patient plasma.

# Chapter 8 ADAMTS13 splice site mutant (type 1b)

## 8.1 Introduction

### 8.1.1 Overview of the splicing process

Transcription of the DNA sequence of a gene into mRNA occurs within the nucleus of the cell. After transcription, mRNA is capped at the 5' end and polyadenylation occurs at the 3' end. These modifications enable the cell to assess whether both ends of an mRNA molecule are intact before export from the nucleus for translation into protein.

The genomic DNA of a gene typically consists of protein coding sequences (exons), which are separated by long introns. Both exons and introns are transcribed into mRNA. Splicing of mRNA is important to enable removal of introns and join together protein coding sequences. Splicing enables cells to synthesise several proteins from the same gene (Alberts *et al*, 2002).

Each splicing event removes one intron, occurring through two phosphoryl transferase reactions, which join together two exons while removing the intron (Figure 8-1a). Introns range in size from 10 to over 100,000 nucleotides. The 'machinery' that catalyses this process consists of many proteins and other RNA molecules. Intron sequence removal involves three positions on the RNA molecule, the 5' splice site, 3' splice site and the branch point. Each of these sites have a consensus DNA sequence (Figure 8-1b) (Alberts *et al*, 2002).

Only when all the steps of mRNA production have occurred (5' capping, 3' polyadenylation and splicing) can an mRNA molecule be exported from the nucleus. Eukaryotic cells have an additional mechanism, nonsense mediated mRNA decay that can eliminate mRNA containing premature stop codons, before they can be translated into protein. Stop codons can arise from mutations or from incomplete splicing. The ability of the nonsense-mediated decay system to detect these premature stop codons within mRNA depends upon the spatial relationship between the first in frame termination codon and exon-exon boundaries. If the codon lies downstream (3') of an exon-exon boundaries the mRNA does not undergo nonsense

mediated decay. If on the other hand it is upstream (5') of an exon-exon boundary the mRNA is degraded (Alberts *et al*, 2002).

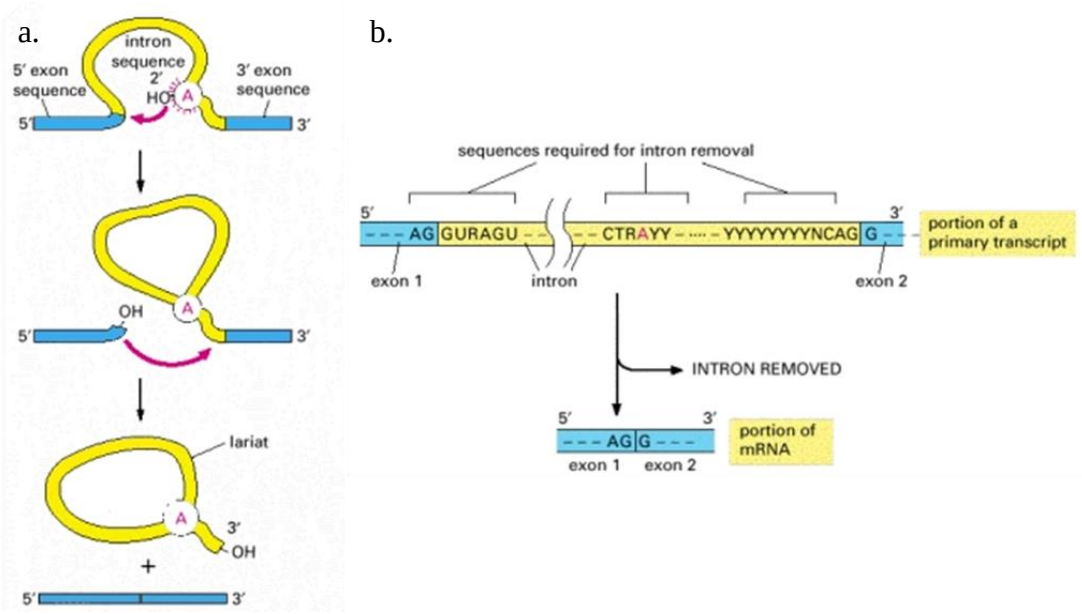


**Figure 8-1 Splicing process**

Figure a shows a simplified diagram of the splicing process. A specific nucleotide within the intron (A) attacks the 5' splice site, cutting the sugar-phosphate backbone of the RNA at this point. The released free 3'-OH end of the exon then reacts with the start of the next exon sequence. The two exons are joined together and the intronic sequence is released. Figure b shows the consensus sequence required for splicing. The three blocks of nucleotide sequences highlighted are required to remove an intron sequence. R stands for an A or G nucleotide, Y stands for a C or U nucleotide. Only the GU at the start of the intron and the AG at its end are invariant nucleotides in the splicing consensus sequence. The remaining positions can be occupied by a variety of nucleotides but the ones shown are preferred. Images from: (Alberts *et al*, 2002).

### 8.1.2 *ADAMTS13* splice site mutations

In patients with congenital TTP nine different splice site mutations (6% of all mutations) have been described (Lotta *et al*, 2012;Uchida *et al*, 2004;Matsumoto *et al*, 2004;Studt *et al*, 2005;Veyradier *et al*, 2004;Levy *et al*, 2001;Prestidge *et al*, 2012). The effect of these mutations on the splicing process has been analysed for three of these mutations. Matsumoto *et al* analysed *in vivo* two splice site mutations: c.414+1G>A within intron 4 and c.1244+2T>G within intron 10 (Matsumoto *et al*, 2004). The mRNA from patients with these mutations was reverse transcribed and analysed and the authors found that these mutations did affect splicing. Uchida *et al* analysed the splice site mutation c.330+1G>A, within intron 3, through the creation

of a mini gene (Uchida *et al*, 2004). The authors similarly found this mutation affected the splicing process.

### 8.1.3 Predicted effect of splice site mutation

At the start of this project a mutation (c.106-1G>C) predicted to affect splicing, not previously characterised *in vitro* or *in vivo*, was analysed as described in the methods (Chapter 2.14) to assess the effect of the mutation on splicing. The predicted effect of this mutation is illustrated in Figure 8-2.

The c.106-1G>C splice site mutation results in the exchange of a G residue with a C residue in the last nucleotide of the intron just before exon 2. For splicing to occur an 'AG' acceptor site is required at the end of the intron. In this patient the AG acceptor site at the end on intron 1 is affected by the mutation. The cell splicing machinery is predicted to use the AG residue at the beginning of exon 2 instead as the acceptor site. If this new acceptor site was to be used then these two nucleotides (AG) are no longer part of exon 2 and instead exon 2 would begin with the third nucleotide present, which is a T nucleotide. The deletion of these two nucleotides would lead to a frame shift and the introduction of a stop codon 102 amino acids later at the end of exon 4.

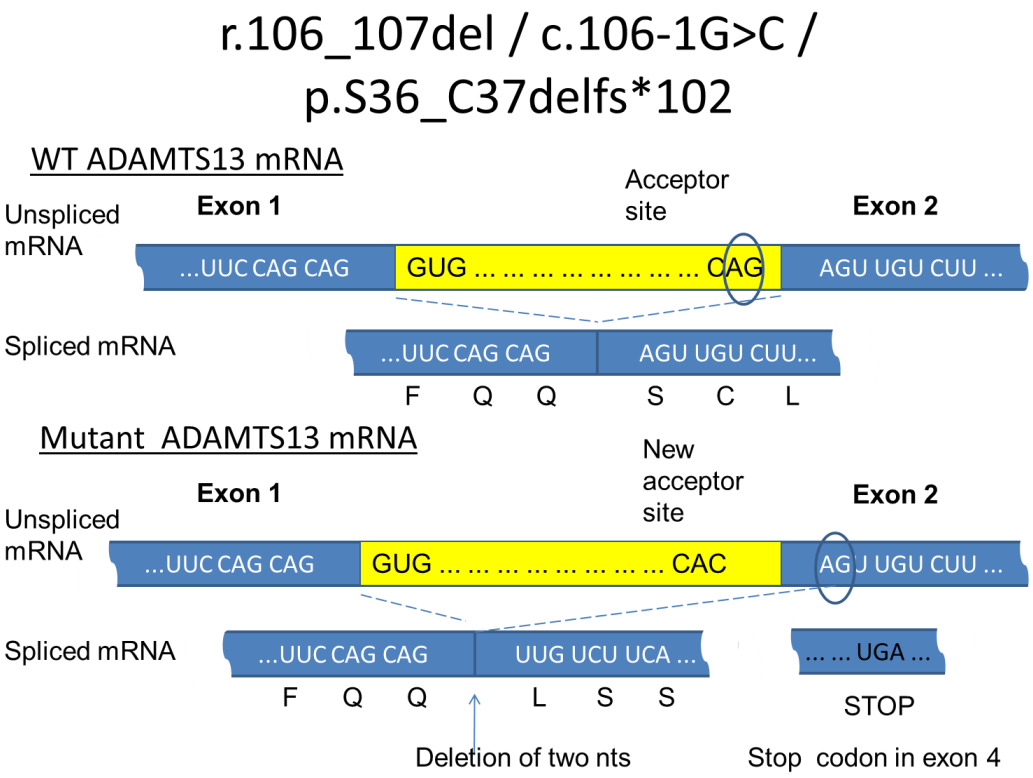


**Figure 8-2 Predicted effect of mutation on splicing**

nt: nucleotide. The mutation is predicted to lead to the use of an alternative acceptor site, located at the beginning of exon 2.

### 8.1.4 Patient information

The patient with the c.106-1G>C (p.S36_C37delfs*102, r.106_107del) mutation (patient 4) had no exonic mutations or non-synonymous polymorphisms. This patient is female and first presented with TTP at 8 months. The patient has had 3 subsequent episodes which were triggered by viral infections. The patient had undetectable ADAMTS13 antigen and activity in her plasma. The patient plasma activity was also measured using SELDI-TOF and was 0.67% of PNP (Lotta *et al*, 2012).

## 8.2 *ADAMTS13* whole blood RNA extraction

One way to assess whether this mutation affects splicing is to analyse the patient's RNA. If this mutation affects splicing as predicted then the RNA of this patient would be slightly different to that of normal controls as two nucleotides would be deleted from the patients RNA. Others have demonstrated that *ADAMTS13* RNA is present within leukocytes (Matsumoto *et al*, 2004). The RNA of this patient was to

be extracted, but first RNA was extracted from two healthy controls to ensure that the technique was working.

RNA extraction, RT and PCR amplification were carried out as described in the methods (Chapter 2.15). Two primer pairs were used to amplify *ADAMTS13* cDNA: F6/R6 to produce a fragment of 169bp and F6/RevJP to produce a fragment of 542bp. Another set of primers (G3PDH F'/R') were used to amplify a housekeeping gene G3PDH as a control. Figure 8-3a shows the PCR fragments obtained after using the primer pair F6/R6 and G3PDHF'/R'. Figure 8-3c shows the PCR fragments obtained after using the primer pair F6/RevJP and G3PDHF'/R'.

The G3PDH gene (expected size 983bp) could be detected in the positive control sample (Figure 8-3a) but *ADAMTS13* could not be detected. Neither *ADAMTS13* nor G3PDH could be detected in the normal controls. Importantly nothing could be detected in the negative control samples. In the PCR fragments shown in Figure 8-3c nothing could be detected in any of the samples when loaded onto a 2% agarose gel.

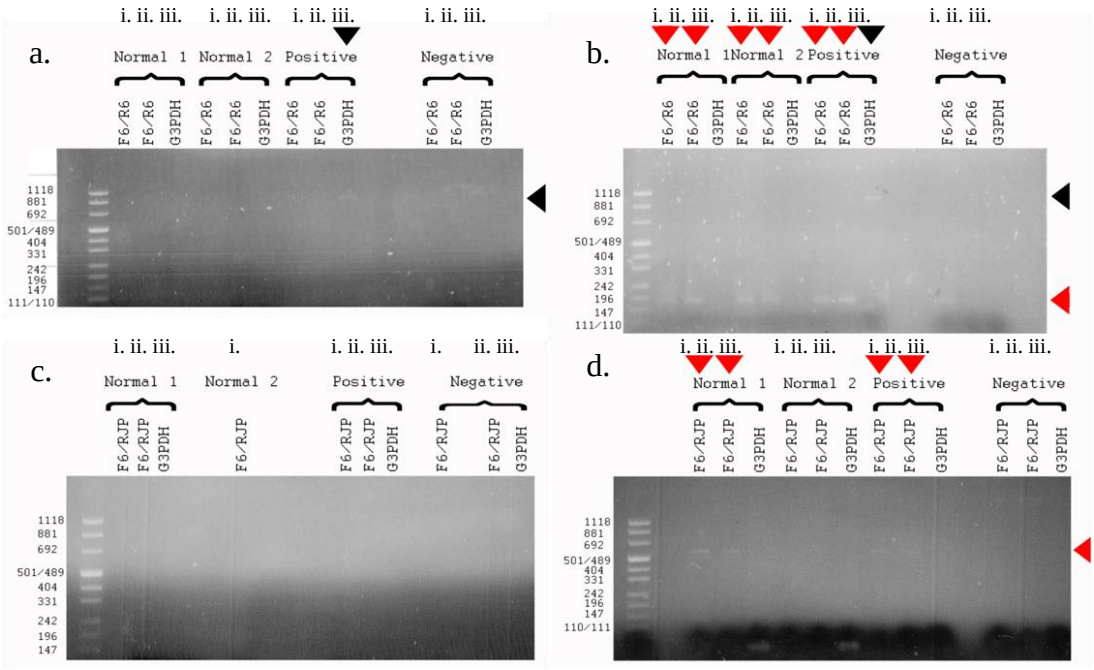


**Figure 8-3 A 2% agarose gel of RT-PCR products**

RT cDNA was amplified using PCR (shown in Figure a and c). For the PCR products obtained in b and d, the PCR products from a and c were used (respectively) as a template. Three reactions each were set up for two healthy controls, a positive control and a negative control. In a and b primers F6 and R6 were used in i and ii and G3PDH primers were used in iii. For c and d, F6 and RevJP were used for i and ii and G3PDH primers were used for iii. For samples i. and ii. slightly different quantities of cDNA were used in the PCR. In the gel shown in Figure c samples ii. and iii. for normal 2 were not loaded as a small amount of sample was available for analysis. The expected size of the products for each pair of primers was as follows: F6/R6:169bp, F6/RevJP: 542bp, G3PDH:983bp. The DNA ladder pUC mix marker 8 (ThermoFischer Scientific) was used.

The samples obtained from the first PCR (Figure 8-3a and c) were used as a template for the second PCR using the same conditions as the first PCR (Figure 8-3b and d). *ADAMTS13* could be detected using primer F6/R6 in both normal controls (Figure 8-3b), the housekeeping gene G3PDH could be detected in the positive control but not in normal control samples. Nothing could be detected in the negative controls. *ADAMTS13* could be detected in the positive control and in normal control 1 using primer pair F6/RevJP (Figure 8-3d). Nothing could be detected in the negative controls.

### 8.2.1 Purification of PCR products

The PCR products from the second PCR (Figure 8-3b) obtained from normal control 1 using primer pair F6/R6 were pooled and purified as described in methods. This was similarly done for the PCR products obtained from normal control 1 (primer pair

F6/RevJP) and normal control 2 (primer pair F6/R6).The purified PCR products were run on a 2% agarose gel and are shown in Figure 8-4. The purified products are barely visible on the agarose gel.

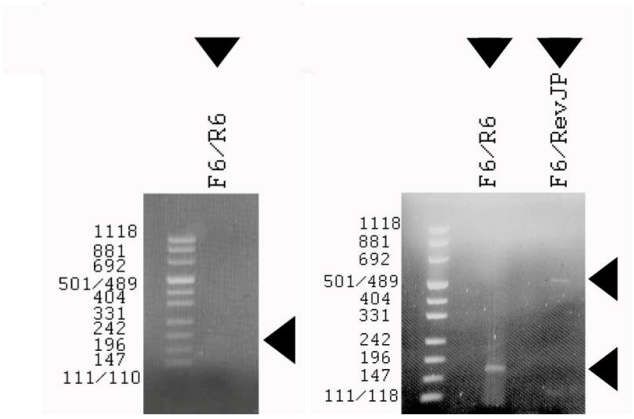


**Figure 8-4 Purified *ADAMTS13* PCR products obtained from RT of normal control mRNA**

Figure a shows the pooled PCR product obtained from normal control 1 using primer pair F6/R6. Figure b shows purified product obtained from normal control 1 using primer pair F6/RevJP and from normal control 2 using primer pair F6/R6. The expected size of products for each pair of primers was as follows: F6/R6:169bp and F6/RevJP: 542bp. The ladder pUC mix marker 8 (ThermoFischer Scientific) was used.

The purified PCR products were sequenced and were confirmed to be ADAMTS13. *ADAMTS13* RNA was therefore successfully extracted, RT into cDNA and PCR amplified from leukocytes. The technique was developed so that RNA could be extracted from the blood of the patient with the splice site mutation. The blood could not be obtained from the patient during the time of this study however, despite trying to obtain a sample.

## 8.3 Creating a mini gene to analyse splice site mutation *in vitro*

An alternative way to assess whether the mutation affects splicing is to construct a mini gene *in vitro*. The vector which had been used in previous experiments Chapter 3 -7 contained the complete cDNA sequence of *ADAMTS13*, i.e. all 29 exons and no introns. This vector has a T7 promoter/priming site which enables *in vitro* transcription of genomic DNA in the sense orientation. It also had a bovine growth hormone (BGH) polyadenylation site which allows its efficient transcription

termination and adenylation of mRNA. This vector therefore is suitable to analyse transcription *in vitro*.

The predicted splice site mutation lies within intron 1, just before exon 2. First it was investigated whether it was possible to remove exon 1 and exon 2 or 3 within the vector expressing *ADAMTS13* cDNA using restriction digestion and then replace this region of the vector with genomic DNA of exon 1→exon 2 or exon1→exon3. A restriction enzyme that could be used to cleave the vector only once within exon 1, 2 or 3 was searched for using web cutter (URL: http://rna.lundberg.gu.se/cutter2/; accessed 17th June 2014). This tool lists the restriction enzymes which cut a given DNA sequence and also shows where in the sequence the enzyme cuts it. A restriction enzyme which cut the vector only once within exon 1 or 2 could not be identified.

Instead it was decided that a fragment containing either exon 1 + intron 1 + exon 2 or exon 1 + intron 1 + exon 2 + intron 2 + exon 3 would be cloned into an empty pcDNA 3.1 D/V5-His-TOPO® vector using a pcDNA 3.1 Directional TOPO expression kit (Life technologies).

Genomic DNA from a normal control and from the patient with the splice site mutation was to be cloned. In order to clone directionally within the TOPO vector the forward primer should contain a Kozak sequence (CACCATG) at the 5'end of the primer (Kozak, 1987). The first 4 nucleotides CACC, base pair with the overhang sequence GTGG within the TOPO vector. The ATG following this is the initiation codon of the protein of interest. Primer SpliceA for TOPO® cloning was designed so that it contained this Kozak sequence.

The C-terminal tag and V5 epitope were also to be included in the protein produced by the vector and so the reverse primer was designed so that the WT open reading frame was in frame with the C-terminal tag encoded by the vector. Three primers were designed (SpliceA, SpliceB and SpliceC). SpliceA was designed to bind within exon 1. Two reverse primers were designed, one to bind within exon 2 (SpliceB) and one to bind within exon 3 (SpliceC). These primers were designed to produce the products illustrated in Figure 8-5.

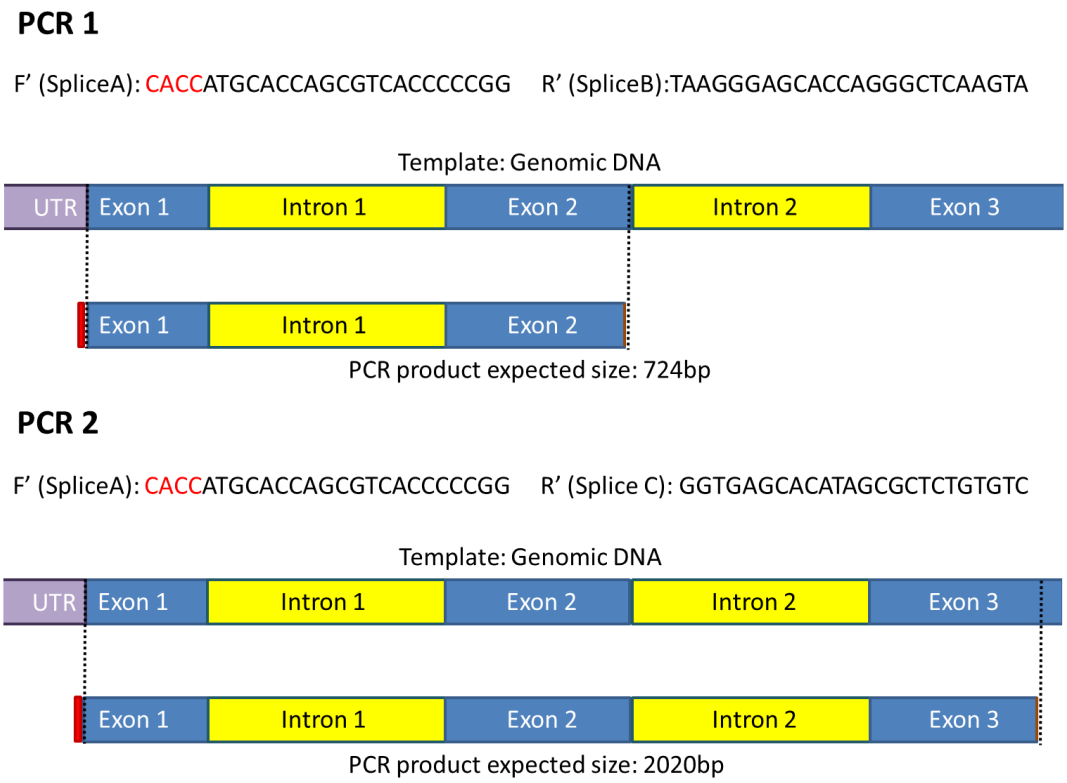


**Figure 8-5 Primers and products designed for TOPO cloning**

Primers were designed to amplify either exon1→exon 2 of *ADAMTS13* genomic DNA (PCR 1) or exon 1→exon 3 of *ADAMTS13* genomic DNA (PCR 2). 5' to 3' sequence of primers are shown. UTR, untranslated region. The CACC region introduced into the PCR product by the primer is shown in red. The brown line indicates that the complete exonic sequence is not included in the PCR fragment.

## 8.4 PCR amplification of WT *ADAMTS13* using primers SpliceA/B and SpliceA/C

PCR was set up to amplify genomic DNA using primers SpliceA/B and SpliceA/C with an annealing temperature of $55^0$C. Multiple bands were observed on the agarose gel so the PCR was repeated varying the annealing temperature. An annealing temperature of $58^0$C produced the expected product for SpliceA/B and SpliceA/C (Figure 8-6a).

The products obtained from the PCR using primers SpliceA/C were used as a template for another PCR which was set up under the same conditions. A band of the expected size was observed on the gel (Figure 8-6b).

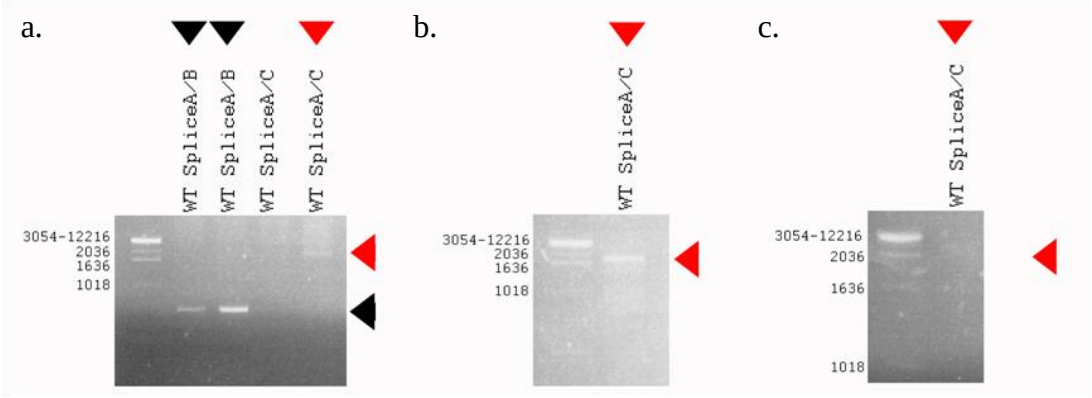


**Figure 8-6 PCR amplification and purification of WT *ADAMTS13***

Figure a shows the products formed using primer SpliceA and primer SpliceB (lanes 1 and 2). Lanes 3 and 4 show the product formed using primer SpliceA and SpliceC. Different quantities of genomic DNA were used in lanes 1 and 2 and also in lanes 3 and 4. Figure b shows the results of another PCR set up under the same conditions using the product in lane 3 of figure a as a template and primers SpliceA and SpliceC. Figure c shows the purified product in figure b. Expected size of product using SpliceA/B was 724bp and for SpliceA/C was 2020bp. DNA ladder marker X (Roche) was used.

The product from the reaction was PCR purified. The purified product is shown in Figure 8-6c. Some of this product was sequenced and confirmed to be *ADAMTS13*. The whole PCR product was not sequenced as there was a limited amount of the product available.

## 8.5 PCR amplification of splice site mutant *ADAMTS13* using primers SpliceA/B or SpliceA/C

PCR was set up for the splice mutant using the same conditions that had been used for WT *ADAMTS13* genomic DNA. A band of the expected size could be detected using Splice A/B but no band could be detected using the primers Splice A/C (Figure 8-7a). A second PCR was set up using the product formed with primers SpliceA/C as a template and using the same PCR conditions that had been used to create the product. Multiple bands were present on the agarose gel (Figure 8-7b), one of which was the expected size.

A number of PCRs were set up with mutant genomic DNA and the annealing temperature was varied but still multiple bands were obtained. Touchdown PCR was set up in order to try and eliminate the non-specific bands, after which a band could

be detected of the incorrect size. The PCR was repeated in the presence of DMSO and again a band of the incorrect size could be detected.

All of the PCR products that were obtained from the initial PCR set up for the mutant (shown in Figure 8-7b) (consisting of many PCR fragments of different sizes) was run on an agarose gel and the DNA of the desired size was cut from the gel (top band) (as shown in Figure 8-7c). The cut piece of gel containing the desired band of DNA was purified. The purified product is shown in Figure 8-7d. Part of this fragment was sequenced and was confirmed to be *ADAMTS13*.

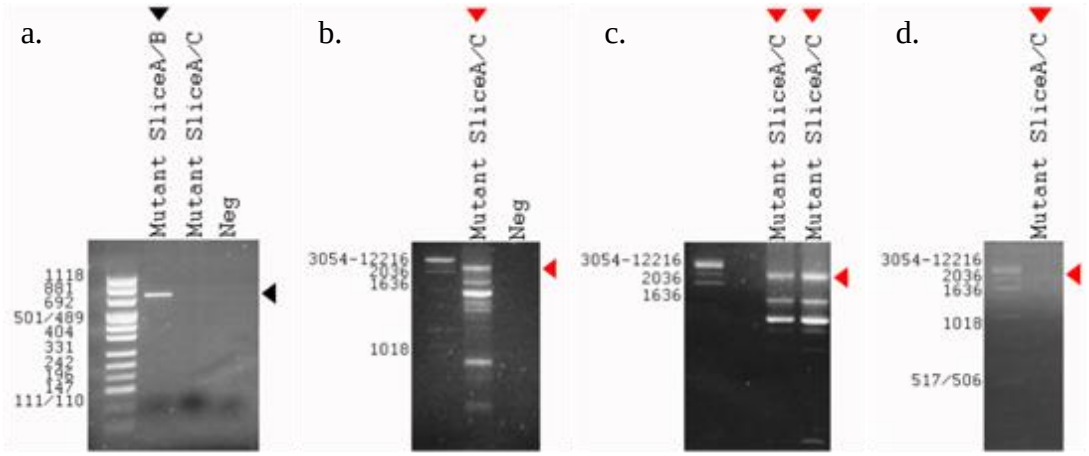


**Figure 8-7 PCR amplification and purification of splice site mutant *ADAMTS13***

Figure a shows the products formed using primer SpliceA and primer SpliceB (lanes 1) and the product formed using primer SpliceA and SpliceC (lane 2). Figure b shows the results of a second PCR using the product in lane 2 of figure a as a template and primers SpliceA and SpliceC. Figure c shows the PCR product that was used for gel DNA extraction. The top band was cut from the gel and extracted. Figure d shows the purified gel extracted product. Expected size of product using SpliceA/B was 724bp and for SpliceA/C was 2020bp. The ladders pUC mix marker 8 (ThermoFischer Scientific) or DNA ladder marker X (Roche) were used.

## 8.6 TOPO cloning of PCR fragment product using primers SpliceA/C

For TOPO cloning the product containing exon1→exon 3 was used as opposed to the product containing exon 1→exon 2 as there would be more of the sequence following the mutation in the product exon1→exon 3. TOPO cloning was set up for WT and mutant *ADAMTS13* as described in the methods (Chapter 2.17). For cloning 4µl of each PCR fragment was used (purified fragment shown in Figure 8-6c and Figure 8-7d). The day after transformation six colonies each were picked for mini

preparation from the plates containing *E. coli* transformed with WT or mutant *ADAMTS13*. No DNA could be detected using a nanodrop or by agarose gel electrophoresis.

A further three colonies underwent mini preparation; DNA could be detected in these clones. Sequencing of this DNA was set up using primers which were part of the TOPO cloning kit (T7 and BGH) which bound to the vector before and after the region which should contain the insert. Nothing could be detected after sequencing. Instead restriction digests were set up to investigate if the cloned fragment could be detected this way. Three restriction enzymes (BstXI, StuI, and XbaI) that would cut both the vector and the insert once were used. If the vector contained the insert two bands would be present after restriction digest, whereas if the vector was empty one band would be present. The DNA obtained from mini preparation was digested with these restriction enzymes but the amount of DNA from this was too low to be observed on a gel.

In a last attempt to investigate whether *ADAMTS13* could be detected within these clones, PCR was used. Two PCRs were set up, one using primer SpliceA and SpliceC and another using primers T7 and BGH. Primers were added to 3µl of the DNA obtained after mini preparation and the PCRs were set up using the conditions used to create the products for cloning. In WT no bands could be observed, in the mutant multiple bands could be seen but these were not of the correct size.

## 8.7 New primers for TOPO cloning

New primers were created to produce a new PCR fragment for TOPO cloning. Primer SpliceA which was used to create the PCR fragment previously was very rich in C nucleotides which may have contributed to the non-specific binding problems that were experienced in the PCR reactions. The basic local alignment search tool (BLAST) was used (URL: http://blast.ncbi.nlm.nih.gov/Blast.cgi; accessed 17$^{th}$ June 2014) to investigate whether the primers that had been used to create the fragment (Primer SpliceA/B/C) were likely to bind to other regions within *ADAMTS13*. This appeared to be the case so new primers were designed. These primers were designed

using NCBI primer blast (URL: http://www.ncbi.nlm.nih.gov/tools/primer-blast/, accessed 17th June 2014).

The primer SpliceD binds to the untranslated region of genomic DNA before the *ADAMTS13* ATG start codon within the signal peptide region of *ADAMTS13*. SpliceE binds within the middle of exon 3. These two new primers were used to produce the fragment shown in Figure 8-8.

Primer SpliceD does not have 'CACC' at the beginning of its sequence and so the PCR fragment produced with this primer could not be cloned directly into the TOPO vector. In addition due to the design of the SpliceE primer, the end of the fragment produced by this primer pair would not be in frame with the V5/His tag encoded by the vector. It was desirable to clone the fragment so that it was in frame with this so that the protein produced by the vector could be detected using an anti-V5 antibody, as with the other ADAMTS13 proteins produced previously.

In order to produce a PCR fragment that could be inserted into the TOPO vector and was in frame with the V5/His tags when expressed, another PCR step was carried out (nested PCR). The DNA fragment produced in the first PCR was used as a template for the second PCR (Figure 8-8). For nested PCR the forward primer used was the same one that had been used previously (SpliceA). This primer should bind within the first PCR fragment. As this primer starts with CACC and is followed by the initiation ATG start codon, it would enable cloning of the fragment into the TOPO vector. A reverse primer was designed, SpliceF which bound within exon 3 to produce a fragment that was in frame with the V5/His tag (Figure 8-8).

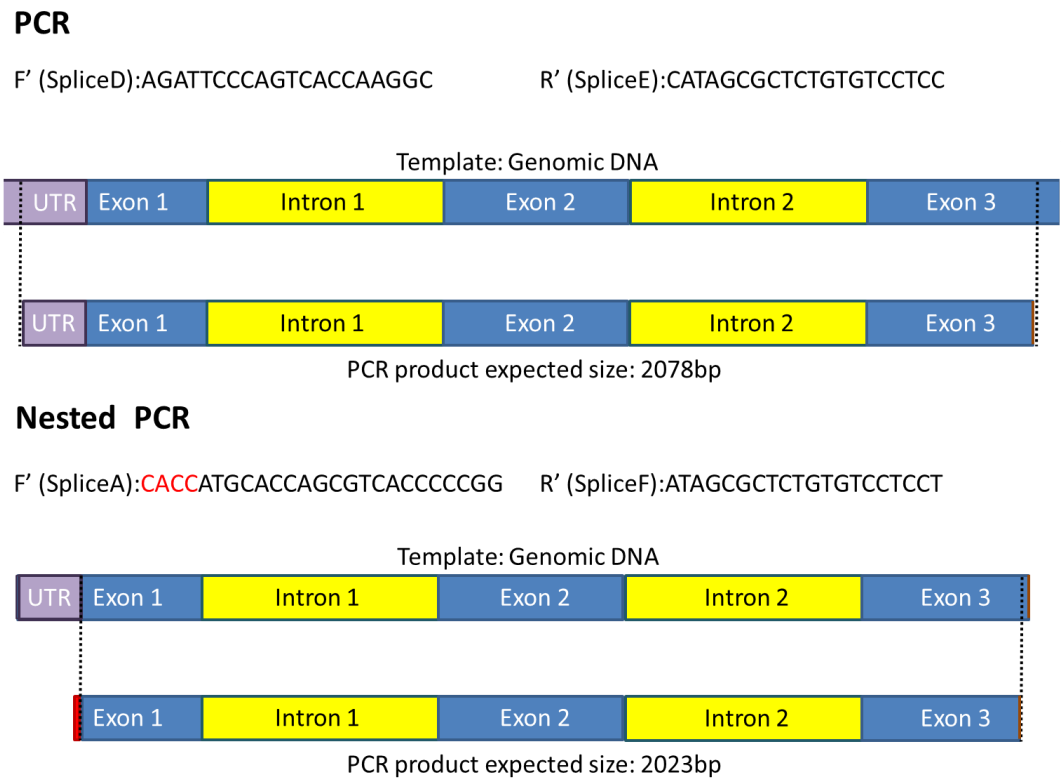


**Figure 8-8 PCR plan**

The brown line at the end of an exon indicates that the whole of the exon sequence is not included in the PCR fragment. The red region at the beginning of PCR fragment 2 illustrates the CACC nucleotides introduced at the beginning of the PCR fragment by the primer SpliceA. UTR: untranslated region. 5' to 3' sequence of primers are shown.

## 8.8 PCR amplification of WT and mutant *ADAMTS13* using primers SpliceD/E and SpliceA/F

PCR was initially set up using WT *ADAMTS13* with an annealing temperature of 55°C in the absence of DMSO. Multiple bands were observed on the agarose gel (Figure 8-9a). PCR was repeated at 58°C in the presence and absence of DMSO (Figure 8-9b). A clear band could be seen in the presence of DMSO. This band was PCR purified (Figure 8-9c) and partially sequenced. This was confirmed to be *ADAMTS13*.

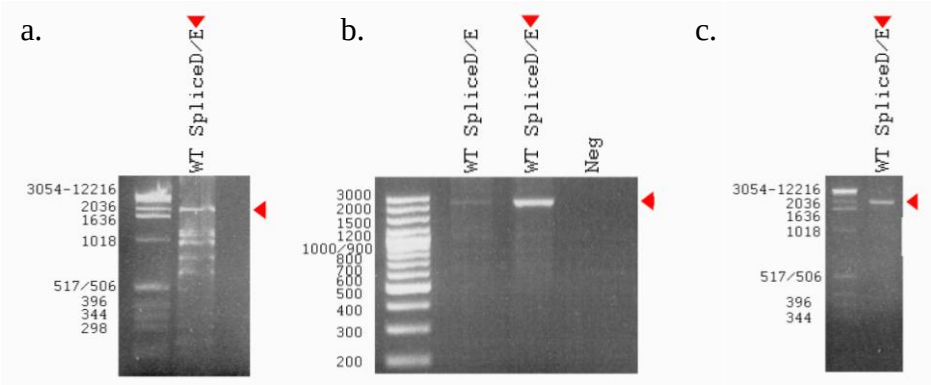


**Figure 8-9 PCR amplification and PCR purification of WT *ADAMTS13***

Figure a shows the PCR amplification of WT *ADAMTS13* genomic DNA at an annealing temperature of 55°C. Figure b shows the PCR amplification of WT *ADAMTS13* genomic DNA at an annealing temperature of 58°C in the absence (lane 1) and presence (lane 2) of DMSO. Figure c shows the purification of the product in lane 2 of figure b. DNA ladder marker X (Roche) or gene ruler 100bp plus DNA ladder (ThermoFischer Scientific) was used.

More of this product was produced so that the entire PCR fragment could be sequenced to be sure that there were no unexpected polymorphisms or mutations in the intronic region of the control. The PCR was repeated using the same conditions but this time multiple bands were obtained, unlike previously. The PCR machine and the annealing temperature (higher and lower) were changed. DMSO was added to the reaction mix and touchdown PCR was used and the volume of the enzyme and buffer were changed to try and obtain one single band. However multiple bands were still obtained.

One possible reason for this problem could be related to the genomic DNA used for PCR, for example if it had sheared during DNA extraction. An agarose gel of the genomic DNA encoding normal and mutant *ADAMTS13* were run on an agarose gel. There did not however appear to be a problem with the genomic DNA (Figure 8-10).

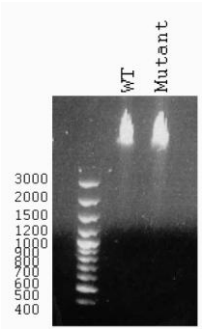


**Figure 8-10 Agarose gel of genomic DNA**

Genomic DNA from WT *ADAMTS13* and splice site mutant genomic DNA was run on a 2% agarose gel. Gene ruler 100bp plus DNA ladder was used (ThermoFischer Scientific).

As one single band could no longer be obtained (Figure 8-11a) I proceeded with nested PCR. Initially the PCR was set up using an annealing temperature of 63°C and multiple bands were obtained. A single band was obtained when the annealing temperature was changed to 61°C (Figure 8-11b). This product was PCR purified and partially sequenced. It was confirmed to be ADAMTS13.

There was not enough of the purified nested PCR fragment to sequence the whole fragment so the nested PCR was repeated. PCR was carried out using the nested PCR product as a template, using the same conditions as before. Multiple bands were observed on the gel, which were not of the correct size. Nested PCR was carried out using the same PCR 1 sample that had been used previously. Strangely one band was not obtained (as had been the case previously) but multiple bands were obtained instead. The annealing temperature and the concentration of DMSO were varied. Additionally a lower concentration of primer and formamide were used but this did not produce any bands. Instead all of the products that had been obtained from nested PCR were pooled together and were run on an agarose gel for DNA gel extraction (Figure 8-11c). The top band was cut for gel extraction; the purified product is shown in Figure 8-11d. This was sequenced and confirmed to be *ADAMTS13*.

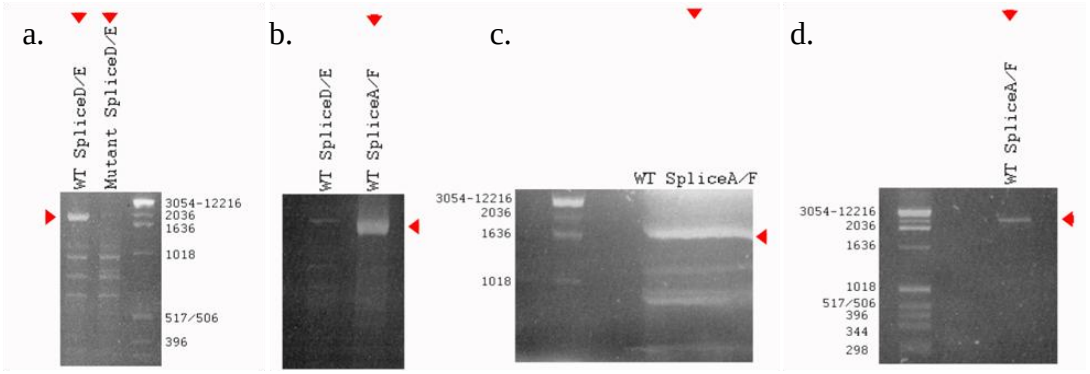


**Figure 8-11 PCR amplification and gel purification of WT *ADAMTS13***

Figure a shows PCR amplification of WT (lane 1) and *ADAMTS13* splice mutant (lane 2) genomic DNA using primers SpliceD and SpliceE. Figure b shows PCR amplification of WT (lane 1) *ADAMTS13* genomic DNA using primers SpliceD and SpliceE (lane 1). This DNA was used as a template for a subsequent PCR using primers SpliceA and SpliceF. The product of this is shown in lane 2. Figure c shows the WT *ADAMTS13* PCR fragment that was used for agarose gel extraction (top band). Figure d shows the purified product. Expected size of product using SpliceD/E was 2078bp and using SpliceA/F was 2023bp. DNA ladder marker X (Roche) was used.

The entire exonic DNA of this product was sequenced and some of the intronic DNA within this fragment. However because of the limited material and the amount of work required to produce this fragment, this fragment was to be cloned into the TOPO vector and the intronic regions of the fragment sequenced after cloning.

With the mutant multiple bands were obtained after the first PCR, with very little of the correct size (Figure 8-11a). I decided therefore to create one mini gene, using WT genomic DNA and then carry out site directed mutagenesis on this vector to create the splice site mutant.

## 8.9 TOPO cloning of PCR fragment produced using primers SpliceA/F

This time for TOPO cloning a control reaction was set up. The PCR fragment used for the control TOPO cloning reaction was produced as recommended by the manufacturers (Figure 8-12)

.

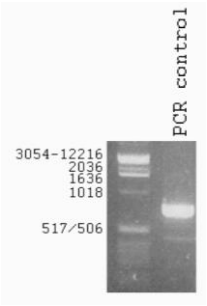


**Figure 8-12 TOPO PCR cloning reaction**

Control PCR was set up for subsequent TOPO cloning. The expected size of the fragment is 750bp.

The TOPO cloning reaction was carried out using 4µl of the WT PCR product. The positive and vector only controls were set up as recommended by the manufacturer. After transformation clones were picked and grown for mini preparation. Restriction digest on the DNA obtained after mini preparation was carried out. Before this however a restriction digest of the TOPO vector expressing full length *ADAMTS13* cDNA using the enzyme StuI was performed to check that the enzyme was working and cleaved at the expected sites.

StuI was predicted to cleave the vector expressing full length WT *ADAMTS13* cDNA at multiple sites and was predicted to cleave the WT splice *ADAMTS13* fragment at one point to produce fragments of 1138bp and 881bp. Results are shown in Figure 8-13. The enzyme cleaved both of the products as expected.

The expected size of the fragments obtained after StuI digestion if the vector contained the WT splice product was 2085bp and 5451bp. No band could be detected at 2085bp suggesting that the vectors were empty or did not contain the full fragment (Figure 8-14). After this three more colonies were picked and the same results were obtained.

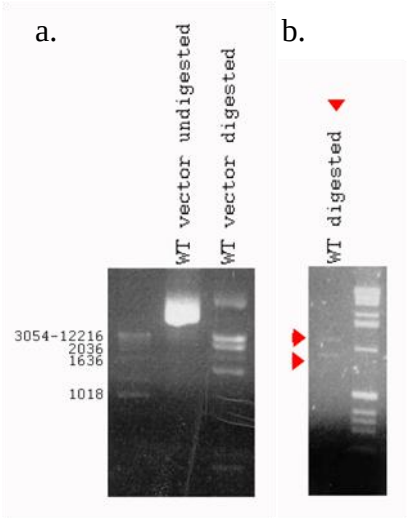


**Figure 8-13 StuI restriction digest of WT *ADAMTS13***

Figure a shows the results before and after restriction digest of the TOPO vector containing *ADAMTS13* full length cDNA. Figure b shows the results after restriction digest of the WT PCR splice fragment used for cloning. The expected size of the PCR splice fragments were 1138 and 889bp. DNA ladder marker X (Roche) was used.

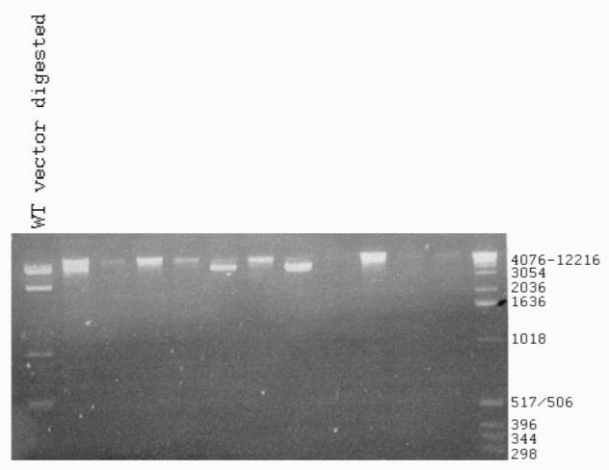


**Figure 8-14 StuI restriction digest of TOPO clones**

Restriction digest with StuI was carried out of DNA obtained after mini preparation of *E. coli* transformed for TOPO cloning. A vector containing the full length PCR fragment should produce fragments of 2085 and 5451bp. In lane 1 the vector expressing full length *ADAMTS13* cDNA was also run as a control. DNA ladder marker X (Roche) was used.

The TOPO cloning reaction was repeated. This time 2µl of the DNA was used for the cloning reaction, however no colonies grew. The cloning reaction was repeated again, this time using 10ng of DNA. In the previous cloning reactions the amount of DNA used for the reaction was not quantified. This transformation worked and

colonies were picked for mini preparation and sequenced (twelve colonies). All of these colonies contained empty vectors except for one which appeared to contain *ADAMTS13*. However this clone contained the beginning and end of the *ADAMTS13* fragment, with the region in the middle absent.

Another transformation was carried out using the same conditions as previously. This time many more colonies (86) were picked and sequenced to check if they contained *ADAMTS13*. From this five clones were found which contained DNA resembling *ADAMTS13*. However there were large deletions of the *ADAMTS13* sequence within these vectors. These deletions were particularly within the intronic region of *ADAMTS13*. The deletions present in each of the clones were different suggesting that the deletion occurred during the cloning process. Due to time constraints I was not able to perform another transformation.

## 8.10 Discussion

RNA was successfully extracted from normal controls, reverse transcribed and used to PCR amplify the *ADAMTS13* gene. Although a sample from the patient with the splice site mutation was not available for mRNA analysis, this technique could be used to analyse other patients which have potential splice site mutations in the future.

A fragment was successfully produced using PCR encoding exon1, intron 1, exon 2, intron 2 and exon 3 of ADAMTS13. There were some difficulties in producing a single band using PCR. To try and optimise the PCR, the annealing temperature, DMSO concentration, DNA concentration, primer concentration and dNTP concentration were varied and new primers were designed. When successful in producing a single PCR band, the results were not always reproducible. Often after repeating a PCR using the same conditions and components multiple bands were obtained rather than a single band as previously obtained. Due to the difficulties in producing a single PCR band, a DNA PCR band of the desired size was extracted from an agarose gel.

After obtaining a PCR fragment it was cloned into a TOPO vector. TOPO cloning was carried out four times but no clones were found which contained the full

*ADAMTS13* sequence. In the initial cloning procedures this may have been because too much of the PCR fragment was used for cloning, which would have reduced the efficiency.

In the last cloning reaction 86 clones were analysed but only 5 of them contained a sequence resembling *ADAMTS13*. This shows that the efficiency of the cloning procedure was poor (the kit states that the cloning efficiency should be 90%). This poor cloning efficiency may have been because a gel purified PCR fragment was used (as opposed to a purified PCR fragment). Additionally the gel purified products were not freshly produced before cloning, which may have further reduced the efficiency.

Although *ADAMTS13* could be detected in 5 clones these clones did not contain the entire expected sequence of *ADAMTS13*. These clones had large regions of the *ADAMTS13* DNA deleted from them (particularly the intronic regions). The regions that were deleted in each of the clones were different suggesting that the problem occurred during the cloning and transformation steps. This problem could be overcome in the future by using an alternative type of *E. coli*. There are some types of *E. coli* which have been specially modified to prevent the deletion of large regions of DNA such as Sure 2 supercompetent cells (Agilent technologies). These *E. coli* lack components of the pathways that catalyse the rearrangement and deletion of non-stranded secondary and tertiary structures that may occur in eukaryotic DNA, which prevents their cloning.

After these problems have been resolved the vector expressing WT ADAMTS13 genomic DNA could be used as a template for site directed mutagenesis to introduce the splice site mutation. The vectors containing WT and mutant ADAMTS13 exonic and intronic DNA could then be transiently transfected in HEK 293T cells. The RNA produced could then be extracted and analysed to check if the splice site mutation did affect splicing leading to the formation of different RNA products. Unfortunately all of these experiments could not be performed during the time of this project, but this is something that could be continued in the future.

# Chapter 9 Summary and conclusions

The clinical presentation of patients with TTP is highly variable. Patients vary with respect to the age of disease onset, number of relapses and need for plasma exchange/infusion. There is evidence to suggest that the *ADAMTS13* genotype of patients may contribute to some of this heterogeneity. Relationships have been shown to exist between *ADAMTS13* genotype and age of disease onset (Lotta *et al*, 2010) and residual ADAMTS13 activity (Lotta *et al*, 2012). Residual ADAMTS13 activity in turn has been shown to be associated with the annual rate of TTP episodes (Lotta *et al*, 2012). This thesis was based upon the hypothesis that the clinical and laboratory phenotype of patients with congenital TTP, relates to the *ADAMTS13* mutations that the patients have. The aim of this study was to express *ADAMTS13* mutants which had been identified in a homozygous form in congenital TTP patients to assess their effect on the secretion and activity of ADAMTS13. I used a variety of methods to assess the effect of three types of *ADAMTS13* mutations: type 1a, type 2 and type 1b.

Two type 1a ADAMTS13 mutants (p.I143T and p.Y570C) were studied *in vitro*. The p.I143T mutation (present in patient 1) and p.Y570C mutation (present in patient 2) were both identified in a homozygous form in the affected patients. Both patients first presented with the disease during adolescence and had undetectable ADAMTS13 activity and antigen in their plasma, in the absence of detectable anti-ADAMTS13 antibodies.

When vectors expressing these mutants were transiently expressed *in vitro* in HEK293T cells, the levels of the mutants within the cell were slightly increased compared to WT ADAMTS13. Therefore, both mutants were synthesised within the cell, demonstrating that the mutations did not prevent protein synthesis. No ADAMTS13 could be detected using western blotting in supernatant samples (concentrated ~20 fold) and ADAMTS13 antigen in the supernatant was also undetectable using an ADAMTS13 antigen ELISA. No ADAMTS13 activity could be detected within supernatant samples using FRETS-VWF73 substrate for analysis (detection limit 2.5% of PNP). Both mutations therefore severely affected the

secretion and subsequently measureable ADAMTS13 activity, which correlated with the undetectable antigen and activity present in the plasma of patients 1 and 2.

These mutants were studied further in order to investigate their subcellular localisation. Immunofluorescence staining and confocal microscopy were used to analyse the localisation of these mutants within the ER and *cis* Golgi of the cell. WT and mutant ADAMTS13 appeared to localise extensively within the ER but appeared to localise less extensively within the *cis* Golgi. Colocalisation quantitative analysis showed that less of the *cis* Golgi voxels within cells expressing the mutants overlapped with the ADAMTS13 voxels in the same cell, when compared to cells expressing WT ADAMTS13. Together these results suggest that less of the mutant protein is transported to the Golgi compared to WT ADAMTS13.

As both mutants appeared to localise within the ER and the *cis* Golgi of the cell but were secreted at a severely reduced level I investigated whether these proteins were degraded within the cell by either the cell proteasome or lysosomes. I initially investigated this by inhibiting the proteasome or lysosomes in HEK293T cells transiently expressing these mutants. However the results from these experiments were unclear and so I decided instead to investigate the effect of proteasome and lysosome inhibition in HEK293 cells stably expressing mutant ADAMTS13. At the time of analysis I did not have a stable line expressing the p.Y570C mutant and so the effect of proteasome and lysosome inhibition was investigated for the p.I143T mutant only.

Addition of the proteasome inhibitor (MG132) and the proteasome and cathepsin inhibitor (ALLN) to HEK 293 cells stably expressing the p.I143T mutant led to an increase in the intracellular levels of ADAMTS13. This increase was not observed in cells stably expressing WT ADAMTS13 after the addition of either drug. These results suggest that a large proportion of the p.I143T mutant, but not WT ADAMTS13 is targeted to the proteasome for degradation.

The quantity of WT and p.I143T mutant ADAMTS13 present in the supernatant of stable line cells in the presence of proteasome inhibitors was also measured. In these experiments the supernatant was concentrated to a greater degree (~100 fold)

compared to the supernatant obtained from transient transfections. At this degree of concentration the p.I143T mutant could be detected in the majority of experiments. In WT ADAMTS13 the addition of MG132 led to a slight decrease in the quantity and activity of ADAMTS13 measured in the supernatant. With the p.I143T mutant however the opposite occurred, there was a slight increase in the quantity secreted and as a result the activity of the mutant. The antigen and activity of the mutant measured in the supernatant incubated in the presence of MG132 however was similar to the values obtained after incubation with DMSO, suggesting that the DMSO solvent was mainly responsible for the increase in the values obtained. In contrast, inhibition of lysosomes with ammonium chloride or Bafilomycin A1 led to similar/slightly increased levels in cells expressing either WT or mutant ADAMTS13, suggesting that the mutant was degraded by lysosomes to a similar extent as WT ADAMTS13.

The addition of DMSO to cells stably expressing WT or p.I143T mutant ADAMTS13 appeared to lead to an increase in the secretion of ADAMTS13. DMSO is a chemical chaperone and has been shown to aid the secretion of some proteins. I investigated whether another chemical chaperone, betaine, could alternatively help promote the folding and subsequent secretion of the p.I143T mutant.

The addition of 100mM betaine led to a slight decrease in the quantity and activity of WT ADAMTS13 detected in the supernatant (expressed by stable line HEK293 cells). After the addition of betaine to cells expressing the p.I143T mutant there was a median 1.8 fold increase in ADAMTS13 antigen in the supernatant compared to in the absence of betaine. The median antigen value obtained in the absence of betaine was 17ng/ml, range :< 10-197ng/ml, the median value in the presence of betaine on the other hand was 28ng/ml, range: 12- 354ng/ml.

For the p.I143T mutant activity in the absence of betaine was undetectable (<2.5% of PNP) in all experiments, but could be detected in 6/11 experiments in the presence of betaine. In the six experiments in which activity could be detected in the presence of betaine there was a several fold increase in the activity of the mutant in the presence of betaine. The median activity of the mutant in the presence of betaine for these six

experiments was: 5.5% of PNP, ranging from 2.7%-7.1% of PNP. The addition of betaine therefore appeared to promote the secretion of the p.I143T mutant.

In cell lysate samples two distinct bands were present, with the upper band more prominent in cells treated with betaine. This band was sensitive to Endoglycosidase H digestion, which cleaves most N-linked glycans except for complex glycans. Complex glycans are formed in the Golgi so ER associated proteins are sensitive to Endoglycosidase H digestion, suggesting that the upper band that was present in cell lysate samples corresponded to ER associated ADAMTS13. The lower band appeared to be unglycosylated ADAMTS13, as it was not sensitive to Endoglycosidase H or PNGase F digestion. The ability of betaine to aid the folding of ADAMTS13 appeared to promote glycosylation of the protein, in turn leading to a greater proportion of glycosylated compared to unglycosylated protein within the ER of the cell. This in turn promoted the secretion of the protein.

In summary, the p.Y570C mutation severely affected the secretion of ADAMTS13 *in vitro* and subsequently no activity could be measured in the supernatant of cells expressing the mutant. This mutant localised within the ER of the cell but appeared to localise less extensively within the *cis* Golgi. Similarly the p.I143T mutant severely affected the secretion and activity of ADAMTS13 *in vitro*. This mutant also localised within the ER but less extensively within the *cis* Golgi compared to WT ADAMTS13. This mutant appeared to be targeted within the cell to the proteasome for degradation. Addition of the chemical chaperone betaine to cells stably expressing the mutant led to increased secretion of the mutant and consequently in some experiments detectable ADAMTS13 activity in the supernatant.

The two patients with the type 1a mutations also had polymorphisms in the *ADAMTS13* gene. Patient 1 (with the p.I143T mutation) was homozygous for the non-synonymous polymorphism (p.Q448E). Patient 2 (with the p.Y570C mutation) was homozygous for two polymorphisms (p.R7W and p.P618A). These polymorphisms have been expressed *in vitro* by other groups (Plaimauer *et al*, 2006) and two of these polymorphisms (p.Q448E and p.P618A) have been expressed separately in WT ADAMTS13 in this study. The effect of these polymorphisms in combination with the secretion defect mutations was not studied *in vitro* here due to

time constraints but they may have modulated slightly the secretion of either of these two mutants. The p.P618A polymorphism significantly affected the secretion of ADAMTS13 when expressed in WT ADAMTS13 as shown in Chapter 7 and by other groups (Plaimauer *et al*, 2006;Edwards *et al*, 2012;Rurali *et al*, 2013) and so it is likely to have further decreased the secretion and activity of the p.Y570C ADAMTS13 mutant. Plaimauer *et al* showed that the expression of p.R7W and p.Q448E in combination with a mutation (p.R1336W) enhanced the detrimental effect of the mutation (Plaimauer *et al*, 2006). These polymorphisms therefore may have further reduced the secretion of ADAMTS13 when expressed with their respective mutations.

One type 2 ADAMTS13 mutant (p.R102H) was analysed *in vitro* to study the effect of this mutation on the secretion and activity of ADAMTS13. The patient with this mutation developed TTP during her third trimester of pregnancy. She had undetectable ADAMTS13 activity in her plasma in the absence of detectable anti-ADAMTS13 antibodies. However the patient had detectable ADAMTS13 antigen in her plasma, 42%±5.4 of PNP (mean±SD).

After transient transfection of the p.R102H mutant in HEK293T cells, reduced ADAMTS13 could be detected in the supernatant by western blotting. ADAMTS13 antigen within the supernatant was measured using an ADAMTS13 antigen ELISA and was found to be partially reduced (30% of WT). The partial defect in secretion *in vitro* observed with the p.R102H mutant correlated with the detectable ADAMTS13 antigen in the plasma of patient 3. Decreased ADAMTS13 activity could also be measured in the supernatant (15% of WT), giving an average specific activity of 48%. The activity of this mutant was studied further using purified ADAMTS13 protein.

Supernatant was collected from HEK293 cells stably expressing WT or p.R102H mutant ADAMTS13 and ADAMTS13 was purified using FPLC. Time course experiments were set up using FRETS-VWF73 as a substrate and equal quantities of WT and mutant ADAMTS13 to assess the catalytic efficiency ($k_{cat}/K_m$) of both proteins. The $k_{cat}/K_m$ for WT was 2.8 x $10^5$($M^{-1}sec^{-1}$), whereas for the mutant this value was approximately 4 fold lower with a value of 0.75 x $10^5$($M^{-1}sec^{-1}$). In the

circulation therefore this mutant is likely to be less efficient at cleaving ADAMTS13 than WT.

The activity of the purified material was analysed further using VWF multimer analysis. Equal quantities of WT or mutant ADAMTS13 were incubated with full length VWF and VWF multimeric pattern was analysed over time. At 30 minutes there appeared to be a slight difference between WT and mutant ADAMTS13, with more of the intermediate molecular weight multimers present in the mutant. However at the remaining time points there did not appear to be a noticeable difference between WT and mutant ADAMTS13.

Together these results suggested that there is a difference in the activity of WT and the p.R102H mutant ADAMTS13. However the activity of the p.R102H mutant was not severely reduced as expected based on the undetectable activity measured in the patient plasma. The results from the transient transfection experiments showed that this mutant is secreted at a reduced level, which would also impact on the activity measured in the patient plasma. However this defect in secretion did not appear to be sufficient to severely reduce the activity to the levels measured in the patient plasma *in vivo*.

The patient with the p.R102H mutation was also homozygous for three ADAMTS13 non-synonymous polymorphisms (p.Q448E, p.P618A and p.A900V). I investigated whether these polymorphisms in combination with the p.R102H mutation could further affect the activity of ADAMTS13. Each polymorphism was also expressed separately in WT ADAMTS13.

When expressed separately the p.P618A polymorphism had the greatest effect on the secretion of ADAMTS13, reducing the secretion of ADAMTS13 more than the p.R102H mutation. The p.Q448E polymorphism appeared to decrease slightly the secretion of ADAMTS13 whereas the p.A900V polymorphism increased it. When all three polymorphisms were expressed in WT ADAMTS13 or in combination with the p.R102H mutation they reduced the secretion of ADAMTS13 further, when compared to WT or the p.R102H mutant alone.

The p.Q448E and p.P618A polymorphisms did not appear to affect the activity of ADAMTS13, whereas the p.A900V polymorphism did. The specific activity of WT and the p.R102H mutant in the presence of all three polymorphisms was reduced.

No activity could be detected in the p.R102H+p.Q448E+p.P618A+p.A900V construct which correlated with the undetectable ADAMTS13 activity measured in the patient plasma. This suggests that the p.R102H mutation in combination with the three polymorphisms was responsible for the reduced activity measured in the patient plasma. However the quantity of ADAMTS13 in the supernatant was reduced (6% of PNP), which is lower than the quantity of antigen measured in the patient plasma (42%±5.4 of PNP, mean±SD). So although ADAMTS13 antigen could be detected in the supernatant it was lower than the quantity measured in the patient plasma.

In summary the p.R102H mutation partially affects both the secretion and the activity of ADAMTS13. However this mutation did not appear to severely affect the activity of ADAMTS13 as predicted based upon the undetectable ADAMTS13 activity measured in the patient plasma. When this mutation was expressed in combination with three *ADAMTS13* polymorphisms also present in the patient with this mutation, the secretion was further reduced and the activity was undetectable, suggesting that the mutation in combination with the three polymorphisms was responsible for the undetectable ADAMTS13 activity measured in the patient plasma.

I attempted to analyse the effect of a splice site mutation (p.S36_C37delfs*102) on the splicing process by creating a mini gene. I successfully created the ADAMTS13 coding fragment (exon 1→exon 3) to be inserted into the expression vector for cloning; however the cloning reaction was not successful despite trying a number of different technical procedures. Further work is required in order to assess the effect of this mutation on splicing.

In this study I fulfilled my aim to assess how *ADAMTS13* mutations can lead to some of the laboratory features measured in patient plasma (i.e. ADAMTS13 antigen and activity). I successfully studied type 1a and type 2 ADAMTS13 mutants and investigated whether and how these mutations contributed to the undetectable ADAMTS13 activity measured in the patient plasma. I attempted to characterise a

splice site mutant in addition but during the time of this study I have not been able to complete this.

It is difficult to assess how these mutations relate to other features of the disease phenotype because of the small number of mutations analysed. In order to study how these *ADAMTS13* mutations relate to other features of the disease would require a large number of patients to be studied with the same genotype. To the best of my knowledge, patients 1,2 and 4 are the only congenital TTP patients described in the literature with the mutations studied here and only one other patient with the p.R102H mutation has been described (Scully *et al*, 2014). In fact for the majority of ADAMTS13 mutations that have been described to date, most of them have been described in only one patient in the literature. The exceptions to this is the p.R1060W mutation, predominantly present in patients with adult onset TTP (Moatti-Cohen *et al*, 2012;Scully *et al*, 2014) and the p.E1382RfsX6 mutation, predominantly present in patients with childhood onset TTP (Schneppenheim *et al*, 2006).

If looking at just the effect of the mutations (i.e. not in combination with ADAMTS13 polymorphisms also present in the patient), then the p.R102H mutation does not appear to affect ADAMTS13 function as severely as the p.I143T and p.Y570C mutations. The p.I143T and p.Y570C mutations were identified in patients with adolescent onset TTP, who both require regular plasma infusion. On the other hand the p.R102H mutation was identified in a patient with a less severe disease, who developed the disease during adulthood and only requires plasma infusion/exchange when pregnant or after an episode. However the effect of ADAMTS13 polymorphisms also needs to be considered as my results have shown. Ideally residual ADAMTS13 activity should be measured in all of the mutants, when expressed in combination with their respective polymorphisms in order to establish whether residual ADAMTS13 activity is higher in the type 2 mutant compared to the type 1a mutants.

Residual ADAMTS13 activity appears to be associated with disease severity and with *ADAMTS13* genotype (Lotta *et al*, 2012) so it is important to understand the mechanisms and to what extent different mutations within *ADAMTS13* affect its function. Of the mutations identified approximately 30% have been expressed *in*

*vitro* (Lotta *et al*, 2010;Feys *et al*, 2009b;Camilleri *et al*, 2012;Taguchi *et al*, 2012). Patients homozygous for *ADAMTS13* mutations are particularly useful in order to study genotype phenotype relationships that may exist. Of the 43 mutations which have been expressed only 16 are present in a homozygous form in at least one patient in the literature. The results from my study have contributed another three mutations to this list. However more of these homozygous mutations need be expressed *in vitro* in order to assess this relationship more fully.

ADAMTS13 appears to play an important role in determining a patient's phenotype but other factors should also be considered. Other genetic modifiers may be important in the development of TTP. Noris *et al* described two sisters with congenital TTP who presented with TTP during pregnancy and with a slightly different clinical course. One sister had a predominance of neurological symptoms and the other renal symptoms. The sister with renal involvement had a mutation within complement factor H (Noris *et al*, 2005). Complement deficiencies have been found in patients with atypical HUS patients, a disease characterised by renal impairment (Malina *et al*, 2012).

My work has highlighted the importance of *ADAMTS13* polymorphisms to the contribution of laboratory disease phenotype. Other groups have shown the importance of *ADAMTS13* polymorphisms (Plaimauer *et al*, 2006;Edwards *et al*, 2012;Rurali *et al*, 2013) and their effects in combination with *ADAMTS13* mutations (Plaimauer *et al*, 2006). My work has shown however that the ADAMTS13 polymorphisms present in patient 3 along with the mutation identified are vital for disease laboratory phenotype.

The effect of chemical chaperones on the secretion of ADAMTS13 mutants has not been investigated before and is a novel concept in the treatment of TTP. The *ADAMTS13* mutations which have been identified in patients with congenital TTP and expressed *in vitro*, affect to various degrees the secretion pathways of these proteins and the activity of ADAMTS13 (Lotta *et al*, 2010). The majority (86%), lead to reduced (<50% of WT) secretion of mutant recombinant ADAMTS13. The use of a chemical chaperone such as betaine, to aid the secretion of misfolded

ADAMTS13 proteins may be an attractive therapeutic option as potentially a large number of secretion defect mutants could be treated using a similar mechanism.

In my experiments, betaine caused a slight increase in ADAMTS13 activity. It has been shown that residual ADAMTS13 activity is associated with disease severity so even a small increase in activity could be beneficial clinically (Lotta *et al*, 2012). I investigated the effect of betaine, but there are a number of other chemical chaperones that could be investigated that could potentially lead to a larger increase in secretion and activity. The development of pharmacological chaperones could lead to a more potent effect. Currently patients with congenital TTP are treated with plasma infusion or an intermediate purity FVIII concentrate with measurable ADAMTS13 activity and plasma exchange for acute episodes (Scully & Goodship, 2014;Scully *et al*, 2012). Plasma exchange can be expensive, citrate reactions, allergic reactions can occur and there is also the risk of venous thromboembolism (McGuckin *et al*, 2014). It also requires specialised equipment, personnel, and insertion of a central venous access line (George, 2010). Chemical chaperones however can be orally administered so if these could one day be used as a replacement for plasma exchange or infusion it would be highly beneficial.

Chemical chaperones or the development of pharmacological chaperones could be used in combination with current therapies or potentially by themselves as a novel therapeutic option in the treatment of congenital TTP.

# Appendix

| Paralog | GI number | Ortholog | GI number |
|---|---|---|---|
| *Ailuropoda melanoleuca* | 301770673 | ADAMTS1 | 50845384 |
| *Bos taurus* | 297480872 | ADAMTS2 | 3928000 |
| *Calithrix jacchus* | 296191110 | ADAMTS3 | 333360873 |
| *Canis lupus familiaris* | 337298368 | ADAMTS4 | 12643637 |
| *Cavia porcellus* | 348574536 | ADAMTS5 | 12643903 |
| *Cricetulus griseus* | 354499351 | ADAMTS6 | 64276808 |
| *Danio Rerio* | 326670284 | ADAMTS7 | 38197242 |
| *Equus caballus* | 194225985 | ADAMTS8 | 153792351 |
| *Felis catus* | 410979457 | ADAMTS9 | 33624896 |
| *Gallus gallus* | 363740569 | ADAMTS10 | 56121815 |
| *Gorilla gorilla gorilla* | 426363476 | ADAMTS12 | 51558724 |
| *Homo Sapiens* | 15963593 | ADAMTS13 | 15963593 |
| *Mus musculus* | 47604978 | ADAMTS14 | 21265052 |
| *Nomascus leucogenys* | 332255397 | ADAMTS15 | 21265058 |
| *Otolemur garretti* | 395844537 | ADAMTS16 | 32363141 |
| *Ovis aries* | 426226011 | ADAMTS17 | 37999850 |
| *Pan troglodytes* | 332833255 | ADAMTS18 | 76800647 |
| *Pango abelli* | 395741139 | ADAMTS19 | 29336810 |
| *Papio anubis* | 402896179 | ADAMTS20 | 28316229 |
| *Saimiri boliviensis boliviensis* | 403301620 | - | - |
| *Sarophilus harrisii* | 395506393 | - | - |
| *Taeriopygia guttata* | 449478260 | - | - |

**Table S 1 GI number of sequences used for alignment**

| Primer Name | Sequence | Exon position |
|---|---|---|
| T7 (Life technologies) | TAATACGACTCACTATAGGG | Vector sequence |
| For1 | ATGCACCAGCGTCACCCCCG | 1 |
| For2 | GAGCCACAGGCCGTGTCTTCTTA | 2 |
| For3 | GTCTTCAGGCTTTGGAGCCAC | 2 |
| Rev1 | CCTGGTGAGCCTGGAAGACATCG | 3 |
| For4 | GCTGACCTGGTCCTCTATATCAC | 5 |
| Rev2 | AATGGTGACTCCCAGGTCGA | 6 |
| For5 | TGCGCAGCCTGGCCTCTACTACA | 8 |
| Rev3 | GCAGGAGAGGGCCTGGCACATATC | 9 |
| For6 | CATAGCAGCAGTGCATGGGC | 10 |
| For7 | CCCCAGACCTGCCTTTGGGGGGCGTG | 10/11 |
| For8 | GACATTTGGCTGTGATGGTAGG | 13/14 |
| For9 | AGAGTGGCCCTCACCGAGGACCGG | 16 |
| Rev4 | AAACCTGGATGTCAGCATCTTC | 16/17 |
| For10 | TACTTCCAGCCTAAGCCACGG | 17 |
| For11 | GGACCAGGCCAGGAAGGAGTTGGT | 18 |
| For12 | AGACTTCGGCCCATGCAGCG | 19 |
| For13 | GCGGGAGGTCTGCCAGGCTGTC | 22 |
| Rrv5 | GCTGCAGGCCGCCAGCTTGTACT | 23 |
| For14 | GCCAACAGGAACCATTGACATGC | 26 |
| For15 | CGCTGAGTCCAGCCACGAGTAAT | 28 |
| BGH Reverse (Life technologies) | TAGAAGGCACAGTCGAGG | Vector sequence |

**Table S 2 Primers used to sequence ADAMTS13 cDNA**

| Mutation | Forward Primer | Reverse Primer | Primer position | Domain |
|---|---|---|---|---|
| c.106-1G>C | CCATCTCTTTTT GTCTTGCACAG TTGTCTTCAGGC | GCCTGAAGACAA CTGTGCAAGACA AAAAGAGATGG | Intron 1/ Exon 2 | Propeptide |
| p. R102H (c.305G>A) | CAGGAGGACAC AGAGCACTATG TGCTCACCAAC | GTTGGTGAGCAC ATAGTGCTCTGT GTCCTCCTG | Exon 3 | Metalloprotease |
| p. I143T (c.428T>C) | GAGGGTGCTCC AAATACCACAG CCAACCTCACC | GGTGAGGTTGGC TGTGGTATTTGG AGCACCCTC | Exons 4/ Exon 5 | Metalloprotease |
| p.T196I (c.C587T) | GTGCGGGGCGT CATCCAGCTGG GCGG | CCGCCCAGCTGG ATGACGCCCCGC AC | Exon 6 | Metalloprotease |
| p.R409W (c.C1225T) | GTGGTCACCAG GAGGTGGCAGT GCAACAACC | GGTTGTTGCACTG CCACCTCCTGGTG ACCAC | Exon 10 | TSP-1 |
| p. Y570C (c.1709A>G) | GGCAGAGCGAG AGAATGTGTCA CGTTTCTGAC | GTCAGAAACGTG ACACATTCTCTCG CTCTGCC | Exon 14/ Exon 15 | Spacer |
| p.A596V (c.C1787T) | CTCTTCACACAC TTGGTGGTGAG GATCGGAGGG | CCCTCCGATCCTC ACCACCAAGTGT GTGAAGAG | Exon 15/ Exon 16 | Spacer |
| p.C754R (c.T2260C) | GACTTCGGCCC ACGCAGCGCCT CCTG | CAGGAGGCGCTG CGTGGGCCGAAG TC | Exon 19 | TSP-1:3 |
| p.C977F (c.G2930T) | GAGGATCCTGT ATTTTGCCCGG GCCCATG | CATGGGCCCGGG CAAAATACAGGA TCCTC | Exon 23 | TSP-1:6 |

**Table S 3 Primers used for site directed mutagenesis to introduce mutations. The substituted nucleotide is shown in red**

| Polymorphism | Forward Primer | Reverse Primer | Primer position | Domain |
|---|---|---|---|---|
| p. Q448E (i) (c.1342C>G) | GCTGGAGTTC ATGTCGGAAC AGTGCGCCAG GAC | GTCCTGGCGCAC TGTTCCGACATG AACTCCAGC | Exon 11 | Cysteine-rich |
| p. Q448E (ii) (c.1342C>G) | CCAGCTGGAG TTCATGTCGGA ACAGTGCGCC AGGACCGACG | CGTCGGTCCTGGC GCACTGTTCCGAC ATGAACTCCAGCT GG | Exon 11 | Cysteine-rich |
| p. P618A (c.1852C>G) | CTAACACCAC CTACGCCTCCC TCCTGGAG | CTCCAGGAGGGA GGCGTAGGTGGT GTTA | Exon 16 | Spacer |
| p. A900V (c.2699C>T) | GTGTGGACCC CTGTGGCAGG GTCGTGC | GCACGACCCTGC CACAGGGGTCCA CAC | Exon 21 | TSP 1-5 |

**Table S 4 Primers used for site directed mutagenesis to introduce polymorphisms. The substituted nucleotide is shown in red**

| | Primer | Forward Primer | Exon/Intron position |
|---|---|---|---|
| **RNA** | F6 | GAGCCACAGGCCGTGTCTTCTTA | Exon 2 |
| | R6 | CCTGGTGAGCCTGGAAGACATCG | Exon 3 |
| | RevJP | AATGGTGACTCCCAGGTCGA | Exon 6 |
| **Mini-gene: creation and seq** | SpliceA (F) | CACCATGCACCAGCGTCACCCCCGG | Exon 1 |
| | SpliceB (R) | TAAGGGAGCACCAGGGCTCAAGTA | Exon 2 |
| | SpliceC (R) | GGTGAGCACATAGCGCTCTGTGTC | Exon 3 |
| | SpliceD (F) | AGATTCCCAGTCACCAAGGC | Untranslated region |
| | SpliceE (R) | CATAGCGCTCTGTGTCCTCC | Exon 3 |
| | SpliceF (R) | ATAGCGCTCTGTGTCCTCCT | Exon 3 |
| **Mini-gene: seq** | F3/4 | TGTTAGCTTTCCACTGCTTG | Intron 3 |
| | T7 (LT) | TAATACGACTCACTATAGGG | Vector sequence |
| | BGH Reverse (LT) | TAGAAGGCACAGTCGAGG | Vector sequence |

**Table S 5 Primers used for splicing**

RNA: Primers used for RNA extraction, LT: Primers provided by Life technologies, seq: sequencing, F: forward primer, R: reverse primer.

| | No | Type | Location | DNA | Protein | Reference |
|---|---|---|---|---|---|---|
| **S** | 1 | Insertion | Exon 1 | c.82dupT | p.W28LfsX111 | (Donadelli *et al*, 2006) |
| **Pro** | 2 | Splice | Intron 1 | c.106-1G>C | p.S36_C37delfs*102 | (Lotta *et al*, 2012) |
| | 3 | Nonsense | Exon 2 | c.130C>T | p.Q44X | (Antoine *et al*, 2003) |
| **Metalloprotease** | 4 | Missense | Exon 3 | c.237C>G | p.I79M | (Veyradier *et al*, 2004) |
| | 5 | Missense | Exon 3 | c.262G>A | p.V88M | (Bestetti *et al*, 2003) |
| | 6 | Missense | Exon 3 | c.262G>C | p.V88L | (Moatti-Cohen *et al*, 2012) |
| | 7 | Missense | Exon 3 | c.283G>C | p.A95P | (Moatti-Cohen *et al*, 2012) |
| | 8 | Missense | Exon 3 | c.286C>G | p.H96D | (Levy *et al*, 2001) |
| | 9 | Deletion | Exon 3 | c.291_319del | p.E98PfsX31 | (Garagiola *et al*, 2008) |
| | 10 | Missense | Exon 3 | c.304C>T | p.R102C | (Levy *et al*, 2001) |
| | 11 | Missense | Exon 3 | c.305G>A | p. R102H | (Camilleri *et al*, 2012) |
| | 12 | Splice | Intron 3 | c.330+1G>A | r.[330_331ins105, 330_331ins27] | (Uchida *et al*, 2004) |
| | 13 | Deletion | Exon 4 | c.334del | p.A111QfsX18 | (Scully *et al*, 2014) |
| | 14 | Missense | Exon 4 | c.356C>T | p.S119F | (Meyer *et al*, 2008) |
| | 15 | Insertion | Exon 4 | c.372_373insGT | p.R125VfsX6 | (Fujimura *et al*, 2009) |
| | 16 | Splice | Intron 4 | c.414+1G>A | r.spl? | (Matsumoto *et al*, 2004) |
| | 17 | Missense | Exon 5 | c.428T>C | p.I143T | (Lotta *et al*, 2012) |
| | 18 | Missense | Exon 5 | c.448T>C | p.S150P | (Lotta *et al*, 2012) |
| | 19 | Missense | Exon 5 | c.533T>C | p.I178T | (Fujimura *et al*, 2009) |
| | 20 | Missense | Exon 6 | c.577C>T | p.R193W | (Matsumoto *et al*, 2004) |
| | 21 | Missense | Exon 6 | c.578G>A | p.R193Q | (Lotta *et al*, 2012) |
| | 22 | Missense | Exon 6 | c.581G>T | p.G194V | (Ma *et al*, 2006) |
| | 23 | Missense | Exon 6 | c.587C>T | p.T196I | (Levy *et al*, 2001) |
| | 24 | Missense | Exon 6 | c.607T>C | p.S203P | (Veyradier *et al*, 2004) |
| | 25 | Missense | Exon 6 | c.649G>C | p.D217H | (Camilleri *et al*, 2012) |
| | 26 | Missense | Exon 6 | c.681G>C | p.G227R | (Fujimura *et al*, 2011) |
| | 27 | Splice | Intron 6 | c.686+1G>A | | (Matsumoto *et al*, 2004) |
| | 28 | Splice | Intron 6 | c.687-2 A>G | | (Studt *et al*, 2005) |
| | 29 | Missense | Exon 7 | c.695T>A | p.L232Q | (Schneppenheim *et al*, 2003) |
| | 30 | Missense | Exon 7 | c.702C>A | p.H234Q | (Shibagaki *et al*, 2006) |
| | 31 | Missense | Exon 7 | c.701A>G | p.H234R | (Fujimura *et al*, 2011) |
| | 32 | Missense | Exon 7 | c.703G>C | p.D235H | (Assink *et al*, 2003) |
| | 33 | Missense | Exon 7 | c.703G>T | p.D235Y | (Lotta *et al*, 2012) |
| | 34 | Missense | Exon 7 | c.706G>T | p.G236C | (Lotta *et al*, 2012) |
| | 35 | Deletion | Exon 7 | c.718_724del | p.S240AfsX9 | (Assink *et al*, 2003) |
| | 36 | Deletion | Exon 7 | c.719_724del | p.G241_C242del | (Camilleri *et al*, 2012) |
| | 37 | Deletion | Exon 7 | c.746_987+ 373del1782 | p.M249TdelfsX50 | (Eura *et al*, 2014) |
| | 38 | Missense | Exon 7 | c.749C>T | p.A250V | (Uchida *et al*, 2004) |
| | 39 | Deletion | Exon 7 | c.768_774del | p.R257AfsX13 | (Prestidge *et al*, 2012) |

| | | | | | | |
|---|---|---|---|---|---|---|
| | 40 | Missense | Exon 7 | c.788C>G | p.S263C | (Schneppenheim *et al*, 2003) |
| | 41 | Missense | Exon 7 | c.788C>T | p.S263F | (Rossio *et al*, 2013) |
| | 42 | Missense | Exon 7 | c.794G>C_ 796A>T | p.C265S+S266C | (Camilleri *et al*, 2012) |
| | 43 | Missense | Exon 7 | c.803G>C | p.R268P | (Kokame *et al*, 2002) |
| | 44 | Deletion | Intron 8_ Exon 8 | c.825-10_843del | | (Veyradier *et al*, 2004) |
| | 45 | Missense | Exon 8 | c.841T>A | p.C281S | (Eura *et al*, 2014) |
| **Disintegrin-like** | 46 | Missense | Exon 8 | c.911A>G | p.Y304C | (Fujimura *et al*, 2009) |
| | 47 | Missense | Exon 8 | c.932G>A | p.C311Y | (Assink *et al*, 2003) |
| | 48 | Missense | Exon 8 | c.? | p.R312C | (Fujimura *et al*, 2011) |
| | 49 | Missense | Exon 8 | c.964T>G (+) 968C>G (+) 969C>A (+) 970T>C | p.C322G + T323R + F324L | (Kokame *et al*, 2008) |
| | 50 | Missense | Exon 9 | c.1039T>A | p.C347S | (Schneppenheim *et al*, 2006) |
| | 51 | Missense | Exon 9 | c.1045C>T | p.R349C | (Fujimura *et al*, 2009) |
| | 52 | Missense | Exon 9 | c.1058C>T | p.P353L | (Schneppenheim *et al*, 2003) |
| | 53 | Deletion | Exon 10 | c.1095_1112del | p.W365_R370del | (Tao *et al*, 2006) |
| | 54 | Missense | Exon 10 | c.? | p.G385E | (Fujimura *et al*, 2011) |
| **T1** | 55 | Nonsense | Exon 10 | c.1169G>A | p.W390X | (Schneppenheim *et al*, 2003) |
| | 56 | Missense | Exon 10 | c.1170G>C | p.W390C | (Licht *et al*, 2004) |
| | 57 | Missense | Exon 10 | c.1192C>T | p.R398C | (Fujimura *et al*, 2011) |
| | 58 | Missense | Exon 10 | c.1193G>A | p.R398H | (Levy *et al*, 2001) |
| | 59 | Missense | Exon 10 | c.1201G>A | p.G401R | (Scully *et al*, 2014) |
| | 60 | Missense | Exon 10 | c.1225C>T | p.R409W | (Camilleri *et al*, 2012) |
| | 61 | Splice | Intron 10 | c.1244+2T>G | r.spl? | (Matsumoto *et al*, 2004) |
| | 62 | Missense | Exon 11 | c. 1308G>C | p.Q436H | (Camilleri *et al*, 2012) |
| | 63 | Splice | Intron 11 | c.1309_?G>A | | (Veyradier *et al*, 2004) |
| | 64 | Missense | Exon 12 | c.? | p.C438S | (Fujimura *et al*, 2011) |
| **Cysteine-rich** | 65 | Nonsense | Exon 12 | c.1345C>T | p.Q449X | (Kokame *et al*, 2002) |
| | 66 | Missense | Exon 12 | c.1368G>T | p.Q456H | (Camilleri *et al*, 2012) |
| | 67 | Missense | Exon 12 | c.1370C>T | p.P457L | (Assink *et al*, 2003) |
| | 68 | Deletion | Exon 13 | c.1456_1457del | p.M486VfsX47 | (Scully *et al*, 2014) |
| | 69 | Missense | Exon 13 | c.1492C>T | p.R498C | (Scully *et al*, 2014) |
| | 70 | Missense | Exon 13 | c.1520G>A | p.R507Q | (Veyradier *et al*, 2004) |
| | 71 | Missense | Exon 13 | c.1523G>A | p.C508Y | (Kokame *et al*, 2002) |
| | 72 | Missense | Exon 13 | c.1574G>A | p.G525D | (Fujimura *et al*, 2009) |
| | 73 | Missense | Exon 13 | c.1582A>G | p.R528G | (Levy *et al*, 2001) |
| | 74 | Splice | Intron 13 | c.1584+5G>A | | (Levy *et al*, 2001) |
| | 75 | Missense | Exon 14 | c.1648G>A | p.G550R | (Fujimura *et al*, 2011) |
| | 76 | Deletion | Exon 14 | c.1649_1664del | p.D551QfsX58 | (Alsultan *et al*, 2013) |
| **Spacer** | 77 | Missense | Exon 15 | c.1709A>G | p.Y570C | (Metin *et al*, 2013) |
| | 78 | Deletion | Exon 15 | c.1783_1784del | p.L595GfsX19 | (Savasan *et al*, 2003) |
| | 79 | Splicing | Exon 15 | c.1786+1G>A | p.E569_A596 delinsA | (Prestidge *et al*, 2012) |

| | | | | | | |
|---|---|---|---|---|---|---|
| | 80 | Missense | Exon 16 | c.1787C>T | p.A596V | (Veyradier *et al*, 2004) |
| | 81 | Missense | Exon 16 | c.1816G>C | p.A606P | (Fujimura *et al*, 2009) |
| | 82 | Deletion | Exon 16 | c.1885del | p.R629EfsX69 | (Fujimura *et al*, 2011) |
| | 83 | Missense | Exon 16 | c.1892C>T | p.A631V | (Moatti-Cohen *et al*, 2012) |
| | 84 | Missense | Exon 16 | c.1921G>A | p.E641K | (Scully *et al*, 2014) |
| | 85 | Deletion | Exon 16 | c.1922del | p.E641GfsX57 | (Alsultan *et al*, 2013) |
| | 86 | Missense | Exon 16 | c.1973A>G | p.Y658C | (Lee *et al*, 2011) |
| | 87 | Deletion | Exon 17 | c.1999del | p.N667TfsX31 | (Scully *et al*, 2014) |
| | 88 | Missense | Exon 17 | c.2012C>T | p.P671L | (Schneppenheim *et al*, 2006) |
| | 89 | Missense | Exon 17 | c.2017A>T | p.I673F | (Matsumoto *et al*, 2004) |
| | 90 | Deletion | Exon 17 | c.2042del | p.K681CfsX16 | (Rank *et al*, 2014) |
| **T2** | 91 | Missense | Exon 17 | c.2068G>A | p.A690T | (Camilleri *et al*, 2012) |
| | 92 | Missense | Exon 17 | c.2074C>T | p.R692C | (Levy *et al*, 2001) |
| | 93 | Missense | Exon 18 | c.2167C>A | p.Q723K | (Fujimura *et al*, 2011) |
| | 94 | Nonsense | Exon 18 | c.2203G>T | p.E735X | (Borgi *et al*, 2013) |
| **T3** | 95 | Deletion | Exon 19 | c.2259del | p.C754AfsX24 | (Fujimura *et al*, 2011) |
| | 96 | Missense | Exon 19 | c.2260T>C | p.C754R | (Camilleri *et al*, 2012) |
| | 97 | Missense | Exon 19 | c.2272T>C | p.C758R | (Veyradier *et al*, 2004) |
| | 98 | Deletion | Exon 19 | c.2279del | p.G760AfsX18 | (Assink *et al*, 2003) |
| | 99 | Deletion | Exon 19 | c.2376_2401del | p.A793PfsX43 | (Levy *et al*, 2001) |
| **T4** | 100 | Nonsense | Exon 20 | c.2434G>T | p.E812X | (Moatti-Cohen *et al*, 2012) |
| | 101 | Deletion | Exon 20 | c.2455del | p.A819LfsX24 | (Moatti-Cohen *et al*, 2012) |
| | 102 | Deletion | Exon 20 | c.2549_2550del | p.D850GfsX7 | (Schneppenheim *et al*, 2003) |
| **T5** | 103 | Missense | Exon 21 | c.2723G>C | p.C908S | (Veyradier *et al*, 2004) |
| | 104 | Missense | Exon 21 | c.2723G>A | p.C908Y | (Matsumoto *et al*, 2004) |
| | 105 | Missense | Exon 21 | c.2725G>C | p.G909R | (Fujimura *et al*, 2011) |
| | 106 | Nonsense | Exon 21 | c.2728C>T | p.R910X | (Schneppenheim *et al*, 2003) |
| | 107 | Missense | Exon 22 | c.2746C>T | p.R916C | (Deal *et al*, 2012) |
| | 108 | Nonsense | Exon 22 | c.2785C>T | p.Q929X | (Fujimura *et al*, 2009) |
| | 109 | Missense | Exon 22 | c.2851T>G | p.C951G | (Levy *et al*, 2001) |
| **T6** | 110 | Deletion | Exon 23 | c.2930_2935del | p.C977_R979 delinsW | (Palla *et al*, 2009) |
| | 111 | Missense | Exon 23 | c.2930G>T | p.C977F | (Camilleri *et al*, 2012) |
| **T7** | 112 | Nonsense | Exon 24 | c.3047G>A | p.W1016X | (Donadelli *et al*, 2006) |
| | 113 | Missense | Exon 24 | c.3070T>G | p.C1024G | (Levy *et al*, 2001) |
| | 114 | Missense | Exon 24 | c.? | p.C1024R | (Fujimura *et al*, 2011) |
| | 115 | Nonsense | Exon 24 | c.3100A>T | p.R1034X | (Schneppenheim *et al*, 2003) |
| | 116 | Nonsense | Exon 24 | c.3107C>A | p.S1036X | (Klukowska *et al*, 2010) |
| | 117 | Missense | Exon 24 | c.3178C>T | p.R1060W | (Tao *et al*, 2006) |
| | 118 | Deletion | Exon 24 | c.3198_3199del | p.C1067SfsX30 | (Fujimura *et al*, 2011) |
| | 119 | Deletion | Exon 24 | c.3220_3223del | p.Y1074AfsX46 | (Fujimura *et al*, 2011) |
| **T8** | 120 | Nonsense | Exon 24 | c.? | p.W1081X | (Fujimura *et al*, 2011) |
| | 121 | Missense | Exon 25 | c.3251G>A | p.C1084Y | (Lotta *et al*, 2012) |

| | | | | | | |
|---|---|---|---|---|---|---|
| | 122 | Deletion | Exon 25 | c.3254_3255del | p.S1085CfsX12 | (Veyradier *et al*, 2004) |
| | 123 | Missense | Exon 25 | c.3283C>T | p.R1095W | (Lotta *et al*, 2012) |
| | 124 | Missense | Exon 25 | c.3284G>A | p.R1095Q | (Camilleri *et al*, 2012) |
| | 125 | Missense | Exon 25 | c.3313C>T | p.Q1105X | (Moatti-Cohen *et al*, 2012) |
| | 126 | Missense | Exon 25 | c.3367C>T | p.R1123C | (Matsumoto *et al*, 2004) |
| | 127 | Missense | Exon 25 | c.3368G>A | p.R1123H | (Rank *et al*, 2014) |
| **CUB-1** | 128 | Nonsense | Exon 26 | c.3616C>T | p.R1206X | (Shibagaki *et al*, 2006) |
| | 129 | Missense | Exon 26 | c.3638G>A | p.C1213Y | (Levy *et al*, 2001) |
| | 130 | Missense | Exon 26 | c.3650T>C | p.I1217T | (Park *et al*, 2008) |
| | 131 | Missense | Exon 26 | c.3655C>T | p.R1219W | (Donadelli *et al*, 2006) |
| | 132 | Missense | Exon 26 | c.3656G>A | p.R1219Q | (Scully *et al*, 2014) |
| | 133 | Missense | Exon 27 | c.3716G>T | p.G1239V | (Bestetti *et al*, 2003) |
| | 134 | Nonsense | Exon 27 | c.3735G>A | p.W1245X | (Licht *et al*, 2004) |
| | 135 | Deletion | Eon 27 | c.3751_3892 +587del729 | p.R1251SfsX2 | (Eura *et al*, 2014) |
| | 136 | Insertion | Exon 27 | c.3770dupT | p.L1258VfsX36 | (Levy *et al*, 2001) |
| **CUB-2** | 137 | Nonsense | Exon 28 | c.3904C>T | p.Q1302X | (Fujimura *et al*, 2009) |
| | 138 | Missense | Exon 28 | c.4006C>T | p.R1336W | (Antoine *et al*, 2003) |
| | 139 | Deletion | Exon 28 | c.4015del | p.I1339SfsX21 | (Scully *et al*, 2014) |
| | 140 | Missense | Exon 29 | c.4085A>T | p.D1362V | (Calderazzo *et al*, 2012) |
| | 141 | Deletion | Exon 29 | c.4119del | p.Q1374SfsX22 | (Fujimura *et al*, 2011) |
| | 142 | Insertion | Exon 29 | c.4143dupA | p.E1382RfsX6 | (Schneppenheim *et al*, 2003) |

**Table S 6 ADAMTS13 mutations identified in patients with congenital TTP and published in the literature**

S: Signal Peptide, Pro: Propeptide. Reference refers to the first case published in the literature in which mutation was identified. T1→TSP-1; T2→TSP-1:2; T3→TSP-1:3; T4→TSP-1:4; T5→TSP-1:5; T6→TSP-1:6; T7→TSP-1:7 and T8→TSP-1:8.

| No | DNA | Protein | Domain | Reference |
|---|---|---|---|---|
| 1 | c.130C>T | p.Q44X | P | (Plaimauer *et al*, 2006) |
| 2 | c.262G>A | p.V88M | MP | (Donadelli *et al*, 2006;Peyvandi *et al*, 2006) |
| 3 | c.291_319del | p.E98PfsX31 | MP | (Garagiola *et al*, 2008) |
| 4 | c.305G>A | p. R102H | MP | (Camilleri *et al*, 2012) |
| 5 | c.330+1G>A | r.[330_331ins105, 330_331ins27] | MP | (Uchida *et al*, 2004) |
| 6 | c.356C>T | p.S119F | MP | (Feys *et al*, 2009b) |
| 7 | c.577C>T | p.R193W | MP | (Matsumoto *et al*, 2004) |
| 8 | c.587C>T | p.T196I | MP | (Camilleri *et al*, 2012) |
| 9 | c.607T>C | p.S203P | MP | (Hommais *et al*, 2007) |
| 10 | c.649G>C | p.D217H | MP | (Camilleri *et al*, 2012) |
| 11 | c.749C>T | p.A250V | MP | (Uchida *et al*, 2004) |
| 12 | c.794G>C_796A>T | p.C265S+S266C | MP | (Camilleri *et al*, 2012) |
| 13 | c.803G>C | p.R268P | MP | (Kokame *et al*, 2002;Hommais *et al*, 2007;Camilleri *et al*, 2012) |
| 14 | c.719_724del | p.G241_C242del | MP | (Camilleri *et al*, 2012) |
| 15 | c.1058C>T | p.P353L | Dis | (Manea *et al*, 2007a) |
| 16 | c.1095_1112del | p.W365_R370del | Dis | (Tao *et al*, 2006) |
| 17 | c.1192C>T | p.R398C | TSP1 | (Camilleri *et al*, 2012) |
| 18 | c.1225C>T | p.R409W | TSP1 | (Camilleri *et al*, 2012) |
| 19 | c. 1308G>C | p.Q436H | TSP1 | (Camilleri *et al*, 2012) |
| 20 | c.1345C>T | p.Q449X | Cys | (Kokame *et al*, 2002;Soejima *et al*, 2003) |
| 21 | c.1368G>T | p.Q456H | Cys | (Camilleri *et al*, 2012) |
| 22 | c.1370C>T | p.P457L | Cys | (Manea *et al*, 2007a) |
| 23 | c.1520G>A | p.R507Q | Cys | (Hommais *et al*, 2007) |
| 24 | c.1523G>A | p.C508Y | Cys | (Kokame *et al*, 2002) |
| 25 | c.1787C>T | p.A596V | Spac | (Hommais *et al*, 2007;Camilleri *et al*, 2012) |
| 26 | c.2017A>T | p.I673F | Spac | (Matsumoto *et al*, 2004) |
| 27 | c.2068G>A | p.A690T | TSP-1:2 | (Camilleri *et al*, 2012) |
| 28 | c.2260T>C | p.C754R | TSP-1:3 | (Camilleri *et al*, 2012) |
| 29 | c.2723G>A | p.C908Y | TSP-1:5 | (Matsumoto *et al*, 2004) |
| 30 | c.2728C>T | p.R910X | TSP-1:5 | (Camilleri *et al*, 2012) |
| 31 | c.2930_2935del | p.C977_R979delinsW | TSP-1:6 | (Palla *et al*, 2009) |
| 32 | c.2930G>T | p.C977F | TSP-1:6 | (Camilleri *et al*, 2012) |
| 33 | c.3047G>A | p.W1016X | TSP-1:7 | (Soejima *et al*, 2003) |
| 34 | c.? | p.C1024R | TSP-1:7 | (Taguchi *et al*, 2012) |
| 35 | c.3178C>T | p.R1060W | TSP-1:7 | (Camilleri *et al*, 2008;Tao *et al*, 2006) |
| 36 | c.3367C>T | p.R1123C | TSP-1:8 | (Matsumoto *et al*, 2004;Donadelli *et al*, 2006) |
| 37 | c.3638G>A | p.C1213Y | CUB-1 | (Zhou *et al*, 2009b) |
| 38 | c.3655C>T | p.R1219W | CUB-1 | (Donadelli *et al*, 2006) |
| 39 | c.3716G>T | p.G1239V | CUB-1 | (Donadelli *et al*, 2006;Peyvandi *et al*, 2006) |
| 40 | c.3735G>A | p.W1245X | CUB-1 | (Zhou *et al*, 2009b) |
| 41 | c.3770dupT | p.L1258VfsX36 | CUB-1 | (Zhou *et al*, 2009b) |
| 42 | c.4006C>T | p.R1336W | CUB-2 | (Plaimauer *et al*, 2006) |
| 43 | c.4143dupA | p.E1382RfsX6 | CUB-2 | (Pimanda *et al*, 2004;Garagiola *et al*, 2008) |

**Table S 7 ADAMTS13 mutations identified in patients with congenital TTP expressed *in vitro***

P: propeptide, MP: metalloprotease, Dis: disintegrin-like, Cys: cysteine-rich, Spa: spacer

>NG_011934 reference sequence, modifications in red according to vector ADAMTS13

▼ Signal peptide

1/1 31/11

atg cac cag cgt cac ccc cgg gca aga tgc cct ccc ctc tgt gtg gcc gga atc ctt gccExon1

M H Q R H P R A R C P P L C V A G I L A

▼ Propeptide

61/21 91/31

tgt ggc ttt ctc ctg ggc tgc tgg gga ccc tcc cat ttc cag cag agc tgt ctt cag gctExon 2

C G F L L G C W G P S H F Q Q S C L Q A

121/41 151/51

ctg gag cca cag gcc gtg tct tct tac ttg agc cct ggt gct ccc tta aaa ggc cgc cct

L E P Q A V S S Y L S P G A P L K G R P

▼ Metalloprotease

181/61 211/71

cct tcc cct ggc ttc cag agg cag agg cag agg cag agg cgg gct gca ggc ggc atc ctaExon 3

P S P G F Q R Q R Q R Q R R A A G G I L

241/81 271/91

cac ctg gag ctg ctg gtg gcc gtg ggc ccc gat gtc ttc cag gct cac cag gag gac aca

H L E L L V A V G P D V F Q A H Q E D T

301/101 331/111

gag cgc tat gtg ctc acc aac ctc aac atc ggg gca gaa ctg ctt cgg gac ccg tcc ctgExon 4

E R Y V L T N L N I G A E L L R D P S L

361/121 391/131

ggg gct cag ttt cgg gtg cac ctg gtg aag atg gtc att ctg aca gag cct gag ggt gct

G A Q F R V H L V K M V I L T E P E G A

421/141 451/151

cca aat atc aca gcc aac ctc acc tcg tcc ctg ctg agc gtc tgt ggg tgg agc cag accExon 5

P N I T A N L T S S L L S V C G W S Q T

481/161 511/151

atc aac cct gag gac gac acg gat cct ggc cat gct gac ctg gtc ctc tat atc act agg

I N P E D D T D P G H A D L V L Y I T R

541/181 571/191

ttt gac ctg gag ttg cct gat ggt aac cgg cag gtg cgg ggc gtc acc cag ctg ggc ggtExon 6

F D L E L P D G N R Q V R G V T Q L G G

601/201 631/211

gcc tgc tcc cca acc tgg agc tgc ctc att acc gag gac act ggc ttc gac ctg gga gtc

A C S P T W S C L I T E D T G F D L G V

661/221 691/231

acc att gcc cat gag att ggg cac agc ttc ggc ctg gag cac gac ggc gcg ccc ggc agc

T I A H E I G H S F G L E H D G A P G S

721/241 751/251

ggc tgc ggc ccc agc gga cac gtg atg gct tcg gac ggc gcc gcg ccc cgc gcc ggc ctcExon 7

G C G P S G H V M A S D G A A P R A G L

781/261 811/271

gcc tgg tcc ccc tgc agc cgc cgg cag ctg ctg agc ctg ctc agc gca gga cgg gcg cgc

A W S P C S R R Q L L S L L S A G R A R

▼ Disintegrin-like

841/281 871/291

tgc gtg tgg gac ccg ccg cgg cct caa ccc ggg tcc gcg ggg cac ccg ccg gat gcg caaExon 8

C V W D P P R P Q P G S A G H P P D A Q

901/301 931/311

cct ggc ctc tac tac agc gcc aac gag cag tgc cgc gtg gcc ttc ggc ccc aag gct gtc

P G L Y Y S A N E Q C R V A F G P K A V

961/321 991/331

gcc tgc acc ttc gcc agg gag cac ctg gat atg tgc cag gcc ctc tcc tgc cac aca gac

A C T F A R E H L D M C Q A L S C H T D

1021/341 1051/351

ccg ctg gac caa agc agc tgc agc cgc ctc ctc gtt cct ctc ctg gat ggg aca gaa tgtExon 9

P L D Q S S C S R L L V P L L D G T E C

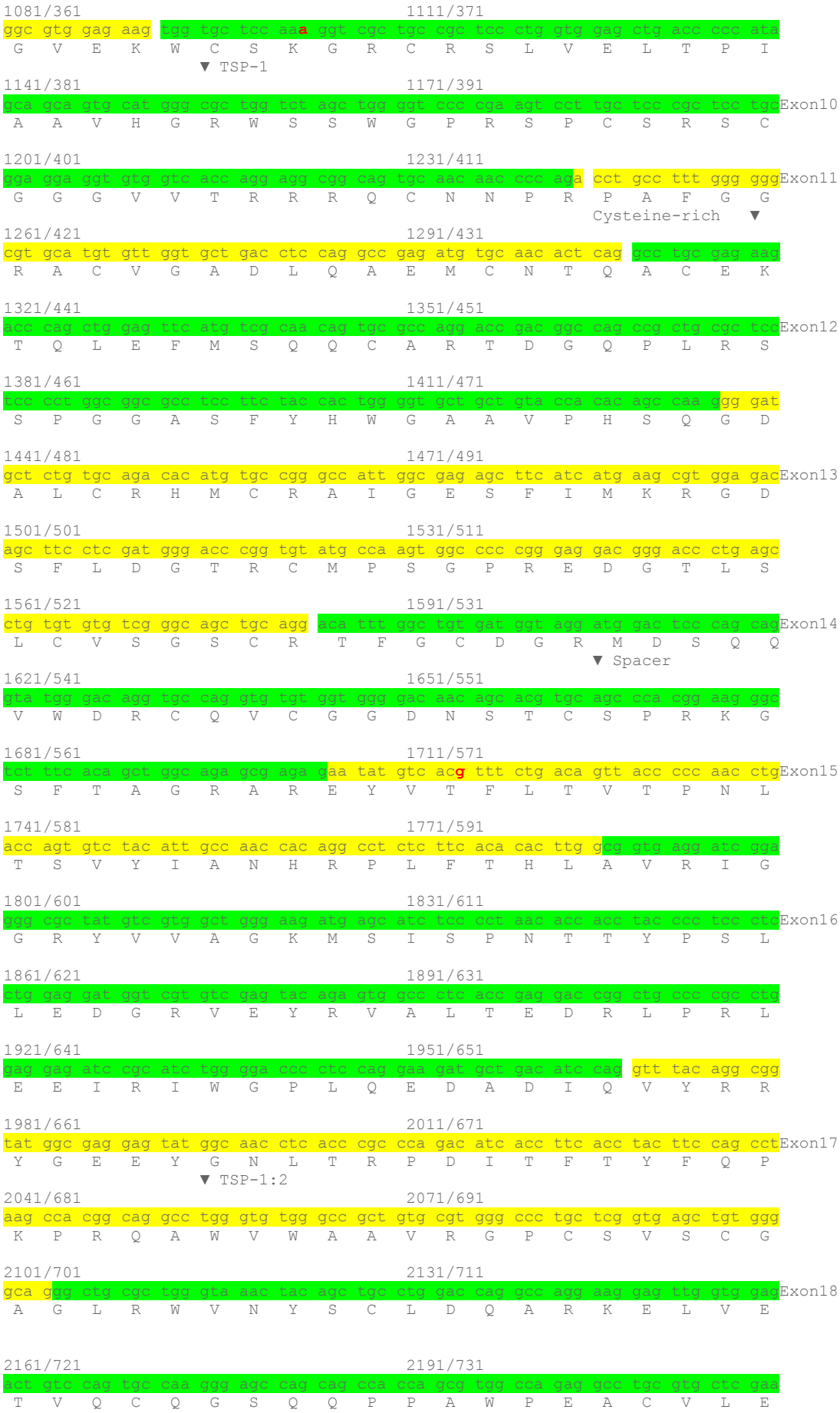
1081/361
1111/371
ggc gtg gag aag tgg tgc tcc aaa ggt cgc tgc cgc tcc ctg gtg gag ctg acc ccc atc
G V E K W C S K G R C R S L V E L T P I
▼ TSP-1
1141/381
1171/391
gca gca gtg cat ggg cgc tgg tct agc tgg ggt ccc cga agt cct tgc tcc cgc tcc tgcExon10
A A V H G R W S S W G P R S P C S R S C
1201/401
1231/411
gga gga ggt gtg gtc acc agg agg cgg cag tgc aac aac ccc aga cct gcc ttt ggg gggExon11
G G G V V T R R R Q C N N P R P A F G G
Cysteine-rich ▼
1261/421
1291/431
cgt gca tgt gtt ggt gct gac ctc cag gcc gag atg tgc aac act cag gcc tgc gag aag
R A C V G A D L Q A E M C N T Q A C E K
1321/441
1351/451
acc cag ctg gag ttc atg tcg caa cag tgc gcc agg acc gac ggc cag ccg ctg cgc tccExon12
T Q L E F M S Q Q C A R T D G Q P L R S
1381/461
1411/471
tcc cct ggc ggc gcc tcc ttc tac cac tgg ggt gct gct gta cca cac agc caa ggg gat
S P G G A S F Y H W G A A V P H S Q G D
1441/481
1471/491
gct ctg tgc aga cac atg tgc cgg gcc att ggc gag agc ttc atc atg aag cgt gga gacExon13
A L C R H M C R A I G E S F I M K R G D
1501/501
1531/511
agc ttc ctc gat ggg acc cgg tgt atg cca agt ggc ccc cgg gag gac ggg acc ctg agc
S F L D G T R C M P S G P R E D G T L S
1561/521
1591/531
ctg tgt gtg tcg ggc agc tgc agg aca ttt ggc tgt gat ggt agg atg gac tcc cag cagExon14
L C V S G S C R T F G C D G R M D S Q Q
▼ Spacer
1621/541
1651/551
gta tgg gac agg tgc cag gtg tgt ggt ggg gac aac agc acg tgc agc cca cgg aag ggc
V W D R C Q V C G G D N S T C S P R K G
1681/561
1711/571
tct ttc aca gct ggc aga gcg aga caa tat gtc acg ttt ctg aca gtt acc ccc aac ctgExon15
S F T A G R A R E Y V T F L T V T P N L
1741/581
1771/591
acc agt gtc tac att gcc aac cac agg cct ctc ttc aca cac ttg gcg gtg agg atc ggc
T S V Y I A N H R P L F T H L A V R I G
1801/601
1831/611
ggg cgc tat gtc gtg gct ggg aag atg agc atc tcc cct aac acc acc tac ccc tcc ctcExon16
G R Y V V A G K M S I S P N T T Y P S L
1861/621
1891/631
ctg gag gat ggt cgt gtc gag tac aga gtg gcc ctc acc gag gac cgg ctg ccc cgc ctg
L E D G R V E Y R V A L T E D R L P R L
1921/641
1951/651
gag gag atc cgc atc tgg gga ccc ctc cag gaa gat gct gac atc cag gtt tac agg cgg
E E I R I W G P L Q E D A D I Q V Y R R
1981/661
2011/671
tat ggc gag gag tat ggc aac ctc acc cgc cca gac atc acc ttc acc tac ttc cag cctExon17
Y G E E Y G N L T R P D I T F T Y F Q P
▼ TSP-1:2
2041/681
2071/691
aag cca cgg cag gcc tgg gtg tgg gcc gct gtg cgt ggg ccc tgc tcg gtg agc tgt ggg
K P R Q A W V W A A V R G P C S V S C G
2101/701
2131/711
gca ggg ctg cgc tgg gta aac tac agc tgc ctg gac cag gcc agg aag gag ttg gtg gagExon18
A G L R W V N Y S C L D Q A R K E L V E
2161/721
2191/731
act gtc cag tgc caa ggg agc cag cag cca cca gcg tgg cca gag gcc tgc gtg ctc gac
T V Q C Q G S Q Q P P A W P E A C V L E

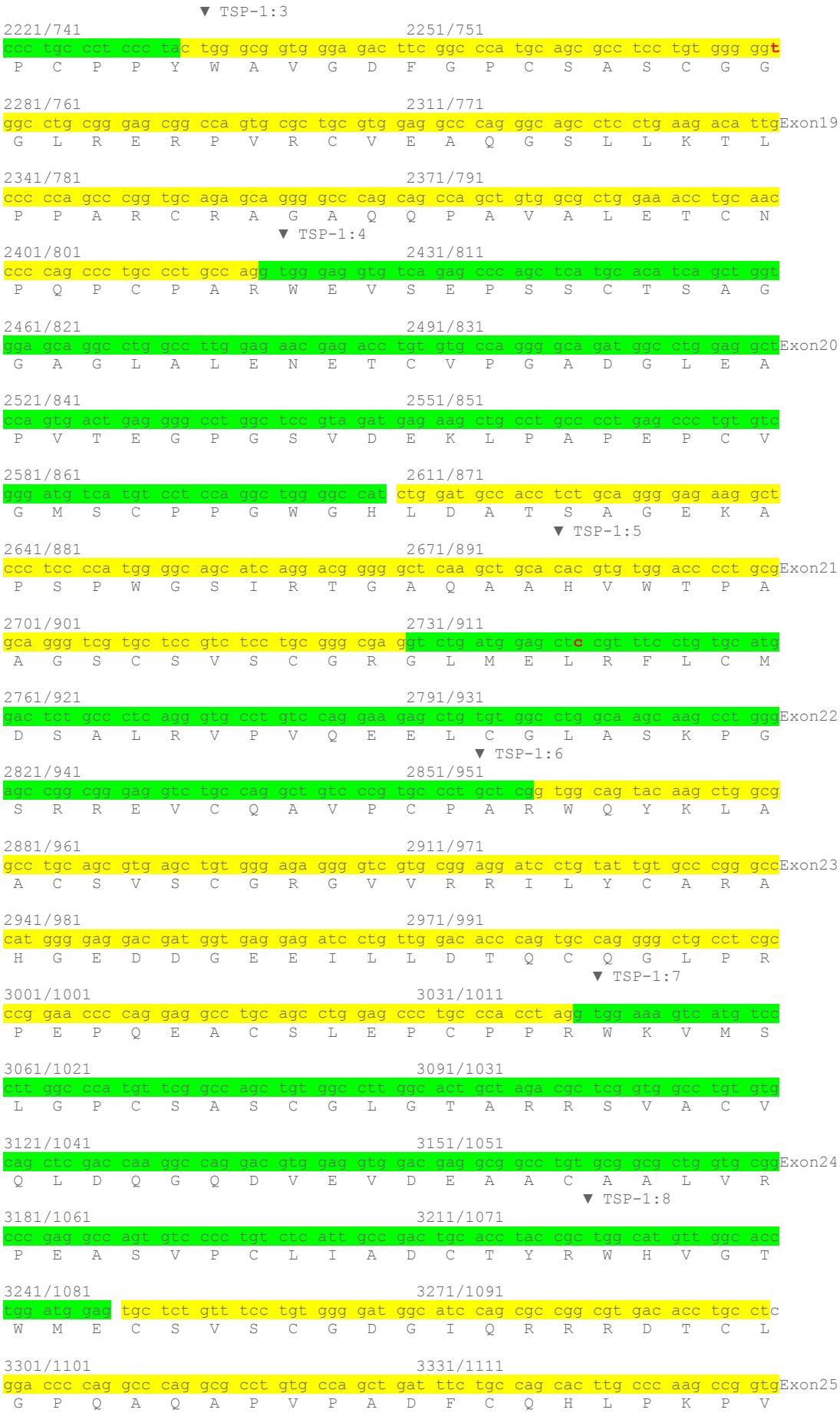
▼ TSP-1:3
2221/741
2251/751
ccc tgc cct ccc tac tgg gcg gtg gga gac ttc ggc cca tgc agc gcc tcc tgt ggg ggt
P C P P Y W A V G D F G P C S A S C G G
2281/761
2311/771
ggc ctg cgg gag cgg cca gtg cgc tgc gtg gag gcc cag ggc agc ctc ctg aag aca ttgExon19
G L R E R P V R C V E A Q G S L L K T L
2341/781
2371/791
ccc cca gcc cgg tgc aga gca ggg gcc cag cag cca gct gtg gcg ctg gaa acc tgc aac
P P A R C R A G A Q Q P A V A L E T C N
▼ TSP-1:4
2401/801
2431/811
ccc cag ccc tgc cct gcc agg tgg gag gtg tca gag ccc agc tca tgc aca tca gct ggt
P Q P C P A R W E V S E P S S C T S A G
2461/821
2491/831
gga gca ggc ctg gcc ttg gag aac gag acc tgt gtg cca ggg gca gat ggc ctg gag gctExon20
G A G L A L E N E T C V P G A D G L E A
2521/841
2551/851
cca gtg act gag ggg cct ggc tcc gta gat gag aag ctg cct gcc cct gag ccc tgt gtc
P V T E G P G S V D E K L P A P E P C V
2581/861
2611/871
ggg atg tca tgt cct cca ggc tgg ggc cat ctg gat gcc acc tct gca ggg gag aag gct
G M S C P P G W G H L D A T S A G E K A
▼ TSP-1:5
2641/881
2671/891
ccc tcc cca tgg ggc agc atc agg acg ggg gct caa gct gca cac gtg tgg acc cct gcgExon21
P S P W G S I R T G A Q A A H V W T P A
2701/901
2731/911
gca ggg tcg tgc tcc gtc tcc tgc ggg cga ggt ctg atg gag ctc cgt ttc ctg tgc atg
A G S C S V S C G R G L M E L R F L C M
2761/921
2791/931
gac tct gcc ctc agg gtg cct gtc cag gaa gag ctg tgt ggc ctg gca agc aag cct gggExon22
D S A L R V P V Q E E L C G L A S K P G
▼ TSP-1:6
2821/941
2851/951
agc cgg cgg gag gtc tgc cag gct gtc ccg tgc cct gct cgg tgg cag tac aag ctg gcg
S R R E V C Q A V P C P A R W Q Y K L A
2881/961
2911/971
gcc tgc agc gtg agc tgt ggg aga ggg gtc gtg cgg agg atc ctg tat tgt gcc cgg gccExon23
A C S V S C G R G V V R R I L Y C A R A
2941/981
2971/991
cat ggg gag gac gat ggt gag gag atc ctg ttg gac acc cag tgc cag ggg ctg cct cgc
H G E D D G E E I L L D T Q C Q G L P R
▼ TSP-1:7
3001/1001
3031/1011
ccg gaa ccc cag gag gcc tgc agc ctg gag ccc tgc cca cct agg tgg aaa gtc atg tcc
P E P Q E A C S L E P C P P R W K V M S
3061/1021
3091/1031
ctt ggc cca tgt tcg gcc agc tgt ggc ctt ggc act gct aga cgc tcg gtg gcc tgt gtg
L G P C S A S C G L G T A R R S V A C V
3121/1041
3151/1051
cag ctc gac caa ggc cag gac gtg gag gtg gac gag gcg gcc tgt gcg gcg ctg gtg cggExon24
Q L D Q G Q D V E V D E A A C A A L V R
▼ TSP-1:8
3181/1061
3211/1071
ccc gag gcc agt gtc ccc tgt ctc att gcc gac tgc acc tac cgc tgg cat gtt ggc acc
P E A S V P C L I A D C T Y R W H V G T
3241/1081
3271/1091
tgg atg gag tgc tct gtt tcc tgt ggg gat ggc atc cag cgc cgg cgt gac acc tgc ctc
W M E C S V S C G D G I Q R R R D T C L
3301/1101
3331/1111
gga ccc cag gcc cag gcg cct gtg cca gct gat ttc tgc cag cac ttg ccc aag ccg gtgExon25
G P Q A Q A P V P A D F C Q H L P K P V

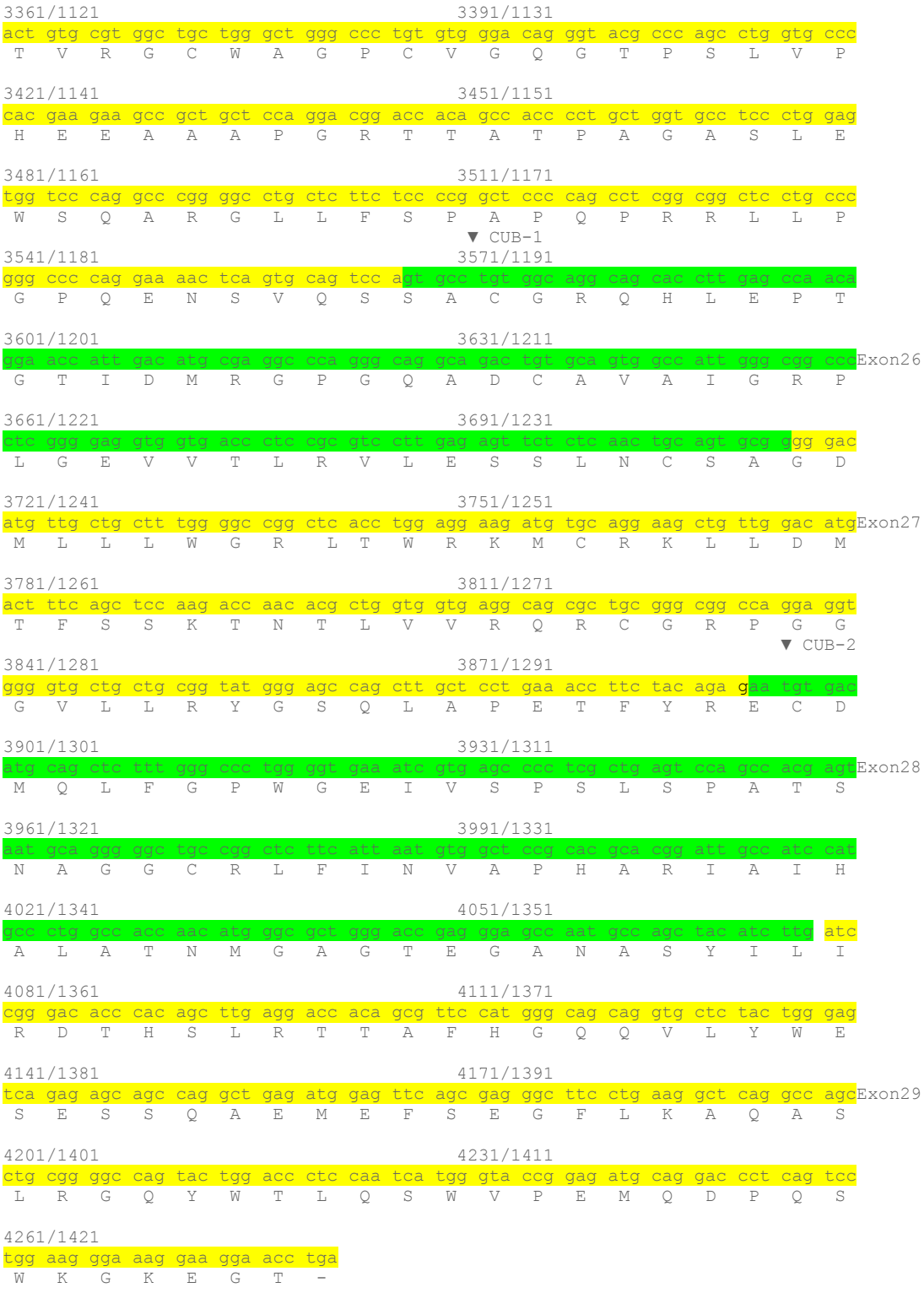


**Figure S 1 ADAMTS13 DNA vector sequence. Exons and domains are highlighted. Domains highlighted based on annotation by (Zheng *et al*, 2001)**

a.

```
Taeniopygia 1   -------MRVGWALRALAVLPLGLCWLPQKFLGALDGEDVLSYFGTSSVPDVP------- 46
Gallus      1   ------------------------------------------------------------
Bos         1   --------------------------------MPAASLRKDSWAQPGWESALS------- 21
Ovis        1   -----MKKVMFGLKLDCEDQRKRLRVNPASWSSPAALPARHSRSTPGFRQMIAGSMAPST 55
Gorilla     1   --------------------------------MHQRHP--RARCPPLCVAGFL------- 19
Pan         1   --------------------------------MHQRHP--RARCPPLCVAGIL------- 19
ADAMTS13    1   --------------------------------MHQRHP--RARCPPLCVAGIL------- 19
Nomascus    1   --------------------------------MRQHHPRARARCPPLCVAGIL------- 21
Pango       1   --------------------------------MYQRHP--RARCPPLCVAGIL------- 19
Papio       1   --------------------------------MRQRHP--QARCPSLCVAGIL------- 19
Callithrix  1   --------------------------------MRQRHP--WARCPPFCVAGIL------- 19
Saimin      1   --------------------------------MCQRHL--RARCPSLCVAGIL------- 19
Otolemur    1   --------------------------------MHTDWG---------------------- 6
Mus         1   ------------------------------MSQLCLWLTCQPCYAVSVRGILT------- 23
Cricetulus  1   ------------------------------MSELCLWVTCQPFHAASIRGVLT------- 23
Cava        1   ----------------------------------MSPWARGTLLQAASAGGILT------- 20
Canus       1   --------------------------------MREPRP-----WGRCVGAILT------- 16
Felis       1   --------------------------------MREPRP-----WGRCVGATLT------- 16
Ailuropoda  1   --------------------------------MRK----------HCNNAVL--------- 10
Equus       1   --------------------------------MSELQL-----WGRCVQGILT------- 16
Sarcophilus 1   MSFHSFILAHLRKGRRQPSRQNHSSSLSSPFTPPPPHLPLVAPRSSSARRDRTKADNQSE 60
Danio       1   -------------------------------------------MRLYIRPVLEQ------ 11
```

b.

```
ADAMTS1     1   ---------------SGSETPLPETDLAHCFYSGTVN--GDPSSAAALSLCEG-VRGAFY 150
ADAMTS4     1   -----------------QAPELLGGAEPGTYLTGTIN--GDPESVASLHWDGGALLGVLQ 154
ADAMTS15    1   ---------------PLQGLTGGSSDLRRCFYSGDVN--AEPDSFAAVSLCGG-LRGAFG 128
ADAMTS8     1   ---------------GSGRATGGERGLRGCFFSGTVN--GEPESLAAVSLCRG-LSGSFL 127
ADAMTS5     1   -------------------TSAPWRHRSHCFYRGTVD--ASPRSLAVFDLCGG-LDGFFA 157
ADAMTS9     1   -------------NQTKFYSEE-EAELKHCFYKGYVN--TNSEHTAVISLCSG-MLGTFR 177
ADAMTS20    1   -------------ERGAWESDAGPSDLRHCFYRGQVN--SQEDYKAVVSLCGG-LVGTFK 156
ADAMTS3     1   PGNITDPINNHQPGSATYRIRRTEPLQTNCAYVGDIV--DIPGTS-VAISNCDGLAGMIK 173
ADAMTS14    1   -----------------FRELFRQPLRQECVYTGGVT--GMPGAA-VAISNCDGLAGLIR 179
ADAMTS2     1   -----------------KGTTRVEPLLGSCLYVGDVA--GLAEASSVALSNCDGLAGLIR 183
ADAMTS6     1   -------------------GPQWKHDFLDNCHYTGYLQ-DQRSTT-KVALSNCVGLHGVIA 159
ADAMTS10    1   -------------------GLAWQRAARPHCLYAGHLQ-GQASTS-HVAISTCGGLHGLIV 150
ADAMTS7     1   -----------------LGRAHIRAHTPACHLLGEVQ-DPELEGGLAAISACDGLKGVFQ 157
ADAMTS12    1   -----------------SHVKMMASSAPLCHLSGTVL-QQGTRVGTAALSACHGLTGFFQ 168
ADAMTS16    1   -----------------TKSVQTLPPEDFCFYQGSLR-SHRNSS--VALSTCQGLSGMIR 172
ADAMTS18    1   -----------------ASETQ-KPEVQQCFYQGFIR-NDSSSS--VAVSTCAGLSGLIR 170
ADAMTS17    1   ---------------AGAARRRGRPAELCFYSGRVLGHPGSLVSLSACGAAGGLVGLIQ 155
ADAMTS19    1   G-----------PTGAASAPQPPAPPDAGCFYTGAVLRHPGSLASFSTCG--GGLMGFIQ 248
ADAMTS13    1   --------------------MHQRHPRARCPPLCVAG-----------ILACGFLLGCWG 29
```

**Figure S 2 Alignment of human ADAMTS13 with ADAMTS13 orthologs and paralogs, showing conservation of the p.R7W polymorphism**

Figure a shows conservation in orthologs and b shows conservation in paralogs. Polymorphism is shown in yellow.

| |
|---|
| Abcam, Cambridge, UK |
| Agilent technologies, Wokingham, UK |
| Anachem Ltd, Luton, UK |
| Appelton Woods, Birmingham, UK |
| BD Biosciences, Oxford, UK |
| Beckman Coulter, High Wycombe, UK |
| Bethyl laboratories Inc, Montogomery, USA |
| Bio-rad Laboratories Ltd, Hemel Hempstead, UK |
| BMG Labtech, Aylesbury, UK |
| Dako UK Ltd, Ely, UK |
| GE Healthcare, Little Chalfont, UK |
| Greiner Bio-One Ltd, Stonehouse, UK |
| Katholieke Universiteit Leuven, Laboratory for thrombosis research, Kortruk, Leuven |
| LGC standards, Teddington, UK |
| Life technologies, Paisley, UK |
| Merck chemicals, Nottingham, UK |
| Millipore UK Ltd, Livingston, UK |
| MP Biomedicals, Cambridge, UK |
| New England Biolabs, Hitchin, UK |
| Perkin Elmer, Massachusetts, USA |
| Polysciences Europe, Eppelheim, Germany |
| PreAnalytix, Hombrechtikon, Switzerland |
| Promega, Southampton, UK |
| Qiagen, Sussex, UK |
| Santa Cruz Biotechnology Inc, Heidelberg, Germany |
| Sekisui Diagnostics, Stamford, USA |
| Sigma, Dorset, UK |
| Takara Bio Europe/Clontech, Saint-Germain-en-Laye, France |
| ThermoFischer Scientific, Basingstoke, UK |
| Vector Laboratories Ltd, Peterborough, UK |
| VWR, Lutterworth, UK |
| Roche, Burgess Hill, UK |

**Table S 8 Supplier information**

# Publications and presentations arising from work performed for this thesis

## Publications

Congenital thrombotic thrombocytopenic purpura with novel mutations in three unrelated Turkish children. A. Metin, S. Unal, F. Gumruk, R. Palla, A. Cairo, M. Underwood & A. Gurgey (2013). *Pediatric Blood & Cancer*.

## Oral presentations

*In vitro* characterisation of the p.R102H mutation identified in a patient with congenital thrombotic thrombocytopenic purpura (TTP) and detectable ADAMTS13 antigen in their plasma. M. Underwood, I. Garagiola, I. Mackie, S. Machin, R. De Cristofaro, S. Lancellotti & F. Peyvandi. *Presented at British Society for Haemostasis and Thrombosis/Belgian Society on Thrombosis and Haemostasis joint meeting October 10$^{th}$-11$^{th}$ 2013, Nottingham.*

The effect of ADAMTS13 mutations on its secretion, activity and subcellular location. M. Underwood, I. Garagiola, I. Mackie, S. Machin & F. Peyvandi. *Presented at British Society for Haemostasis and Thrombosis/UK Platelet Group Joint Meeting October 18$^{th}$-19$^{th}$ 2012, Bath.*

## Poster presentations

*In vitro* characterisation of two ADAMTS13 mutants (p.I143T, p.Y570C) identified in two patients with congenital thrombotic thrombocytopenic purpura (TTP). M. Underwood, I. Garagiola, I. Mackie, S. Machin, A. Metin, A. Gurgey, F. Peyvandi. *Presented at ISTH XXIV congress June 29$^{th}$-July 4$^{th}$ 2013, Amsterdam.*

References


Adler,J., Pagakis,S.N., & Parmryd,I. (2008) Replicate-based noise corrected correlation for accurate measurements of colocalization. *J.Microsc.*, **230**, 121-133.

Ahmad,A., Aggarwal,A., Sharma,D., Dave,H.P., Kinsella,V., Rick,M.E., & Schechter,G.P. (2004) Rituximab for treatment of refractory/relapsing thrombotic thrombocytopenic purpura (TTP). *Am J Hematol.*, **77**, 171-176.

Ai,J., Smith,P., Wang,S., Zhang,P., & Zheng,X.L. (2005) The proximal carboxyl-terminal domains of ADAMTS13 determine substrate specificity and are all required for cleavage of von Willebrand factor. *J.Biol.Chem.*, **280**, 29428-29434.

Akiyama,M., Takeda,S., Kokame,K., Takagi,J., & Miyata,T. (2009) Crystal structures of the noncatalytic domains of ADAMTS13 reveal multiple discontinuous exosites for von Willebrand factor. *Proc.Natl.Acad.Sci.U.S.A*, **106**, 19274-19279.

Alberts,B., Johnson,A., Lewis,J., Raff,M., Roberts,K., & Walter,D. (2002) *Molecular Biology of the Cell,* 4th edn, Garland Science, New York.

Alsultan,A., Jarrar,M., Al-Harbi,T., & Balwi,A.L. (2013) Novel frameshift mutations in ADAMTS13 in two families with hereditary thrombotic thrombocytopenic purpura. *Pediatr.Blood Cancer*, **60**, 1559-1560.

Anderson,P.J., Kokame,K., & Sadler,J.E. (2006) Zinc and calcium ions cooperatively modulate ADAMTS13 activity. *J.Biol.Chem.*, **281**, 850-857.

Andersson,H.M., Siegerink,B., Luken,B.M., Crawley,J.T., Algra,A., Lane,D.A., & Rosendaal,F.R. (2012) High VWF, low ADAMTS13, and oral contraceptives increase the risk of ischemic stroke and myocardial infarction in young women. *Blood*, **119**, 1555-1560.

Andreini,C., Banci,L., Bertini,I., Elmi,S., & Rosato,A. (2005) Comparative analysis of the ADAM and ADAMTS families. *J.Proteome.Res.*, **4**, 881-888.

Antoine,G., Zimmermann,K., Plaimauer,B., Grillowitzer,M., Studt,J.D., Lammle,B., & Scheiflinger,F. (2003) ADAMTS13 gene defects in two brothers with constitutional thrombotic thrombocytopenic purpura and normalization of von Willebrand factor-cleaving protease activity by recombinant human ADAMTS13. *Br.J.Haematol.*, **120**, 821-824.

Apte,S.S. (2004) A disintegrin-like and metalloprotease (reprolysin type) with thrombospondin type 1 motifs: the ADAMTS family. *Int.J Biochem.Cell Biol.*, **36**, 981-985.

Arakawa,T. & Timasheff,S.N. (1983) Preferential interactions of proteins with solvent components in aqueous amino acid solutions. *Arch.Biochem.Biophys.*, **224**, 169-177.

Arakawa,T. & Timasheff,S.N. (1985) The stabilization of proteins by osmolytes. *Biophys.J*, **47**, 411-414.

Arora,A., Ha,C., & Park,C.B. (2004) Inhibition of insulin amyloid formation by small stress molecules. *FEBS Lett.*, **564**, 121-125.

Asada,Y., Sumiyoshi,A., Hayashi,T., Suzumiya,J., & Kaketani,K. (1985) Immunohistochemistry of vascular lesion in thrombotic thrombocytopenic purpura, with special reference to factor VIII related antigen. *Thromb.Res.*, **38**, 469-479.

Assink,K., Schiphorst,R., Allford,S., Karpman,D., Etzioni,A., Brichard,B., van de Kar,N., Monnens,L., & van den Heuvel,L. (2003) Mutation analysis and clinical implications of von Willebrand factor-cleaving protease deficiency. *Kidney Int.*, **63**, 1995-1999.

Azuma,H., Sugimoto,M., Ruggeri,Z.M., & Ware,J. (1993) A role for von Willebrand factor proline residues 702-704 in ristocetin-mediated binding to platelet glycoprotein Ib. *Thromb.Haemost.*, **69**, 192-196.

Bai,C., Biwersi,J., Verkman,A.S., & Matthay,M.A. (1998) A mouse model to test the in vivo efficacy of chemical chaperones. *J Pharmacol.Toxicol.Methods*, **40**, 39-45.

Banno,F., Chauhan,A.K., Kokame,K., Yang,J., Miyata,S., Wagner,D.D., & Miyata,T. (2009) The distal carboxyl-terminal domains of ADAMTS13 are required for regulation of in vivo thrombus formation. *Blood*, **113**, 5323-5329.

Banno,F., Kaminaka,K., Soejima,K., Kokame,K., & Miyata,T. (2004) Identification of strain-specific variants of mouse Adamts13 gene encoding von Willebrand factor-cleaving protease. *J Biol.Chem.*, **279**, 30896-30903.

Banno,F., Kokame,K., Okuda,T., Honda,S., Miyata,S., Kato,H., Tomiyama,Y., & Miyata,T. (2006) Complete deficiency in ADAMTS13 is prothrombotic, but it alone is not sufficient to cause thrombotic thrombocytopenic purpura. *Blood*, **107**, 3161-3166.

Bao,J., Xiao,J., Mao,Y., & Zheng,X.L. (2014) Carboxyl terminus of ADAMTS13 directly inhibits platelet aggregation and ultra large von Willebrand factor string formation under flow in a free-thiol-dependent manner. *Arterioscler.Thromb.Vasc.Biol.*, **34**, 397-407.

Barg,A., Ossig,R., Goerge,T., Schneider,M.F., Schillers,H., Oberleithner,H., & Schneider,S.W. (2007) Soluble plasma-derived von Willebrand factor assembles to a haemostatically active filamentous network. *Thromb.Haemost.*, **97**, 514-526.

Barlow,A.L., Macleod,A., Noppen,S., Sanderson,J., & Guerin,C.J. (2010) Colocalization analysis in fluorescence micrographs: verification of a more accurate calculation of pearson's correlation coefficient. *Microsc.Microanal.*, **16**, 710-724.

Bebok,Z., Venglarik,C.J., Panczel,Z., Jilling,T., Kirk,K.L., & Sorscher,E.J. (1998) Activation of DeltaF508 CFTR in an epithelial monolayer. *Am.J Physiol*, **275**, C599-C607.

Benito,J.M., Garcia Fernandez,J.M., & Ortiz,M.C. (2011) Pharmacological chaperone therapy for Gaucher disease: a patent review. *Expert.Opin.Ther.Pat*, **21**, 885-903.

Benjamin,E.R., Khanna,R., Schilling,A., Flanagan,J.J., Pellegrino,L.J., Brignol,N., Lun,Y., Guillen,D., Ranes,B.E., Frascella,M., Soska,R., Feng,J., Dungan,L., Young,B.,

Lockhart,D.J., & Valenzano,K.J. (2012) Co-administration with the pharmacological chaperone AT1001 increases recombinant human alpha-galactosidase A tissue uptake and improves substrate reduction in Fabry mice. *Mol.Ther.*, **20**, 717-726.

Bennett,E.J., Bence,N.F., Jayakumar,R., & Kopito,R.R. (2005) Global impairment of the ubiquitin-proteasome system by nuclear or cytoplasmic protein aggregates precedes inclusion body formation. *Mol.Cell*, **17**, 351-365.

Berardi,A.S., Pannuzzo,G., Graziano,A., Costantino-Ceccarini,E., Piomboni,P., & Luddi,A. (2014) Pharmacological chaperones increase residual beta-galactocerebrosidase activity in fibroblasts from Krabbe patients. *Mol.Genet.Metab.*, Prepublished online May 23 2014; doi:10.1016/j.ymgme2014.05.009.

Berendse,K., Ebberink,M.S., Ijlst,L., Poll-The BT, Wanders,R.J., & Waterham,H.R. (2013) Arginine improves peroxisome functioning in cells from patients with a mild peroxisome biogenesis disorder. *Orphanet.J Rare.Dis.*, **8**, 138.

Berg,J.M., Tymoczko,J.L., & Stryer,L. (2002) *Biochemistry,* 5th edn, W H Freeman, New York.

Bernardo,A., Ball,C., Nolasco,L., Moake,J.F., & Dong,J.F. (2004) Effects of inflammatory cytokines on the release and cleavage of the endothelial cell-derived ultralarge von Willebrand factor multimers under flow. *Blood*, **104**, 100-106.

Berndt,M.C., Ward,C.M., Booth,W.J., Castaldi,P.A., Mazurov,A.V., & Andrews,R.K. (1992) Identification of aspartic acid 514 through glutamic acid 542 as a glycoprotein Ib-IX complex receptor recognition sequence in von Willebrand factor. Mechanism of modulation of von Willebrand factor by ristocetin and botrocetin. *Biochemistry*, **31**, 11144-11151.

Bernier,V., Morello,J.P., Zarruk,A., Debrand,N., Salahpour,A., Lonergan,M., Arthus,M.F., Laperriere,A., Brouard,R., Bouvier,M., & Bichet,D.G. (2006) Pharmacologic chaperones as a potential treatment for X-linked nephrogenic diabetes insipidus. *J Am.Soc.Nephrol.*, **17**, 232-243.

Bestetti,G., Stellari,A., Lattuada,A., Corbellino,M., Parravicini,C., Calzarossa,C., Cenzuales,S., Moroni,M., Galli,M., & Rossi,E. (2003) ADAMTS 13 genotype and vWF protease activity in an Italian family with TTP. *Thromb.Haemost.*, **90**, 955-956.

Bettoni,G., Palla,R., Valsecchi,C., Consonni,D., Lotta,L.A., Trisolini,S.M., Mancini,I., Musallam,K.M., Rosendaal,F.R., & Peyvandi,F. (2012) ADAMTS-13 activity and autoantibodies classes and subclasses as prognostic predictors in acquired thrombotic thrombocytopenic purpura. *Journal of Thrombosis and Haemostasis*, **10**, 1556-1565.

Bohm,M., Betz,C., Miesbach,W., Krause,M., von Auer,C., Geiger,H., & Scharrer,I. (2005) The course of ADAMTS-13 activity and inhibitor titre in the treatment of thrombotic thrombocytopenic purpura with plasma exchange and vincristine. *Br.J Haematol.*, **129**, 644-652.

Bolte,S. & Cordelieres,F.P. (2006) A guided tour into subcellular colocalization analysis in light microscopy. *J.Microsc.*, **224**, 213-232.

Bonapace,G., Waheed,A., Shah,G.N., & Sly,W.S. (2004) Chemical chaperones protect from effects of apoptosis-inducing mutation in carbonic anhydrase IV identified in retinitis pigmentosa 17. *Proc.Natl.Acad.Sci.U.S.A*, **101**, 12300-12305.

Bongers,T.N., de Bruijne,E.L., Dippel,D.W., de Jong,A.J., Deckers,J.W., Poldermans,D., de Maat,M.P., & Leebeek,F.W. (2009) Lower levels of ADAMTS13 are associated with cardiovascular disease in young patients. *Atherosclerosis*, **207**, 250-254.

Bonnefoy,A., Daenens,K., Feys,H.B., De Vos,R., Vandervoort,P., Vermylen,J., Lawler,J., & Hoylaerts,M.F. (2006a) Thrombospondin-1 controls vascular platelet recruitment and thrombus adherence in mice by protecting (sub)endothelial VWF from cleavage by ADAMTS13. *Blood*, **107**, 955-964.

Bonnefoy,A., Romijn,R.A., Vandervoort,P.A., Van Rompaey,I., Vermylen,J., & Hoylaerts,M.F. (2006b) von Willebrand factor A1 domain can adequately substitute for A3 domain in recruitment of flowing platelets to collagen. *Journal of Thrombosis and Haemostasis*, **4**, 2151-2161.

Borden,L.A., Smith,K.E., Gustafson,E.L., Branchek,T.A., & Weinshank,R.L. (1995) Cloning and expression of a betaine/GABA transporter from human brain. *J Neurochem.*, **64**, 977-984.

Borgi,A., Khemiri,M., Veyradier,A., Kazdaghli,K., & Barsaoui,S. (2013) Congenital Thrombotic Thrombocytopenic Purpura: Atypical Presentation and New ADAMTS 13 Mutation in a Tunisian Child. *Mediterr.J.Hematol.Infect.Dis.*, **5**, e2013041.

Bork,P. & Beckmann,G. (1993) The CUB domain. A widespread module in developmentally regulated proteins. *J Mol.Biol.*, **231**, 539-545.

Bouley,R., Lu,H.A., Nunes,P., Da Silva,N., McLaughlin,M., Chen,Y., & Brown,D. (2011) Calcitonin has a vasopressin-like effect on aquaporin-2 trafficking and urinary concentration. *J Am.Soc.Nephrol.*, **22**, 59-72.

Bouley,R., Pastor-Soler,N., Cohen,O., McLaughlin,M., Breton,S., & Brown,D. (2005) Stimulation of AQP2 membrane insertion in renal epithelial cells in vitro and in vivo by the cGMP phosphodiesterase inhibitor sildenafil citrate (Viagra). *Am.J Physiol.Renal Physiol.*, **288**, F1103-F1112.

Bowen,D.J. & Collins,P.W. (2004) An amino acid polymorphism in von Willebrand factor correlates with increased susceptibility to proteolysis by ADAMTS13. *Blood*, **103**, 941-947.

Bowman,E.J., Siebers,A., & Altendorf,K. (1988) Bafilomycins: a class of inhibitors of membrane ATPases from microorganisms, animal cells, and plant cells. *Proc.Natl.Acad.Sci.U.S.A*, **85**, 7972-7976.

Brown,C.R., Hong-Brown,L.Q., Biwersi,J., Verkman,A.S., & Welch,W.J. (1996) Chemical chaperones correct the mutant phenotype of the delta F508 cystic fibrosis transmembrane conductance regulator protein. *Cell Stress.Chaperones.*, **1**, 117-125.

Burrows,J.A., Willis,L.K., & Perlmutter,D.H. (2000) Chemical chaperones mediate increased secretion of mutant alpha 1-antitrypsin (alpha 1-AT) Z: A potential pharmacological

strategy for prevention of liver injury and emphysema in alpha 1-AT deficiency. *Proc.Natl.Acad.Sci.U.S.A*, **97**, 1796-1801.

Buzza,M.S., Dyson,J.M., Choi,H., Gardiner,E.E., Andrews,R.K., Kaiserman,D., Mitchell,C.A., Berndt,M.C., Dong,J.F., & Bird,P.I. (2008) Antihemostatic activity of human granzyme B mediated by cleavage of von Willebrand factor. *J.Biol.Chem.*, **283**, 22498-22504.

Calderazzo,J.C., Kempfer,A., Powazniak,Y., Lopez,I.R., Sanchez-Luceros,A., Woods,A.I., & Lazzari,M.A. (2012) A new ADAMTS13 missense mutation (D1362V) in thrombotic thrombocytopenic purpura diagnosed during pregnancy. *Thromb.Haemost.*, **108**, 401-403.

Callewaert,F., Roodt,J., Ulrichts,H., Stohr,T., van Rensburg,W.J., Lamprecht,S., Rossenu,S., Priem,S., Willems,W., & Holz,J.B. (2012) Evaluation of efficacy and safety of the anti-VWF Nanobody ALX-0681 in a preclinical baboon model of acquired thrombotic thrombocytopenic purpura. *Blood*, **120**, 3603-3610.

Camilleri,R.S., Cohen,H., Mackie,I.J., Scully,M., Starke,R.D., Crawley,J.T., Lane,D.A., & Machin,S.J. (2008) Prevalence of the ADAMTS-13 missense mutation R1060W in late onset adult thrombotic thrombocytopenic purpura. *J.Thromb.Haemost.*, **6**, 331-338.

Camilleri,R.S., Scully,M., Thomas,M., Mackie,I.J., Liesner,R., Chen,W.J., Manns,K., & Machin,S.J. (2012) A phenotype-genotype correlation of ADAMTS13 mutations in congenital thrombotic thrombocytopenic purpura patients treated in the United Kingdom. *J.Thromb.Haemost.*, **10**, 1792-1801.

Canaff,L., Vanbellinghen,J.F., Kanazawa,I., Kwak,H., Garfield,N., Vautour,L., & Hendy,G.N. (2012) Menin missense mutants encoded by the MEN1 gene that are targeted to the proteasome: restoration of expression and activity by CHIP siRNA. *J Clin.Endocrinol.Metab*, **97**, E282-E291.

Canis,K., McKinnon,T.A., Nowak,A., Panico,M., Morris,H.R., Laffan,M., & Dell,A. (2010) The plasma von Willebrand factor O-glycome comprises a surprising variety of structures including ABH antigens and disialosyl motifs. *Journal of Thrombosis and Haemostasis*, **8**, 137-145.

Cao,W., Krishnaswamy,S., Camire,R.M., Lenting,P.J., & Zheng,X.L. (2008a) Factor VIII accelerates proteolytic cleavage of von Willebrand factor by ADAMTS13. *Proc.Natl.Acad.Sci.U.S.A*, **105**, 7416-7421.

Cao,W., Sabatino,D.E., Altynova,E., Lange,A.M., Casina,V.C., Camire,R.M., & Zheng,X.L. (2012) Light chain of factor VIII is sufficient for accelerating cleavage of von Willebrand factor by ADAMTS13 metalloprotease. *J.Biol.Chem.*, **287**, 32459-32466.

Cao,W.J., Niiya,M., Zheng,X.W., Shang,D.Z., & Zheng,X.L. (2008b) Inflammatory cytokines inhibit ADAMTS13 synthesis in hepatic stellate cells and endothelial cells. *Journal of Thrombosis and Haemostasis*, **6**, 1233-1235.

Cataland,S.R., Peyvandi,F., Mannucci,P.M., Lammle,B., Kremer Hovinga,J.A., Machin,S.J., Scully,M., Rock,G., Gilbert,J.C., Yang,S., Wu,H., Jilma,B., & Knoebl,P. (2012) Initial experience from a double-blind, placebo-controlled, clinical outcome study of

ARC1779 in patients with thrombotic thrombocytopenic purpura. *Am.J Hematol.*, **87**, 430-432.

Chauhan,A.K., Goerge,T., Schneider,S.W., & Wagner,D.D. (2007) Formation of platelet strings and microthrombi in the presence of ADAMTS-13 inhibitor does not require P-selectin or beta3 integrin. *J.Thromb.Haemost.*, **5**, 583-589.

Chauhan,A.K., Motto,D.G., Lamb,C.B., Bergmeier,W., Dockal,M., Plaimauer,B., Scheiflinger,F., Ginsburg,D., & Wagner,D.D. (2006) Systemic antithrombotic effects of ADAMTS13. *J.Exp.Med.*, **203**, 767-776.

Chauhan,A.K., Walsh,M.T., Zhu,G., Ginsburg,D., Wagner,D.D., & Motto,D.G. (2008) The combined roles of ADAMTS13 and VWF in murine models of TTP, endotoxemia, and thrombosis. *Blood*, **111**, 3452-3457.

Chen,J., Chung,D.W., Le,J., Ling,M., Konkle,B.A., & Lopez,J.A. (2013) Normal cleavage of von Willebrand factor by ADAMTS-13 in the absence of factor VIII in patients with severe hemophilia A. *J.Thromb.Haemost.*, **11**, 1769-1772.

Chen,J., Fu,X., Wang,Y., Ling,M., McMullen,B., Kulman,J., Chung,D.W., & Lopez,J.A. (2010) Oxidative modification of von Willebrand factor by neutrophil oxidants inhibits its cleavage by ADAMTS13. *Blood*, **115**, 706-712.

Chen,J., Ling,M., Fu,X., Lopez,J.A., & Chung,D.W. (2012) Simultaneous exposure of sites in von Willebrand factor for glycoprotein Ib binding and ADAMTS13 cleavage: studies with ristocetin. *Arterioscler.Thromb.Vasc.Biol.*, **32**, 2625-2630.

Chen,J., Reheman,A., Gushiken,F.C., Nolasco,L., Fu,X., Moake,J.L., Ni,H., & Lopez,J.A. (2011) N-acetylcysteine reduces the size and activity of von Willebrand factor in human plasma and mice. *J Clin.Invest*, **121**, 593-603.

Chen,W., Lou,J., & Zhu,C. (2009) Molecular Dynamics Simulated Unfolding of von Willebrand Factor A Domains by Force. *Cel.Mol.Bioeng.*, **2**, 75-86.

Christophe,O., Obert,B., Meyer,D., & Girma,J.P. (1991) The binding domain of von Willebrand factor to sulfatides is distinct from those interacting with glycoprotein Ib, heparin, and collagen and resides between amino acid residues Leu 512 and Lys 673. *Blood*, **78**, 2310-2317.

Clancy,J.P., Rowe,S.M., Accurso,F.J., Aitken,M.L., Amin,R.S., Ashlock,M.A., Ballmann,M., Boyle,M.P., Bronsveld,I., Campbell,P.W., De Boeck,K., Donaldson,S.H., Dorkin,H.L., Dunitz,J.M., Durie,P.R., Jain,M., Leonard,A., McCoy,K.S., Moss,R.B., Pilewski,J.M., Rosenbluth,D.B., Rubenstein,R.C., Schechter,M.S., Botfield,M., Ordonez,C.L., Spencer-Green,G.T., Vernillet,L., Wisseh,S., Yen,K., & Konstan,M.W. (2012) Results of a phase IIa study of VX-809, an investigational CFTR corrector compound, in subjects with cystic fibrosis homozygous for the F508del-CFTR mutation. *Thorax*, **67**, 12-18.

Claus,R.A., Bockmeyer,C.L., Kentouche,K., Sieber,M.W., Oberle,V., Kaufmann,R., Deigner,H.P., & Losche,W. (2005) Transcriptional regulation of ADAMTS13. *Thromb Haemost*, **94**, 41-45.

Costes,S.V., Daelemans,D., Cho,E.H., Dobbin,Z., Pavlakis,G., & Lockett,S. (2004) Automatic and quantitative measurement of protein-protein colocalization in live cells. *Biophys.J.*, **86**, 3993-4003.

Cramer,E.M., Meyer,D., le Menn,R., & Breton-Gorius,J. (1985) Eccentric localization of von Willebrand factor in an internal structure of platelet alpha-granule resembling that of Weibel-Palade bodies. *Blood*, **66**, 710-713.

Crawley,J.T., de Groot,R., Xiang,Y., Luken,B.M., & Lane,D.A. (2011) Unraveling the scissile bond: how ADAMTS13 recognizes and cleaves von Willebrand factor. *Blood*, **118**, 3212-3221.

Crawley,J.T., Lam,J.K., Rance,J.B., Mollica,L.R., O'Donnell,J.S., & Lane,D.A. (2005) Proteolytic inactivation of ADAMTS13 by thrombin and plasmin. *Blood*, **105**, 1085-1093.

Crawley,J.T., Lane,D.A., Woodward,M., Rumley,A., & Lowe,G.D. (2008) Evidence that high von Willebrand factor and low ADAMTS-13 levels independently increase the risk of a non-fatal heart attack. *J.Thromb.Haemost.*, **6**, 583-588.

Cruz,M.A., Yuan,H., Lee,J.R., Wise,R.J., & Handin,R.I. (1995) Interaction of the von Willebrand factor (vWF) with collagen. Localization of the primary collagen-binding site by analysis of recombinant vWF a domain polypeptides. *J Biol.Chem.*, **270**, 10822-10827.

Davies,J.E., Sarkar,S., & Rubinsztein,D.C. (2006) Trehalose reduces aggregate formation and delays pathology in a transgenic mouse model of oculopharyngeal muscular dystrophy. *Hum.Mol.Genet.*, **15**, 23-31.

Davis,A.K., Makar,R.S., Stowell,C.P., Kuter,D.J., & Dzik,W.H. (2009) ADAMTS13 binds to CD36: a potential mechanism for platelet and endothelial localization of ADAMTS13. *Transfusion*, **49**, 206-213.

De Cristofaro,R., Peyvandi,F., Baronciani,L., Palla,R., Lavoretano,S., Lombardi,R., Di Stasio,E., Federici,A.B., & Mannucci,P.M. (2006) Molecular mapping of the chloride-binding site in von Willebrand factor (VWF): energetics and conformational effects on the VWF/ADAMTS-13 interaction. *J.Biol.Chem.*, **281**, 30400-30411.

De Cristofaro,R., Peyvandi,F., Palla,R., Lavoretano,S., Lombardi,R., Merati,G., Romitelli,F., Di Stasio,E., & Mannucci,P.M. (2005) Role of chloride ions in modulation of the interaction between von Willebrand factor and ADAMTS-13. *J.Biol.Chem.*, **280**, 23295-23302.

de Groot,R., Bardhan,A., Ramroop,N., Lane,D.A., & Crawley,J.T. (2009) Essential role of the disintegrin-like domain in ADAMTS13 function. *Blood*, **113**, 5609-5616.

de Groot,R., Lane,D.A., & Crawley,J.T. (2010) The ADAMTS13 metalloprotease domain: roles of subsites in enzyme activity and specificity. *Blood*, **116**, 3064-3072.

De Maeyer,B., De Meyer,S.F., Feys,H.B., Pareyn,I., Vandeputte,N., Deckmyn,H., & Vanhoorelbeke,K. (2010) The distal carboxyterminal domains of murine ADAMTS13 influence proteolysis of platelet-decorated VWF strings in vivo. *Journal of Thrombosis and Haemostasis*, **8**, 2305-2312.

De Meyer,S.F., Savchenko,A.S., Haas,M.S., Schatzberg,D., Carroll,M.C., Schiviz,A., Dietrich,B., Rottensteiner,H., Scheiflinger,F., & Wagner,D.D. (2012) Protective anti-inflammatory effect of ADAMTS13 on myocardial ischemia/reperfusion injury in mice. *Blood*, **120**, 5217-5223.

Deal,T., Kremer Hovinga,J.A., Marques,M.B., & Adamski,J. (2012) Novel ADAMTS13 mutations in an obstetric patient with upshaw-schulman syndrome. *J.Clin.Apher.*, **28**, 311-316.

Di Stasio,E., Lancellotti,S., Peyvandi,F., Palla,R., Mannucci,P.M., & De Cristofaro,R. (2008) Mechanistic studies on ADAMTS13 catalysis. *Biophys.J*, **95**, 2450-2461.

Ding,W.X., Ni,H.M., Gao,W., Yoshimori,T., Stolz,D.B., Ron,D., & Yin,X.M. (2007) Linking of autophagy to ubiquitin-proteasome system is important for the regulation of endoplasmic reticulum stress and cell viability. *Am.J Pathol.*, **171**, 513-524.

Ding,W.X. & Yin,X.M. (2008) Sorting, recognition and activation of the misfolded protein degradation pathways through macroautophagy and the proteasome. *Autophagy.*, **4**, 141-150.

Doi,M., Matsui,H., Takeda,H., Saito,Y., Takeda,M., Matsunari,Y., Nishio,K., Shima,M., Banno,F., Akiyama,M., Kokame,K., Miyata,T., & Sugimoto,M. (2012) ADAMTS13 safeguards the myocardium in a mouse model of acute myocardial infarction. *Thromb.Haemost.*, **108**, 1236-1238.

Donadelli,R., Banterla,F., Galbusera,M., Capoferri,C., Bucchioni,S., Gastoldi,S., Nosari,S., Monteferrante,G., Ruggeri,Z.M., Bresin,E., Scheiflinger,F., Rossi,E., Martinez,C., Coppo,R., Remuzzi,G., & Noris,M. (2006) In-vitro and in-vivo consequences of mutations in the von Willebrand factor cleaving protease ADAMTS13 in thrombotic thrombocytopenic purpura. *Thromb.Haemost.*, **96**, 454-464.

Dong,J.F., Cruz,M.A., Aboulfatova,K., Martin,C., Choi,H., Bergeron,A.L., Martini,S.R., Kroll,M.H., & Kent,T.A. (2008) Magnesium maintains endothelial integrity, up-regulates proteolysis of ultra-large von Willebrand factor, and reduces platelet aggregation under flow conditions. *Thromb.Haemost.*, **99**, 586-593.

Dong,J.F., Moake,J.L., Nolasco,L., Bernardo,A., Arceneaux,W., Shrimpton,C.N., Schade,A.J., McIntire,L.V., Fujikawa,K., & Lopez,J.A. (2002) ADAMTS-13 rapidly cleaves newly secreted ultralarge von Willebrand factor multimers on the endothelial surface under flowing conditions. *Blood*, **100**, 4033-4039.

Edwards,N.C., Hing,Z.A., Perry,A., Blaisdell,A., Kopelman,D.B., Fathke,R., Plum,W., Newell,J., Allen,C.E., Geetha,S., Shapiro,A., Okunji,C., Kosti,I., Shomron,N., Grigoryan,V., Przytycka,T.M., Sauna,Z.E., Salari,R., Mandel-Gutfreund,Y., Komar,A.A., & Kimchi-Sarfaty,C. (2012) Characterization of coding synonymous and non-synonymous variants in ADAMTS13 using ex vivo and in silico approaches. *PLoS.One.*, **7**, e38864.

Ellgaard,L. & Helenius,A. (2003) Quality control in the endoplasmic reticulum. *Nat.Rev.Mol.Cell Biol.*, **4**, 181-191.

Engin,F. & Hotamisligil,G.S. (2010) Restoring endoplasmic reticulum function by chemical chaperones: an emerging therapeutic approach for metabolic diseases. *Diabetes Obes.Metab*, **12 Suppl 2**, 108-115.

Eura,Y., Kokame,K., Takafuta,T., Tanaka,R., Kobayashi,H., Ishida,F., Hisanaga,S., Matsumoto,M., Fujimura,Y., & Miyata,T. (2014) Candidate gene analysis using genomic quantitative PCR: identification of ADAMTS13 large deletions in two patients with Upshaw-Schulman syndrome. *Mol.Genet.Genomic.Med.*, **2**, 240-244.

Fakhouri,F., Vernant,J.P., Veyradier,A., Wolf,M., Kaplanski,G., Binaut,R., Rieger,M., Scheiflinger,F., Poullin,P., Deroure,B., Delarue,R., Lesavre,P., Vanhille,P., Hermine,O., Remuzzi,G., & Grunfeld,J.P. (2005) Efficiency of curative and prophylactic treatment with rituximab in ADAMTS13-deficient thrombotic thrombocytopenic purpura: a study of 11 cases. *Blood*, **106**, 1932-1937.

Fan,J., Perry,S.J., Gao,Y., Schwarz,D.A., & Maki,R.A. (2005) A point mutation in the human melanin concentrating hormone receptor 1 reveals an important domain for cellular trafficking. *Mol.Endocrinol.*, **19**, 2579-2590.

Fan,J.Q., Ishii,S., Asano,N., & Suzuki,Y. (1999) Accelerated transport and maturation of lysosomal alpha-galactosidase A in Fabry lymphoblasts by an enzyme inhibitor. *Nat.Med.*, **5**, 112-115.

Fan,Z.C. & Tao,Y.X. (2009) Functional characterization and pharmacological rescue of melanocortin-4 receptor mutations identified from obese patients. *J Cell Mol.Med.*, **13**, 3268-3282.

Federici,A.B., Bader,R., Pagani,S., Colibretti,M.L., De Marco,L., & Mannucci,P.M. (1989) Binding of von Willebrand factor to glycoproteins Ib and IIb/IIIa complex: affinity is related to multimeric size. *Br.J.Haematol.*, **73**, 93-99.

Feldhammer,M., Durand,S., & Pshezhetsky,A.V. (2009) Protein misfolding as an underlying molecular defect in mucopolysaccharidosis III type C. *PLoS.One.*, **4**, e7434.

Feng,S., Eyler,S.J., Zhang,Y., Maga,T., Nester,C.M., Kroll,M.H., Smith,R.J., & Afshar-Kharghan,V. (2013a) Partial ADAMTS13 deficiency in atypical hemolytic uremic syndrome. *Blood*, **122**, 1487-1493.

Feng,S., Liang,X., Cruz,M.A., Vu,H., Zhou,Z., Pemmaraju,N., Dong,J.F., Kroll,M.H., & Afshar-Kharghan,V. (2013b) The interaction between factor H and Von Willebrand factor. *PLoS.One.*, **8**, e73715.

Ferrari,S., Scheiflinger,F., Rieger,M., Mudde,G., Wolf,M., Coppo,P., Girma,J.P., Azoulay,E., Brun-Buisson,C., Fakhouri,F., Mira,J.P., Oksenhendler,E., Poullin,P., Rondeau,E., Schleinitz,N., Schlemmer,B., Teboul,J.L., Vanhille,P., Vernant,J.P., Meyer,D., & Veyradier,A. (2007) Prognostic value of anti-ADAMTS 13 antibody features (Ig isotype, titer, and inhibitory effect) in a cohort of 35 adult French patients undergoing a first episode of thrombotic microangiopathy with undetectable ADAMTS 13 activity. *Blood*, **109**, 2815-2822.

Fersht,A. (1985) *Enzyme structure and mechanism,* 2nd edn, W. H. Freeman and Co, New York.

Feys,H.B., Anderson,P.J., Vanhoorelbeke,K., Majerus,E.M., & Sadler,J.E. (2009a) Multi-step binding of ADAMTS-13 to von Willebrand factor. *J.Thromb.Haemost.*, **7**, 2088-2095.

Feys,H.B., Canciani,M.T., Peyvandi,F., Deckmyn,H., Vanhoorelbeke,K., & Mannucci,P.M. (2007) ADAMTS13 activity to antigen ratio in physiological and pathological conditions associated with an increased risk of thrombosis. *Br.J Haematol.*, **138**, 534-540.

Feys,H.B., Pareyn,I., Vancraenenbroeck,R., De Maeyer,M., Deckmyn,H., Van Geet,C., & Vanhoorelbeke,K. (2009b) Mutation of the H-bond acceptor S119 in the ADAMTS13 metalloprotease domain reduces secretion and substrate turnover in a patient with congenital thrombotic thrombocytopenic purpura. *Blood*, **114**, 4749-4752.

Feys,H.B., Roodt,J., Vandeputte,N., Pareyn,I., Lamprecht,S., van Rensburg,W.J., Anderson,P.J., Budde,U., Louw,V.J., Badenhorst,P.N., Deckmyn,H., & Vanhoorelbeke,K. (2010) Thrombotic thrombocytopenic purpura directly linked with ADAMTS13 inhibition in the baboon (Papio ursinus). *Blood*, **116**, 2005-2010.

Florijn,R.J., Slats,J., Tanke,H.J., & Raap,A.K. (1995) Analysis of antifading reagents for fluorescence microscopy. *Cytometry*, **19**, 177-182.

Forster,R.P. & Goldstein,L. (1976) Intracellular osmoregulatory role of amino acids and urea in marine elasmobranchs. *Am.J Physiol*, **230**, 925-931.

Foster,P.A., Fulcher,C.A., Marti,T., Titani,K., & Zimmerman,T.S. (1987) A major factor VIII binding domain resides within the amino-terminal 272 amino acid residues of von Willebrand factor. *J Biol.Chem.*, **262**, 8443-8446.

Frustaci,A., Chimenti,C., Ricci,R., Natale,L., Russo,M.A., Pieroni,M., Eng,C.M., & Desnick,R.J. (2001) Improvement in cardiac function in the cardiac variant of Fabry's disease with galactose-infusion therapy. *N.Engl.J Med.*, **345**, 25-32.

Fujimoto,T., Ohara,S., & Hawiger,J. (1982) Thrombin-induced exposure and prostacyclin inhibition of the receptor for factor VIII/von Willebrand factor on human platelets. *J Clin.Invest*, **69**, 1212-1222.

Fujimura,Y. & Matsumoto,M. (2010) Registry of 919 patients with thrombotic microangiopathies across Japan: database of Nara Medical University during 1998-2008. *Intern.Med.*, **49**, 7-15.

Fujimura,Y., Matsumoto,M., Isonishi,A., Yagi,H., Kokame,K., Soejima,K., Murata,M., & Miyata,T. (2011) Natural history of Upshaw-Schulman syndrome based on ADAMTS13 gene analysis in Japan. *J.Thromb.Haemost.*, **9 Suppl 1**, 283-301.

Fujimura,Y., Matsumoto,M., Kokame,K., Isonishi,A., Soejima,K., Akiyama,N., Tomiyama,J., Natori,K., Kuranishi,Y., Imamura,Y., Inoue,N., Higasa,S., Seike,M., Kozuka,T., Hara,M., Wada,H., Murata,M., Ikeda,Y., Miyata,T., & George,J.N. (2009) Pregnancy-induced thrombocytopenia and TTP, and the risk of fetal death, in Upshaw-Schulman syndrome: a series of 15 pregnancies in 9 genotyped patients. *Br.J.Haematol.*, **144**, 742-754.

Fujimura,Y., Titani,K., Holland,L.Z., Roberts,J.R., Kostel,P., Ruggeri,Z.M., & Zimmerman,T.S. (1987) A heparin-binding domain of human von Willebrand factor. Characterization and localization to a tryptic fragment extending from amino acid residue Val-449 to Lys-728. *J Biol.Chem.*, **262**, 1734-1739.

Fujimura,Y., Titani,K., Holland,L.Z., Russell,S.R., Roberts,J.R., Elder,J.H., Ruggeri,Z.M., & Zimmerman,T.S. (1986) von Willebrand factor. A reduced and alkylated 52/48-kDa fragment beginning at amino acid residue 449 contains the domain interacting with platelet glycoprotein Ib. *J Biol.Chem.*, **261**, 381-385.

Fujioka,M., Hayakawa,K., Mishima,K., Kunizawa,A., Irie,K., Higuchi,S., Nakano,T., Muroi,C., Fukushima,H., Sugimoto,M., Banno,F., Kokame,K., Miyata,T., Fujiwara,M., Okuchi,K., & Nishio,K. (2010) ADAMTS13 gene deletion aggravates ischemic brain damage: a possible neuroprotective role of ADAMTS13 by ameliorating postischemic hypoperfusion. *Blood*, **115**, 1650-1653.

Fujioka,M., Nakano,T., Hayakawa,K., Irie,K., Akitake,Y., Sakamoto,Y., Mishima,K., Muroi,C., Yonekawa,Y., Banno,F., Kokame,K., Miyata,T., Nishio,K., Okuchi,K., Iwasaki,K., Fujiwara,M., & Siesjo,B.K. (2012) ADAMTS13 gene deletion enhances plasma high-mobility group box1 elevation and neuroinflammation in brain ischemia-reperfusion injury. *Neurol.Sci.*, **33**, 1107-1115.

Furlan,M., Robles,R., Galbusera,M., Remuzzi,G., Kyrle,P.A., Brenner,B., Krause,M., Scharrer,I., Aumann,V., Mittler,U., Solenthaler,M., & Lammle,B. (1998a) von Willebrand factor-cleaving protease in thrombotic thrombocytopenic purpura and the hemolytic-uremic syndrome. *N.Engl.J.Med.*, **339**, 1578-1584.

Furlan,M., Robles,R., & Lammle,B. (1996) Partial purification and characterization of a protease from human plasma cleaving von Willebrand factor to fragments produced by in vivo proteolysis. *Blood*, **87**, 4223-4234.

Furlan,M., Robles,R., Morselli,B., Sandoz,P., & Lammle,B. (1999) Recovery and half-life of von Willebrand factor-cleaving protease after plasma therapy in patients with thrombotic thrombocytopenic purpura. *Thromb.Haemost.*, **81**, 8-13.

Furlan,M., Robles,R., Solenthaler,M., & Lammle,B. (1998b) Acquired deficiency of von Willebrand factor-cleaving protease in a patient with thrombotic thrombocytopenic purpura. *Blood*, **91**, 2839-2846.

Furlan,M., Robles,R., Solenthaler,M., Wassmer,M., Sandoz,P., & Lammle,B. (1997) Deficient activity of von Willebrand factor-cleaving protease in chronic relapsing thrombotic thrombocytopenic purpura. *Blood*, **89**, 3097-3103.

Furusho,K., Yoshizawa,T., & Shoji,S. (2005) Ectoine alters subcellular localization of inclusions and reduces apoptotic cell death induced by the truncated Machado-Joseph disease gene product with an expanded polyglutamine stretch. *Neurobiol.Dis.*, **20**, 170-178.

Gandhi,C., Ahmad,A., Wilson,K.M., & Chauhan,A.K. (2014) ADAMTS13 modulates atherosclerotic plaque progression in mice via a VWF-dependent mechanism. *J.Thromb.Haemost.*, **12**, 255-260.

Gandhi,C., Khan,M.M., Lentz,S.R., & Chauhan,A.K. (2012a) ADAMTS13 reduces vascular inflammation and the development of early atherosclerosis in mice. *Blood*, **119**, 2385-2391.

Gandhi,C., Motto,D.G., Jensen,M., Lentz,S.R., & Chauhan,A.K. (2012b) ADAMTS13 deficiency exacerbates VWF-dependent acute myocardial ischemia/reperfusion injury in mice. *Blood*, **120**, 5224-5230.

Gao,W., Anderson,P.J., Majerus,E.M., Tuley,E.A., & Sadler,J.E. (2006) Exosite interactions contribute to tension-induced cleavage of von Willebrand factor by the antithrombotic ADAMTS13 metalloprotease. *Proc.Natl.Acad.Sci.U.S.A*, **103**, 19099-19104.

Gao,W., Anderson,P.J., & Sadler,J.E. (2008) Extensive contacts between ADAMTS13 exosites and von Willebrand factor domain A2 contribute to substrate specificity. *Blood*, **112**, 1713-1719.

Gao,W., Zhu,J., Westfield,L.A., Tuley,E.A., Anderson,P.J., & Sadler,J.E. (2012) Rearranging exosites in noncatalytic domains can redirect the substrate specificity of ADAMTS proteases. *J Biol.Chem.*, **287**, 26944-26952.

Garagiola,I., Valsecchi,C., Lavoretano,S., Oren,H., Bohm,M., & Peyvandi,F. (2008) Nonsense-mediated mRNA decay in the ADAMTS13 gene caused by a 29-nucleotide deletion. *Haematologica*, **93**, 1678-1685.

Gardner,M.D., Chion,C.K., de Groot,R., Shah,A., Crawley,J.T., & Lane,D.A. (2009) A functional calcium-binding site in the metalloprotease domain of ADAMTS13. *Blood*, **113**, 1149-1157.

George,J.N. (2010) How I treat patients with thrombotic thrombocytopenic purpura: 2010. *Blood*, **116**, 4060-4069.

George,J.N., Kremer Hovinga,J.A., Terrell,D.R., Vesely,S.K., & Lammle,B. (2008) The Oklahoma Thrombotic Thrombocytopenic Purpura-Hemolytic Uremic Syndrome Registry: the Swiss connection. *Eur.J Haematol.*, **80**, 277-286.

George,J.N., Lopez,J.A., & Konkle,B.A. (2014) N-Acetylcysteine: an old drug, a new insight, a potentially effective treatment for thrombotic thrombocytopenic purpura. *Transfusion*, **54**, 1205-1207.

Gerhardt,S., Hassall,G., Hawtin,P., McCall,E., Flavell,L., Minshull,C., Hargreaves,D., Ting,A., Pauptit,R.A., Parker,A.E., & Abbott,W.M. (2007) Crystal structures of human ADAMTS-1 reveal a conserved catalytic domain and a disintegrin-like domain with a fold homologous to cysteine-rich domains. *J Mol.Biol.*, **373**, 891-902.

Giblin,J.P., Hewlett,L.J., & Hannah,M.J. (2008) Basal secretion of von Willebrand factor from human endothelial cells. *Blood*, **112**, 957-964.

Gill,J.C., Endres-Brooks,J., Bauer,P.J., Marks,W.J., Jr., & Montgomery,R.R. (1987) The effect of ABO blood group on the diagnosis of von Willebrand disease. *Blood*, **69**, 1691-1695.

Ginsburg,D., Handin,R.I., Bonthron,D.T., Donlon,T.A., Bruns,G.A., Latt,S.A., & Orkin,S.H. (1985) Human von Willebrand factor (vWF): isolation of complementary DNA (cDNA) clones and chromosomal localization. *Science*, **228**, 1401-1406.

Girma,J.P., Kalafatis,M., Pietu,G., Lavergne,J.M., Chopek,M.W., Edgington,T.S., & Meyer,D. (1986) Mapping of distinct von Willebrand factor domains interacting with platelet GPIb and GPIIb/IIIa and with collagen using monoclonal antibodies. *Blood*, **67**, 1356-1366.

Girma,J.P., Takahashi,Y., Yoshioka,A., Diaz,J., & Meyer,D. (1990) Ristocetin and botrocetin involve two distinct domains of von Willebrand factor for binding to platelet membrane glycoprotein Ib. *Thromb.Haemost.*, **64**, 326-332.

Gong,B., Zhang,L.Y., Lam,D.S., Pang,C.P., & Yam,G.H. (2010) Sodium 4-phenylbutyrate ameliorates the effects of cataract-causing mutant gammaD-crystallin in cultured cells. *Mol.Vis.*, **16**, 997-1003.

Gong,B., Zhang,L.Y., Pang,C.P., Lam,D.S., & Yam,G.H. (2009) Trimethylamine N-oxide alleviates the severe aggregation and ER stress caused by G98R alphaA-crystallin. *Mol.Vis.*, **15**, 2829-2840.

Gordon,A.H., Hart,P.D., & Young,M.R. (1980) Ammonia inhibits phagosome-lysosome fusion in macrophages. *Nature*, **286**, 79-80.

Gorner,K., Holtorf,E., Odoy,S., Nuscher,B., Yamamoto,A., Regula,J.T., Beyer,K., Haass,C., & Kahle,P.J. (2004) Differential effects of Parkinson's disease-associated mutations on stability and folding of DJ-1. *J Biol.Chem.*, **279**, 6943-6951.

Hamamy,H. (2012) Consanguineous marriages : Preconception consultation in primary health care settings. *J Community Genet.*, **3**, 185-192.

Hamilton,K.K. & Sims,P.J. (1987) Changes in cytosolic Ca2+ associated with von Willebrand factor release in human endothelial cells exposed to histamine. Study of microcarrier cell monolayers using the fluorescent probe indo-1. *J Clin.Invest*, **79**, 600-608.

Hammond,C., Braakman,I., & Helenius,A. (1994) Role of N-linked oligosaccharide recognition, glucose trimming, and calnexin in glycoprotein folding and quality control. *Proc.Natl.Acad.Sci.U.S.A*, **91**, 913-917.

Hanson,E., Jood,K., Nilsson,S., Blomstrand,C., & Jern,C. (2009) Association between genetic variation at the ADAMTS13 locus and ischemic stroke. *J.Thromb.Haemost.*, **7**, 2147-2148.

Harrison,R.L. & McKee,P.A. (1984) Estrogen stimulates von Willebrand factor production by cultured endothelial cells. *Blood*, **63**, 657-664.

Hassenpflug,W.A., Budde,U., Obser,T., Angerhaus,D., Drewke,E., Schneppenheim,S., & Schneppenheim,R. (2006) Impact of mutations in the von Willebrand factor A2 domain on ADAMTS13-dependent proteolysis. *Blood*, **107**, 2339-2345.

Hayashi,H. & Sugiyama,Y. (2007) 4-phenylbutyrate enhances the cell surface expression and the transport capacity of wild-type and mutated bile salt export pumps. *Hepatology*, **45**, 1506-1516.

He,Y., Chen,Y., Zhao,Y., Zhang,Y., & Yang,W. (2010) Clinical study on five cases of thrombotic thrombocytopenic purpura complicating pregnancy. *Aust.N.Z.J.Obstet.Gynaecol.*, **50**, 519-522.

Henzler Wildman,K.A., Lee,D.K., & Ramamoorthy,A. (2002) Determination of alpha-helix and beta-sheet stability in the solid state: a solid-state NMR investigation of poly(L-alanine). *Biopolymers*, **64**, 246-254.

Hershko,A. & Ciechanover,A. (1998) The ubiquitin system. *Annu.Rev.Biochem.*, **67**, 425-479.

Hing,Z.A., Schiller,T., Wu,A., Hamasaki-Katagiri,N., Struble,E.B., Russek-Cohen,E., & Kimchi-Sarfaty,C. (2013) Multiple in silico tools predict phenotypic manifestations in congenital thrombotic thrombocytopenic purpura. *Br.J.Haematol.*, **160**, 825-837.

Hiura,H., Matsui,T., Matsumoto,M., Hori,Y., Isonishi,A., Kato,S., Iwamoto,T., Mori,T., & Fujimura,Y. (2010) Proteolytic fragmentation and sugar chains of plasma ADAMTS13 purified by a conformation-dependent monoclonal antibody. *J.Biochem.*, **148**, 403-411.

Holden,P. & Horton,W.A. (2009) Crude subcellular fractionation of cultured mammalian cell lines. *BMC.Res.Notes*, **2**, 243.

Hollestelle,M.J., Lai,K.W., van Deuren,M., Lenting,P.J., de Groot,P.G., Sprong,T., & Bovenschen,N. (2011) Cleavage of von Willebrand factor by granzyme M destroys its factor VIII binding capacity. *PLoS.One.*, **6**, e24216.

Holz,J.B. (2012) The TITAN trial--assessing the efficacy and safety of an anti-von Willebrand factor Nanobody in patients with acquired thrombotic thrombocytopenic purpura. *Transfus.Apher.Sci.*, **46**, 343-346.

Hommais,A., Rayes,J., Houllier,A., Obert,B., Legendre,P., Veyradier,A., Girma,J.P., & Ribba,A.S. (2007) Molecular characterization of four ADAMTS13 mutations responsible for congenital thrombotic thrombocytopenic purpura (Upshaw-Schulman syndrome). *Thromb.Haemost.*, **98**, 593-599.

Hosokawa,N., You,Z., Tremblay,L.O., Nagata,K., & Herscovics,A. (2007) Stimulation of ERAD of misfolded null Hong Kong alpha1-antitrypsin by Golgi alpha1,2-mannosidases. *Biochem.Biophys.Res.Commun.*, **362**, 626-632.

Howard,M., Fischer,H., Roux,J., Santos,B.C., Gullans,S.R., Yancey,P.H., & Welch,W.J. (2003) Mammalian osmolytes and S-nitrosoglutathione promote Delta F508 cystic fibrosis transmembrane conductance regulator (CFTR) protein maturation and function. *J.Biol.Chem.*, **278**, 35159-35167.

Hunault,M., Arbini,A.A., Carew,J.A., Peyvandi,F., & Bauer,K.A. (1999) Characterization of two naturally occurring mutations in the second epidermal growth factor-like domain of factor VII. *Blood*, **93**, 1237-1244.

Huxley-Jones,J., Apte,S.S., Robertson,D.L., & Boot-Handford,R.P. (2005) The characterisation of six ADAMTS proteases in the basal chordate Ciona intestinalis provides new insights into the vertebrate ADAMTS family. *Int.J Biochem.Cell Biol.*, **37**, 1838-1845.

Inden,M., Kitamura,Y., Takeuchi,H., Yanagida,T., Takata,K., Kobayashi,Y., Taniguchi,T., Yoshimoto,K., Kaneko,M., Okuma,Y., Taira,T., Ariga,H., & Shimohama,S. (2007) Neurodegeneration of mouse nigrostriatal dopaminergic system induced by repeated oral administration of rotenone is prevented by 4-phenylbutyrate, a chemical chaperone. *J Neurochem.*, **101**, 1491-1504.

Ishii,S., Chang,H.H., Kawasaki,K., Yasuda,K., Wu,H.L., Garman,S.C., & Fan,J.Q. (2007) Mutant alpha-galactosidase A enzymes identified in Fabry disease patients with residual enzyme activity: biochemical characterization and restoration of normal intracellular processing by 1-deoxygalactonojirimycin. *Biochem.J*, **406**, 285-295.

Ishizashi,H., Yagi,H., Matsumoto,M., Soejima,K., Nakagaki,T., & Fujimura,Y. (2007) Quantitative Western blot analysis of plasma ADAMTS13 antigen in patients with Upshaw-Schulman syndrome. *Thromb.Res.*, **120**, 381-386.

Iwata,A., Riley,B.E., Johnston,J.A., & Kopito,R.R. (2005) HDAC6 and microtubules are required for autophagic degradation of aggregated huntingtin. *J Biol.Chem.*, **280**, 40282-40292.

Jaffe,E.A., Hoyer,L.W., & Nachman,R.L. (1973) Synthesis of antihemophilic factor antigen by cultured human endothelial cells. *J.Clin.Invest*, **52**, 2757-2764.

Jamur,M.C. & Oliver,C. (2010) Cell fixatives for immunostaining. *Methods Mol.Biol.*, **588**, 55-61.

Janovick,J.A., Maya-Nunez,G., & Conn,P.M. (2002) Rescue of hypogonadotropic hypogonadism-causing and manufactured GnRH receptor mutants by a specific protein-folding template: misrouted proteins as a novel disease etiology and therapeutic target. *J Clin.Endocrinol.Metab*, **87**, 3255-3262.

Jensen,T.J., Loo,M.A., Pind,S., Williams,D.B., Goldberg,A.L., & Riordan,J.R. (1995) Multiple proteolytic systems, including the proteasome, contribute to CFTR processing. *Cell*, **83**, 129-135.

Jian,C., Xiao,J., Gong,L., Skipwith,C.G., Jin,S.Y., Kwaan,H.C., & Zheng,X.L. (2012) Gain-of-function ADAMTS13 variants that are resistant to autoantibodies against ADAMTS13 in patients with acquired thrombotic thrombocytopenic purpura. *Blood*, **119**, 3836-3843.

Jin,S.Y., Skipwith,C.G., & Zheng,X.L. (2010) Amino acid residues Arg(659), Arg(660), and Tyr(661) in the spacer domain of ADAMTS13 are critical for cleavage of von Willebrand factor. *Blood*, **115**, 2300-2310.

Jin,S.Y., Tohyama,J., Bauer,R.C., Cao,N.N., Rader,D.J., & Zheng,X.L. (2012) Genetic ablation of Adamts13 gene dramatically accelerates the formation of early atherosclerosis in a murine model. *Arterioscler.Thromb.Vasc.Biol.*, **32**, 1817-1823.

Jin,S.Y., Xiao,J., Bao,J., Zhou,S., Wright,J.F., & Zheng,X.L. (2013) AAV-mediated expression of an ADAMTS13 variant prevents shigatoxin-induced thrombotic thrombocytopenic purpura. *Blood*, **121**, 3825-3.

Jones,G.C. & Riley,G.P. (2005) ADAMTS proteinases: a multi-domain, multi-functional family with roles in extracellular matrix turnover and arthritis. *Arthritis Res.Ther.*, **7**, 160-169.

Kang,M., Wilson,L., & Kermode,J.C. (2008) Evidence from limited proteolysis of a ristocetin-induced conformational change in human von Willebrand factor that promotes its binding to platelet glycoprotein Ib-IX-V. *Blood Cells Mol.Dis.*, **40**, 433-443.

Katsumi,A., Tuley,E.A., Bodo,I., & Sadler,J.E. (2000) Localization of disulfide bonds in the cystine knot domain of human von Willebrand factor. *J Biol.Chem.*, **275**, 25585-25594.

Khan,M.M., Motto,D.G., Lentz,S.R., & Chauhan,A.K. (2012) ADAMTS13 reduces VWF-mediated acute inflammation following focal cerebral ischemia in mice. *J.Thromb.Haemost.*, **10**, 1665-1671.

Kim,B., Hing,Z.A., Wu,A., Schiller,T., Struble,E.B., Liuwantara,D., Kempert,P.H., Broxham,E.J., Edwards,N.C., Marder,V.J., Simhadri,V.L., Sauna,Z.E., Howard,T.E., & Kimchi-Sarfaty,C. (2014) Single-nucleotide variations defining previously unreported ADAMTS13 haplotypes are associated with differential expression and activity of the VWF-cleaving protease in a Salvadoran congenital thrombotic thrombocytopenic purpura family. *Br.J.Haematol.*, **165**, 154-158.

Kinoshita,S., Yoshioka,A., Park,Y.D., Ishizashi,H., Konno,M., Funato,M., Matsui,T., Titani,K., Yagi,H., Matsumoto,M., & Fujimura,Y. (2001) Upshaw-Schulman syndrome revisited: a concept of congenital thrombotic thrombocytopenic purpura. *Int.J Hematol.*, **74**, 101-108.

Klaus,C., Plaimauer,B., Studt,J.D., Dorner,F., Lammle,B., Mannucci,P.M., & Scheiflinger,F. (2004) Epitope mapping of ADAMTS13 autoantibodies in acquired thrombotic thrombocytopenic purpura. *Blood*, **103**, 4514-4519.

Kleinschnitz,C., De Meyer,S.F., Schwarz,T., Austinat,M., Vanhoorelbeke,K., Nieswandt,B., Deckmyn,H., & Stoll,G. (2009) Deficiency of von Willebrand factor protects mice from ischemic stroke. *Blood*, **113**, 3600-3603.

Klukowska,A., Niewiadomska,E., Budde,U., Oyen,F., & Schneppenheim,R. (2010) Difficulties in diagnosing congenital thrombotic thrombocytopenic purpura. *J.Pediatr.Hematol.Oncol.*, **32**, 103-107.

Kokame,K., Aoyama,Y., Matsumoto,M., Fujimura,Y., & Miyata,T. (2008) Inherited and de novo mutations of ADAMTS13 in a patient with Upshaw-Schulman syndrome. *J.Thromb.Haemost.*, **6**, 213-215.

Kokame,K., Kokubo,Y., & Miyata,T. (2011) Polymorphisms and mutations of ADAMTS13 in the Japanese population and estimation of the number of patients with Upshaw-Schulman syndrome. *J Thromb.Haemost.*, **9**, 1654-1656.

Kokame,K., Matsumoto,M., Soejima,K., Yagi,H., Ishizashi,H., Funato,M., Tamai,H., Konno,M., Kamide,K., Kawano,Y., Miyata,T., & Fujimura,Y. (2002) Mutations and common polymorphisms in ADAMTS13 gene responsible for von Willebrand factor-cleaving protease activity. *Proc.Natl.Acad.Sci.U.S.A*, **99**, 11902-11907.

Kokame,K., Nobe,Y., Kokubo,Y., Okayama,A., & Miyata,T. (2005) FRETS-VWF73, a first fluorogenic substrate for ADAMTS13 assay. *Br.J Haematol.*, **129**, 93-100.

Kopecka,J., Krijt,J., Rakova,K., & Kozich,V. (2011) Restoring assembly and activity of cystathionine beta-synthase mutants by ligands and chemical chaperones. *J Inherit.Metab Dis.*, **34**, 39-48.

Kozak,M. (1987) At least six nucleotides preceding the AUG initiator codon enhance translation in mammalian cells. *J Mol.Biol.*, **196**, 947-950.

Kraisin,S., Palasuwan,A., Popruk,S., & Nantakomol,D. (2014) Reduced ADAMTS13 activity is associated with an ADAMTS13 SNP, fever and microparticles in a malaria-like model. *Malar.J*, **13**, 3.

Krebs,M.P., Holden,D.C., Joshi,P., Clark,C.L., III, Lee,A.H., & Kaushal,S. (2010) Molecular mechanisms of rhodopsin retinitis pigmentosa and the efficacy of pharmacological rescue. *J Mol.Biol.*, **395**, 1063-1078.

Kubota,K., Niinuma,Y., Kaneko,M., Okuma,Y., Sugai,M., Omura,T., Uesugi,M., Uehara,T., Hosoi,T., & Nomura,Y. (2006) Suppressive effects of 4-phenylbutyrate on the aggregation of Pael receptors and endoplasmic reticulum stress. *J Neurochem.*, **97**, 1259-1268.

Laje,P., Shang,D., Cao,W., Niiya,M., Endo,M., Radu,A., De Rogatis,N., Scheiflinger,F., Zoltick,P.W., Flake,A.W., & Zheng,X.L. (2009) Correction of murine ADAMTS13 deficiency by hematopoietic progenitor cell-mediated gene therapy. *Blood*, **113**, 2172-2180.

Lam,J.K., Chion,C.K., Zanardelli,S., Lane,D.A., & Crawley,J.T. (2007) Further characterization of ADAMTS-13 inactivation by thrombin. *J Thromb.Haemost.*, **5**, 1010-1018.

Lambers,M., Goldenberg,N.A., Kenet,G., Kirkham,F.J., Manner,D., Bernard,T., Mesters,R.M., Junker,R., Stoll,M., & Nowak-Gottl,U. (2013) Role of reduced ADAMTS13 in arterial ischemic stroke: a pediatric cohort study. *Ann.Neurol.*, **73**, 58-64.

Lancellotti,S. & De Cristofaro,R. (2011) Structure and proteolytic properties of ADAMTS13, a metalloprotease involved in the pathogenesis of thrombotic microangiopathies. *Prog.Mol.Biol.Transl.Sci.*, **99**, 105-144.

Lancellotti,S., De Filippis,V., Pozzi,N., Peyvandi,F., Palla,R., Rocca,B., Rutella,S., Pitocco,D., Mannucci,P.M., & De Cristofaro,R. (2010) Formation of methionine sulfoxide by peroxynitrite at position 1606 of von Willebrand factor inhibits its cleavage by ADAMTS-13: A new prothrombotic mechanism in diseases associated with oxidative stress. *Free Radic.Biol.Med.*, **48**, 446-456.

Lankhof,H., van Hoeij,M., Schiphorst,M.E., Bracke,M., Wu,Y.P., Ijsseldijk,M.J., Vink,T., de Groot,P.G., & Sixma,J.J. (1996) A3 domain is essential for interaction of von Willebrand factor with collagen type III. *Thromb Haemost*, **75**, 950-958.

Lawson-Yuen,A. & Levy,H.L. (2006) The use of betaine in the treatment of elevated homocysteine. *Mol.Genet.Metab*, **88**, 201-207.

Le,S.O., Fulop,K., Yamaguchi,Y., Ilias,A., Szabo,Z., Brampton,C.N., Pomozi,V., Huszar,K., Aranyi,T., & Varadi,A. (2011) Expression and in vivo rescue of human ABCC6 disease-causing mutants in mouse liver. *PLoS.One.*, **6**, e24738.

Leanos-Miranda,A., Janovick,J.A., & Conn,P.M. (2002) Receptor-misrouting: an unexpectedly prevalent and rescuable etiology in gonadotropin-releasing hormone receptor-mediated hypogonadotropic hypogonadism. *J Clin.Endocrinol.Metab*, **87**, 4825-4828.

Lee,D.H. & Goldberg,A.L. (1998) Proteasome inhibitors: valuable new tools for cell biologists. *Trends Cell Biol.*, **8**, 397-403.

Lee,J.C. & Timasheff,S.N. (1981) The stabilization of proteins by sucrose. *J Biol.Chem.*, **256**, 7193-7201.

Lee,S.H., Park,J.H., Park,S.K., Lee,E.H., Choi,J.I., Visentin,G.P., Park,T.S., Oh,S.H., & Kim,S.R. (2011) A novel homozygous missense ADAMTS13 mutation Y658C in a patient with recurrent thrombotic thrombocytopenic purpura. *Ann.Clin.Lab Sci.*, **41**, 273-276.

Lee,W.C., Kang,D., Causevic,E., Herdt,A.R., Eckman,E.A., & Eckman,C.B. (2010) Molecular characterization of mutations that cause globoid cell leukodystrophy and pharmacological rescue using small molecule chemical chaperones. *J Neurosci.*, **30**, 5489-5497.

Levine,B. & Kroemer,G. (2008) Autophagy in the pathogenesis of disease. *Cell*, **132**, 27-42.

Levine,J.D., Harlan,J.M., Harker,L.A., Joseph,M.L., & Counts,R.B. (1982) Thrombin-mediated release of factor VIII antigen from human umbilical vein endothelial cells in culture. *Blood*, **60**, 531-534.

Levy,G.G., Nichols,W.C., Lian,E.C., Foroud,T., McClintick,J.N., McGee,B.M., Yang,A.Y., Siemieniak,D.R., Stark,K.R., Gruppo,R., Sarode,R., Shurin,S.B., Chandrasekaran,V., Stabler,S.P., Sabio,H., Bouhassira,E.E., Upshaw,J.D., Jr., Ginsburg,D., & Tsai,H.M. (2001) Mutations in a member of the ADAMTS gene family cause thrombotic thrombocytopenic purpura. *Nature*, **413**, 488-494.

Li,G.W., Rambally,S., Kamboj,J., Reilly,S., Moake,J.L., Udden,M.M., & Mims,M.P. (2014) Treatment of refractory thrombotic thrombocytopenic purpura with N-acetylcysteine: a case report. *Transfusion*, **54**, 1221-1224.

Licht,C., Stapenhorst,L., Simon,T., Budde,U., Schneppenheim,R., & Hoppe,B. (2004) Two novel ADAMTS13 gene mutations in thrombotic thrombocytopenic purpura/hemolytic-uremic syndrome (TTP/HUS). *Kidney Int.*, **66**, 955-958.

Ling,J., Su,J., Ma,Z., & Ruan,C. (2013) The WXXW motif in the TSR1 of ADAMTS13 is important for its secretion and proteolytic activity. *Thromb.Res.*, **131**, 529-534.

Liu,L., Choi,H., Bernardo,A., Bergeron,A.L., Nolasco,L., Ruan,C., Moake,J.L., & Dong,J.F. (2005) Platelet-derived VWF-cleaving metalloprotease ADAMTS-13. *J.Thromb.Haemost.*, **3**, 2536-2544.

Liu,X.L., Done,S.C., Yan,K., Kilpelainen,P., Pikkarainen,T., & Tryggvason,K. (2004) Defective trafficking of nephrin missense mutants rescued by a chemical chaperone. *J Am.Soc.Nephrol.*, **15**, 1731-1738.

Lo,N.C., Turner,N.A., Cruz,M.A., & Moake,J. (2013) Interaction of Shiga toxin with the A-domains and multimers of von Willebrand Factor. *J.Biol.Chem.*, **288**, 33118-33123.

Loesberg,C., Gonsalves,M.D., Zandbergen,J., Willems,C., van Aken,W.G., Stel,H.V., Van Mourik,J.A., & de Groot,P.G. (1983) The effect of calcium on the secretion of factor VIII-related antigen by cultured human endothelial cells. *Biochim.Biophys.Acta*, **763**, 160-168.

Longin,A., Souchier,C., Ffrench,M., & Bryon,P.A. (1993) Comparison of anti-fading agents used in fluorescence microscopy: image analysis and laser confocal microscopy study. *J Histochem.Cytochem.*, **41**, 1833-1840.

Loo,T.W. & Clarke,D.M. (2007) Chemical and pharmacological chaperones as new therapeutic agents. *Expert.Rev.Mol.Med.*, **9**, 1-18.

Lotta,L.A., Garagiola,I., Palla,R., Cairo,A., & Peyvandi,F. (2010) ADAMTS13 mutations and polymorphisms in congenital thrombotic thrombocytopenic purpura. *Hum.Mutat.*, **31**, 11-19.

Lotta,L.A., Tuana,G., Yu,J., Martinelli,I., Wang,M., Yu,F., Passamonti,S.M., Pappalardo,E., Valsecchi,C., Scherer,S.E., Hale,W., Muzny,D.M., Randi,G., Rosendaal,F.R., Gibbs,R.A., & Peyvandi,F. (2013) Next-generation sequencing study finds an excess of rare, coding single-nucleotide variants of ADAMTS13 in patients with deep vein thrombosis. *J.Thromb.Haemost.*, **11**, 1228-1239.

Lotta,L.A., Wu,H.M., Mackie,I.J., Noris,M., Veyradier,A., Scully,M.A., Remuzzi,G., Coppo,P., Liesner,R., Donadelli,R., Loirat,C., Gibbs,R.A., Horne,A., Yang,S., Garagiola,I., Musallam,K.M., & Peyvandi,F. (2012) Residual plasmatic activity of ADAMTS13 is correlated with phenotype severity in congenital thrombotic thrombocytopenic purpura. *Blood*, **120**, 440-448.

Luken,B.M., Turenhout,E.A., Hulstein,J.J., Van Mourik,J.A., Fijnheer,R., & Voorberg,J. (2005) The spacer domain of ADAMTS13 contains a major binding site for antibodies in patients with thrombotic thrombocytopenic purpura. *Thromb.Haemost.*, **93**, 267-274.

Ma,E.S.K., Li,Y.H., Kwok,J.S.Y., Ling,S.C., Yau,P.W., & Chan,G.C.F. (2006) ADAMTS13 mutational analysis in Chinese patients with chronic relapsing thrombotic thrombocytopenic purpura. *Hong Kong Journal of Paediatrics*, **11**, 22-27.

Mackie,I., Langley,K., Chitolie,A., Liesner,R., Scully,M., Machin,S., & Peyvandi,F. (2013) Discrepancies between ADAMTS13 activity assays in patients with thrombotic microangiopathies. *Thromb Haemost*, **109**, 488-496.

Maegawa,G.H., Tropak,M., Buttner,J., Stockley,T., Kok,F., Clarke,J.T., & Mahuran,D.J. (2007) Pyrimethamine as a potential pharmacological chaperone for late-onset forms of GM2 gangliosidosis. *J Biol.Chem.*, **282**, 9150-9161.

Majerus,E.M., Zheng,X., Tuley,E.A., & Sadler,J.E. (2003) Cleavage of the ADAMTS13 propeptide is not required for protease activity. *J.Biol.Chem.*, **278**, 46643-46648.

Malina,M., Roumenina,L.T., Seeman,T., Le,Q.M., Dragon-Durey,M.A., Schaefer,F., & Fremeaux-Bacchi,V. (2012) Genetics of hemolytic uremic syndromes. *Presse Med.*, **41**, e105-e114.

Mancini,I., Valsecchi,C., Lotta,L.A., Deforche,L., Pontiggia,S., Bajetta,M., Palla,R., Vanhoorelbeke,K., & Peyvandi,F. (2014) FRETS-VWF73 rather than CBA assay reflects ADAMTS13 proteolytic activity in acquired thrombotic thrombocytopenic purpura patients. *Thromb.Haemost.*, Prepublished online April 17 2014; doi:10.1160/TH13-08-0688.

Mancuso,D.J., Tuley,E.A., Westfield,L.A., Worrall,N.K., Shelton-Inloes,B.B., Sorace,J.M., Alevy,Y.G., & Sadler,J.E. (1989) Structure of the gene for human von Willebrand factor. *J Biol.Chem.*, **264**, 19514-19527.

Manders,E.M., Stap,J., Brakenhoff,G.J., van Driel,R., & Aten,J.A. (1992) Dynamics of three-dimensional replication patterns during the S-phase, analysed by double labelling of DNA and confocal microscopy. *J.Cell Sci.*, **103 ( Pt 3)**, 857-862.

Manders,E.M.M., Verbeek,F.J., & Aten,J.A. (1993) Measurement of co-localization of objects in dual-colour confocal images. *Journal of Microscopy*, **169**, 375-382.

Manea,M., Kristoffersson,A., Schneppenheim,R., Saleem,M.A., Mathieson,P.W., Morgelin,M., Bjork,P., Holmberg,L., & Karpman,D. (2007a) Podocytes express ADAMTS13 in normal renal cortex and in patients with thrombotic thrombocytopenic purpura. *Br.J.Haematol.*, **138**, 651-662.

Manea,M., Kristoffersson,A., Tsai,H.M., Zhou,W., Winqvist,I., Oldaeus,G., Billstrom,R., Bjork,P., Holmberg,L., & Karpman,D. (2007b) ADAMTS13 phenotype in plasma from normal individuals and patients with thrombotic thrombocytopenic purpura. *Eur.J.Pediatr.*, **166**, 249-257.

Manea,M., Tati,R., Karlsson,J., Bekassy,Z.D., & Karpman,D. (2010) Biologically active ADAMTS13 is expressed in renal tubular epithelial cells. *Pediatr.Nephrol.*, **25**, 87-96.

Mannucci,P.M., Aberg,M., Nilsson,I.M., & Robertson,B. (1975) Mechanism of plasminogen activator and factor VIII increase after vasoactive drugs. *Br.J Haematol.*, **30**, 81-93.

Mannucci,P.M., Canciani,M.T., Forza,I., Lussana,F., Lattuada,A., & Rossi,E. (2001) Changes in health and disease of the metalloprotease that cleaves von Willebrand factor. *Blood*, **98**, 2730-2735.

Marteijn,J.A., Jansen,J.H., & van der Reijden,B.A. (2006) Ubiquitylation in normal and malignant hematopoiesis: novel therapeutic targets. *Leukemia*, **20**, 1511-1518.

Marti,T., Rosselet,S.J., Titani,K., & Walsh,K.A. (1987) Identification of disulfide-bridged substructures within human von Willebrand factor. *Biochemistry*, **26**, 8099-8109.

Matsuda,J., Suzuki,O., Oshima,A., Yamamoto,Y., Noguchi,A., Takimoto,K., Itoh,M., Matsuzaki,Y., Yasuda,Y., Ogawa,S., Sakata,Y., Nanba,E., Higaki,K., Ogawa,Y., Tominaga,L., Ohno,K., Iwasaki,H., Watanabe,H., Brady,R.O., & Suzuki,Y. (2003)

Chemical chaperone therapy for brain pathology in G(M1)-gangliosidosis. *Proc.Natl.Acad.Sci.U.S.A*, **100**, 15912-15917.

Matsui,T., Titani,K., & Mizuochi,T. (1992) Structures of the asparagine-linked oligosaccharide chains of human von Willebrand factor. Occurrence of blood group A, B, and H(O) structures. *J Biol.Chem.*, **267**, 8723-8731.

Matsumoto,M., Kokame,K., Soejima,K., Miura,M., Hayashi,S., Fujii,Y., Iwai,A., Ito,E., Tsuji,Y., Takeda-Shitaka,M., Iwadate,M., Umeyama,H., Yagi,H., Ishizashi,H., Banno,F., Nakagaki,T., Miyata,T., & Fujimura,Y. (2004) Molecular characterization of ADAMTS13 gene mutations in Japanese patients with Upshaw-Schulman syndrome. *Blood*, **103**, 1305-1310.

Mayadas,T.N. & Wagner,D.D. (1992) Vicinal cysteines in the prosequence play a role in von Willebrand factor multimer assembly. *Proc.Natl.Acad.Sci.U.S.A*, **89**, 3531-3535.

Mazzucato,M., Spessotto,P., Masotti,A., De Appollonia,L., Cozzi,M.R., Yoshioka,A., Perris,R., Colombatti,A., & De Marco,L. (1999) Identification of domains responsible for von Willebrand factor type VI collagen interaction mediating platelet adhesion under high flow. *J Biol.Chem.*, **274**, 3033-3041.

McGrath,R.T., McKinnon,T.A., Byrne,B., O'Kennedy,R., Terraube,V., McRae,E., Preston,R.J., Laffan,M.A., & O'Donnell,J.S. (2010) Expression of terminal alpha2-6-linked sialic acid on von Willebrand factor specifically enhances proteolysis by ADAMTS13. *Blood*, **115**, 2666-2673.

McGrath,R.T., van den Biggelaar,M., Byrne,B., O'Sullivan,J.M., Rawley,O., O'Kennedy,R., Voorberg,J., Preston,R.J., & O'Donnell,J.S. (2013) Altered glycosylation of platelet-derived von Willebrand factor confers resistance to ADAMTS13 proteolysis. *Blood*, **122**, 4107-4110.

McGuckin,S., Westwood,J.P., Webster,H., Collier,D., Leverett,D., & Scully,M. (2014) Characterization of the complications associated with plasma exchange for thrombotic thrombocytopaenic purpura and related thrombotic microangiopathic anaemias: a single institution experience. *Vox Sang.*, **106**, 161-166.

McKinnon,T.A., Chion,A.C., Millington,A.J., Lane,D.A., & Laffan,M.A. (2008) N-linked glycosylation of VWF modulates its interaction with ADAMTS13. *Blood*, **111**, 3042-3049.

Melan,M.A. & Sluder,G. (1992) Redistribution and differential extraction of soluble proteins in permeabilized cultured cells. Implications for immunofluorescence microscopy. *J Cell Sci.*, **101 ( Pt 4)**, 731-743.

Metin,A., Unal,S., Gumruk,F., Palla,R., Cairo,A., Underwood,M., & Gurgey,A. (2013) Congenital thrombotic thrombocytopenic purpura with novel mutations in three unrelated turkish children. *Pediatr.Blood Cancer*, **61**, 558-561.

Meyer,S.C., Jeddi,R., Meddeb,B., Gouider,E., Lammle,B., & Kremer Hovinga,J.A. (2008) A first case of congenital TTP on the African continent due to a new homozygous mutation in the catalytic domain of ADAMTS13. *Ann.Hematol.*, **87**, 663-666.

Miller,D.P., Kaye,J.A., Shea,K., Ziyadeh,N., Cali,C., Black,C., & Walker,A.M. (2004) Incidence of thrombotic thrombocytopenic purpura/hemolytic uremic syndrome. *Epidemiology*, **15**, 208-215.

Misawa,T., Hayashi,H., Sugiyama,Y., & Hashimoto,Y. (2012) Discovery and structural development of small molecules that enhance transport activity of bile salt export pump mutant associated with progressive familial intrahepatic cholestasis type 2. *Bioorg.Med.Chem.*, **20**, 2940-2949.

Moake,J.L., Turner,N.A., Stathopoulos,N.A., Nolasco,L.H., & Hellums,J.D. (1986) Involvement of large plasma von Willebrand factor (vWF) multimers and unusually large vWF forms derived from endothelial cells in shear stress-induced platelet aggregation. *J.Clin.Invest*, **78**, 1456-1461.

Moatti-Cohen,M., Garrec,C., Wolf,M., Boisseau,P., Galicier,L., Azoulay,E., Stepanian,A., Delmas,Y., Rondeau,E., Bezieau,S., Coppo,P., & Veyradier,A. (2012) Unexpected frequency of Upshaw-Schulman syndrome in pregnancy-onset thrombotic thrombocytopenic purpura. *Blood*, **119**, 5888-5897.

Mohlke,K.L., Purkayastha,A.A., Westrick,R.J., Smith,P.L., Petryniak,B., Lowe,J.B., & Ginsburg,D. (1999) Mvwf, a dominant modifier of murine von Willebrand factor, results from altered lineage-specific expression of a glycosyltransferase. *Cell*, **96**, 111-120.

Morales,L.D., Martin,C., & Cruz,M.A. (2006) The interaction of von Willebrand factor-A1 domain with collagen: mutation G1324S (type 2M von Willebrand disease) impairs the conformational change in A1 domain induced by collagen. *Journal of Thrombosis and Haemostasis*, **4**, 417-425.

Morello,J.P., Salahpour,A., Laperriere,A., Bernier,V., Arthus,M.F., Lonergan,M., Petaja-Repo,U., Angers,S., Morin,D., Bichet,D.G., & Bouvier,M. (2000) Pharmacological chaperones rescue cell-surface expression and function of misfolded V2 vasopressin receptor mutants. *J Clin.Invest*, **105**, 887-895.

Morgand,M., Buffet,M., Busson,M., Loiseau,P., Malot,S., Amokrane,K., Fortier,C., London,J., Bonmarchand,G., Wynckel,A., Provot,F., Poullin,P., Vanhille,P., Presne,C., Bordessoule,D., Girault,S., Delmas,Y., Hamidou,M., Mousson,C., Vigneau,C., Lautrette,A., Pourrat,J., Galicier,L., Azoulay,E., Pene,F., Mira,J.P., Rondeau,E., Ojeda-Uribe,M., Charron,D., Maury,E., Guidet,B., Veyradier,A., Tamouza,R., & Coppo,P. (2014) High prevalence of infectious events in thrombotic thrombocytopenic purpura and genetic relationship with toll-like receptor 9 polymorphisms: experience of the French Thrombotic Microangiopathies Reference Center. *Transfusion*, **54**, 389-397.

Mori,Y., Wada,H., Gabazza,E.C., Minami,N., Nobori,T., Shiku,H., Yagi,H., Ishizashi,H., Matsumoto,M., & Fujimura,Y. (2002) Predicting response to plasma exchange in patients with thrombotic thrombocytopenic purpura with measurement of vWF-cleaving protease activity. *Transfusion*, **42**, 572-580.

Morioka,Y., Casari,C., Wohner,N., Cho,S., Kurata,S., Kitano,A., Christophe,O.D., Lenting,P.J., Li,R., Denis,C.V., & Prevost,N. (2014) Expression of a structurally constrained von Willebrand factor variant triggers acute thrombotic thrombocytopenic purpura in mice. *Blood*, **123**, 3344-3353.

Moschcowitz,E. (1924) Hyaline thrombosis of the terminal arterioles and capillaries: a hithero undescribed disease. *Proceedings of the New York Pathological Society*, **24**, 21-24.

Mosyak,L., Georgiadis,K., Shane,T., Svenson,K., Hebert,T., McDonagh,T., Mackie,S., Olland,S., Lin,L., Zhong,X., Kriz,R., Reifenberg,E.L., Collins-Racie,L.A., Corcoran,C., Freeman,B., Zollner,R., Marvell,T., Vera,M., Sum,P.E., Lavallie,E.R., Stahl,M., & Somers,W. (2008) Crystal structures of the two major aggrecan degrading enzymes, ADAMTS4 and ADAMTS5. *Protein Sci.*, **17**, 16-21.

Motto,D.G., Chauhan,A.K., Zhu,G., Homeister,J., Lamb,C.B., Desch,K.C., Zhang,W., Tsai,H.M., Wagner,D.D., & Ginsburg,D. (2005) Shigatoxin triggers thrombotic thrombocytopenic purpura in genetically susceptible ADAMTS13-deficient mice. *J.Clin.Invest*, **115**, 2752-2761.

Nachman,R., Levine,R., & Jaffe,E.A. (1977) Synthesis of factor VIII antigen by cultured guinea pig megakaryocytes. *J Clin.Invest*, **60**, 914-921.

Neuhaus,E.M., Horstmann,H., Almers,W., Maniak,M., & Soldati,T. (1998) Ethane-freezing/methanol-fixation of cell monolayers: a procedure for improved preservation of structure and antigenicity for light and electron microscopies. *J Struct.Biol.*, **121**, 326-342.

Nicholson,A.C., Malik,S.B., Logsdon,J.M., Jr., & Van Meir,E.G. (2005) Functional evolution of ADAMTS genes: evidence from analyses of phylogeny and gene organization. *BMC.Evol.Biol.*, **5**, 11.

Niiya,M., Endo,M., Shang,D., Zoltick,P.W., Muvarak,N.E., Cao,W., Jin,S.Y., Skipwith,C.G., Motto,D.G., Flake,A.W., & Zheng,X.L. (2009) Correction of ADAMTS13 deficiency by in utero gene transfer of lentiviral vector encoding ADAMTS13 genes. *Mol.Ther.*, **17**, 34-41.

Nishio,K., Anderson,P.J., Zheng,X.L., & Sadler,J.E. (2004) Binding of platelet glycoprotein Ibalpha to von Willebrand factor domain A1 stimulates the cleavage of the adjacent domain A2 by ADAMTS13. *Proc.Natl.Acad.Sci.U.S.A*, **101**, 10578-10583.

Nolasco,L.H., Turner,N.A., Bernardo,A., Tao,Z., Cleary,T.G., Dong,J.F., & Moake,J.L. (2005) Hemolytic uremic syndrome-associated Shiga toxins promote endothelial-cell secretion and impair ADAMTS13 cleavage of unusually large von Willebrand factor multimers. *Blood*, **106**, 4199-4209.

Noorwez,S.M., Kuksa,V., Imanishi,Y., Zhu,L., Filipek,S., Palczewski,K., & Kaushal,S. (2003) Pharmacological chaperone-mediated in vivo folding and stabilization of the P23H-opsin mutant associated with autosomal dominant retinitis pigmentosa. *J Biol.Chem.*, **278**, 14442-14450.

Noorwez,S.M., Malhotra,R., McDowell,J.H., Smith,K.A., Krebs,M.P., & Kaushal,S. (2004) Retinoids assist the cellular folding of the autosomal dominant retinitis pigmentosa opsin mutant P23H. *J Biol.Chem.*, **279**, 16278-16284.

Noris,M., Bucchioni,S., Galbusera,M., Donadelli,R., Bresin,E., Castelletti,F., Caprioli,J., Brioschi,S., Scheiflinger,F., & Remuzzi,G. (2005) Complement factor H mutation in

familial thrombotic thrombocytopenic purpura with ADAMTS13 deficiency and renal involvement. *J.Am.Soc.Nephrol.*, **16**, 1177-1183.

North,A.J. (2006) Seeing is believing? A beginners' guide to practical pitfalls in image acquisition. *J.Cell Biol.*, **172**, 9-18.

Nowak,A.A., McKinnon,T.A., Hughes,J.M., Chion,A.C., & Laffan,M.A. (2014) The O-linked glycans of human von Willebrand factor modulate its interaction with ADAMTS-13. *J.Thromb.Haemost.*, **12**, 54-61.

O'Donnell,J.S., McKinnon,T.A., Crawley,J.T., Lane,D.A., & Laffan,M.A. (2005) Bombay phenotype is associated with reduced plasma-VWF levels and an increased susceptibility to ADAMTS13 proteolysis. *Blood*, **106**, 1988-1991.

Ohgane,K., Dodo,K., & Hashimoto,Y. (2010) Retinobenzaldehydes as proper-trafficking inducers of folding-defective P23H rhodopsin mutant responsible for retinitis pigmentosa. *Bioorg.Med.Chem.*, **18**, 7022-7028.

Okumiya,T., Ishii,S., Takenaka,T., Kase,R., Kamei,S., Sakuraba,H., & Suzuki,Y. (1995) Galactose stabilizes various missense mutants of alpha-galactosidase in Fabry disease. *Biochem.Biophys.Res.Commun.*, **214**, 1219-1224.

Okumiya,T., Kroos,M.A., Vliet,L.V., Takeuchi,H., Van der Ploeg,A.T., & Reuser,A.J. (2007) Chemical chaperones improve transport and enhance stability of mutant alpha-glucosidases in glycogen storage disease type II. *Mol.Genet.Metab*, **90**, 49-57.

Ono,T., Mimuro,J., Madoiwa,S., Soejima,K., Kashiwakura,Y., Ishiwata,A., Takano,K., Ohmori,T., & Sakata,Y. (2006) Severe secondary deficiency of von Willebrand factor-cleaving protease (ADAMTS13) in patients with sepsis-induced disseminated intravascular coagulation: its correlation with development of renal failure. *Blood*, **107**, 528-534.

Oppenheim,A.V., Willsky,A.S., & Young,I.T. (1983) *Signals and systems,* Prentice-Hall, New Jersey.

Orenstein,S.J., Kuo,S.H., Tasset,I., Arias,E., Koga,H., Fernandez-Carasa,I., Cortes,E., Honig,L.S., Dauer,W., Consiglio,A., Raya,A., Sulzer,D., & Cuervo,A.M. (2013) Interplay of LRRK2 with chaperone-mediated autophagy. *Nat.Neurosci.*, **16**, 394-406.

Paddock,S. (1999) *Confocal microscopy, methods and protocols (Methods in molecular biology),* Humana Press, New Jersey.

Padilla,A., Moake,J.L., Bernardo,A., Ball,C., Wang,Y., Arya,M., Nolasco,L., Turner,N., Berndt,M.C., Anvari,B., Lopez,J.A., & Dong,J.F. (2004) P-selectin anchors newly released ultralarge von Willebrand factor multimers to the endothelial cell surface. *Blood*, **103**, 2150-2156.

Palla,R., Lavoretano,S., Lombardi,R., Garagiola,I., Karimi,M., Afrasiabi,A., Ramzi,M., De Cristofaro,R., & Peyvandi,F. (2009) The first deletion mutation in the TSP1-6 repeat domain of ADAMTS13 in a family with inherited thrombotic thrombocytopenic purpura. *Haematologica*, **94**, 289-293.

Palla,R., Valsecchi,C., Bajetta,M., Spreafico,M., De Cristofaro,R., & Peyvandi,F. (2011) Evaluation of assay methods to measure plasma ADAMTS13 activity in thrombotic microangiopathies. *Thromb.Haemost.*, **105**, 381-385.

Pan,S., Cheng,X., & Sifers,R.N. (2013) Golgi-situated endoplasmic reticulum alpha-1, 2-mannosidase contributes to the retrieval of ERAD substrates through a direct interaction with gamma-COP. *Mol.Biol.Cell*, **24**, 1111-1121.

Pan,S., Wang,S., Utama,B., Huang,L., Blok,N., Estes,M.K., Moremen,K.W., & Sifers,R.N. (2011) Golgi localization of ERManI defines spatial separation of the mammalian glycoprotein quality control system. *Mol.Biol.Cell*, **22**, 2810-2822.

Parenti,G., Zuppaldi,A., Gabriela,P.M., Rosaria,T.M., Annunziata,I., Meroni,G., Porto,C., Donaudy,F., Rossi,B., Rossi,M., Filocamo,M., Donati,A., Bembi,B., Ballabio,A., & Andria,G. (2007) Pharmacological enhancement of mutated alpha-glucosidase activity in fibroblasts from patients with Pompe disease. *Mol.Ther.*, **15**, 508-514.

Park,H.S., Jun,d.Y., Han,C.R., Woo,H.J., & Kim,Y.H. (2011) Proteasome inhibitor MG132-induced apoptosis via ER stress-mediated apoptotic pathway and its potentiation by protein tyrosine kinase p56lck in human Jurkat T cells. *Biochem.Pharmacol.*, **82**, 1110-1125.

Park,H.W., Oh,D., Kim,N., Cho,H.Y., Moon,K.C., Chae,J.H., Ahn,H.S., Choi,Y., & Cheong,H.I. (2008) Congenital thrombotic thrombocytopenic purpura associated with unilateral moyamoya disease. *Pediatr.Nephrol.*, **23**, 1555-1558.

Park,J.E., Son,A.I., Hua,R., Wang,L., Zhang,X., & Zhou,R. (2012) Human cataract mutations in EPHA2 SAM domain alter receptor stability and function. *PLoS.One.*, **7**, e36564.

Parmryd,I., Adler,J., Patel,R., & Magee,A.I. (2003) Imaging metabolism of phosphatidylinositol 4,5-bisphosphate in T-cell GM1-enriched domains containing Ras proteins. *Exp.Cell Res.*, **285**, 27-38.

Pedemonte,N., Lukacs,G.L., Du,K., Caci,E., Zegarra-Moran,O., Galietta,L.J., & Verkman,A.S. (2005) Small-molecule correctors of defective DeltaF508-CFTR cellular processing identified by high-throughput screening. *J Clin.Invest*, **115**, 2564-2571.

Perucho,J., Casarejos,M.J., Gomez,A., Solano,R.M., de Yebenes,J.G., & Mena,M.A. (2012) Trehalose protects from aggravation of amyloid pathology induced by isoflurane anesthesia in APP(swe) mutant mice. *Curr.Alzheimer.Res.*, **9**, 334-343.

Pey,A.L., Ying,M., Cremades,N., Velazquez-Campoy,A., Scherer,T., Thony,B., Sancho,J., & Martinez,A. (2008) Identification of pharmacological chaperones as potential therapeutic agents to treat phenylketonuria. *J Clin.Invest*, **118**, 2858-2867.

Peyvandi,F., Ferrari,S., Lavoretano,S., Canciani,M.T., & Mannucci,P.M. (2004) von Willebrand factor cleaving protease (ADAMTS-13) and ADAMTS-13 neutralizing autoantibodies in 100 patients with thrombotic thrombocytopenic purpura. *Br.J.Haematol.*, **127**, 433-439.

Peyvandi,F., Lavoretano,S., Palla,R., Valsecchi,C., Merati,G., De Cristofaro,R., Rossi,E., & Mannucci,M.P. (2006) Mechanisms of the interaction between two ADAMTS13

gene mutations leading to severe deficiency of enzymatic activity. *Hum.Mutat.*, **27**, 330-336.

Peyvandi,F., Palla,R., Lotta,L.A., Mackie,I., Scully,M.A., & Machin,S.J. (2010) ADAMTS-13 assays in thrombotic thrombocytopenic purpura. *J Thromb.Haemost.*, **8**, 631-640.

Pimanda,J.E., Maekawa,A., Wind,T., Paxton,J., Chesterman,C.N., & Hogg,P.J. (2004) Congenital thrombotic thrombocytopenic purpura in association with a mutation in the second CUB domain of ADAMTS13. *Blood*, **103**, 627-629.

Pinsky,D.J., Naka,Y., Liao,H., Oz,M.C., Wagner,D.D., Mayadas,T.N., Johnson,R.C., Hynes,R.O., Heath,M., Lawson,C.A., & Stern,D.M. (1996) Hypoxia-induced exocytosis of endothelial cell Weibel-Palade bodies. A mechanism for rapid neutrophil recruitment after cardiac preservation. *J.Clin.Invest*, **97**, 493-500.

Plaimauer,B., Fuhrmann,J., Mohr,G., Wernhart,W., Bruno,K., Ferrari,S., Konetschny,C., Antoine,G., Rieger,M., & Scheiflinger,F. (2006) Modulation of ADAMTS13 secretion and specific activity by a combination of common amino acid polymorphisms and a missense mutation. *Blood*, **107**, 118-125.

Plaimauer,B., Kremer Hovinga,J.A., Juno,C., Wolfsegger,M.J., Skalicky,S., Schmidt,M., Grillberger,L., Hasslacher,M., Knobl,P., Ehrlich,H., & Scheiflinger,F. (2011) Recombinant ADAMTS13 normalizes von Willebrand factor-cleaving activity in plasma of acquired TTP patients by overriding inhibitory antibodies. *J Thromb.Haemost.*, **9**, 936-944.

Plaimauer,B. & Scheiflinger,F. (2004) Expression and characterization of recombinant human ADAMTS-13. *Semin.Hematol.*, **41**, 24-33.

Pollard,A. & Wyn Jones,R.G. (1979) Enzyme activities in concentrated solutions of glycinebetaine and other solutes. *Planta*, **144**, 291-298.

Pos,W., Crawley,J.T., Fijnheer,R., Voorberg,J., Lane,D.A., & Luken,B.M. (2010) An autoantibody epitope comprising residues R660, Y661, and Y665 in the ADAMTS13 spacer domain identifies a binding site for the A2 domain of VWF. *Blood*, **115**, 1640-1649.

Pozzi,N., Lancellotti,S., De Cristofaro,R., & De Filippis,V. (2012) Modeling ADAMTS13-von Willebrand factor interaction: Implications for oxidative stress-related cardiovascular diseases and type 2A von Willebrand disease. *Biophys.Chem.*, **160**, 1-11.

Prestidge,T.D., Rurali,E., Wadsworth,L., Wu,J.K., Moore,J.C., & Bresin,E. (2012) Congenital thrombotic thrombocytopenic purpura (cTTP) with two novel mutations. *Pediatr.Blood Cancer*, **59**, 1296-1298.

Pruss,C.M., Notley,C.R., Hegadorn,C.A., O'Brien,L.A., & Lillicrap,D. (2008) ADAMTS13 cleavage efficiency is altered by mutagenic and, to a lesser extent, polymorphic sequence changes in the A1 and A2 domains of von Willebrand factor. *Br.J Haematol.*, **143**, 552-558.

Puthalakath,H., O'Reilly,L.A., Gunn,P., Lee,L., Kelly,P.N., Huntington,N.D., Hughes,P.D., Michalak,E.M., McKimm-Breschkin,J., Motoyama,N., Gotoh,T., Akira,S., Bouillet,P.,

& Strasser,A. (2007) ER stress triggers apoptosis by activating BH3-only protein Bim. *Cell*, **129**, 1337-1349.

Qu,Y., Bolen,C.L., & Bolen,D.W. (1998) Osmolyte-driven contraction of a random coil protein. *Proc.Natl.Acad.Sci.U.S.A*, **95**, 9268-9273.

Raife,T.J., Cao,W., Atkinson,B.S., Bedell,B., Montgomery,R.R., Lentz,S.R., Johnson,G.F., & Zheng,X.L. (2009) Leukocyte proteases cleave von Willebrand factor at or near the ADAMTS13 cleavage site. *Blood*, **114**, 1666-1674.

Rand,J.H., Gordon,R.E., Sussman,I.I., Chu,S.V., & Solomon,V. (1982) Electron microscopic localization of factor-VIII-related antigen in adult human blood vessels. *Blood*, **60**, 627-634.

Rand,J.H., Sussman,I.I., Gordon,R.E., Chu,S.V., & Solomon,V. (1980) Localization of factor-VIII-related antigen in human vascular subendothelium. *Blood*, **55**, 752-756.

Rank,C.U., Kremer,H.J., Taleghani,M.M., Lammle,B., Gotze,J.P., & Nielsen,O.J. (2014) Congenital thrombotic thrombocytopenic purpura caused by new compound heterozygous mutations of the ADAMTS13 gene. *Eur.J.Haematol.*, **92**, 168-171.

Rasola,A., Galietta,L.J., Barone,V., Romeo,G., & Bagnasco,S. (1995) Molecular cloning and functional characterization of a GABA/betaine transporter from human kidney. *FEBS Lett.*, **373**, 229-233.

Rayes,J., Hollestelle,M.J., Legendre,P., Marx,I., de Groot,P.G., Christophe,O.D., Lenting,P.J., & Denis,C.V. (2010) Mutation and ADAMTS13-dependent modulation of disease severity in a mouse model for von Willebrand disease type 2B. *Blood*, **115**, 4870-4877.

Rayes,J., Hommais,A., Legendre,P., Tout,H., Veyradier,A., Obert,B., Ribba,A.S., & Girma,J.P. (2007) Effect of von Willebrand disease type 2B and type 2M mutations on the susceptibility of von Willebrand factor to ADAMTS-13. *J.Thromb.Haemost.*, **5**, 321-328.

Rayes,J., Roumenina,L.T., Dimitrov,J.D., Repesse,Y., Ing,M., Christophe,O., Jokiranta,T.S., Halbwachs-Mecarelli,L., Borel-Derlon,A., Kaveri,S.V., Fremeaux-Bacchi,V., & Lacroix-Desmazes,S. (2014) The interaction between factor H and VWF increases factor H cofactor activity and regulates VWF prothrombotic status. *Blood*, **123**, 121-125.

Reed,R.H., Chudek,J.A., Foster,R., & Gadd,G.M. (1987) Osmotic significance of glycerol accumulation in exponentially growing yeasts. *Appl.Environ.Microbiol.*, **53**, 2119-2123.

Rene,P., Le Gouill,C., Pogozheva,I.D., Lee,G., Mosberg,H.I., Farooqi,I.S., Valenzano,K.J., & Bouvier,M. (2010) Pharmacological chaperones restore function to MC4R mutants responsible for severe early-onset obesity. *J Pharmacol.Exp.Ther.*, **335**, 520-532.

Renshaw,S. (2007) *Immunohistochemistry: Methods Express,* 1st edn, Scion Publishing Limited, Boxham.

Ribes,J.A., Francis,C.W., & Wagner,D.D. (1987) Fibrin induces release of von Willebrand factor from endothelial cells. *J Clin.Invest*, **79**, 117-123.

Ricketts,L.M., Dlugosz,M., Luther,K.B., Haltiwanger,R.S., & Majerus,E.M. (2007) O-fucosylation is required for ADAMTS13 secretion. *J.Biol.Chem.*, **282**, 17014-17023.

Rieger,M., Mannucci,P.M., Kremer Hovinga,J.A., Herzog,A., Gerstenbauer,G., Konetschny,C., Zimmermann,K., Scharrer,I., Peyvandi,F., Galbusera,M., Remuzzi,G., Bohm,M., Plaimauer,B., Lammle,B., & Scheiflinger,F. (2005) ADAMTS13 autoantibodies in patients with thrombotic microangiopathies and other immunomediated diseases. *Blood*, **106**, 1262-1267.

Robben,J.H., Sze,M., Knoers,N.V., & Deen,P.M. (2006) Rescue of vasopressin V2 receptor mutants by chemical chaperones: specificity and mechanism. *Mol.Biol.Cell*, **17**, 379-386.

Romijn,R.A., Bouma,B., Wuyster,W., Gros,P., Kroon,J., Sixma,J.J., & Huizinga,E.G. (2001) Identification of the collagen-binding site of the von Willebrand factor A3-domain. *J Biol.Chem.*, **276**, 9985-9991.

Rossio,R., Ferrari,B., Cairo,A., Mancini,I., Pisapia,G., Palazzo,G., & Peyvandi,F. (2013) Two novel heterozygote missense mutations of the ADAMTS13 gene in a child with recurrent thrombotic thrombocytopenic purpura. *Blood Transfus.*, **11**, 241-244.

Roth,S.D., Schuttrumpf,J., Milanov,P., Abriss,D., Ungerer,C., Quade-Lyssy,P., Simpson,J.C., Pepperkok,R., Seifried,E., & Tonn,T. (2012) Chemical chaperones improve protein secretion and rescue mutant factor VIII in mice with hemophilia A. *PLoS.One.*, **7**, e44505.

Rountree,J.S., Butters,T.D., Wormald,M.R., Boomkamp,S.D., Dwek,R.A., Asano,N., Ikeda,K., Evinson,E.L., Nash,R.J., & Fleet,G.W. (2009) Design, synthesis, and biological evaluation of enantiomeric beta-N-acetylhexosaminidase inhibitors LABNAc and DABNAc as potential agents against Tay-Sachs and Sandhoff disease. *ChemMedChem.*, **4**, 378-392.

Rubenstein,R.C., Egan,M.E., & Zeitlin,P.L. (1997) In vitro pharmacologic restoration of CFTR-mediated chloride transport with sodium 4-phenylbutyrate in cystic fibrosis epithelial cells containing delta F508-CFTR. *J Clin.Invest*, **100**, 2457-2465.

Rubinsztein,D.C. (2006) The roles of intracellular protein-degradation pathways in neurodegeneration. *Nature*, **443**, 780-786.

Ruggeri,Z.M. (1997) von Willebrand factor. *J Clin.Invest*, **100**, S41-S46.

Rurali,E., Noris,M., Chianca,A., Donadelli,R., Banterla,F., Galbusera,M., Gherardi,G., Gastoldi,S., Parvanova,A., Iliev,I., Bossi,A., Haefliger,C., Trevisan,R., Remuzzi,G., & Ruggenenti,P. (2013) ADAMTS13 predicts renal and cardiovascular events in type 2 diabetic patients and response to therapy. *Diabetes*, **62**, 3599-3609.

Sadler,J.E. (1998) Biochemistry and genetics of von Willebrand factor. *Annu.Rev.Biochem.*, **67**, 395-424.

Sakariassen,K.S., Nievelstein,P.F., Coller,B.S., & Sixma,J.J. (1986) The role of platelet membrane glycoproteins Ib and IIb-IIIa in platelet adherence to human artery subendothelium. *Br.J Haematol.*, **63**, 681-691.

Sala,G., Arosio,A., Stefanoni,G., Melchionda,L., Riva,C., Marinig,D., Brighina,L., & Ferrarese,C. (2013) Rotenone upregulates alpha-synuclein and myocyte enhancer factor 2D independently from lysosomal degradation inhibition. *Biomed.Res.Int.*, **2013**, 846725.

Sallah,S., Husain,A., Wan,J.Y., & Nguyen,N.P. (2004) Rituximab in patients with refractory thrombotic thrombocytopenic purpura. *J Thromb.Haemost.*, **2**, 834-836.

Sanchez-Luceros,A., Farias,C.E., Amaral,M.M., Kempfer,A.C., Votta,R., Marchese,C., Salviu,M.J., Woods,A.I., Meschengieser,S.S., & Lazzari,M.A. (2004) von Willebrand factor-cleaving protease (ADAMTS13) activity in normal non-pregnant women, pregnant and post-delivery women. *Thromb.Haemost.*, **92**, 1320-1326.

Sanger,F., Nicklen,S., & Coulson,A.R. (1977) DNA sequencing with chain-terminating inhibitors. *Proc.Natl.Acad.Sci.U.S.A*, **74**, 5463-5467.

Santana,A., Salido,E., Torres,A., & Shapiro,L.J. (2003) Primary hyperoxaluria type 1 in the Canary Islands: a conformational disease due to I244T mutation in the P11L-containing alanine:glyoxylate aminotransferase. *Proc.Natl.Acad.Sci.U.S.A*, **100**, 7277-7282.

Santos-Sierra,S., Kirchmair,J., Perna,A.M., Reiss,D., Kemter,K., Roschinger,W., Glossmann,H., Gersting,S.W., Muntau,A.C., Wolber,G., & Lagler,F.B. (2012) Novel pharmacological chaperones that correct phenylketonuria in mice. *Hum.Mol.Genet.*, **21**, 1877-1887.

Sato,S., Ward,C.L., Krouse,M.E., Wine,J.J., & Kopito,R.R. (1996) Glycerol reverses the misfolding phenotype of the most common cystic fibrosis mutation. *J Biol.Chem.*, **271**, 635-638.

Savage,B., Saldivar,E., & Ruggeri,Z.M. (1996) Initiation of platelet adhesion by arrest onto fibrinogen or translocation on von Willebrand factor. *Cell*, **84**, 289-297.

Savage,B., Sixma,J.J., & Ruggeri,Z.M. (2002) Functional self-association of von Willebrand factor during platelet adhesion under flow. *Proc.Natl.Acad.Sci.U.S.A*, **99**, 425-430.

Savasan,S., Lee,S.K., Ginsburg,D., & Tsai,H.M. (2003) ADAMTS13 gene mutation in congenital thrombotic thrombocytopenic purpura with previously reported normal VWF cleaving protease activity. *Blood*, **101**, 4449-4451.

Scheiflinger,F., Knobl,P., Trattner,B., Plaimauer,B., Mohr,G., Dockal,M., Dorner,F., & Rieger,M. (2003) Nonneutralizing IgM and IgG antibodies to von Willebrand factor-cleaving protease (ADAMTS-13) in a patient with thrombotic thrombocytopenic purpura. *Blood*, **102**, 3241-3243.

Schettert,I.T., Pereira,A.C., Lopes,N.H., Hueb,W.A., & Krieger,J.E. (2010) Association between ADAMTS13 polymorphisms and risk of cardiovascular events in chronic coronary disease. *Thromb.Res.*, **125**, 61-66.

Schiviz,A., Wuersch,K., Piskernik,C., Dietrich,B., Hoellriegl,W., Rottensteiner,H., Scheiflinger,F., Schwarz,H.P., & Muchitsch,E.M. (2012) A new mouse model mimicking thrombotic thrombocytopenic purpura: correction of symptoms by recombinant human ADAMTS13. *Blood*, **119**, 6128-6135.

Schneider,S.W., Nuschele,S., Wixforth,A., Gorzelanny,C., Alexander-Katz,A., Netz,R.R., & Schneider,M.F. (2007) Shear-induced unfolding triggers adhesion of von Willebrand factor fibers. *Proc.Natl.Acad.Sci.U.S.A*, **104**, 7899-7903.

Schneider-Poetsch,T., Ju,J., Eyler,D.E., Dang,Y., Bhat,S., Merrick,W.C., Green,R., Shen,B., & Liu,J.O. (2010) Inhibition of eukaryotic translation elongation by cycloheximide and lactimidomycin. *Nat.Chem.Biol.*, **6**, 209-217.

Schnell,U., Dijk,F., Sjollema,K.A., & Giepmans,B.N. (2012) Immunolabeling artifacts and the need for live-cell imaging. *Nat.Methods*, **9**, 152-158.

Schneppenheim,R., Budde,U., Oyen,F., Angerhaus,D., Aumann,V., Drewke,E., Hassenpflug,W., Haberle,J., Kentouche,K., Kohne,E., Kurnik,K., Mueller-Wiefel,D., Obser,T., Santer,R., & Sykora,K.W. (2003) von Willebrand factor cleaving protease and ADAMTS13 mutations in childhood TTP. *Blood*, **101**, 1845-1850.

Schneppenheim,R., Kremer Hovinga,J.A., Becker,T., Budde,U., Karpman,D., Brockhaus,W., Hrachovinova,I., Korczowski,B., Oyen,F., Rittich,S., von Rosen,J., Tjonnfjord,G.E., Pimanda,J.E., Wienker,T.F., & Lammle,B. (2006) A common origin of the 4143insA ADAMTS13 mutation. *Thromb.Haemost.*, **96**, 3-6.

Schultz,D.R., Arnold,P.I., Jy,W., Valant,P.A., Gruber,J., Ahn,Y.S., Mao,F.W., Mao,W.W., & Horstman,L.L. (1998) Anti-CD36 autoantibodies in thrombotic thrombocytopenic purpura and other thrombotic disorders: identification of an 85 kD form of CD36 as a target antigen. *Br.J Haematol.*, **103**, 849-857.

Scully,M., Cohen,H., Cavenagh,J., Benjamin,S., Starke,R., Killick,S., Mackie,I., & Machin,S.J. (2007) Remission in acute refractory and relapsing thrombotic thrombocytopenic purpura following rituximab is associated with a reduction in IgG antibodies to ADAMTS-13. *Br.J Haematol.*, **136**, 451-461.

Scully,M. & Goodship,T. (2014) How I treat thrombotic thrombocytopenic purpura and atypical haemolytic uraemic syndrome. *Br.J Haematol.*, **164**, 759-766.

Scully,M., Hunt,B.J., Benjamin,S., Liesner,R., Rose,P., Peyvandi,F., Cheung,B., & Machin,S.J. (2012) Guidelines on the diagnosis and management of thrombotic thrombocytopenic purpura and other thrombotic microangiopathies. *Br.J.Haematol.*, **158**, 323-335.

Scully,M., Mcdonald,V., Cavenagh,J., Hunt,B.J., Longair,I., Cohen,H., & Machin,S.J. (2011) A phase 2 study of the safety and efficacy of rituximab with plasma exchange in acute acquired thrombotic thrombocytopenic purpura. *Blood*, **118**, 1746-1753.

Scully,M., Starke,R., Lee,R., Mackie,I., Machin,S., & Cohen,H. (2006) Successful management of pregnancy in women with a history of thrombotic thrombocytopaenic purpura. *Blood Coagul.Fibrinolysis*, **17**, 459-463.

Scully,M., Thomas,M., Underwood,M., Watson,H., Langley,K., Camilleri,R.S., Clark,A., Creagh,D., Rayment,R., Mcdonald,V., Roy,A., Evans,G., McGuckin,S., Ni Ainle,F., Maclean,R., Lester,W., Nash,M., Scott,R., & O'Brien,P. (2014) Congenital and acquired thrombotic thrombocytopenic purpura and pregnancy: presentation, management and outcome of subsequent pregnancies. *Blood*, Prepublished online May 23 2014; doi:10.1182/blood-2014-02-553131.

Scully,M., Yarranton,H., Liesner,R., Cavenagh,J., Hunt,B., Benjamin,S., Bevan,D., Mackie,I., & Machin,S. (2008) Regional UK TTP registry: correlation with laboratory ADAMTS 13 analysis and clinical features. *Br.J.Haematol.*, **142**, 819-826.

Segel,I. (1993) *Enzyme Kinetics: Behavior and Analysis of Rapid Equilibrium and Steady-State Enzyme Systems,* John Wiley and Sons, Inc, New York.

Shang,D., Zheng,X.W., Niiya,M., & Zheng,X.L. (2006) Apical sorting of ADAMTS13 in vascular endothelial cells and Madin-Darby canine kidney cells depends on the CUB domains and their association with lipid rafts. *Blood*, **108**, 2207-2215.

Shibagaki,Y., Matsumoto,M., Kokame,K., Ohba,S., Miyata,T., Fujimura,Y., & Fujita,T. (2006) Novel compound heterozygote mutations (H234Q/R1206X) of the ADAMTS13 gene in an adult patient with Upshaw-Schulman syndrome showing predominant episodes of repeated acute renal failure. *Nephrol.Dial.Transplant.*, **21**, 1289-1292.

Shida,Y., Nishio,K., Sugimoto,M., Mizuno,T., Hamada,M., Kato,S., Matsumoto,M., Okuchi,K., Fujimura,Y., & Yoshioka,A. (2008) Functional imaging of shear-dependent activity of ADAMTS13 in regulating mural thrombus growth under whole blood flow conditions. *Blood*, **111**, 1295-1298.

Shim,K., Anderson,P.J., Tuley,E.A., Wiswall,E., & Sadler,J.E. (2008) Platelet-VWF complexes are preferred substrates of ADAMTS13 under fluid shear stress. *Blood*, **111**, 651-657.

Shin,S.H., Kluepfel-Stahl,S., Cooney,A.M., Kaneski,C.R., Quirk,J.M., Schiffmann,R., Brady,R.O., & Murray,G.J. (2008) Prediction of response of mutated alpha-galactosidase A to a pharmacological chaperone. *Pharmacogenet.Genomics*, **18**, 773-780.

Shuman,S. (1991) Recombination mediated by vaccinia virus DNA topoisomerase I in Escherichia coli is sequence specific. *Proc.Natl.Acad.Sci.U.S.A*, **88**, 10104-10108.

Sidoryk-Wegrzynowicz,M., Lee,E.S., Ni,M., & Aschner,M. (2010) Manganese-induced downregulation of astroglial glutamine transporter SNAT3 involves ubiquitin-mediated proteolytic system. *Glia*, **58**, 1905-1912.

Siedlecki,C.A., Lestini,B.J., Kottke-Marchant,K.K., Eppell,S.J., Wilson,D.L., & Marchant,R.E. (1996) Shear-dependent changes in the three-dimensional structure of human von Willebrand factor. *Blood*, **88**, 2939-2950.

Singh,L.R., Chen,X., Kozich,V., & Kruger,W.D. (2007) Chemical chaperone rescue of mutant human cystathionine beta-synthase. *Mol.Genet.Metab.*, **91**, 335-342.

Skipwith,C.G., Cao,W., & Zheng,X.L. (2010) Factor VIII and platelets synergistically accelerate cleavage of von Willebrand factor by ADAMTS13 under fluid shear stress. *J.Biol.Chem.*, **285**, 28596-28603.

Smith,J.L., Reloj,A.R., Nataraj,P.S., Bartos,D.C., Schroder,E.A., Moss,A.J., Ohno,S., Horie,M., Anderson,C.L., January,C.T., & Delisle,B.P. (2013) Pharmacological correction of long QT-linked mutations in KCNH2 (hERG) increases the trafficking of Kv11.1 channels stored in the transitional endoplasmic reticulum. *Am.J Physiol.Cell.Physiol.*, **305**, C919-C930.

Snider,C.E., Moore,J.C., Warkentin,T.E., Finch,C.N., Hayward,C.P., & Kelton,J.G. (2004) Dissociation between the level of von Willebrand factor-cleaving protease activity and disease in a patient with congenital thrombotic thrombocytopenic purpura. *Am.J.Hematol.*, **77**, 387-390.

Soejima,K., Matsumoto,M., Kokame,K., Yagi,H., Ishizashi,H., Maeda,H., Nozaki,C., Miyata,T., Fujimura,Y., & Nakagaki,T. (2003) ADAMTS-13 cysteine-rich/spacer domains are functionally essential for von Willebrand factor cleavage. *Blood*, **102**, 3232-3237.

Soejima,K., Nakamura,H., Hirashima,M., Morikawa,W., Nozaki,C., & Nakagaki,T. (2006) Analysis on the molecular species and concentration of circulating ADAMTS13 in Blood. *J Biochem.*, **139**, 147-154.

Somero,G.N. (1986) Protons, osmolytes, and fitness of internal milieu for protein function. *Am.J Physiol*, **251**, R197-R213.

Song,J.L. & Chuang,D.T. (2001) Natural osmolyte trimethylamine N-oxide corrects assembly defects of mutant branched-chain alpha-ketoacid decarboxylase in maple syrup urine disease. *J Biol.Chem.*, **276**, 40241-40246.

Sorvillo,N., Kaijen,P.H., Matsumoto,M., Fujimura,Y., van der Zwaan,C., Verbij,F.C., Pos,W., Fijnheer,R., Voorberg,J., & Meijer,A.B. (2014) Identification of N-linked glycosylation and putative O-fucosylation, C-mannosylation sites in plasma derived ADAMTS13. *Journal of Thrombosis and Haemostasis*, **12**, 670-679.

Sporn,L.A., Chavin,S.I., Marder,V.J., & Wagner,D.D. (1985) Biosynthesis of von Willebrand protein by human megakaryocytes. *J.Clin.Invest*, **76**, 1102-1106.

Stadler,C., Skogs,M., Brismar,H., Uhlen,M., & Lundberg,E. (2010) A single fixation protocol for proteome-wide immunofluorescence localization studies. *J Proteomics.*, **73**, 1067-1078.

Stasi,R. (2010) Rituximab in autoimmune hematologic diseases: not just a matter of B cells. *Semin.Hematol.*, **47**, 170-179.

Stewart,G.A., Ridsdale,R., Martin,E.P., Na,C.L., Xu,Y., Mandapaka,K., & Weaver,T.E. (2012) 4-Phenylbutyric acid treatment rescues trafficking and processing of a mutant surfactant protein-C. *Am.J Respir.Cell Mol.Biol.*, **47**, 324-331.

Stirling,Y., Woolf,L., North,W.R., Seghatchian,M.J., & Meade,T.W. (1984) Haemostasis in normal pregnancy. *Thromb Haemost*, **52**, 176-182.

Stock,D., Nederlof,P.M., Seemuller,E., Baumeister,W., Huber,R., & Lowe,J. (1996) Proteasome: from structure to function. *Curr.Opin.Biotechnol.*, **7**, 376-385.

Studt,J.D., Kremer Hovinga,J.A., Antoine,G., Hermann,M., Rieger,M., Scheiflinger,F., & Lammle,B. (2005) Fatal congenital thrombotic thrombocytopenic purpura with apparent ADAMTS13 inhibitor: in vitro inhibition of ADAMTS13 activity by hemoglobin. *Blood*, **105**, 542-544.

Su,H. & Wang,X. (2010) The ubiquitin-proteasome system in cardiac proteinopathy: a quality control perspective. *Cardiovasc.Res.*, **85**, 253-262.

Sullivan,D.C., Huminiecki,L., Moore,J.W., Boyle,J.J., Poulsom,R., Creamer,D., Barker,J., & Bicknell,R. (2003) EndoPDI, a novel protein-disulfide isomerase-like protein that is preferentially expressed in endothelial cells acts as a stress survival factor. *J Biol.Chem.*, **278**, 47079-47088.

Suzuki,M., Murata,M., Matsubara,Y., Uchida,T., Ishihara,H., Shibano,T., Ashida,S., Soejima,K., Okada,Y., & Ikeda,Y. (2004) Detection of von Willebrand factor-cleaving protease (ADAMTS-13) in human platelets. *Biochem.Biophys.Res.Commun.*, **313**, 212-216.

Taguchi,F., Yagi,H., Matsumoto,M., Sadamura,S., Isonishi,A., Soejima,K., & Fujimura,Y. (2012) The homozygous p.C1024R-ADAMTS13 gene mutation links to a late-onset phenotype of Upshaw-Schulman syndrome in Japan. *Thromb.Haemost.*, **107**, 1003-1005.

Tamarappoo,B.K. & Verkman,A.S. (1998) Defective aquaporin-2 trafficking in nephrogenic diabetes insipidus and correction by chemical chaperones. *J Clin.Invest*, **101**, 2257-2267.

Tamarappoo,B.K., Yang,B., & Verkman,A.S. (1999) Misfolding of mutant aquaporin-2 water channels in nephrogenic diabetes insipidus. *J Biol.Chem.*, **274**, 34825-34831.

Tan,C.M., Nickols,H.H., & Limbird,L.E. (2003) Appropriate polarization following pharmacological rescue of V2 vasopressin receptors encoded by X-linked nephrogenic diabetes insipidus alleles involves a conformation of the receptor that also attains mature glycosylation. *J Biol.Chem.*, **278**, 35678-35686.

Tanaka,M., Machida,Y., Niu,S., Ikeda,T., Jana,N.R., Doi,H., Kurosawa,M., Nekooki,M., & Nukina,N. (2004) Trehalose alleviates polyglutamine-mediated pathology in a mouse model of Huntington disease. *Nat.Med.*, **10**, 148-154.

Tandon,N.N., Rock,G., & Jamieson,G.A. (1994) Anti-CD36 antibodies in thrombotic thrombocytopenic purpura. *Br.J Haematol.*, **88**, 816-825.

Tao,Z., Anthony,K., Peng,Y., Choi,H., Nolasco,L., Rice,L., Moake,J.L., & Dong,J.F. (2006) Novel ADAMTS-13 mutations in an adult with delayed onset thrombotic thrombocytopenic purpura. *J.Thromb.Haemost.*, **4**, 1931-1935.

Tati,R., Kristoffersson,A.C., Stahl,A.L., Morgelin,M., Motto,D., Satchell,S., Mathieson,P., Manea-Hedstrom,M., & Karpman,D. (2011) Phenotypic expression of ADAMTS13 in glomerular endothelial cells. *PLoS.One.*, **6**, e21587.

Tatzelt,J., Prusiner,S.B., & Welch,W.J. (1996) Chemical chaperones interfere with the formation of scrapie prion protein. *EMBO.J*, **15**, 6363-6373.

Teckman,J.H. (2004) Lack of effect of oral 4-phenylbutyrate on serum alpha-1-antitrypsin in patients with alpha-1-antitrypsin deficiency: a preliminary study. *J Pediatr.Gastroenterol.Nutr.*, **39**, 34-37.

Terrell,D.R., Williams,L.A., Vesely,S.K., Lammle,B., Hovinga,J.A., & George,J.N. (2005) The incidence of thrombotic thrombocytopenic purpura-hemolytic uremic syndrome: all patients, idiopathic patients, and patients with severe ADAMTS-13 deficiency. *J.Thromb.Haemost.*, **3**, 1432-1436.

Tersteeg,C., de Maat,S., De Meyer,S.F., Smeets,M.W., Barendrecht,A.D., Roest,M., Pasterkamp,G., Fijnheer,R., Vanhoorelbeke,K., de Groot,P.G., & Maas,C. (2014) Plasmin cleavage of von Willebrand factor as an emergency bypass for ADAMTS13 deficiency in thrombotic microangiopathy. *Circulation*, **129**, 1320-1331.

Titani,K., Kumar,S., Takio,K., Ericsson,L.H., Wade,R.D., Ashida,K., Walsh,K.A., Chopek,M.W., Sadler,J.E., & Fujikawa,K. (1986) Amino acid sequence of human von Willebrand factor. *Biochemistry*, **25**, 3171-3184.

Tjeldhorn,L., Iversen,N., Sandvig,K., Bergan,J., Sandset,P.M., & Skretting,G. (2011) Protein C mutation (A267T) results in ER retention and unfolded protein response activation. *PLoS.One.*, **6**, e24009.

Trionfini,P., Tomasoni,S., Galbusera,M., Motto,D., Longaretti,L., Corna,D., Remuzzi,G., & Benigni,A. (2009) Adenoviral-mediated gene transfer restores plasma ADAMTS13 antigen and activity in ADAMTS13 knockout mice. *Gene Ther.*, **16**, 1373-1379.

Tripodi,A., Peyvandi,F., Chantarangkul,V., Palla,R., Afrasiabi,A., Canciani,M.T., Chung,D.W., Ferrari,S., Fujimura,Y., Karimi,M., Kokame,K., Kremer Hovinga,J.A., Lammle,B., De Meyer,S.F., Plaimauer,B., Vanhoorelbeke,K., Varadi,K., & Mannucci,P.M. (2008) Second international collaborative study evaluating performance characteristics of methods measuring the von Willebrand factor cleaving protease (ADAMTS-13). *J Thromb.Haemost.*, **6**, 1534-1541.

Tropak,M.B., Reid,S.P., Guiral,M., Withers,S.G., & Mahuran,D. (2004) Pharmacological enhancement of beta-hexosaminidase activity in fibroblasts from adult Tay-Sachs and Sandhoff Patients. *J Biol.Chem.*, **279**, 13478-13487.

Tsai,B., Ye,Y., & Rapoport,T.A. (2002) Retro-translocation of proteins from the endoplasmic reticulum into the cytosol. *Nat.Rev.Mol.Cell Biol.*, **3**, 246-255.

Tsai,H.M. (1996) Physiologic cleavage of von Willebrand factor by a plasma protease is dependent on its conformation and requires calcium ion. *Blood*, **87**, 4235-4244.

Tsai,H.M. & Lian,E.C. (1998) Antibodies to von Willebrand factor-cleaving protease in acute thrombotic thrombocytopenic purpura. *N.Engl.J.Med.*, **339**, 1585-1594.

Tseng,S.C. & Kimchi-Sarfaty,C. (2011) SNPs in ADAMTS13. *Pharmacogenomics.*, **12**, 1147-1160.

Tuddenham,E.G., Lane,R.S., Rotblat,F., Johnson,A.J., Snape,T.J., Middleton,S., & Kernoff,P.B. (1982) Response to infusions of polyelectrolyte fractionated human factor VIII concentrate in human haemophilia A and von Willebrand's disease. *Br.J Haematol.*, **52**, 259-267.

Turner,N., Nolasco,L., Tao,Z., Dong,J.F., & Moake,J. (2006) Human endothelial cells synthesize and release ADAMTS-13. *J.Thromb.Haemost.*, **4**, 1396-1404.

Uchida,T., Wada,H., Mizutani,M., Iwashita,M., Ishihara,H., Shibano,T., Suzuki,M., Matsubara,Y., Soejima,K., Matsumoto,M., Fujimura,Y., Ikeda,Y., & Murata,M. (2004) Identification of novel mutations in ADAMTS13 in an adult patient with congenital thrombotic thrombocytopenic purpura. *Blood*, **104**, 2081-2083.

Uemura,M., Tatsumi,K., Matsumoto,M., Fujimoto,M., Matsuyama,T., Ishikawa,M., Iwamoto,T.A., Mori,T., Wanaka,A., Fukui,H., & Fujimura,Y. (2005) Localization of ADAMTS13 to the stellate cells of human liver. *Blood*, **106**, 922-924.

Van,G.F., Straley,K.S., Cao,D., Gonzalez,J., Hadida,S., Hazlewood,A., Joubran,J., Knapp,T., Makings,L.R., Miller,M., Neuberger,T., Olson,E., Panchenko,V., Rader,J., Singh,A., Stack,J.H., Tung,R., Grootenhuis,P.D., & Negulescu,P. (2006) Rescue of DeltaF508-CFTR trafficking and gating in human cystic fibrosis airway primary cultures by small molecules. *Am.J Physiol Lung Cell Mol.Physiol*, **290**, L1117-L1130.

Vanhoorelbeke,K. & Deckmyn,H. (2003) The role of VWF-collagen interaction in acute platelet thrombus formation., **28**, 61-67.

Vavassori,S., Cortini,M., Masui,S., Sannino,S., Anelli,T., Caserta,I.R., Fagioli,C., Mossuto,M.F., Fornili,A., van Anken,E., Degano,M., Inaba,K., & Sitia,R. (2013) A pH-regulated quality control cycle for surveillance of secretory protein assembly. *Mol.Cell*, **50**, 783-792.

Veyradier,A., Lavergne,J.M., Ribba,A.S., Obert,B., Loirat,C., Meyer,D., & Girma,J.P. (2004) Ten candidate ADAMTS13 mutations in six French families with congenital thrombotic thrombocytopenic purpura (Upshaw-Schulman syndrome). *J.Thromb.Haemost.*, **2**, 424-429.

Vomund,A.N. & Majerus,E.M. (2009) ADAMTS13 bound to endothelial cells exhibits enhanced cleavage of von Willebrand factor. *J.Biol.Chem.*, **284**, 30925-30932.

Von Langenbeck,J.M. (1966) Mucolytic agent. *Br.Med.J*, **2**, 603-604.

Wagner,D.D. & Marder,V.J. (1984) Biosynthesis of von Willebrand protein by human endothelial cells: processing steps and their intracellular localization. *J Cell Biol.*, **99**, 2123-2130.

Wagner,D.D., Olmsted,J.B., & Marder,V.J. (1982) Immunolocalization of von Willebrand protein in Weibel-Palade bodies of human endothelial cells. *J Cell Biol.*, **95**, 355-360.

Wagner,D.D., Saffaripour,S., Bonfanti,R., Sadler,J.E., Cramer,E.M., Chapman,B., & Mayadas,T.N. (1991) Induction of specific storage organelles by von Willebrand factor propolypeptide. *Cell*, **64**, 403-413.

Wang,A., Liu,F., Dong,N., Ma,Z., Zhang,J., Su,J., Zhao,Y., & Ruan,C. (2010) Thrombospondin-1 and ADAMTS13 competitively bind to VWF A2 and A3 domains in vitro. *Thromb.Res.*, **126**, e260-e265.

Wang,X., Su,H., & Ranek,M.J. (2008) Protein quality control and degradation in cardiomyocytes. *J Mol.Cell Cardiol.*, **45**, 11-27.

Wang,Y., Bartlett,M.C., Loo,T.W., & Clarke,D.M. (2006) Specific rescue of cystic fibrosis transmembrane conductance regulator processing mutants using pharmacological chaperones. *Mol.Pharmacol.*, **70**, 297-302.

Watanabe-Asano,T., Kuma,A., & Mizushima,N. (2014) Cycloheximide inhibits starvation-induced autophagy through mTORC1 activation. *Biochem.Biophys.Res.Commun.*, **445**, 334-339.

Waters,P.J. (2001) Degradation of mutant proteins, underlying "loss of function" phenotypes, plays a major role in genetic disease. *Curr.Issues Mol.Biol.*, **3**, 57-65.

Weiss,H.J., Sussman,I.I., & Hoyer,L.W. (1977) Stabilization of factor VIII in plasma by the von Willebrand factor. Studies on posttransfusion and dissociated factor VIII and in patients with von Willebrand's disease. *J Clin.Invest*, **60**, 390-404.

Welch,W.J. & Brown,C.R. (1996) Influence of molecular and chemical chaperones on protein folding. *Cell Stress.Chaperones.*, **1**, 109-115.

Wolins,N., Bosshart,H., Kuster,H., & Bonifacino,J.S. (1997) Aggregation as a determinant of protein fate in post-Golgi compartments: role of the luminal domain of furin in lysosomal targeting. *J Cell Biol.*, **139**, 1735-1745.

Wu,X., Katz,E., Della Valle,M.C., Mascioli,K., Flanagan,J.J., Castelli,J.P., Schiffmann,R., Boudes,P., Lockhart,D.J., Valenzano,K.J., & Benjamin,E.R. (2011) A pharmacogenetic approach to identify mutant forms of alpha-galactosidase A that respond to a pharmacological chaperone for Fabry disease. *Hum.Mutat.*, **32**, 965-977.

Xiang,Y., de Groot,R., Crawley,J.T., & Lane,D.A. (2011) Mechanism of von Willebrand factor scissile bond cleavage by a disintegrin and metalloproteinase with a thrombospondin type 1 motif, member 13 (ADAMTS13). *Proc.Natl.Acad.Sci.U.S.A*, **108**, 11602-11607.

Yancey,P.H. (2005) Organic osmolytes as compatible, metabolic and counteracting cytoprotectants in high osmolarity and other stresses. *J Exp.Biol.*, **208**, 2819-2830.

Yancey,P.H., Clark,M.E., Hand,S.C., Bowlus,R.D., & Somero,G.N. (1982) Living with water stress: evolution of osmolyte systems. *Science*, **217**, 1214-1222.

Yancey,P.H. & Somero,G.N. (1979) Counteraction of urea destabilization of protein structure by methylamine osmoregulatory compounds of elasmobranch fishes. *Biochem.J*, **183**, 317-323.

Yee,A. & Kretz,C.A. (2014) Von Willebrand factor: form for function. *Semin.Thromb Hemost.*, **40**, 17-27.

Yeh,H.C., Zhou,Z., Choi,H., Tekeoglu,S., May,W., III, Wang,C., Turner,N., Scheiflinger,F., Moake,J.L., & Dong,J.F. (2010) Disulfide bond reduction of von Willebrand factor by ADAMTS-13. *J.Thromb.Haemost.*, **8**, 2778-2788.

Yorimitsu,T. & Klionsky,D.J. (2007) Endoplasmic reticulum stress: a new pathway to induce autophagy. *Autophagy.*, **3**, 160-162.

Yoshida,H., Yoshizawa,T., Shibasaki,F., Shoji,S., & Kanazawa,I. (2002) Chemical chaperones reduce aggregate formation and cell death caused by the truncated Machado-Joseph disease gene product with an expanded polyglutamine stretch. *Neurobiol.Dis.*, **10**, 88-99.

Yoshimori,T., Yamamoto,A., Moriyama,Y., Futai,M., & Tashiro,Y. (1991) Bafilomycin A1, a specific inhibitor of vacuolar-type H(+)-ATPase, inhibits acidification and protein degradation in lysosomes of cultured cells. *J Biol.Chem.*, **266**, 17707-17712.

Zanardelli,S., Chion,A.C., Groot,E., Lenting,P.J., McKinnon,T.A., Laffan,M.A., Tseng,M., & Lane,D.A. (2009) A novel binding site for ADAMTS13 constitutively exposed on the surface of globular VWF. *Blood*, **114**, 2819-2828.

Zanardelli,S., Crawley,J.T., Chion,C.K., Lam,J.K., Preston,R.J., & Lane,D.A. (2006) ADAMTS13 substrate recognition of von Willebrand factor A2 domain. *J Biol.Chem.*, **281**, 1555-1563.

Zeisel,S.H., Mar,M.H., Howe,J.C., & Holden,J.M. (2003) Concentrations of choline-containing compounds and betaine in common foods. *J Nutr.*, **133**, 1302-1307.

Zeitlin,P.L., Diener-West,M., Rubenstein,R.C., Boyle,M.P., Lee,C.K., & Brass-Ernst,L. (2002) Evidence of CFTR function in cystic fibrosis after systemic administration of 4-phenylbutyrate. *Mol.Ther.*, **6**, 119-126.

Zhang,P., Pan,W., Rux,A.H., Sachais,B.S., & Zheng,X.L. (2007) The cooperative activity between the carboxyl-terminal TSP1 repeats and the CUB domains of ADAMTS13 is crucial for recognition of von Willebrand factor under flow. *Blood*, **110**, 1887-1894.

Zhang,R., Chen,L., Jiralerspong,S., Snowden,A., Steinberg,S., & Braverman,N. (2010) Recovery of PEX1-Gly843Asp peroxisome dysfunction by small-molecule compounds. *Proc.Natl.Acad.Sci.U.S.A*, **107**, 5569-5574.

Zhang,X., Halvorsen,K., Zhang,C.Z., Wong,W.P., & Springer,T.A. (2009) Mechanoenzymatic cleavage of the ultralarge vascular protein von Willebrand factor. *Science*, **324**, 1330-1334.

Zhang,X.M., Wang,X.T., Yue,H., Leung,S.W., Thibodeau,P.H., Thomas,P.J., & Guggino,S.E. (2003) Organic solutes rescue the functional defect in delta F508 cystic fibrosis transmembrane conductance regulator. *J Biol.Chem.*, **278**, 51232-51242.

Zhao,B.Q., Chauhan,A.K., Canault,M., Patten,I.S., Yang,J.J., Dockal,M., Scheiflinger,F., & Wagner,D.D. (2009) von Willebrand factor-cleaving protease ADAMTS13 reduces ischemic brain injury in experimental stroke. *Blood*, **114**, 3329-3334.

Zheng,X., Chung,D., Takayama,T.K., Majerus,E.M., Sadler,J.E., & Fujikawa,K. (2001) Structure of von Willebrand factor-cleaving protease (ADAMTS13), a metalloprotease involved in thrombotic thrombocytopenic purpura. *J.Biol.Chem.*, **276**, 41059-41063.

Zheng,X., Nishio,K., Majerus,E.M., & Sadler,J.E. (2003) Cleavage of von Willebrand factor requires the spacer domain of the metalloprotease ADAMTS13. *J.Biol.Chem.*, **278**, 30136-30141.

Zheng,X.L., Wu,H.M., Shang,D., Falls,E., Skipwith,C.G., Cataland,S.R., Bennett,C.L., & Kwaan,H.C. (2010) Multiple domains of ADAMTS13 are targeted by autoantibodies against ADAMTS13 in patients with acquired idiopathic thrombotic thrombocytopenic purpura. *Haematologica*, **95**, 1555-1562.

Zhou,M., Dong,X., Baldauf,C., Chen,H., Zhou,Y., Springer,T.A., Luo,X., Zhong,C., Grater,F., & Ding,J. (2011) A novel calcium-binding site of von Willebrand factor A2 domain regulates its cleavage by ADAMTS13. *Blood*, **117**, 4623-4631.

Zhou,W., Bouhassira,E.E., & Tsai,H.M. (2007) An IAP retrotransposon in the mouse ADAMTS13 gene creates ADAMTS13 variant proteins that are less effective in cleaving von Willebrand factor multimers. *Blood*, **110**, 886-893.

Zhou,W., Inada,M., Lee,T.P., Benten,D., Lyubsky,S., Bouhassira,E.E., Gupta,S., & Tsai,H.M. (2005) ADAMTS13 is expressed in hepatic stellate cells. *Lab Invest*, **85**, 780-788.

Zhou,W. & Tsai,H.M. (2009) N-Glycans of ADAMTS13 modulate its secretion and von Willebrand factor cleaving activity. *Blood*, **113**, 929-935.

Zhou,Z., Gong,Q., & January,C.T. (1999) Correction of defective protein trafficking of a mutant HERG potassium channel in human long QT syndrome. Pharmacological and temperature effects. *J Biol.Chem.*, **274**, 31123-31126.

Zhou,Z., Han,H., Cruz,M.A., Lopez,J.A., Dong,J.F., & Guchhait,P. (2009a) Haemoglobin blocks von Willebrand factor proteolysis by ADAMTS-13: a mechanism associated with sickle cell disease. *Thromb.Haemost.*, **101**, 1070-1077.

Zhou,Z., Jing,H., Tao,Z., Choi,H., Aboulfatova,K., Moake,J., Li,R., & Dong,J.F. (2009b) Effects of naturally occurring mutations in CUB-1 domain on synthesis, stability, and activity of ADAMTS-13. *Thromb.Res.*, **124**, 323-327.

Zhou,Z., Nguyen,T.C., Guchhait,P., & Dong,J.F. (2010) Von Willebrand factor, ADAMTS-13, and thrombotic thrombocytopenic purpura. *Semin.Thromb.Hemost.*, **36**, 71-81.